The synthesis, chemical and physical characterisation of selected energetic binder systems
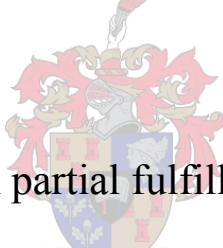
By

Khalifa Alkaabi

Dissertation presented in partial fulfillment of requirements for

the degree:

PhD (Polymer Science)

Supervisor: Dr. Albert van Reenen

2009

Stellenbosch

Declaration

I hereby declare that the work contained in this dissertation is my own original work and that I have not previously, in its entirety or in part, submitted it at any university for a degree.

---------------------   2009

  Khalifa Al-Kaabi   Stellenbosch

ABSTRACT

Due to numerous accidents involving munitions, recent interest has focused on the development and use of insensitive munitions (IM). Polymeric materials are used in insensitive munitions as binders or plasticizers. Most of the polymeric binders used are based on polycondensation reaction via using urethane linkages.

The main aim of this study was the synthesis and characterization of selected energetic thermoplastic elastomers binder based on utilizing controlled free radical polymerization. This was achieved by using hydroxyl terminated poly (epichlorohydrin) (PECH-diol) and hydroxyl terminated glycidyl azide polymer (GAP-diol) as starting materials, and the subsequent synthesis of different macro-initiators. These macro-initiators were used to polymerize methyl methacrylate (MMA) to obtain thermoplastic elastomers.

PECH-diol was prepared by cationic ring-opening polymerization (CROP) based on using borontrifluoride etherate (BF_3-etherate) as catalyst and a low molecular weight diol as initiator. GAP-diol was synthesized by the reaction of PECH-diol with sodium azide in organic solvent..

Poly(epichlorohydrin-methyl methacrylate) (PECH-PMMA) and poly(glycidyl azide-methyl methacrylate) (GAP-PMMA) block copolymers were prepared by free radical polymerization of MMA monomer in presence of PECH and GAP macro-azo-initiator (MAI). The MAIs were prepared by the polycondensation reaction of hydroxyl terminated groups of elastomer with 4,4' azobis (4-cyanopentanoyl chloride) (ACPC). The phase behavior of blends of amorphous PMMA/PECH-diol and PMMA/GAP-diol was also investigated.

Poly(epichlorohydrin-methyl methacrylate) (PECH-PMMA) and poly(glycidyl azide-methyl methacrylate) (GAP-PMMA) graft copolymers were synthesized by photopolymerization of MMA in presence of PECH and GAP with pendant *N,N*-diethyldithiocarbamate groups as macro-photoiniferters. . Photopolymerization of MMA proceeded in a controlled fashion.

A macro RAFT agent, based on the reaction of PECH with pendent dithiobenzoate was prepared. The macro-RAFT agent was used in the controlled thermal bulk polymerization of methyl methacrylate. Finally, living/controlled radical

polymerization of MMA with four different photoiniferters, namely benzyl diethyl dithiocarbamate (BDC), 2-(*N,N*-diethyldithiocarbamyl) propionic acid (PDC), 2-(*N,N*-diethyldithiocarbamyl) isobutyric acid (DTCA), and diethyl dithiocarbamate-epichlorohydrin was achieved.

Opsomming

As gevolg van verskeie ongelukke waar plofstowwe betrokke was, is daar onlangs baie aandag geskenk aan die ontwikkeling en gebruik van nie-sensitiewe plofstowwe en dryfmiddels. Polimeriese materials word in hierdie toepassings gebruik as binders en plastiseermiddels. Meeste van die polimere in hierdie toepassings word vervaardig deur polikondensasie-reaksies wat lei tot uretaan-bindings.

Die hoofdoel van hiersie studie was die sintese en karakterisering van gelselkteerde energetiese termoplastiese elastomere deur gebruik te maak van beheerde vrye radikaal polimerisasie.. Dit is bereik deur hidroksie-getermineerde poli(epichlorohidrien) (PECH-diol) en hidroksie-getermineerde glisidiel asied polimeer (GAP-diol) as uitgangsmateriale te gebruik. Die daaropvolgende sintese van verskillende makro-inisisieerders het gelei tot spesies wat gebruik kon word vir die polimerisasie van metiel metakrilaat (MMA) met die vorming van termoplasitese elastomere.

PECH-diol is berei deur kationiese ringopeningspolimerisasie met borontrifluoried eteraat (BF_3-eteraat) as katalis en 'n lae molekulêre massa diol as afsetter.. GAP-diol is berei deur die reaksie van PECH-diol met nariumasied.

Poli(epichlorohidirien-metiel metakrilaat) (PECH-PMMA) en poli(glisidiel asied-metiel metakrilaat) (GAP-PMMA) blok koploimere is berei deur vrye radikaal polimerisasie van MMA in die teenwoordigheid van PECH en GAP makro-aso-afsetter (MAA). Die MAA is berei deur die polikondensasie-reaksie van terminale hidroksie-groepe van die uitgangstowwe met 4,4' asobis (4-sianopentanoiel chloried) (ACPC). Die fase-gedrag van amorfe PMMA/PECH-diol en PMMA/GAP-diol is ook ondersoek.

Poli(epichlorohidirien-metiel metakrilaat) (PECH-PMMA) en poli(glisidiel asied-metiel metakrilaat) (GAP-PMMA) ent-kopolimere is berei deur die fotopolimerisasie van MMA in teenwoordigheid van PECH en GAP met *N,N*-dietieldithiokarbamaat groepe as makro-fotoiniferters. Fotopolimerisasie van MMA MMA het op 'n beheerde manier verloop.

'n Makro RAFT agent, gebaseer op die reaksie van PECH met dithiobensoaat sygroepe is berei. Die makro RAFT agent is gebruik in die beheerde termiese

massapolimerisasie van MMA. Laastens is lewende/beheerde radikaal polimerisasie van MMA met vire verskillende fotoiniferters, naamlik bensiel dietiel dithiokarbamaat (BDC), 2-(*N,N*-dietiel dithiokarbamiel) propioonsuur (PDC), 2-(*N,N*-dietiel dithiokarbamiel) isobutiriese suur (DTCA), en dietiel dithiokarbamat-epichlorohidirien susksesvol uitgevoer.

Dedication

This work is dedicated to H. H. General Sheikh Mohammed Bin Zayed Al Nahyan, inspiration of new UAE generation toward R&D.

Acknowledgements

All praise and thanks are due to (GOD), the one and only, the Indivisible Creator and Sustainer of the World. To Him we belong and to Him we shall return. I wish to thank Him for all that He has bestowed on us, although He can never be praised or thanked enough.

Also, I would like to express my sincerest gratitude to all who guided, advised and supported me during the presented study. I would like to thank the following individuals and companies for their contributions:

- My family, for their love, patience, and support.

- My promoter Dr. A.J van Reenen for his guidance and support.

- My supervisors Mr. Jum'ah Ahmed Albowardi and Mr. Mohamed Salem Alfalasi for there support, encouragements, and belief that I would succeed.

- Dr. M.J. Hurndall, for her advice on the writing of this thesis and publications and Dr. WG Weber for his continues advice and co-operation.

- Elsa Malherbe and Jean McKenzie for the recording NMR spectra and Jean for the interpretation and help with the results.

- My colleagues in the Olefins Lab and all other colleagues who worked with me in the polymer science laboratories during this study.

- NASCHEM, a division of Denel Pty Ltd for the financial support for this work.

- Kannetjie Fouche and Hannes Bester from NASCHEM for their support and organization for this study.

- Susan Meyer from Naschem and Charles Wiehahn from Cape land system for their help in the DSC and TGA analyses of the energetic binders.

Table of contents

Chapter 4 Synthesis and characterizations of poly(methyl methacrylate-*b*-epichlorohydrin) and poly(methyl methacrylate-*b*-glycidyl azide) copolymers by using nitroxide-mediated polymerization

Chapter 7 Synthesis and characterization of poly(epichlorohydrin-methyl methacrylate) graft copolymers prepared using reversible addition-fragmentation chain-transfer polymerization

List of Figures

List of Schemes

List of Tables

List of Symbols

$[M]_o$	Initial concentration of the initiator
$[M]$	Monomer concentration
$\overline{M_n}$	Number average molar mass
$\overline{M_{wt}}$	Weight average molar mass

List of Abbreviation

ACPA	4,4'Azobis (4-cyanopentanoyl Acid)
ACPC	4,4'Azobis (4-cyanopentanoyl chloride)
AIBN	2,2'Azobis(isobutyronitrile)
Akardite II	1,1-Diphenyl-3-methylurea
AMM	Active monomer mechanism
AMMO	3-Azidomethyl-3-methyl oxetane
AP	Ammonium perchlorate
ATRP	Atom transfer radical polymerization
BAMO	3,3-Bis(azidomethyl)oxetane
BCMO	3,3-Bis(chloromethyl)oxetane
BDC	Benzyl diethyl dithiocarbamate
BDNPA/F	Bis(2,2-dinitropropyl)acetal/formal
BDNPF	Bis(2,2-dinitropropyl)acetal/bis(2,2-dinitropropyl)formal
BF_3-etherate	Borontrifluoride etherate
BU	1,4-butanediol
Butyl-NENA	*N*-n-butyl-*N*-(2-nitroxy-ethyl)nitramine
CAB	Cellulose acetate butyrate
Centrallite I	1,3-Diethyl-1,3-diphenylurea
CFRP	Control free radical polymerization
CROP	Cationic ring opening polymerization
DBTL	Dibutyltin dilaurate
DCM	Dichloromethane
DEG	Di(ethylene glycol)
DEGBAA	Azido-acetic-acid-2-[2'-(2''-azido-acetoxy)-ethoxy]-ethylester
DMF	Dimethyl formamide
DMA	Dynamic mechanical analysis
DOP	dioctyl adipate
DP	Degree of Polymerization
DPA	Diphenylamine
DSC	Differential scanning calorimetry
DTCA	2-(*N,N*-diethyldithiocarbamyl) isobutyric acid
ECH	Epichlorohydrin
ECH-DDC	*N,N*-diethyl dithiocarbamate-epichlorohydrin
EGBAA	Azido-acetic-acid-2-(2'-azido-acetoxy)-ethylester

EG	Ethylene glycol
ETPEs	Energetic thermoplastic elastomers
EVA	Ethylene-vinyl acetate
GAP	Glycidyl azide polymer
GAP-DDC	*N,N*-diethyl dithiocarbamate glycidyl azide polymer
GAP-TDDC	*N,N*-diethyl dithiocarbamate terminated glycidyl azide polymer
GAP-*b*-PMMA	Poly (glycidyl azide-methyl methacrylate) block copolymer
GAP-*g*-PMMA	Poly (glycidyl azide-methyl methacrylate) graft copolymer
Gly	Glycerol
GLYN	Glycidyl nitrate
HDI	Hexamethylene diisocyanate
HIMMO	3-Hydroxymethyl-3-methyloxetane
HMX	Octahydro 1,3,5,7-tetranitro-1,3,5,7-tetrazocine
IM	Insensitive Munitions
IPDI	Isophorone diisocyanate
LOVA	Low vulnerability ammunition
MAI	Macro-azo-initiator
MDI	4,4'-Diisocyanato diphenylmethane
MMA	Methyl methacrylate
MP	2-methyl-2,4-pentandiol
MWD	Molecular weight distribution
NaN$_3$	Sodium azide
2-NDPA	2-Nitro-diphenylamine
NHTPB	Nitrated hydroxyl terminated polybutadiene
NMP	Nitroxide-mediated polymerization
NPN	2,2-Dinitro-1,3-bis-nitrooxy-propane
NQ	Nitroguanidine
PBX	Plastic bonded explosive
PDC	2-(*N,N*-diethyldithiocarbamyl) proponic acid
PDI	Polydispersity index
PECH	Poly(epichlorohydrin)
PECH-DDC	*N,N*-diethyl dithiocarbamate poly(epichlorohydrin)
PECH-*g*-PMMA	Poly(epichlorohydrin-methyl methacrylate) graft copolymer
PECH-*b*-PMMA	Poly(epichlorohydrin-methyl methacrylate) block copolymer
PECH-*g*-PS	Poly (epichlorohydrin-styrene) graft copolymer
PEG	Polyethylene glycol
PMMA	Poly(methyl methacrylate)
PNP	Poly(nitropolyphenylene)
polyNIMMO	Poly(3-nitratomethyl-3-methyl-oxetane)
PS	Poly(styrene)
PR	1,3-propandiol
PVA	Poly(vinyl acetate) and poly(vinyl alcohol)
PVN	Polyvinyl nitrate
RAFT	Reversible addition-fragmentation chain transfer
RDX	Cyclotrimethylenetrinitramine
S	Strong
SBS	Styrene-butadiene-styrene
SEM	Scanning electron microscopy

SEC	Size exclsion chromatography
TDI	Toluene diisocyanate
T_g	Glass transition temperature
TGA	Thermal gravimetrical analysis
THF	Tetrahydrofuran
TMNTA	Azido-acetic-acid-3-(2'-azido-acetoxy)-2-(2'-azido-acetoxymethyl)-2-nitro-ropylester
TPEs	Thermoplastic elastomers
TPU	Thermoplastic polyurethane
W	Weak

Various aspects of the work carried out during this study have been published and presented:

Presentations:

1- Synthesis and Characterization of Energetic Thermoplastic Elastomers by Using Controlled Free Radical Polymerization, Insensitive Munitions & Energetic Materials Technology Symposium, Miami, FL, October 15-17, 2007.

2- Applied of Living/Controlled Radical Polymerization in Synthesis of Energetic Thermoplastic Elastomers, PARARI 8th Australian Explosives Ordnance Symposium, 13-15 November, 2007.

3- Comparison between Polymerization Techniques for synthesis of Energetic Thermoplastic Elastomers, Insensitive Munitions & Energetic Materials Technology Symposium, Tucson, AZ, May 11-14, 2009.

Posters:

1- Synthesis of energetic thermoplastic elastomers using living or controlled radical polymerization, 38th International ICT-Conference, Karlsruhe, Germany, 26-29 June, 2007.

2- Synthesis and characterization of poly(methyl methacrylate-epichlorohydrin) grafted copolymers by using reversible addition-fragmentation chain-transfer (RAFT) polymerization, Zing Polymer Synthesis Conference, Cancun, Mexico 17-20 March, 2008.

Publications:

1- Controlled radical polymerization of poly(methyl methacrylate-*g*-epichlorohydrin) using *N, N*-dithiocarbamate-mediated iniferters, Accepted in Journal of Applied Polymer Science, Vol.108, 2528-2534-2008.

2- Synthesis of poly(methyl methacrylate-*g*-glycidyl azide) graft copolymers using *N ,N*-dithiocarbamate-mediated iniferters,. Accepted in Journal of Applied Polymer Science, 2009.

3- Synthesis and characterization of poly(epichlorohydrin-*g*-methyl methacrylate) graft copolymers prepared using reversible addition-

fragmentation chain-transfer polymerization , submitted to Journal of Polymer bulletin, 2008.

4- Controlled radical polymerization of methyl methacrylate using *N, N*-dithiocarbamate-mediated iniferter derivatives, submitted to Journal of Polymer bulletin, 2008.

Chapter 1

Introduction and Objectives

Chapter 1

Introduction and Objectives

This chapter presents a brief introduction to the thesis and its structure. It also includes its purpose, goal, objectives and methodology.

1.1 Introduction

There is a demand for materials with novel properties for specific advanced applications such as biomaterial, aerospace, and military. New materials should provide unique properties or be used to eliminate some deficiencies of older products. New materials should have better physical (strength, density, modulus, glass transition temperature) and chemical (compatibility, miscibility, functional groups, wettability) properties, when compared with older materials. Polymers provide an exciting array of possibilities for novel applications. New polymeric materials may be derived from the design and synthesis of new monomers, controlling the microstructure by utilizing existing, inexpensive, and readily available monomers in conjunction with novel catalyst, blend of homopolymers, and chemical modification of existing polymers.

This research projects new polymeric binders to be utilized in insensitive munitions (IM) that have been prepared by inexpensive and readily available monomers using controlled free radical polymerization.

1.1.1 Polymeric binders and insensitive munitions

Polymeric materials have a very wide range of applications. This is attributed, in part, to their very wide range of properties, good availability of their raw materials (hydrocarbons), and their ease of modification with changing in their molecular

2

Chapter 1

structure. In addition to every day's applications of polymeric materials, these materials are also used in many different advanced applications, such as medical devices, drug delivery, military equipment, and in the aerospace industry. Polymers used in military applications vary from simple applications such as military bags and tents, food packaging, etc., to advanced and complex applications such as ammunitions and explosive packaging, anti-chemical protective clothes, and high energetic material and additives. These sophisticated applications require materials with superior properties and special characteristics, where deficiency could lead to catastrophe damage and loss of lives [1, 2].

Numerous accidents have taken place during the last fifty years, especially onboard a United States aircraft carrier, such as USS Forestall, Oriskany, and Enterprise. Munitions were involved, either as the source of the accident or as an aggravating factor that contributed to the magnitude of these catastrophes. This found an action to reduce the vulnerability of ammunition. Over the past decade, determined attempts have been made by military services to reduce the vulnerability of their munitions platforms [1, 2]. This has been done by launching research projects to develop low vulnerability ammunition (LOVA) and identify the technology requirements for the production of insensitive munitions.

The design of future weapon systems requires safer, less sensitivities, and high performance munitions. There are several approaches that can be used to provide IM solutions, including weapon design, mitigation devices, packaging, and the use of less sensitive materials in explosive and propellant formulations. The use of energetic binders in explosive and propellant formulations is considered potentially a very useful method to formulate high performance LOVA. This could be attributed to the possibility to transplant energetic groups into polymer backbone or side chains and the availability of polymeric materials. There is a rapid development in using polymeric materials in propellant technology. The main function of polymeric binder

3

Chapter 1

is to provide a matrix that contains other ingredients and to act as protecting and encapsulating agent for other ingredients of the formulation. Usually, it produces final products with better mechanical resistance and simple processing requirements for the desired shape and dimensions.

1.1.2 Types of polymeric binders in insensitive munitions

Polymers and plasticizers may in themselves be inert, or energetic (capable of undergoing internal oxidation-reduction, exothermic, gas-forming decomposition), or they may serve as fuels for suspended oxidizer particles [1]. The classification of polymeric materials used in IM is given in **Figure 1.1**.
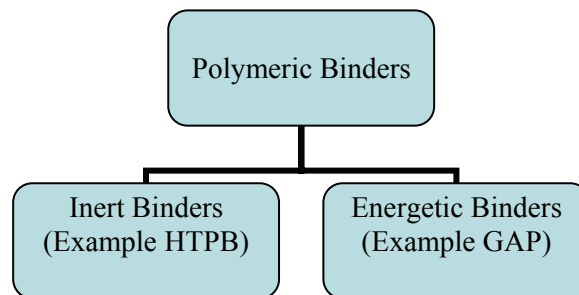
Figure 1.1 Classification of polymeric binders used in insensitive munitions.

Hydroxyl terminated polybutadiene (HTPB) is a popular example of inert binder. HTPB is used to encapsulate the explosive. The polymers react with isocyanates and plasticized with dioctyl adipate (DOA). In most solid rocket propellants the inert polymer content (binder) comprises only 5-15% of the total propellant formulation. The inert polymeric ingredient affects the final properties of the propellant and reduces the achievable output energy. Prior to the development of energetic binders, the polymeric component of most binders was the least energetic material in the entire mixture. It was not possible to extend a certain quantity of binder in the final

Chapter 1

formulation to avoid drawback in the performance (energy output). Glycidyl azide polymer (GAP) was first synthesized in 1972 by Vandenburg and lately a number of binders containing azide and nitro groups were developed and used in advanced rocket propellant formulations [1-3]. The most popular energetic binders are nitrocellulose, GAP, poly(3-nitratomethyl-3-methyl-oxetane) (polyNIMMO), and poly(3-azidomethyl-3-methyl oxetane) (polyAMMO). Some cited advantages of GAP are a low glass transition temperature, high energy from the decomposition of N_3 groups, high density, good safety, and compatibility [2]. Many other polymeric materials examined as binder for the IM. Some of the desired characteristics of good polymeric binders are [2, 3]:

1. Reduce vulnerability during storage and transportation, or upon exposure to unplanned hazardous stimuli.

2. Improve the mechanical properties and maintain the geometric integrity of the propellant charge when subject to external conditions such a change in temperature, stresses resulting from thermal coefficient of expansion differences between the propellant and the case materials, stresses resulting from case pressurization, storage at elevated temperature, vibration and acceleration, and weight loads.

3. Possibly enhance performance (energy output).

4. Reduce environmental impact in manufacture, use and disposal, and contribute to more economical production.

5. Enhance the processing, together with the solid additives, and can be mixed into a homogeneous mass and made to flow from the mixing vessel into the motor chamber, where the bore mandrel may present a complex geometric pattern.

6. Reduce fracture mechanics associated with the missile launching.

Chapter 1

1.1.3 Living/controlled radical polymerization

In order to obtain control over polymer chain architecture a so-called "living system" must be established. In a living polymerization system, the probabilities of termination and chain transfer reactions are kept to a minimum. Some of the characteristics of living polymerization are [4, 5]:

1. Polymerization proceeds until all monomer is consumed and commences again upon addition of new or more monomer.
2. Polymers with complex architectures can be synthesized.
3. Narrow molecular weight distribution is achieved.

Living polymerization has been achieved by using ionic polymerization techniques. Practical requirements for this polymerization include very stringent reaction conditions, such as high vacuum or an inert atmosphere, and the absence of water or other impurities. On the other hand, free radical polymerization is a powerful tool to synthesize polymers, where wide range of monomers can undergo radical polymerization under relatively simple conditions[4]. In addition, living or controlled radical polymerization has been successfully used to pursue some of the main goals in the development of macromolecules. For example, synthesis of polymers with well-defined chemical structures, and control of the molecular weight and low polydispersity. Literature reports many radical polymerization methods, that exhibit controlled or living characteristic, such as (I) dithiocarbamate iniferters [6, 7], (II) nitroxide-mediated processes, (III) transition metal complex-mediated atom transfer radical polymerization (ATRP), and (VI) reversible addition-fragmentation chain transfer (RAFT) [4].

Chapter 1

1.2 Aims

The following are the aims of this study:

1. Synthesize the soft segment pre-polymer, namely hydroxyl terminated poly(epichlorohydrin) (PECH-diols) and GAP-diols.
2. Convert the pre-polymer to the maro-initiator after reaction with active groups such as dithiocarbamate, both to produce block and graft copolymers.
3. Use of the macro-initiators in control free radical polymerization of acrylate or vinyl monomers to yield two different copolymers (block and graft). A schematic representation of the study methodology that was undertaken is shown in **Scheme 1.1**.
4. Chemical and physical characterization.
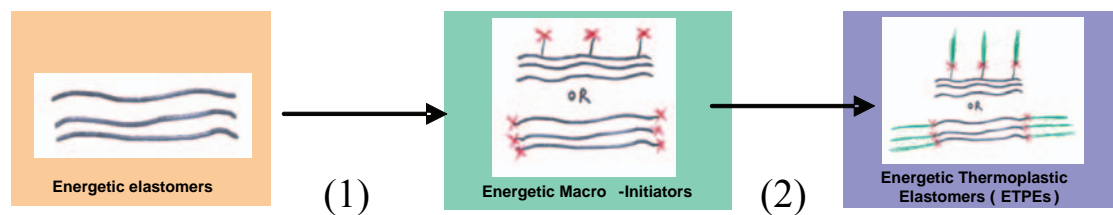
Scheme 1.1 Flow diagram of the approach followed in this work: (1) preparation of energetic macro-initiators, (2) controlled free radical polymerization in the presence of energetic macro-initiators, (3) yield of the final energetic thermoplastic elastomers binders.

1.3 Objectives

The main objective of this study is to use a novel approach based on utilizing control free radical polymerization (CFRP) to synthesize energetic thermoplastic elastomers

Chapter 1

binders. GAP was identified as suitable soft energetic segment, and poly(methyl methacrylate) (PMMA) as a thermoplastic hard segment. An energetic thermoplastic elastomers conventionally synthesized by the isocyanate cross linking of hydroxyl terminated GAP, which drawback during manufacturing and storage [2]. The objective of this study is to develop thermoplastic elastomers as energetic binder by using alternative method compared to the conventional materials.

1.4 Layout of the thesis

Chapter one presents a brief introduction to the topics and the objectives of the study. Chapter two describes the synthesis and characterization of PECH-diols produced via cationic ring opening polymerization (CROP), which will be used latter in the project.

Chapter three deals with the synthesis and characterizations of GAP-diols and conventional energetic thermoplastic elastomers based on reaction of GAP-diols with different isocyanate monomers. Synthesis was achieved via azidation reaction of PECH-diols. The preparation, and characterization, of energetic thermoplastic elastomers (ETPEs) by reaction of GAP-diols with isocyanate (IPDI) and (TDI) will also be reported. The literature review focuses on the different types of energetic binders (polymer and plasticisers) and the most important factors effecting synthesis of energetic thermoplastic elastomers via the urethane reaction.

Chapter four reports on the synthesis and characterizations of poly(methyl methacrylate-*b*-epichlorohydrin) (PMMA-*b*-PECH) and poly(methyl methacrylate-*b*-glycidyl azide) (PMMA-*b*-GAP) copolymers by using 4,4' azobis (4-cyanopentanoyl acid), where hydroxyl terminated groups of two different

elastomers were polycondensed with 4,4' azobis (4-cyanopentanoyl chloride) (ACPC) to prepare macro-azo-initiator (MAI) containing scissile –N=N– units. This macro-azo-initiator was used in the free radical polymerization of methyl methacrylate (MMA) to yield block copolymers.

Chapter five deals with the study of the miscibility of PECH-diols, GAP-diols and high molecular weight rubbery poly(epichlorohydrin) (RPECH) with PMMA and poly(styrene). The miscibility behavior of blends was examined using different analytical techniques.

Chapter six can be considered as the main part of this thesis. It presents comprehensive study for the synthesis and characterizations of poly(methyl methacrylate-*g*-epichlorohydrin) (PMMA-*g*-PECH) and poly(methyl methacrylate-*g*-glycidyl azide) (PMMA-*g*-PECH) copolymers based using *N,N*-dithiocarbamate-mediated iniferter. The preparation of poly(epichlorohydrin) and glycidyl azide polymer with pendant *N,N*-diethyldithiocarbamate groups as macro-photoiniferters was successfully carried out and the products confirmed by using different spectroscopic techniques. The synthesis of three different types of thermoplastic elastomers namely, PMMA-*g*-PECH, PS-*g*-PECH, PMMA-*g*-GAP, and PMMA-*b*-GAP copolymers based using *N,N*-diethyldithiocarbamate as macro-photoiniferters, and throughout photopolymerization, have been achieved and the final product was characterized. The literature review of this chapter reported living/control radical polymerization methods with focus on photoiniferters, especially dithiocarbamate iniferters.

Chapter seven deals with controlled radical polymerization of poly(methyl methacrylate-*g*-epichlorohydrin) graft copolymer by using RAFT polymerization. A macro-RAFT-agent was prepared by the reaction of PECH with pendant dithiobenzoate groups be used in thermal polymerization to synthesis thermoplastic elastomers.

Chapter 1

The last chapter reports about controlled radical polymerization of MMA by using *N,N*-dithiocarbamate-mediated iniferters derivatives. Four different photoiniferters namely benzyl diethyl dithiocarbamate, 2-(*N,N*-diethyldithiocarbamyl) proponic acid, 2-(*N,N*-diethyldithiocarbamyl) isobutyric acid, and epichlorohydrin-*N,N*-diethyl dithiocarbamate were synthesized and examined in the living/controlled radical polymerization of MMA. The effect of different iniferter structures on the polymer yield properties, and effect of the concentration (monomer-to-photoiniferter) was examined.

1.5 References

1. Boyars C., Klager K., Propellants Manufacture, Hazards, and Testing. Advances in Chemistry series 88, American Chemical Society 1969.
2. Gaur B., Lochab B., Choudhary V., Varma I. K., J. Macromol. Sci., Polym. Rev 2003, C43(4), 505.
3. Provatas A., Energetic Polymers and Plasticisers for Explosive Formulations-A Review of Recent Advances 2000
   www.dsto.defence.gov.au/corporate/reports/DSTO-TR-0966.**pdf** (accessed on 15/6/2004)
4. Moad G., Solomon D. H., The Chemistry of Radical Polymerization, 1st Edition, Elsevier 2006.
5. Moad G., Rizzardo E., Thany S. H., Aust. J. Chem 2005, 58, 379.
6. Sebenik A., Prog. Polym. Sci 1998, 23, 875.
7. Destarac M., Charmot D., Frank X., Zard S. Z., Macromol. Rapid Commun 2000, 21, 1035.

Chapter 2

Synthesis and characterization of poly(epichlorohydrin)diols produced via cationic ring-opening polymerization

Chapter 2

Synthesis and characterization of poly(epichlorohydrin)diols produced via cationic ring-opening polymerization

Abstract

Poly(epichlorohydrin) with hydroxyl end groups (PECH-diols) was prepared reproducibly by the cationic ring-opening polymerization (CROP) of epichlorohydrin (ECH) by using borontrifluoride etherate (BF_3-etherate) as catalyst and a low molecular weight diol as initiator. The polymerization reaction was terminated by the addition of water. Products were obtained in high yields and with low polydispersity (1.1-1.4). PECH-diols were characterized by UV, FTIR, ^{13}C-NMR and ^{1}H-NMR spectroscopy, GPC and DSC. The terminal hydroxyl groups of the polymer were characterized by derivatizing them using trifluoro acetic anhydride and analyzing the resulting ester by NMR. Both primary and secondary hydroxyl groups were present in the polymer and ^{1}H-NMR showed that about 90% of the terminal hydroxyl groups were secondary. Different diols were used in the CROP, without significantly affecting the final polymer properties.

Keywords: Poly(epichlorohydrin); cationic ring-opening polymerization; rubber degradation.

Chapter 2

2.1 Introduction and objectives

The literature review is subdivided into two main parts. The first part deals with cationic polymerization and will focus on cationic ring-opening polymerization (CROP) of cyclic monomers. The second part deals with the degradation of rubber, particularly the degradation of PECH rubber.

2.1.1 Cationic polymerization

Cationic polymerization proceeds by an addition mechanism, and comprises initiation, propagation, and termination, similar to radical reactions. **Equation 2.1** represents a typical cationic initiation reaction, where I^+ is a typical strong Lewis acid.

$$M + I^+ \rightarrow MI^+ \qquad \text{.........................} [2.1]$$

There are three groups of electrophilic initiators: classical protonic acids such as HCl, H_2SO_4, $HClO_4$; Lewis acids or Friedel-Crafts catalysts such as BF_3, $AlCl_3$, $TiCl_4$, $SnCl_4$; and carbonation ion salts [1]. Lewis acids alone are not particularly active and require a co-catalyst to act as a proton donor. Lewis acids, such as borontrifloride, usually gives a rapid reaction when trace quantities of water are present but remain dormant under anhydrous conditions (**Scheme 2.1**) [1, 2].

$$BF_3 \quad + \quad H_2O \quad \rightleftharpoons \quad H^+ BF_3 OH^-$$
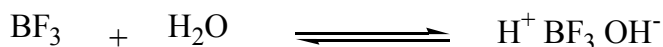
Scheme 2.1 Proposed reaction mechanism of borontrifloride with water to yield an active cationic initiator.

2.1.2 Cationic ring-opening polymerization

Cationic ring-opening polymerization has contributed to macromolecular science and polymer technology in a number of ways. The importance of cationic polymerization arises from the commercial importance of polymers that are synthesized via this method, such as poly(N-vinylcarbazole), poly(vinyl ether), polyisobutylene and its copolymer

13

Chapter 2
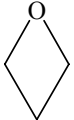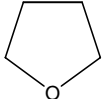
with isoprene (butyl rubber) [2]. A number of industrially important polymers are also produced by cationic ring-opening polymerization, including poly(tetramethylene glycol), poly(epichlorohydrin), poly(dimethylsiloxane), poly(ethylene imine), poly(ethylene oxide), and polytetrahydrofuran [3]. The latter was first studied by Meerwein and it has become an important product, where the α,ω-dihydroxy oligomers with $\overline{M_n}$ values ranging from 1 000 to 3 000 g/mol are used as the soft elastic segments in thermoplastic elastomers like polyurethanes (Lycra ®), polyesters (Hytrel ®), and polyamides [4].

There are several books that discuss cationic polymerization [1, 2, 5-7]. In addition, there are several review articles on this subject [4, 6, 7]. In this study the focus will be on the polymerization of the three-membered cyclic ether (oxirane) monomers via CROP. The following is a description of the important parameters affecting the cationic ring-opening polymerization of cyclic monomers.

2.1.2.1 Cyclic monomers and ring strains

The ring strain of cyclic monomers is affected by the geometry of the cyclic ethers and by the number of atoms in the ring [5]. Ring strain decreases with increasing ring size. **Table 2.1** shows the ring strain of typical, unsubstituted cyclic ethers. Three-, four-, and five-membered cyclic ethers are the most important types of cyclic ethers. They can be easily polymerized due to the strain present in the cyclic ring [5]. Ring strain of highly cyclic monomers is very low, making polymerization more difficult, and hence they are less important commercially.

Table 2.1 The ring strain of typical unsubstituted cyclic ethers [7].

Unsubstituted cyclic ether	Ring strain (kJ mol^{-1})
Oxirane (ethylene oxide)	114
Oxetane (trimethylene oxide)	107
Oxolane (tetrahydrofuran)	23

Chapter 2

2.1.2.2 Nucleophilicity or basicity of cyclic ethers

Nucleophilicity or basicity reflects the same property, namely the ability to share the lone electron pair (or pairs) with an electron acceptor and; thus, to combine with an electrophilic substrate. Linear and cyclic ethers belong to the group of weak organic bases [7]. The basicity is affected by the chemical structure, ring size and substituents. The basicity of cyclic ethers decreases as the ring strain increases (oxirane<oxetane< oxolane). Substitution affects the basicity; it is reported that methyl substitution increases the basicity, where as chloromethyl substitution decreases the basicity [7].

2.1.2.3 Polymerizability of cyclic ethers

Polymerizabililty is related to the free energy changes (ΔG_p) (**equation 2.2**) associated with a conversion of monomer molecule into polymer unit. ΔG_p of polymerization is a function of enthalpy (ΔH_p) and entropy (ΔS_p) of polymerization [2].

$$\Delta G_p = \Delta H_p - T\Delta S_p \qquad \text{.........................[2.2]}$$

The thermodynamic parameter that has the greatest effect on the polymerizability is the enthalpy of polymerization (ΔH_p). In the case of cyclic monomers this parameter is related to the ring strain. Hence, polymerization of highly strained three- and four-member cyclic ethers is practically irreversible, whereas polymerization of the five-members such as THF is reversible and a significant concentration of monomer remains in equilibrium with the growing polymer chains.

2.1.2.3.1 Initiation

The initiation of cyclic ether polymerization can be achieved by three different methods: (a) direct addition of initiator to monomer molecule (protonic acids); (b) abstraction of a hydride ion (H$^-$) from monomer (carbonation salts); and (c) formation of zwitterions between initiator and monomer (BF$_3$) [5].

Chapter 2

2.1.2.3.2 Propagation

Propagation in cyclic ether polymerization proceeds either by the active chain end (ACE) mechanism, in which active species are located at the end of the growing macromolecule, and/or by the active monomer (AM) mechanism, where the positive charge is located on the monomer and the growing macromolecule is terminated with a non-ionic nucleophilic group (e.g. HO⁻ group). **Scheme 2.2** shows a schematic representation of the two different mechanisms. The ACE and AM mechanisms may coexist in the same system [5, 7].
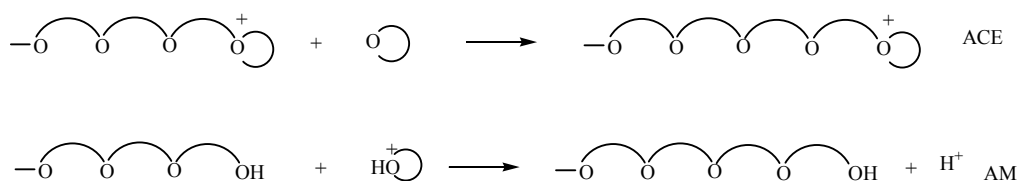
Scheme 2.2 Polymerization of a cyclic monomer may proceed by the active chain end mechanism, and/or by the active monomer mechanism.

2.1.2.3.3 Transfer and termination reactions

Transfer and termination reactions can occur as inherent features of the system or can be induced in order to introduce the desired end group. An undesirable transfer or termination reaction can be avoided, even in the presence of a certain level of impurities due to lower reactivity of oxonium ions and basic character of monomers, which make termination less critical than in vinyl polymerization [5, 7].

2.1.2.4 Copolymerization of cyclic ethers

Cyclic ethers are capable of copolymerizing with other cyclic ethers, as well as with a variety of other compounds, and extensive studies have been carried out on the copolymerization of cyclic ethers using cationic ring-opening copolymerization [6]. Saegusa *et al*. [8] reported on the copolymerization of tetrahydrofuran and epichlorohydrin using triethyl aluminum (AlEt₃) or AlEt₃.H2O, which produces block copolymers. Epichlorohydrin can be copolymerized with ethylene oxide to produce poly(epichlorohydrin-co-ethylene oxide) rubber by using AlEt₃.H₂O as an initiator.

Copolymerization of cyclic monomers leads to modified properties compared to those found in the homopolymers of certain cyclic monomers. For example, copolymerization

Chapter 2

of oxirane with four- or five-membered cyclic compounds leads to less crystalline and lower melting materials than is the case with the homopolymers of the four- and five-membered cyclic monomers [6]. On the other hand, tetrahydrofuran can be copolymerized with an energetic monomer like 3,3-bis(azidomethyl)oxetane to improve processing and modify its glass transition temperature [6]. In the cationic ring-opening polymerization of an oxirane monomer such as epichlorohydrin, utilization of a low molecular weight diol such as ethylene glycol or 1,4-butanediol as initiator usually yields a copolymer of epichlorohydrin with these diols [9]. In contrast, carrying out the CROP of ECH monomer in the presence of water yields pure poly(epichlorohydrin) [10].

2.1.2.5 Cationic ring-opening polymerization of oxiran monomers

Oxiran monomers such as ethylene oxide and propylene oxide are directly prepared by the oxidation of corresponding alkenes. On the other hand, epichlorohydrin is produced from the corresponding chlorohydrin (**Equation 2.3**) [6].

Propylene + Cl$_2$ → allyl chloride + HOCl → glycerol dichlorohydrin → epichlorohydrin .... [2.3]
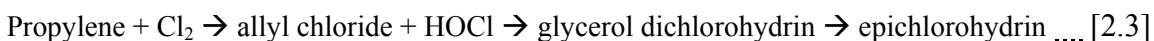
In spite of the availability of monomers, cationic polymerization of oxirans is of little industrial interest. Thus is due to the side reactions that prohibit the preparation of well-defined, high molecular weight polymers. The two important exceptions are preparation of poly(epichlorohydrin) elastomers and curing of the epoxy resins, and polymerization of epichlorohydrin in presence of low molecular weight diols to prepare reactive (telechelic) oligomers [5].

2.1.2.6 Cationic ring-opening polymerization of epichlorohydrin monomers

The microstructure of PECH obtained from CROP depends on the type of initiator employed. Literature reported three microstructures obtained from utilizing different intitators. First, cationic initiators such as Lewis acids or tertiary oxonium salts, often complexed with water, alcohol or ether, result in an atactic low molecular weight polymer ($\overline{M_n}$ <4000 g/mol) with hydroxyl end groups when polymerization is quenched with water or alcohol [9]. Second, telechelic polymers of molecular weight up to 15 000

17

Chapter 2

g/mol can be obtained where 1,4-butanediyl ditriflate is used as initiator [11]. The most important industrial method is the Vandenberg process, based on the use of organometallic initiators, which yields polymers of high molecular weight (rubber) that are often fractionated into there atactic and isotactic components [12].

2.1.4 Objectives

The major objective of the present study is to prepare PECH-diols by using CROP and understanding its synthesis conditions, microstructure, and properties to be used later in further experiments.

2.2 Experimental

Materials, equipments and methods are described in this section.

2.2.1 Materials

Epichlorohydrin monomer, borontrifluoride etherate, deuterated chloroform, trifluoro acetic anhydride, ethylene glycol, 1,4-butanediol, 1,3-propane diol, 2-methyl-2,4-pentane diol, poly(ethylene glycol), di(ethylene glycol), and glycerol were obtained from Aldrich and used without further purification. Toluene and dichloromethane were purified by standard procedures. Magnesium sulfide was obtained from Fluka and used as received. All purified solvents and diols were stored over molecular sieves. Nitrogen was dried by passing it through a calcium chloride tower.

2.2.2 Analytical equipment and methods

2.2.2.1 UV analysis

The UV spectra of polymers were recorded on a GBC UV/visible 920 spectrometer. Samples were dissolved in dichloromethane, in concentrations of 1 mg/mL.

Chapter 2

2.2.2.2 FTIR analysis

FTIR spectra of polymers were recorded with a Perkin-Elmer spectrophotometer. Samples were placed between NaCl windows. The FTIR spectra were recorded in the range from 500 to 4000 cm^{-1} using 32 scans.

2.2.2.3 NMR analysis

NMR spectra were recorded on either a 300 MHz Varian VXR spectrometer operating at 300 MHz for ^{1}H spectra and 75 MHz for ^{13}C spectra; or a 600 MHz Varian Unity Inova spectrometer operating at 400 MHz for ^{1}H and 100 MHz for ^{13}C. Standard pulse sequences were used for obtaining ^{1}H, ^{13}C, and APT spectra.

2.2.2.4 GPC analysis

The molecular weights of the polymers were determined by GPC (Waters). The GPC consisted of a Waters 717 Plus autosampler, a Waters 600E system controller (run by Millennium32 V4 software), and a Waters 610 fluid unit. A Waters 410 differential refractometer was used as a detector at 35 ^{o}C. Tetrahydrofuran (THF, HPLC grade) sparged with IR-grade helium was used as eluent at a flow rate of 1 mL/min and typically 5 mg of sample was dissolved in 1 mL of solvent for analysis. The column oven was kept at 30 ^{o}C and the injection volume was 100 μm. Two PLgel 5 μm Mixed-C columns and a pre-column (PLgel 5 μm Guard) were used. A set of narrow molecular weight polystyrene samples covering a molecular weight range of 350-3 500 000 g/mol were used as GPC standards. All molecular masses are reported as polystyrene equivalents.

2.2.2.5 DSC analysis

DSC analyses of polymer samples were performed with a TA Instruments DSC-Q100. Indium metal was used for the calibration of the instrument according to standard procedures. The analyses were carried out in a nitrogen atmosphere and 10 ^{o}C/min was used as heating rate. About 1-3 mg of sample was hermetically sealed in aluminum sample pan for analysis.

Chapter 2

2.2.3 Experimental techniques

This section is divided into four parts. The first part covers experimental techniques used to produce PECH-diols. The second part reports the experimental method used to study the effect of using different diols in the CROP. The third part describes the experimental techniques used to determine the microstructure of the final product. The last part describes the techniques applied in the degradation of rubbery PECH.

2.2.3.1 Ring-opening polymerization of epichlorohydrin.

The ring-opening polymerization of epichlorohydrin monomers was carried out according to the published procedure described by Ivin [5]. **Scheme 2.3** is a representation of the procedure followed for the cationic ring-opening polymerization of ECH monomer. In a typical experiment, the synthesis of PECH was conducted in the following manner. A clean and dry 250-mL three-necked, round-bottom flask, placed in a temperature controlled water bath, was fitted with a condenser with a calcium chloride guard tube in the top, and an efficient magnetic stirrer bar. Running reaction in closed system lead to the explosion of the reactor. An appropriate quantity of diols was dissolved in 50 mL of polymerization solvent (either toluene or dichloromethane) and the solution mixture stirred for about 15 min in order to ensure homogeneity of the mixture. A few drops of borontrifluoride etherate were added, using a glass pipette. The reaction mixture then changed from a clear, colorless liquid, into a cloudy, white liquid. The reaction mixture was stirred for another 30 min. To this mixture, ECH dissolved in 50 mL of polymerization solvent was then added dropwise over a period of 60-90 min using a dropping funnel. The reaction was carried out at room temperature for 3 hr before being quenched by adding 50 mL of distilled water and vigorously stirring for about 30 min. The resultant turbid appearance could be attributed to the lack of miscibility of the reaction mixture and water.

During addition of ECH monomers to the reaction mixture, a slight increase in the bath temperature was noticed, especially during early stages of the addition. This phenomenon could be attributed to the energy released from the opening of the epoxide ring during polymerization. The crude reaction product was transferred to a separating funnel and the organic layer washed three times with distilled water in order to remove all

Chapter 2

un-reacted monomer, diol, and brontrifluoride. The organic layer was transferred to a round-bottom flask and dried over magnesium sulfate. Finally, the organic layer and product were filtered and the solvent was removed by vacuum distillation. In order to remove of all the solvent, vacuum drying was applied to the product. Typically, the product in the round-bottom flask was heated in an oil bath at 60 °C and vacuum was applied for about 5 hours to extract most traces of solvent remaining in the product. The yield was typically about 90% or more. The final product was characterized by characterization techniques, such as UV, NMR and FTIR spectroscopy, GPC and DSC, in order to explore its properties and microstructure.
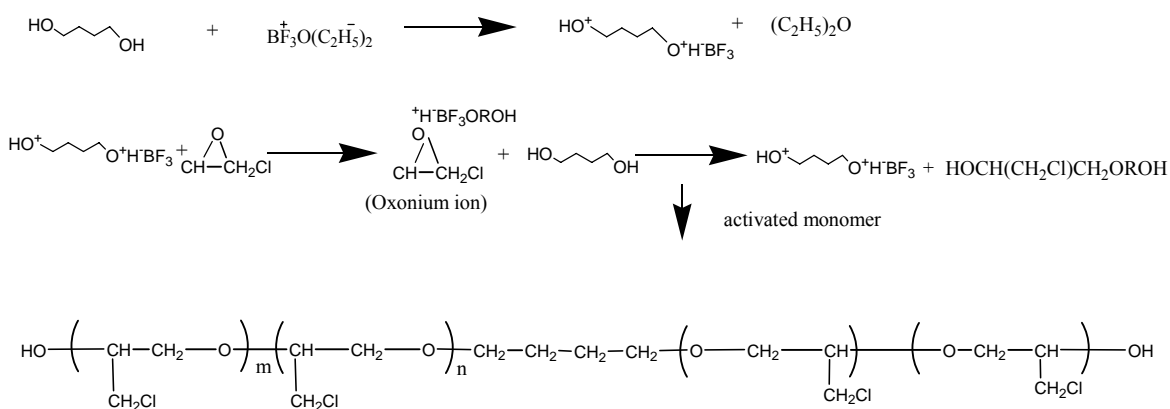
Scheme 2.3 Proposed reaction for the cationic ring-opening polymerization of epichlorohydrin in the presence of 1,4-butanediols (initiator) and brontrifloride etherate (catalyst) [10].

^{1}H-NMR (CDCl$_3$): δ= 1.64 ppm [CH$_2$ protons of 1, 4-butanediol], δ= 3.1 ppm [OH, hydroxyl group proton], δ= 3.8 ppm [CH$_2$, CH protons of polyether], δ= 3.6-4 ppm [CH, CH$_2$, CH$_2$Cl due to protons of methylene, methane, and chloromethyl units].

^{13}C-NMR (CDCl$_3$): δ= 26-26.5 and 75 ppm [–CH$_2$– of 1, 4-butanediol], δ= 43-46 ppm [chloromethyl units –CH$_2$Cl], δ= 69-71 ppm [–O–CH$_2$–], δ= 79 ppm [–O–CH–].

FTIR (NaCl): 3406 (s, –OH), 2906 (s), 2866 (s), 1428 (s), 1292 (w), 1248 (w), 1100 (s, –C–O–C–), 838 (w), 744 (s, –CH$_2$–Cl), 704 (s) cm^{-1}.

Chapter 2

GPC (THF) at 25 $^{\circ}$C: $\overline{M_n}$ = 900-1 430 g/mol and polydispersity = 1.1-1.4 based on polystyrene standards. UV spectrum did not show strong absorption in the range 200-600 nm.

2.2.3.2 Effect of diols in ECH polymerization

Different diols were used as initiators in the CROP of ECH. The same polymerization technique as described in the Section 2.2.3.1 was used. Final products were characterized by UV, FTIR and NMR spectroscopy, and GPC, in order to investigate effect of different diols on the products.

2.2.3.3 Acetalyation of PECH-diol with trifluoro acetic anhydride

The nature of the OH groups in PECH-diol obtained by CROP were investigated by the esterification reaction of OH groups by adding about 15 mg of trifluoroacetic anhydride to the NMR tube containing about 80 mg of PECH-diol dissolved in deuterated chloroform **Scheme 2.4**.
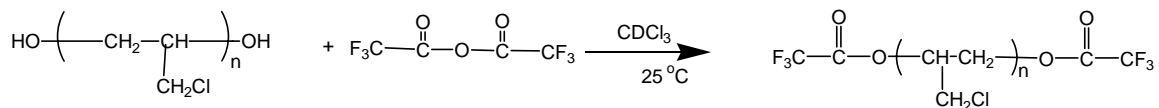
Scheme 2.4 Proposed reaction for the acetalyation of PECH-diol by using trifluoroacetic anhydride in deuterated chloroform.

2.3 Results and discussion

This section includes a description for the results obtained from the synthesis and characterizations of PECH-diols and degradation of rubbery PECH.

2.3.1 Synthesis and characterization of hydroxyl terminated poly(epichlorohydrin)

Section 2.3.1 includes results from the CROP of epichlorohydrin, the effect of using different diols, the effect of using different solvents, and a study of type of OH groups (secondary or primary) produced by acetalyation.

Chapter 2

2.3.1.1 Cationic ring-opening polymerization of epichlorohydrin

Polymerization of ECH by cationic ring-opening polymerization using a combination of brontrifluoride etherate (catalyst) and low molecular weight diol (initiator) is reported to yield polymers with low cyclic oligomer formation [5, 10]. The use of a diol also affords the possibility of producing linear telechelics, when the polymerization is terminated with an alcohol or water. In this study, polymerization of ECH proceeded to a high conversion ($\geq 90\%$) and yielded a polymer with a narrow polydispersity (1.1-1.4). A typical GPC profile of a PECH-diol is shown in **Figure 2.1**. A slight shoulder at about 20 minutes could be attributed to un-reacted ECH monomers. High yields and low molecular weight distributions (MWD) could be an indication that polymerization proceed in a reasonably controlled manner [13].
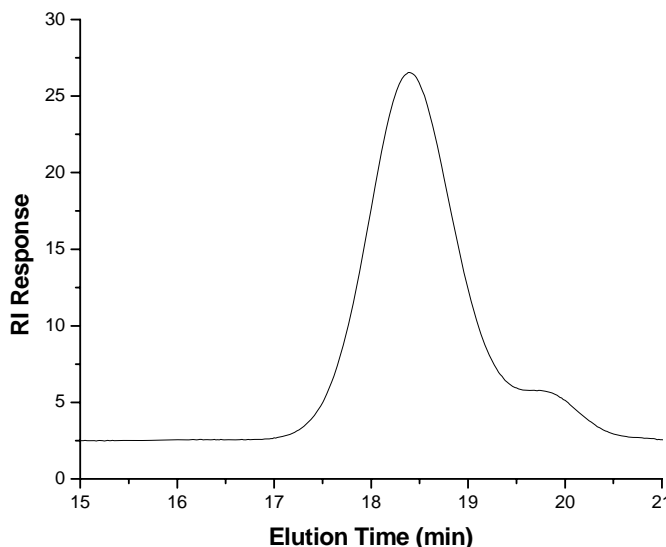
Figure 2.1 GPC trace of PECH-diols, $\overline{M_n}$ =1154 g/mol and polydispersity 1.14.

(Reaction conditions: toluene as solvent, 1, 4-butanediol as initiator, borontrifluoride etherate (BF$_3$-etherate) as catalyst, and [ECH]/[Diol]= 50).

The UV spectrum of PECH-diols is shown in **Figure 2.2**. UV spectrum did not show any absorption peak for PECH-diols in the range of 600-200 nm, which indicates that the chloromethyl pendant groups do not have strong absorption at this UV range. This result is in agreement with the literature [9, 13].

Chapter 2
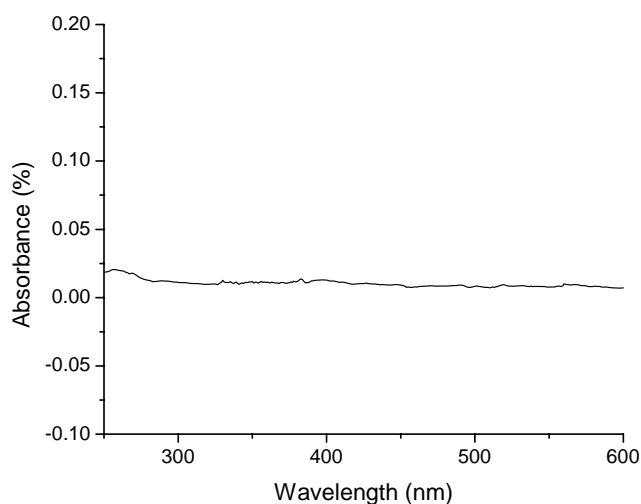
Figure 2.2 UV spectrum of PECH-diol, $\overline{M}_n$ =1154 g/mol and polydispersity 1.14.

(Reaction conditions: toluene as solvent, 1, 4-butanediol as initiator, borontrifluoride

etherate (BF$_3$-etherate) as catalyst, and [ECH]/[Diol]= 50), (Analysis conditions:

dichloromethane as solvent and sample concentration 1 mg/5 mL).

The FTIR spectrum is shown in   **Figure 2.3**. The FTIR spectrum of PECH-diols contains peaks indicative of important features of PECH-diols, namely absorption peaks at 745, and 1150 cm^{-1}, which correspond to a chloromethyl group and polyether linkage, respectively. The absorption at about 2850 and 3450 cm^{-1} could be attributed to methyl and ethyl groups and the hydroxyl groups, respectively.

Chapter 2
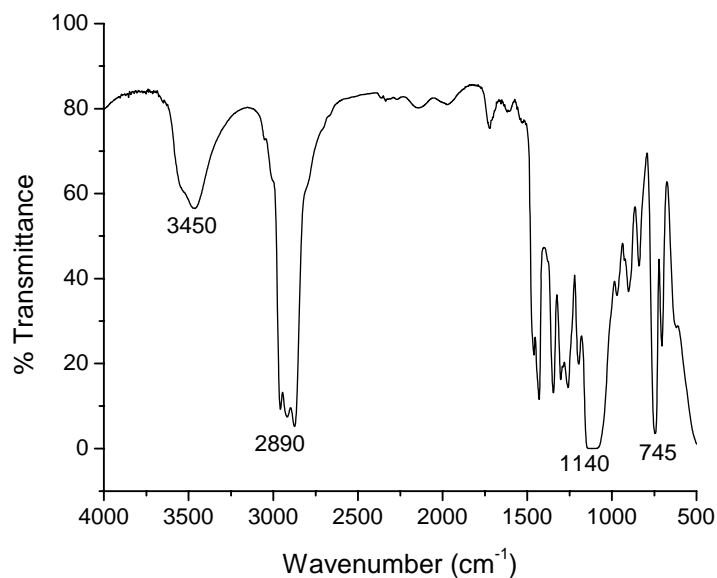
Figure 2.3 FTIR (NaCl) spectrum of PECH-diol elastomers, $\overline{M}_n$ =1154 g/mol and polydispersity 1.14. (Reaction conditions: toluene as solvent, 1, 4-butanediol as initiator, borontrifluoride etherate (BF$_3$-etherate) as catalyst, and [ECH]/[Diol]= 50).

In an attempt to understand the microstructure of PECH-diol produced via CROP, NMR analyses by using ^{1}H-NMR and ^{13}C-NMR were performed. The ^{1}H-NMR spectrum of PECH-diols is shown in **Figure 2.4**, while **Figure 2.5** shows the ^{13}C-NMR.

The most important features of ^{1}H-NMR spectrum are the signals at about 1.6 and 3.1 ppm, which correspond to the CH$_2$ protons of the 1, 4-butanediol included in the PECH-diol, and the hydroxyl group proton, respectively. The peaks between 3.6 and 4 ppm correspond to the PECH protons. The assignments of the PECH-diol structure are illustrated in Figure 2.4.

Significant peaks of ^{13}C-NMR spectrum of PECH-diol are at about 26-26.5 and at 75 ppm. These peaks correspond to the CH$_2$ of the 1, 4-butanediol. Peaks at about 43-46 ppm are attributed to the chloromethyl group of PECH. The polyether linkage –O–CH$_2$– peaks appear at about 69-71 ppm. On the other hand, solvent absorption appears at 77 ppm and peak at about 79 ppm is attributed to the –O–CH–. The assignments of PECH-diol structure are indicated in Figure 2.5.

25

Chapter 2
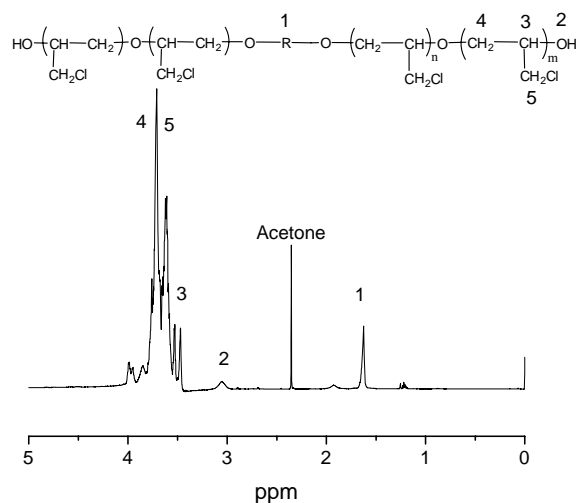
Figure 2.4 ^{1}H-NMR (CDCl$_3$) spectrum of PECH-diols, $\overline{M_n}$ =1154 g/mol and
polydispersity 1.14. (Reaction conditions: toluene as solvent, 1, 4-butanediol as initiator
(R), borontrifluoride etherate (BF$_3$-etherate) as catalyst, and [ECH]/[Diol]= 50).
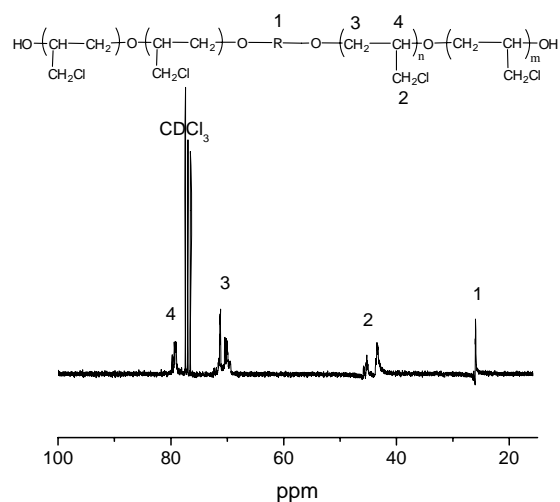
Figure 2.5 ^{13}C-NMR (CDCl$_3$) spectrum of PECH-diols, $\overline{M_n}$ =1154 g/mol and
polydispersity 1.14. (Reaction conditions: toluene as solvent, 1, 4-butanediol as initiator
(R), borontrifluoride etherate (BF$_3$-etherate) as catalyst, and [ECH]/[Diol]= 50).

The PECH-diols are colorless, viscous liquids with a glass transition temperature (T$_g$)
below room temperature. The thermal analysis of PECH-diol by using DSC was

Chapter 2

performed and **Figure 2.6** shows the result. The PECH-diol shows a single glass transition temperature at about -37 °C, which is in agreement with the literature [9].
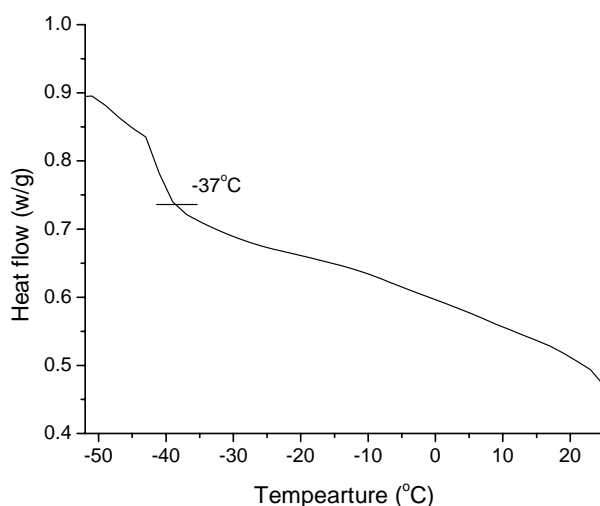
Figure 2.6 DSC thermal analysis curve of PECH-diols, $\overline{M_n}$ =1154 g/mol and polydispersity 1.14.

These results show that polymerization of poly(epichlorohydrin) via cationic ring-opening polymerization using brontrifluoride etherate (catalyst) and 1,4 butanediols (initiator) was successful, and reproducible. The yield (>90%), polydispersity (1.1-1.4), and an absence of cyclic oligomer formation indicate that polymerization followed the activated monomer (AM) mechanism as reported previously [5, 10, 14, 15]. The cationic polymerization of epichlorohydrin without a diol is reported to yield a wide range of products with varying molecular weights [4, 10].

2.3.1.2 Effect of using different types and concentrations of diols on epichlorohydrin polymerization

Different diols were applied in the CROP of ECH. **Table 2.2** shows the $\overline{M_n}$ and PDI of PECH yielded when different types of diols and different [monomer]/ [initiator] ratios used. Generally, the number average molecular weight was ranged from 1000-2000 and the polydispersity from 1.1-1.4, while product yield was ranged from 90-95%. There was no real effect when the monomer/initiator ratio was changed. This could be attributed to the active chain end [10]. The polymerization reactions at lower temperatures (by using

27

Chapter 2

ice bath) did not affect the molecular weight of the products. Changing the type of diol used in the ring-opening polymerization had a slight effect on the $\overline{M_n}$ and PDI. The PECH produced by the reaction when glycerol was used has the lowest PDI (1.09), which could be attributed to the high number of hydroxyl groups in the glycerol. The values of $\overline{M_n}$ were all under 2 000 g/mol and the color of elastomer produced ranged from colorless to yellow due to the complex of BF_3.

Table 2.2 Results of ECH polymerization in the presence of different diols and different [monomer]/[initiator] ratio.[*]

Run number	[ECH]$_o$, mol.L^{-1} (1×10^2)	Type of Diol	[Diol]$_o$, mol.L^{-1} (1×10^2)	Monomer/initiator ratio	Yield (%)	$\overline{M_n}$	PDI
1	6.39	EG	0.537	11	90	1285	1.18
2	12.78	EG	0.537	23	92	1477	1.21
3	6.39	BU	0.127	50	94	1144	1.14
4	12.78	BU	0.127	114	93	1830	1.44
5	6.39	1,3-PR	0.345	18	91	1386	1.18
6	12.78	1,3-PR	0.345	37	90	1420	1.22
7	6.39	MP	0.391	16	95	1392	1.21
8	12.78	MP	0.391	32	94	1363	1.25
9	6.39	PEG(200)	0.281	22	93	1442	1.37
10	12.78	PEG(200)	0.281	45	89	1664	1.44
11	6.39	DEG	0.233	27	94	1614	1.34
12	12.78	DEG	0.233	54	91	1707	1.42
13	19.179	Gly	0.678	28	93	1981	1.09

[*]

- Polymerization conditions: Slow addition of ECH, catalyst BF_3, toluene used as solvent toluene.
- Analysis conditions: in THF and at 25 °C
- EG, ethylene glycol; BU, 1,4-butanediol; 1,3-PR, 1,3-propandiol; MP, 2-methyl-2,4-pentandiol; PEG, polyethylene glycol; DEG, di(ethylene glycol); Gly, glycerol.

Chapter 2

To evaluate the effect of each diol used on the microstructure of PECH-diol the products were analyzed by a number of different analytical techniques, including FTIR, UV, ^{1}H-NMR and ^{13}C-NMR spectroscopy. Strictly speaking, the UV and FTIR spectra did not show any difference when different diols were used. An example of the UV and FTIR spectra of a PECH-diol are shown in Figure 2.2 and Figure 2.3, respectively. This result is in agreement with the results reported in the literature for the same system [9, 13]. DSC analysis also did not show any significant difference between different diols used in CROP, an example of a DSC measurement can be seen in Figure 2.6. T_g values (measurement based on the mid point) were in the range from -25 °C to -43 °C.

NMR was the only technique that was able to discriminate between the PECH-diols produced by different diols. **Figures 2.7** and **2.8** show the ^{13}C-NMR spectra of PECH-diols obtained using ethylene glycol (EG) and 2-methyl-2-4-pentandiol as diol, respectively.
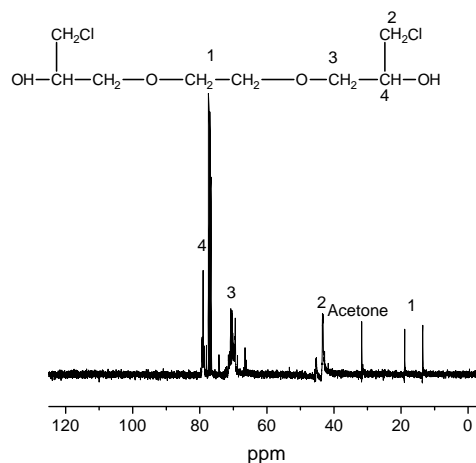
Figure 2.7 ^{13}C-NMR (CDCl$_3$) of the PECH-diols obtained by using EG as an initiator. (Polymerization conditions: borontrifluoride etherate (BF$_3$-etherate) as catalyst, toluene as solvent, and [ECH]/[Diol]=23.)

29

Chapter 2
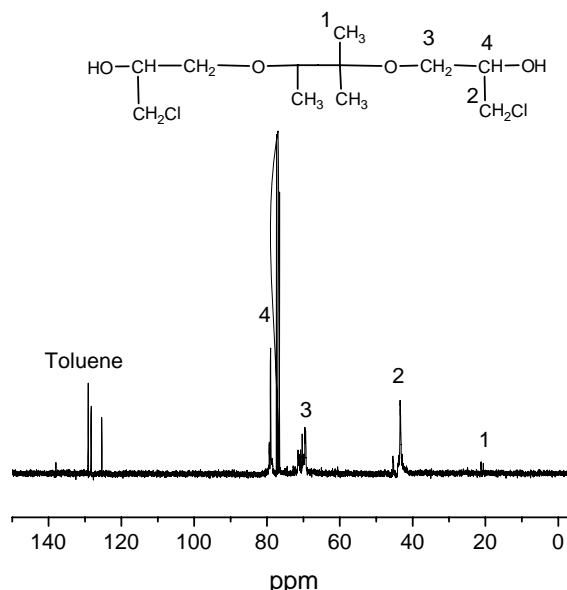
Figure 2.8 ^{13}C-NMR (CDCl$_3$) of the PECH-diols obtained by using 2-methyl-2-4-pentandiol as an initiator. (polymerization conditions: borontrifluoride etherate (BF$_3$-etherate) as catalyst, toluene as solvent, and [ECH]/[Diol]=32.)

The most important feature of the ^{13}C-NMR spectra were the PECH peaks. The most common peaks observed were for the chloromethyl group (CH$_2$Cl), the methyl group (CH$_2$), and the ethyl group (CH), which appear at about 45, 71, and 79 ppm, respectively. When PEG-200 and diethyl glycol were used as initiators, there were no peaks detected in the range 10-25 ppm. When 2-methyl-2-4-pentanediol was used as an initiator there was a peak at about 17 ppm, which could be attributed to the methyl (CH$_3$) group.

2.3.1.3 Effect of using different solvents

The use of either toluene or dichloromethane had a very little effect on the product. However, when DCM was used as reagent, viscosity increased to such an extent that stirring with a magnetic stir bar was no longer possible.

2.3.1.4 Nature of terminal hydroxyl groups

The presence of OH terminal groups was proved by using FTIR and NMR spectroscopy. This result was expected due to the use of a low molecular weight diol as initiator and termination of polymerization with water, which is reported to yield linear telechelic

Chapter 2

polymers with OH terminated groups [10]. It is reported that two types of end-groups (secondary and primary) can be present in PECH-diols obtained by CROP when a low molecular weight diol is used as initiator and boron trifloride etherate as catalyst [10, 17]. In order to study the nature of PECH-diols end groups, the hydroxyl groups were esterified using trifloro acetic anhydride $(CF_3CO)_2O$. The esterfication reaction was carried out in a NMR tube that contained a solution of PECH-diol in CD_3Cl, and ^{1}H-NMR spectra were recorded. A typical ^{1}H-NMR spectrum of PECH after esterification is shown in **Figure 2.9**. Protons of the esterified secondary groups give the expected quintuplet at about 5.34 ppm (shown in detail in the upper-left corner of Figure 2.9). Protons of the primary groups give a multiplet at about 4.45-4.6 ppm. Integration shows that the ratio of the primary to secondary hydroxyl groups in the polymer is about 91% secondary hydroxyl groups and about 9% primary hydroxyl groups. This result is in agreement with literature [10, 17].
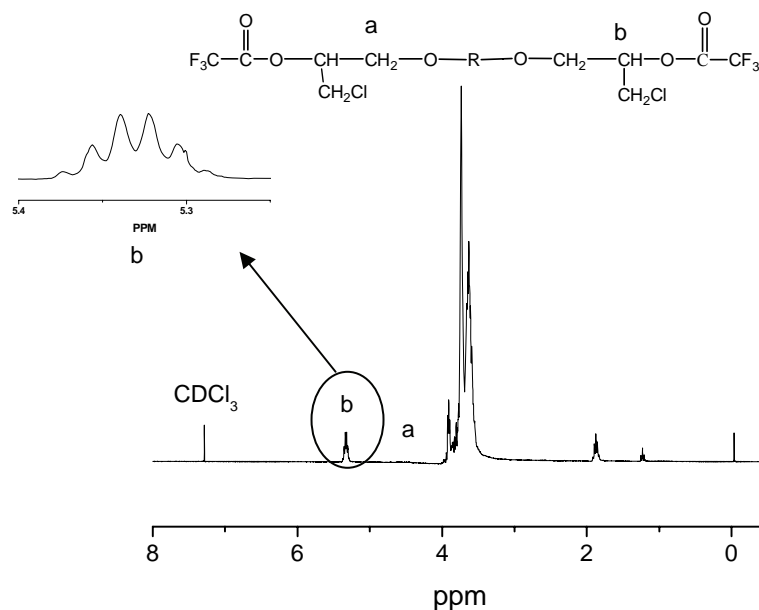
Figure 2.9 ^{1}H-NMR ($CDCl_3$) spectrum of PECH-diols, after esterification with trifloro acetic anhydride. (Reaction conditions: toluene as solvent, 1, 4-butanediols as initiator, borontrifluoride etherate (BF_3-etherate) as catalyst, and [ECH]/[Diol]= 50.)

31

Chapter 2

2.4. Summary

The main objective of this part of the study was achieved by applying cationic ring-opening polymerization of ECH monomers in reactions, using low molecular weight diols as initiator and BF_3 etherate as catalyst to yield PECH-diols. The products were characterized by using different characterization techniques such as GPC, UV, FTIR, proton and carbon NMR, and DSC. The molecular weight of the polymer was in the range 1 000-2 000 and its polydispersity index in the range 1.1-1.4, based on polystyrene standards. The UV spectrum of PECH-diols did not show strong absorption in the range 600-200 nm. FTIR spectrometer showed the most important feature of PECH-diols such as chloromethyl group 745 cm^{-1}, polyether linkage 1110 cm^{-1}, and hydroxyl group 3400 cm^{-1}. The most important feature of ^{1}H-NMR spectrum was the intensity at about 1.6, 3.1, and 3.6-4 ppm, which corresponds to the CH_2 of diols, hydroxyl group proton, and chloromethyl unit, respectively. ^{13}C-NMR spectrum showed intensity at about 26, 45, and 70 ppm, which corresponds to the CH_2 of the 1, 4-butanediols, chloromethyl group of PECH, and methylene, respectively. The thermal analysis by using DSC showed single glass transition temperature at the range (-41 to -25 ^{o}C). The nature of PECH-diols end groups have been studied after esterfication reaction of hydroxyl groups with trifloro acetic anhydride. ^{1}H-NMR spectrum measurement of trifluoro acetyl derivatives of polymer found about 91% secondary hydroxyl groups and about 9% primary hydroxyl groups. Effects of different reaction conditions such as temperature, diols type, monomer/diols ratio, and solvent on the product have been investigated. Using different diols and different [monomer]/[Diol] ratio in the CROP of ECH monomer did not form a significant difference in the polymerization yield and product properties such as molecular weight and glass transition temperature. Thus PECH diols were successfully produced and will be utilized in the next phase of the study.

Chapter 2

2.5 References

1. Cowie J. M. G., Polymers: Chemistry & Physics of Modern Materials, 2nd Edition, Chapman and Hall 1991, Chapter 4, 83-8

2. Matyjaszewski K., Cationic Polymerizations Mechanisms, Synthesis, and Applications, Marcel Dekker. INC 1996, 46.

3. Tsukamoto A., Vogl O., Prog. Polym. Sci 1971, 3, 199.

4. Penczek S., J. Polym. Sci., Part A: Polym. Chem 2000, 38, 1919.

5. Ivin K. J., Sagusa T., Ring Opening Polymerization, Elsevier 1984, 185.

6. Dreyfuss P., Dreyfuss M. P., Comprehensive Polymer Science, The Synthesis, Characterization, Reactions & Applications of Polymer, Cationic Ring-opening Polymerization: Copolymerization. 1st Edition, Pergamon Press 1989, Vol. 3, 851.

7. Penczek S., Kubisa P., Comprehensive Polymer Science, The Synthesis, Characterization, Reactions & Applications of Polymer, Cationic Ring-Opening Polymerization: Ethers. 1st Edition, Pergamon Press 1989, Vol. 3, 813.

8. Saeusa T., Ueshima T., Mai H. I., Furukawa J., Mackromol. Chem 1964, 79, 221.

9. Mohan Y. M., Raju M. P., Raju K. M., J. Appl. Polym. Sci 2004, 93, 2157.

10. Biedron T., Kubisa P., Penczek S., J. Polym. Sci. Part A: Polym. Chem 1991. 29, 619.

11. Kim C. S., Kuo L., Fish R., Russell J., Curb P., Immoos J., Macromolecules 1990, 23, 4715.

12. Brochu S., Ampleman G., Macromolecules 1996, 29, 5539.

13. Ito K., Usami N., Yamashita Y., Polym. J 1979, 11(2), 171.

14. Yugci Y., Serhatli I. E., Kubisa P., Biedron T., Macromolecules 1993, 26, 2397.

15. Murali M. Y., Raju M. P., Raju K. M., Int. J. Polymer. Mater 2005, 54, 651.

16. Frankel M. B., Grant L. R., Flanagan J. E., J. Propul. Power 1992, 8, 560.

17. Francis A.U., Venkatachalam S., Kanakavel M., Ravindran P. V., Ninan K. N., Eur. Polym. J 2003, 39, 831.

18. Hesse M., Meier H., Zeeh B., Spectroscopic Methods in Organic Chemistry, Georg Thieme Verlag 1997, 29-45.

Chapter 3

Synthesis and characterization of hydroxyl terminated glycidyl azide polymer and energetic thermoplastic elastomers

Chapter 3

Synthesis and characterization of hydroxyl terminated glycidyl azide polymer and energetic thermoplastic elastomers

Abstract

In an effort to comply with insensitive munitions (IM) criteria, energetic binders comprising polymers and plasticizers are being used in cast-cured polymer bonded explosives and cast composite rocket propellants. Energetic binders such as glycidyl azide polymer (GAP) maintain the overall energy of explosive formulations or improve their performance. Glycidyl azide polymer with terminal hydroxyl groups (GAP-diols) were synthesized by the reaction of hydroxyl terminated poly(epichlorohydrin) (PECH-diols) with sodium azide in organic solvent. The GAP-diols obtained were characterized by using different analytical techniques. Conversion of the chloromethyl groups of PECH-diols to azide groups was confirmed using FTIR and NMR spectroscopy. Thermal analysis using DSC showed a single glass transition temperature at about -45 $^{\circ}$C and exothermic decomposition at about 242 $^{\circ}$C. FTIR spectroscopy confirmed the formation of energetic thermoplastic elastomers from the reaction of GAP-diols with isophorone diisocyanate (IPDI), and toluene diisocyanate (TDI). The thermo mechanical properties of an energetic thermoplastic elastomers and the effect of the NCO/OH ratio were investigated using DMA.

Chapter 3

3.1 Introduction and objectives

The high vulnerability of ammunitions during storage and transportation represents a high risk hazard, especially for the people dealing with it. Besides the safety issue, high performance, low vulnerability, reliability, environmental aspects, and reduced costs of compositions are important requirements in the design of future weapon systems. In the past, high performance was always the main requirement in the field of research and development of ammunitions and weapon systems until 30 years ago when the US Navy started a new program under the title of insensitive munitions (IM) [1]. This was in reaction to high profile accidents on the USN aircraft carriers such as Oriskany, Forrestal, and Enterprise. These accidents and others around the world, required ammunition and weapon designers to take into account, not only the performance of munitions, but also their vulnerability to accidental ignition. However, in the early days of IM, the requirement for performance was not secondary to the requirement for insensitivity, and there was concern that it might not be possible to achieve insensitivity, desirable though it might be, without sacrificing performance. The IM definition has today become, "Munitions which reliably fulfill their performance, readiness and operational demand, but which minimize the probability of inadvertent initiation and severity of collateral damage to weapon platforms, logistic systems and personnel" [2, 3].

Several approaches are available to provide IM solutions, including weapon design, mitigation devices, packaging, use of intrinsically less sensitive explosive, and use of polymeric materials with explosives and propellant formulations. The last approach shows high promise due to many reasons such as flexibility, ease of modification, and low price of polymeric materials [1]. It is important to mention here that, modifying ammunitions formulation with plastic materials reduces the crack formation and

Chapter 3

propagation due to the ductility of polymers and their ability to absorb the energy. The main source of cracks is associated with the high load generated during the launch of missiles. This damage will not only degrade the mechanical properties of explosives, but also influence the shock sensitivity, combustion and even detonation of explosives [4, 5].

IM ammunitions could reduce the number of the dead and the injured, which is very difficult to be quantified in financial terms. For this reason, there is strong motivation and inspiration in developing these new ammunition systems all round the world. There are many research centers around the world working in developing new binder systems such as DERA in UK, SNPE Propulsion in USA, Fraunhofer-Institut in Germany, and Defense Research Establishment Valcartier (DREV) in Canada.

3.1.1 Polymeric binders for insensitive ammunitions

Polymeric binders are used to reduce the sensitivity of energetic crystals by desensitization of high explosives [3, 4]. This is usually achieved by coating the crystals with polymeric binders. A desensitization to mechanical and thermal stimuli in high explosives such as RDX and HMX leads to an increase in safety, in terms of handling, storage, and production of these materials [5]. Since the performance of explosives should not be affected by the coating, only a small amount of inert material should be used. Good polymeric binder should have good adhesion with high explosives, shows good thermal and mechanical properties, and has a low sensitivity to high explosives [3].

A binder could be a cross-linked polymer that provides a matrix that binds the explosive ingredients together with a plasticizer. The plasticizer is added not only to facilitate processing, but also to improve the mechanical properties of the final formulation, such as the glass transition temperature (T_g) and resistance to crack formation and growth. After the curing process, the binder is a rigid and tough

Chapter 3

elastomeric rubber capable of dissipating and absorbing energy from hazardous stimuli [1]. One of the first binders used in energetic materials was a mixture of nitrocellulose and nitroglycerine [4]. The nitrocellulose thickened the nitroglycerin and reduced the impact and friction sensitivity of the propellant [5]. Currently, the favored practice is the encapsulation of the explosive in a binder composed of a polymer such as hydroxyl terminated polybutadiene (HTPB) and glycidyl azide polymer (GAP), which is usually cross-linked with isocyanates and plasticized with standard plasticizers compounds, such as dioctyl adipate (DOP), or energetic plasticizers like 2-nitro-diphenylamine (2-NDPA). The final binder produces a tough, yet flexible, three-dimensional network. **Table 3.1** shows types of propellants based on different binders used in the formulation.

Table 3. 1 Propellant types based on different binders used in the formulation [4].

Propellant type	Binder
Single based propellant	Based on pure nitrocellulose
Double based propellant	Nitrocellulose plasticized with nitroglycerin
Triple based propellant	Nitrocellulose + nitroglycerin + nitroguanidine
Seminitramine propellants	Nitrocellulose + nitramine + energetic plasticizers
LOVA* propellants with inert binder	Nitramine + binder (HTPB) + plasticizers
LOVA propellants with energetic binders	Nitramine+ binder (GAP)+ plasticizer

* LOVA low vulnerability ammunition.

The use of polymeric binders is however not limited to the propellants; it has also been found in applications in the explosives formulations. When an explosive is blended with a plastic, it is known as plastic bonded explosives (PBXs). These are powdered explosives to which plastic or polymeric binders have been added. The

Chapter 3

binder is usually precipitated out of a solution in the preparation process such that it coats the explosive crystals. Agglomerates of these coated crystals form a material for pressing. The beads are then either die pressed or isostatically pressed at temperatures as high as 120 $^{\circ}$C and pressure ranging from 10 000 to 20 000 psi (pounds per square inch) to produce pellets or billets with densities as high as 97% of the theoretical maximum density (TMD). The pellets/billets produced have good mechanical strength and can be machined to very close tolerances [2, 3].

Generally, there are two different types of polymeric binders used in this field. The first type is an inert binder, and the second is an energetic binder. Both, inert polymers and energetic polymers can be used as binders in low vulnerability gun propellants, high impulse rocket propellants, elastomer modified double-base propellants and high energy PBXs. The following is a description of binders (inert/energetic) used in the in ammunition filed.

3.1.1.1 Inert polymeric binders

Different types of inert binders can be used for propellants, explosives, and pyrotechnics for example HTPB. All inert binders have the same disadvantage namely they reduce the overall energy output of the final formulations. Inert binders do have many advantages, such as improving the processing ability and reducing the variability. However, inert binders do need to meet certain requirements in order to be used in propellant formulations. The first requirement is being processable below 120 $^{\circ}$C, which is the instability temperature of many ingredients in propellant systems, particularly the energetic plasticizers and oxidizer particles. The second requirement is that all thermoplastic elastomers used in propellant compositions have good miscibility and compatibility with the remaining ingredients of a propellant system, particularly the energetic plasticizers [6]. The following is a brief description of some polymeric binders utilized as inert binders [7, 8].

Chapter 3

3.1.1.1.1 Hydroxyl terminated polybutadiene

Hydroxyl terminated polybutadiene **(1)** is a very popular polymeric binder and used to encapsulate the explosive and make propellant formulations. There is world wide acceptance in missile and launched vehicle technology for the use of HTPB as binder in propellants and explosive compositions because of its excellent physical properties, high temperature properties, low viscosity, commercial availability, and it provides a good reduction of vulnerability [4]. HTPB is usually cross-linked with isocyanates via a urethane reaction to form the final binder system, and then plasticized with DOA. However, inertness is considered as the main drawback of HTPB. It is responsible for a reduction in the overall energy output of the final formulations. Currently, HTPB is used in different fields, such as propellants, PBXs, and pyrotechnics [1, 4, 9].

$$HO \left(CH_2-CH=CH-CH_2 \right)_x OH$$

(1)
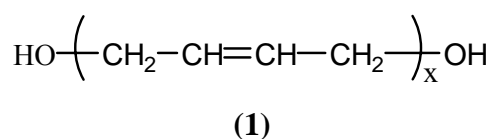
3.1.1.1.2 Ethylene-vinyl acetate copolymer

Ethylene-vinyl acetate (EVA) copolymer **(2)** is another example of an inert binder employed in the same field. It consists of two different segments, where the ethylene (hard segment) constitutes about 60% and vinyl acetate (soft segment) constitutes about 40%. It is usually processed by mixing with the rest of formulation by casting in organic solvents.

$$\left[CH_2CH_2 \right]_n \left[\begin{array}{c} CH_2-CH \\ | \\ OCOCH_3 \end{array} \right]_m$$

(2)
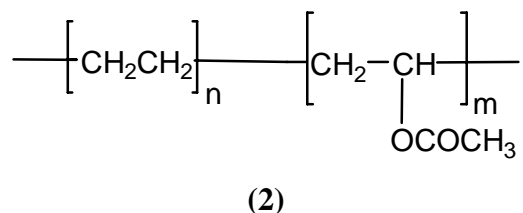
Chapter 3

3.1.1.1.3 Polyvinyl alcohol

Poly(vinyl acetate) (3A) and poly(vinyl alcohol) (PVA) **(3B)** have been used successfully as binders for pyrotechnic compositions for many years [4]. The main challenge associated with these binders is recycling. The advantages of the PVA are good mechanical properties; it is easily plasticized, can be produced in water, resistant to most solvents, not toxic, and had good stability in the dry state.

$$\begin{matrix} & & \\ \left[CH_2{-}CH \right]_n & & \left[CH_2{-}CH \right]_n \\ | & & | \\ OCOCH_3 & & OH \\ \textbf{(3A)} & & \textbf{(3B)} \end{matrix}$$
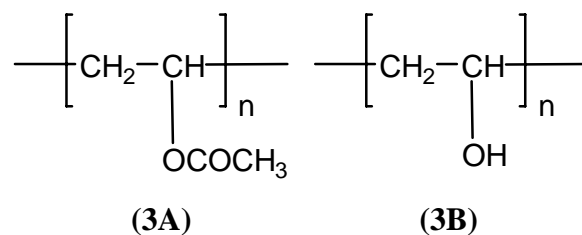
3.1.1.1.4 Cellulose acetate butyrate

Cellulose acetate butyrate (CAB) **(4)** is a modified natural polymer. It is produced by the modification of cellulose with a mixture of acetic and butyric acid. In addition, cellulose acetate (CA) **(4)** is also used as a propellant fuel.
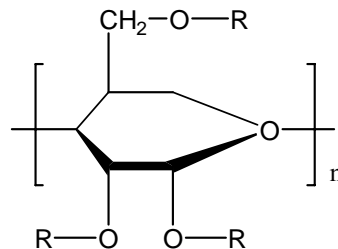
R for CA: $-OCC_2H_5$
R for CAB: $-OCCH_3$ and $-OCC_3H_7$

(4)

Chapter 3

3.1.1.1.5 Styrene-butadiene-styrene block copolymer

Styrene-butadiene-styrene (SBS) **(5)** is manufactured by emulsion polymerization [10]. The presence of styrene (hard block) and butadiene (soft block) makes these copolymers thermoplastic elastomers, which can be processed by conventional thermoplastic processing methods.
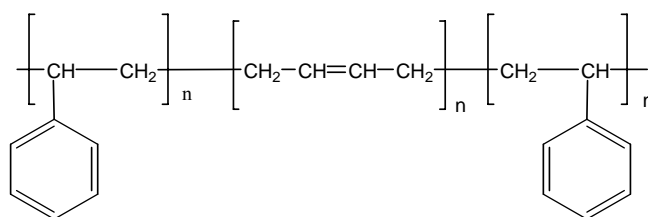
(5)

3.1.1.2 Energetic polymeric binders

In the final formulation a polymeric binder needs to be good a matrix for different components. For that, an appropriate quantity of polymeric binder needs to be used. In the case of inert binders, designers attempt to use a minimum of binder because it will reduce the overall energy output. In contrast, in the case of energetic binders, a higher amount of binder can be used, and the binder will contribute positively to the overall energy output. There are different types of energetic binders used in propellant and explosives formulations. Nitrocellulose is the oldest type of energetic binder used. Single-base propellants are essentially pure nitrocellulose (see Table 3.1) [3]. There are two types of energetic binders, based on the energetic groups. The first type is based on a nitro group, where a hydroxyl group is converted to a nitro via a nitration reaction. Examples of this type of energetic binders are nitrocellulose, nitroglycerine, nitrated hydroxyl terminated polybutadiene, polyvinyl nitrate, polynitropolyphenylenes, poly(3-nitratomethyl-3-methyloxetane) and poly(glycidyl nitrate). The second type of energetic binder is based on an azido group, such as

Chapter 3

poly(3-azidomethyl-3-methyl oxetane) and glycidyl azide polymer. The following is a brief description of some of these energetic binders.

3.1.1.2.1 Nitrocellulose

Nitrocellulose (NC) **(6)**, produced from nitration reaction of cellulose, is probably the first type of energetic binder that was utilized and is still used in gun propellants and double-base rocket propellants today [11]. Nitrocellulose has several advantages, even if its stability and vulnerability is inferior to there of nitramine propellants. The reason to its advantages is that NC combines two very important properties; it exhibits explosive character together with the properties of a polymeric molecule. Further, its mechanical properties which make it possible extrude or press together with plasticizers and other compounds in any given form. This gives the possibility to adjust the burning behavior throughout the adjustment of propellant shape as burning rate affected by shape of propellants pellets [4].
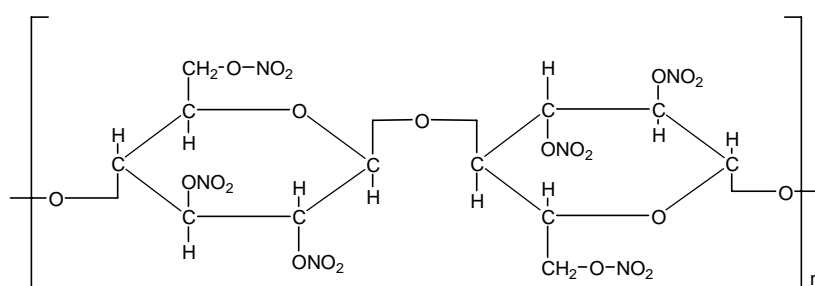
(6)

3.1.1.2.2 Polynitropolyphenylene

Poly(nitropolyphenylene) (PNP) **(7)** is a thermostable, amorphous polymer of relatively low molecular weight (200 g/mol). It is synthesized by Ullmann's reaction, by reacting m-dichlorotrinitrobenzene (styphnyl chloride) and copper powder in

Chapter 3

nitrobenzene [3]. PNP does not melt, and is coated onto fillers by an acetone-ethanol solution. It is used as a heat resistant binder for propellants.
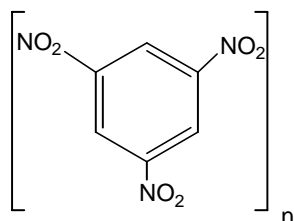
(7)

3.1.1.2.3 Polyvinyl nitrate

Polyvinyl nitrate (PVN) is prepared by the controlled addition of cooled nitric acid to a pre-cooled suspension of polyvinyl alcohol in acetic anhydride, and subsequent processing of the reaction product (**Scheme 3.1**). The energetic value of PVN depends on the % N, which depends on $-ONO_2$ groups, achieved by the nitration process. PVN has the disadvantages of low thermal stability, but like other nitrate polymers, the addition of stabilizers such as carbamite and resorcinol improves its thermal stability [12].
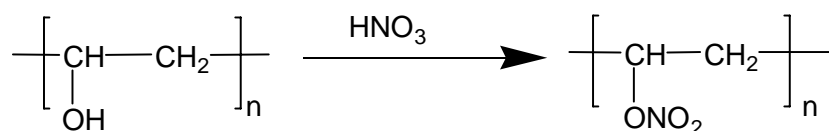
Scheme 3.1 Proposed reaction for nitration of polyvinyl alcohol.

3.1.1.2.4 Poly(3-nitratomethyl-3-methyl oxetane)

Poly(3-nitratomethyl-3-methyl oxetane) (polyNIMMO) **(8)** was developed to be used in polymer bonded explosives and for rocket propellants [3]. It is an energetic polymer, which is used to bind explosive crystals and increase the explosives performance, without compromising its vulnerability to accidental initiation. Poly(NIMMO) consists of a nitrated ester group and an ether linkage. 3-

44

Chapter 3

nitratomethyl-3-methyl oxetane (NIMMO) monomer is synthesized by the selective nitration of the hydroxyl group present in 3-hydroxymethyl-3-methyloxetane (HIMMO), using N_2O_5. The nitrated monomer is polymerized by cationic polymerization to yield a poly(NIMMO) as pale yellow viscous liquid [3, 9]. Poly(NIMMO) has a glass transition temperature at about -25 ^{o}C [3]. The main drawback associated with poly(NIMMO) is its relatively low thermal stability, with decomposition starting at about 170 ^{o}C. This is mainly attributed to the formation of a carbonyl group [13]. Another disadvantage associated with the poly(NIMMO) is that structural changes occur easily, when it is subjected to gamma radiation, especially in halogenated and aromatic solvents [14]. This low stability is attributed to the nitrate esters, which are known to degrade naturally with time by the process that is accelerated by heat and/or light. Akavan et al. [15], have reported that poly(NIMMO) undergoes degradation by three different mechanisms, namely hemolytic scission of the $O-NO_2$ bond, scission of the polyether backbone and cross-linking of the polymer chains when it subjected to high temperature or UV radiation at ambient temperature.

(8)
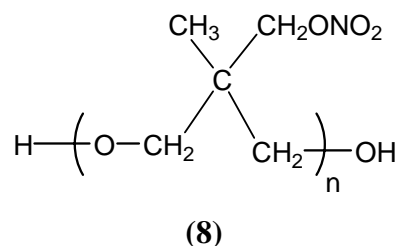
3.1.1.2.5 Nitrated hydroxyl terminated polybutadiene

The synthesis of nitrated hydroxyl terminated polybutadiene (NHTPB) **(9)** synthesized based on the epoxidation of HTPB with acid as the epoxidation reagent in dichloromethane solution. The epoxidized groups then react with N_2O_5 to give a polymer with dinitrate ester groups. NHTPB has many advantages, such as a low T_g

Chapter 3

and acceptable thermal stability. It can also be cured with aliphatic or aromatic diisocyanates [2, 3].

(9)
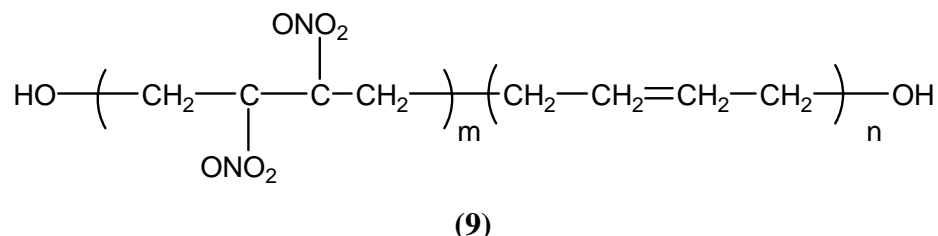
3.1.1.2.6 Glycidyl nitrate

Glycidyl nitrate (GLYN) monomer is prepared by the nitration of glycidol, and it is polymerized to give a hydroxyl terminated prepolymer (**Scheme 3.2**). Poly(GLYN) functions as plasticiser or binder. It is cross-linked by a urethane reaction, where curing with isocyantes leads to the formation of poly(GLYN) rubbers. Poly(GLYN) with molecular weight up to 4 400 g/mol, density 1.39 g/cm^3 and T_g about -35 ^{o}C can be produced from glycidyl nitrate monomers throughout cationic ring-opening polymerization (CROP) in the presence of an excess of low molecular weight diol, such as 1,4-butane diol [16]. It contains about 45 wt% oxygen, which increases its oxygen balance [17].

Although GLYN was first manufactured in the 1960s, it is not a common binder today. There are two reasons. The hazards associated with the polymerization of a nitrated prepolymer and the poor chemical stability characteristics when cured with isocyanate curatives. The latter is due to an intermolecular reaction, and the polymer tends to undergo degradation even at ambient temperature.
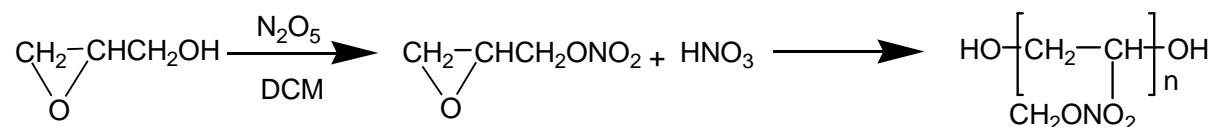
Scheme 3.2 Proposed reaction for synthesis of poly(glycidyl nitrate).

Chapter 3

3.1.1.2.7 Poly(3,3-bis(azidomethyl)oxetane)) and poly(3-azidomethyl-3-methyl oxetane)

Several azido oxetane polymers have shown a promise as energetic thermoplastic elastomers (ETPEs) for the next generation of gun propellants [3]. Examples of these binders are those made by the polymerization of 3,3-bis(azidomethyl)oxetane (BAMO) and 3-azidomethyl-3-methyl oxetane (AMMO) monomers. The synthesis of BAMO monomers involves treating 3,3-bis(chloromethyl)oxetane (BCMO) with sodium azide in dimethylformamide at 85 ^{o}C for 24 h. **Scheme 3.3** shows the proposed synthesis mechanism of BAMO. Propellants based on BAMO show relatively low flame temperatures and smokeless properties [18].
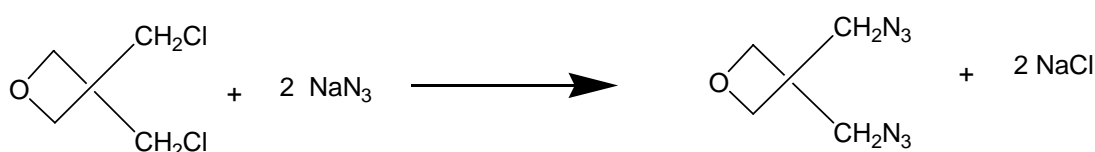
Scheme 3.3 Proposed reaction for the synthesis of BAMO.

The synthesis of AMMO involves azidation, with sodium azide, of the chloro or tosylate product of 3-hydroxy-methyl-3-methyloxetane, as can be seen in **Scheme 3.4**.

R=Cl or OTs
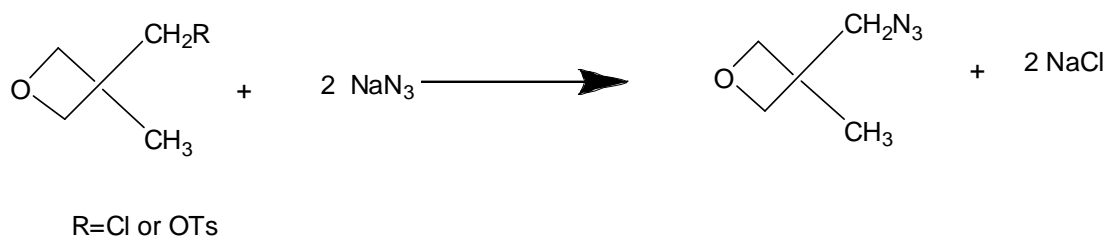
Scheme 3. 4 Proposal reaction for the synthesis of AMMO.

Chapter 3

Homopolymerization and copolymerization of these monomers are carried out using CROP, where BF_3-etherate is used as catalyst and 1,4-butanediol as initiator [19]. Some researchers have investigated the synthesis of ETPE binder based on BAMO/AMMO copolymers by end capping both homopolymers with TDI, followed by a subsequent linking reaction with butanediol [20].

3.1.1.2.8 Glycidyl azide polymer

One of the most promising high-energy binders is glycidyl azide polymer (GAP). GAP applications are not limited to high-energy propellant and plastic bonded explosives only, but can be extended to any other energetic systems, such as safety air bags [1, 3]. Azide polymers are also used for cross-linking, and azide-based surface modifications have been used to improve the biocompatibility of prosthetic implants [21].

GAP is a unique binder of high density, with a positive heat of formation, and is compatible with an advanced oxidizer. It can improve performance in terms of specific impulse and chlorine-free exhaust gases. There are many reasons for the high potential of GAP, such as the presence of a high content of the energetic azide pendant groups, low molecular weight hydroxyl terminated difunctional viscous pre-polymer, high positive heat of formation, low fraction sensitivity, and good compatibility. GAP has a low T_g, low viscosity, and high density. To a certain extent, it is easily prepared compared to other energetic binders [3, 9].

A hydroxyl terminated glycidyl azide polymer (GAP-diol) is usually synthesized by the reaction of the pre-polymer hydroxyl terminated poly(epichlorohydrin) (PECH-diol) with an ionic azide such as lithium azide, sodium azide, or potassium azide, by nucleophilic substitution of the chlorine atoms with N_3. Reactions can be carried out in an organic or an aqueous medium, although the reaction is run in an organic solvent such as dimethyl sulfoxide (DMSO) or dimethyl formamide (DMF). The advantage

Chapter 3

over aqueous medium is the shorter reaction time and the fact that no phase transfer catalyst is needed. Disadvantages of using organic solvents are cost, environmental concerns and difficulty of separation and purification of the final products [22]. Conversion of PECH-diols to GAP-diols can be followed by FTIR and NMR spectroscopy. FTIR analysis is the simplest method of determining the formation of GAP, by the disappearance of the absorption band at about 745cm^{-1}, which is associated with the chloromethyl group of PECH-diols, and formation of 2100cm^{-1} band, which is associated with the azide group of GAP-diols. **Table 3.2** shows the chemical structure and some physical properties of GAP-diols, as mentioned from the literature [3, 9, 23]. Based on type of diols used in the CROP of epichlorohydrin monomers, different forms of GAP can be produced, such as GAP-diol, GAP-triol, and branched GAP. Each one of these structures will reflect in the final mechanical properties of binder after curing. GAP is classified according to the Department of Transportation (DOT) classification as "Propellant Explosive, Liquid Class B Explosives" and it characterized by rapid burning [23].

Table 3.1 GAP-diols chemical structure and selected physical properties [3, 9, 23].

T_g	-45 ^oC
Thermal stability	0.08-0.22 mL N_2/g after 697 h at 50 ^oC
Impact sensitivity	200 kg-cm
Fraction sensitivity	32.4 kg
ΔH_f (experimental)	+0.28 kcal/g (depends on molecular weight)
Burn rate	Self-extinguishes at ambient pressure; 1.96 cm/s at 6.89 MPa

Chapter 3

In new rocket propellant formulations, GAP binder is used with ammonium perchlorate (AP) to increase the power of a propellant. The high generation of gas associated with GAP when it decomposes has found application in gas generates for air bag inflators. Finally, it is very important to mention that GAP is a highly energetic material and should not be handled carelessly. For example, subjecting the pre-polymer to frictional pressure, a blow, or local overheating can cause ignition, with resultant rapid gas generation.

3.1.2 Energetic thermoplastic elastomer binders based on urethane reaction

Thermoplastic elastomers (TPEs) have been developed and have replaced conventional cross-linked or vulcanized elastomers because of their rapid processing advantages. They generally exhibit a continuous two-phase domain structure in which a crystalline, highly polar 'hard' segment serves as tie points or "pseudo cross links" that bind an amorphous "soft" segment into a thermally reversible network resembling that of conventionally cross-linked elastomers [10]. TPEs are typically melted and obtain rubber elasticity without curing. Highly efficient processing techniques of plastics, like extrusion can be employed. The concept of replacing conventional cross-linked binders by thermoplastic binders is very attractive and successful in this area (ammunition manufacturing). In this way, extrusion techniques can be applied for producing composite propellants and PBXs. Add to that, the excess of expired propellants can also be re-melted and reprocessed. Several types of inert TPEs and energetic thermoplastic elastomers (ETPEs) have been investigated in the solid propellants.

Thermoplastic polyurethane (TPU) is an $(ABA)_n$ or AB type thermoplastic elastomer in which the hard segments A (crystalline phase) tend to aggregate, forming microdomains of a physically cross-linked region distributed throughout the soft

Chapter 3

segments B (amorphous phase) [7, 24]. The constitution of A and B in this linear block copolymer and their sequence length play an important role in the physical properties of TPEs. The chemical structure of hard and soft segments and their ratio form an integral part of molecular design for an optimum TPE binder. The hard segment is capable of crystallization or association and leads the thermoplastic behavior to the copolymer, whereas the soft segment leads the elastomeric behavior to the copolymer [24]. This mechanism can happen from slow cooling of the melting temperature, or even slow evaporation from a dilute solution. The crystalline structure can be highly organized, folding back onto itself in switchback fashion that organizes into strands called lamellae, which in turn organizes into spherical structures dense in lamellae, referred to as spherulites. In ETPEs hydroxyl terminated azide or nitro prepolymers are reacted by polyisocyanates via a urethane reaction, as shown in **Scheme 3.5**.

$$R_1\text{—NCO} \quad + \quad HO\text{—}R_2\text{—OH} \xrightarrow{\text{Catalyst}} R_1\text{—OCOHN—O—}R_2\text{—O—NHOCO—}R_1$$
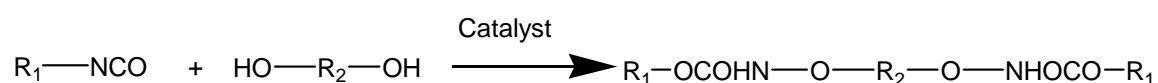
Scheme 3.5 Formation of urethane groups through the reaction of an isocyanate with hydroxyl terminated elastomers.

One of the undesirable features of this urethane reaction is gas evolution. This problem is associated with the reaction of diisocyanates with water, which leads to the release of CO_2 and forms numerous voids in the cured explosives. This will result in a decrease in loading density, mechanical strength, performance, and safety. In addition, the reaction of water with an isocyanate yields a carbamic acid, which decomposes and forms an amine group, which is 100 times more reactive than a primary hydroxyl group [10]. Furthermore, the urea group can react with a second isocyanate to give a biuret group, which will result in cross-linking between two

Chapter 3

polymer chains. Therefore, the presence of water should be avoided by good drying and applying of vacuum in order to obtain linear polyurethane without bubble formation and covalent cross-linking.

Different curing agents can be used, of which the most common isocyanate monomers are isophorone diisocyanate (IPDI), toluene diisocyanate (TDI), 4,4'-diisocyanato diphenylmethane (MDI), hexamethylene diisocyanate (HDI), and 4,4'-dicyclohexyl methane diisocyanate (H_{12}MDI). **Figure 3.1** shows the chemical structures of some of these isocyanates. The choice of appropriate curing agents is very important, because changes in the curing agent will affect the mechanical properties such as strain, stress, and hardness of the final propellant formulation. As an example, TDI is known to yield a binder that is stiffer than one with IPDI. Also, the rate of reaction is different where different isocyanates are used, where MDI exhibits the highest rate of curing compared to IPDI. The choice of an appropriate curing agent and a good understanding of these compounds are of prime importance to achieve binder with preferred properties.
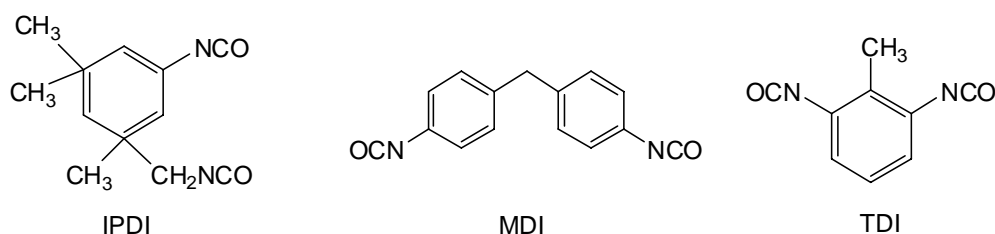
Figure 3.1 Chemical structures of selected polyisocyanates used for curing.

The concentration of isocyanate and hydroxyl groups plays a crucial part in the final properties of a binder. This is usually represented as the NCO/OH ratio. A balance of this ratio leads to a desirable product. A high concentration of NCO forms a stiff and cross-linking binder [9, 25]. On the other hand, a high number of OH groups will

Chapter 3

lead to incomplete reaction and a product with poor mechanical properties. Theoretically, when a diol is reacted with a diisocyanate at a NCO/OH ratio equal to unity, linear copolyurethane with the highest molecular weight is obtained. Precise measurement techniques for OH groups in GAP-diol required obtained NCO/OH ratio equal to unity.

Catalysts are often required to obtain complete curing and also to speed up the reaction. The most common types of catalysts used are organometallic compounds, such as organotin compounds and tertiary amines such as triethyl amine. Dibutyltin dilaurate (DBTL) is known to be a suitable catalyst for the urethane formation between long chain GAP-diol and isocyanates [9]. Also, the nature of a hydroxyl group shows different reaction toward the catalyst. As an example a secondary hydroxyl group has a lower reactivity toward an isocyanate compared to a primary hydroxyl group [9].

3.1.3 Plasticizer used in binder systems

According to the ASTM D-883 definition, a plasticiser is a material incorporated into a plastic to increase its workability and flexibility or dispensability. It is characterized by a high boiling point and low molar mass. The addition of a plasticizer will reduce the melt viscosity, elastic modulus, and glass transition temperature (T_g) [10].

Plasticizers are used in energetic binder systems for PBXs and propellant to fulfill a number of requirements, including lowering viscosity to improve processing, lowering the T_g, to improve mechanical properties, altering the explosive performance, and finally, to improve safety. However, high plasticizing efficiency is not the only criterion for choice of plasticizer. It is necessary to consider other properties such as miscibility, stability, and migration. Some requirements for optimum plasticizers to be used in binders are shown in **Table 3.2.**

Chapter 3

Table 3.2 Some requirements for plasticizers to be used in energetic formulations [10, 26, 27].

Plasticization - lower T_g
Improve processing - lower viscosity
Physical compatibility - polymer-plasticizer interaction parameter
Low migration - diffusion
Low migration - volatility
No adverse effects on cure reactions (terminated plasticizers)
A positive influence on mechanical properties
A positive influence on safety and performance
Stability-long term stability can be crucial
Chemical and physical compatibility with all ingredients
Hazards properties (like toxicity) - particularly in processing Availability, Cost, Purity, Toxicity

Plasticizer migration (exudation) is known to be one of the other problems associated with the degradation and the loss of mechanical properties of composite propellants. It is reported that plasticizer migration is a phenomena related to molecular reactions or diffusion, which will therefore be governed by kinetic relationships and accelerated by increasing the propellant temperature [26]. Most plasticizers used in different formulations commonly display exudation from the binder matrix even under moderate storage conditions [26]. This is highly undesirable as it resulted in degradation of mechanical properties, which lead to an increase in the vulnerability. Furthermore, there is an inverse correlation between molecular weight and plasticizer mobility. The smaller the molecule the quicker it will exude through a polymeric

Chapter 3

matrix. GLYN oligomers have a slower migration rate compared to other smaller plasticizers [27].

Another important aspect of energetic plasticizers is thermal stability. Energetic plasticizers usually exhibit different thermal stabilities based on the energetic group associated with the plasticizers. Plasticizers with nitro groups have a low thermal stability, for example nitrocellulose. On the other hand, plasticizers with azido groups do not have the same problem and don't show autocatalytic decomposition.

However, high plasticizing efficiency is not the only standard of choice of a plasticizer. It is necessary to consider other properties such as miscibility, stability and migration properties. Plasticizer migration across bond lines can cause deterioration of bonding properties and preventing the migration of energetic plasticizers has been a goal of rocket materials research for over 20 years [26]. Finally, it is necessary to consider a range of properties when assessing plasticizers, because no plasticizer is ideal. Some inert and energetic plasticizers in use and their chemical structures are listed in Section 3.1.3.1 and 3.1.3.2, respectively.

3.1.3.1 Inert plasticizers

Dioctyl phthalate (**10**)
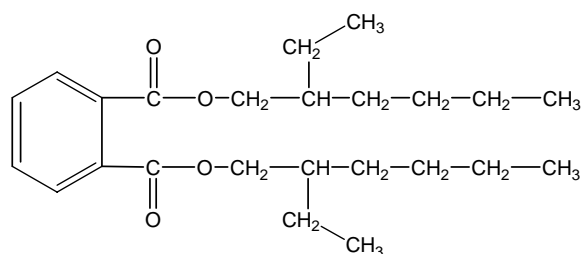
(10)

Chapter 3

Diethyl phthalate **(11)**

(11)
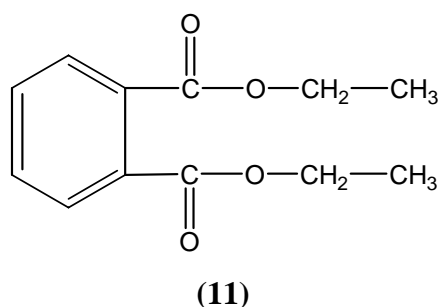
Glycerol **(12)**

(12)
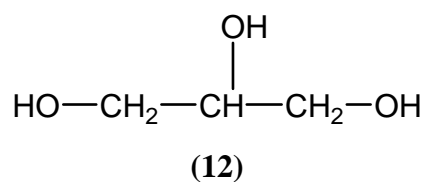
3.1.3.2 Energetic plasticizers

Energetic plasticizers that have been developed and used during the last decade contain the following energetic groups: nitro, nitramine and azido. The main objective of developing energetic plasticizers are: (1) to increase energy content, (2) to adjust the oxygen balance in a formulation, (3) to improve the plasticizer functions in formulations thus reducing the glass transition temperature and the brittle-ductile transition temperature, reducing migration and the so-called exudation, improving an other mechanical properties of the propellant matrix, and (4) to improve the burning behavior of the propellant. Furthermore, for a high specific impulse it is desirable to use energetic plasticizers instead of inert plasticizers. The optimum energetic plasticizers have a low glass transition temperature, a low viscosity, a low ability to

Chapter 3

migrate and a high oxygen balance. They should also be thermally stable and have low impact sensitivity.

Nitro plasticizers depend on nitro moieties (NO_2) in there structure, and are characterized by a high oxygen balance and low glass transition temperature. Nitro plasticizers compounds have the ability to lower the T_g and viscosity of an uncured binder. On the other hand, nitro plasticizers are thermally unstable and different stabilizers such as nitroguanidine (NQ), 1,3-diethyl-1,3-diphenylurea (Centrallite I), diphenylamine (DPA), 2-nitro-diphenylamine (2-NDPA), 1,1-diphenyl-3-methylurea (Akardite II) need to be used. Plasticizers with azido groups is a solution for the low thermal stability and weak compatibility of nitro plasticizers with azido containing compounds (azide binders) [9]. The azido plasticizers have the advantage of delivering extra energy as high amount of nitrogen gases produced on combustion. Also, it decomposed with minimum smoke as it burned without producing smoke [28]. Usually, the synthesis of azido plasticizers is based on reaction of hydroxyl groups of the starting materials with chloroacetic acid. Then, the chloromethyl groups are converted to the azide groups by using sodium azide in DMSO/water as the solvent system. The following are examples of some nitro and azido plasticizers used in ammunition filling and their chemical structures [29].

Bis(2,2-dinitropropyl)acetal/formal (BDNPA/F) **(14)**

(14)
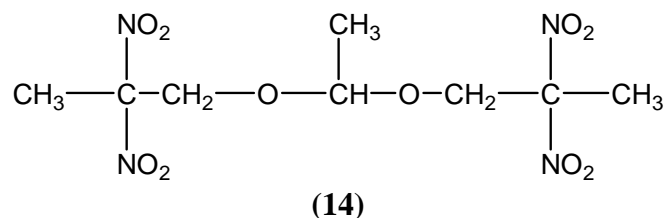
Chapter 3

N-n-butyl-N-(2-nitroxy-ethyl)nitramine (Butyl-NENA) **(15)**

$$CH_2-CH_2-O-NO_2$$
$$NO_2-N$$
$$CH_2-CH_2-CH_2-CH_3$$

(15)

2, 2-Dinitro-1,3-bis-nitrooxy-propane (NPN) **(16)**

$$NO_2$$
$$NO_2-O-CH_2-C-CH_2-O-NO_2$$
$$NO_2$$
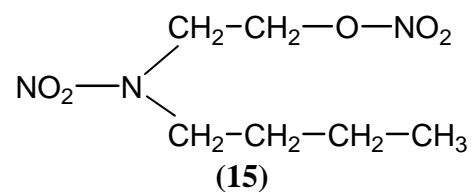
(16)
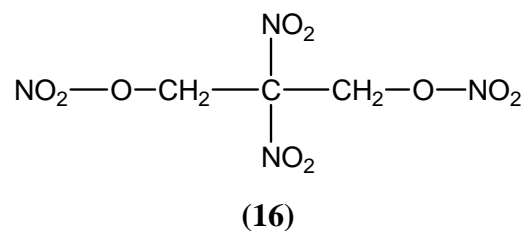
Bis(2, 2-dinitropropyl)acetal/bis(2, 2-dinitropropyl)formal (BDNPF) **(17)**

$$NO_2 \qquad\qquad NO_2$$
$$CH_3-\;-CH_2-O-CH_2-O-CH_2-\;-CH_3$$
$$NO_2 \qquad\qquad NO_2$$

(17)
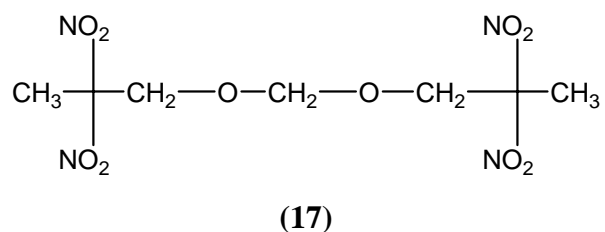
Nitratoethylnitramine **(18)**

$$R-N-CH_2-CH_2-O-NO_2$$
$$NO_2$$

(18)
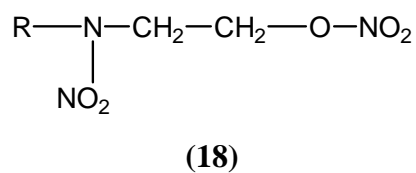
Chapter 3

Azido-acetic-acid-2-(2'-azido-acetoxy)-ethylester (EGBAA) **(19)**

(19)
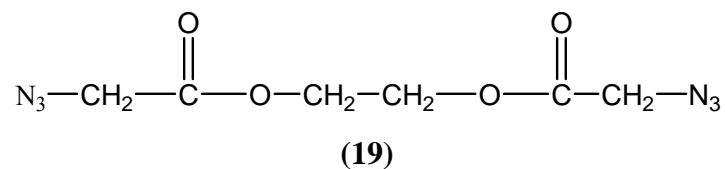
Azido-acetic-acid-2-[2'-(2''-azido-acetoxy)-ethoxy]-ethylester (DEGBAA) **(20)**

(20)
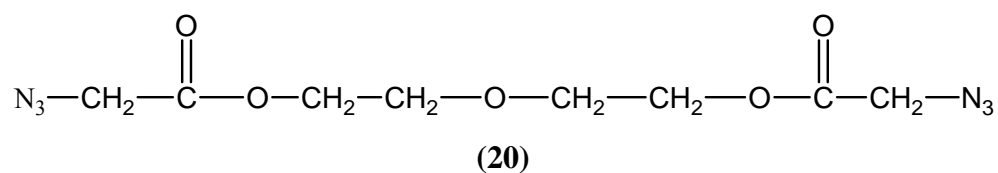
Azido-acetic-acid-3-(2'-azido-acetoxy)-2-(2'-azido-acetoxymethyl)-2-nitro-propylester (TMNTA) **(21)**

(21)
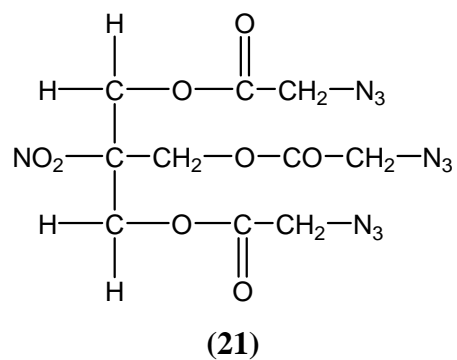
Chapter 3

Azido-acetic-acid-3-(2'-azido-acetoxyl)-2,2-bis-(2'-azido-acetoxymethyl)-propylester (PETKAA) **(22)**

$$C{-}\left(CH_2{-}O{-}\overset{\overset{\displaystyle O}{\|}}{C}{-}CH_2{-}N_3\right)_4$$

(22)
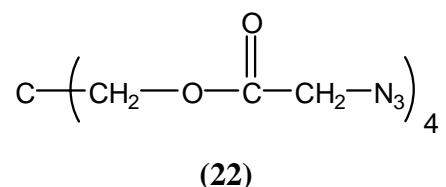
3.1.4 Objectives

The two main objectives were to synthesize and fully characterize GAP-diols and synthesize and characterize of energetic thermoplastice lastomers. The GAP-diols are produced from the azidation reaction of PECH-diols and ETPEs based on reacting hydroxyl terminated GAP with two different isocyanates. Also, GAP-diols obtained will be used later in further work.

3.2 Experimental

3.2.1 Materials

Poly(epichlorohydrin)-diols were produced from cationic ring-opening polymerization under the following conditions: toluene as solvent; 1,4-butane diol as initiator; borontrifluoride etherate (BF$_3$-etherate) as catalyst; and by using [ECH]/[Diol] = 50 ratio (see Chapter 2 Section 2.2.3.1). Isophorone diisocyanate (IPDI), toluene diisocyante (TDI), dibutyl tin dilaurate, triethyl amine, and sodium azide (NaN$_3$, purity > 98%) were used as received from Aldrich without further purification. Dichloromethane (DCM) and dimethylformamide (DMF) were of

Chapter 3

analytical grade and received from Saarchem. Solvents were stored over molecular sieves (5A).

3.2.2 Analytical equipment and methods

3.2.2.1 UV, FTIR, NMR, GPC, and DSC analyses

Equipments description and analysis methods applied for the UV, FTIR, NMR, GPC, and DSC are given in chapter 2 Section 2.2.2.

3.2.2.2 Dynamic mechanical analysis

A Perkin Elmer DMA 7e instrument was used for dynamic mechanical analyses (DMA), using the thin-film mode. Samples were brought to -100 ^{o}C and held there for a minute before being heated to 25 ^{o}C at a heating rate of 5 ^{o}C/min. The frequency was 1 Hz.

3.2.2.3 Thermal gravimetrical analysis

Thermal gravimetrical analyses (TGA) was carried out under nitrogen atmosphere in a Perkin Elmer Thermogravimetric Analyzer Pyris TGA 7, with a Perkin Elmer Thermal Analysis Controller TAC 7/DX. The heating rate was 10 ^{o}C/min.

3.2.3 Experimental techniques

The experimental procedures followed in the syntheses of the hydroxyl terminated glycidyl azide polymer and conventional thermoplastic elastomer via urethane reaction are described here.

3.2.3.1 Synthesis of hydroxyl terminated glycidyl azide polymer

Synthesis of the GAP-diol was based on the azidation reaction of the precursor PECH-diol (1,4-butanediol as initiator and BF$_3$ as catalyst), using sodium azide salts and DMF as solvent [23]. In a typical experiment, a clean and dry 250 mL two-necked round-bottom flask, immersed in an oil bath at room temperature, was connected to a condenser with a calcium chloride guard tube on the top, and with

Chapter 3

magnetic stirrer bar was used in the preparation of GAP. PECH-diols (2 g) was dissolved in dimethylformamide (80 mL) and introduced into the flask. The reaction mixture was heated slowly until the polymer was dissolved in the solvent (maximum temperature 60 ^{o}C). Sodium azide (0.13 g) was slowly added and the temperature rose to 115 ^{o}C. The reaction mixture was allowed to stir for about 10-15 hours before being cooled to room temperature. The polymer solution was then diluted to twice the volume of DMF with dichloromethane. The mixture was filtered to isolate the unreacted sodium azide and the formed sodium chloride. The solution was transferred to a separating funnel and washed with water. Two layers appeared in the separation funnel. DMF extracted in the aqueous phase (top layer). The organic layer (bottom layer) collected and washed several times with water. A solution of polymer in dichloromethane was dried over magnesium sulfate and then the pure polymer was obtained by removing the solvent by rotary evaporator. **Scheme 3.6** gives a representation of the preparation of GAP-diols from PECH-diols.

^{1}H-NMR (CDCl$_3$): δ= 3.3-4 ppm [CH, CH$_2$, CH$_2$N$_3$] due to protons of methylene, methane, and azide units.

^{13}C-NMR (CDCl$_3$): δ= 51-53 ppm [azide group CH$_2$N$_3$], δ= 69-71 ppm [polyether linkage –O–CH$_2$–], δ= 77 ppm [CDCl$_3$] and δ= 79 ppm [due to O–CH–].

FTIR (NaCl): 3406 (s, –OH), 2906 (s), 2866 (s), 2100 (s, –CH$_2$N$_3$), 1658 (s), 1428 (s), 1270 (s), 1130 (s, –C–O–C–), 925 (w), 642 (w), 530 (w) cm^{-1}.

GPC (THF) at 25°C, $\overline{M_n}$ =2000-4035 g/mol, DP=1.2-1.4, UV spectrum shows a weak single absorption at about 285 nm.

Chapter 3
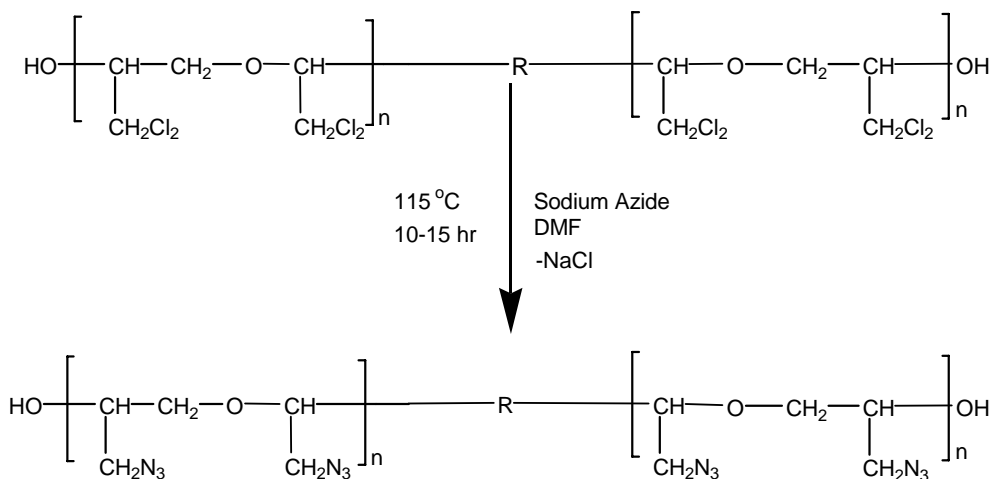
Scheme 3.6 Preparation of GAP-diols (R is 1,4-butanediol).

3.2.3.2 Synthesis of energetic thermoplastic elastomers

The energetic thermoplastic elastomers were prepared by react GAP-diols with either isophorone diisocyanate or tolylene diisocyanate at different NCO/OH ratios. The following is a typical procedure for the synthesis of ETPEs. GAP-diol (0.005 M) was mixed with 1, 4-butanediol (0.0013 M) as a chain extender and kept under vacuum for 2 hours at 80 ^{o}C. During this step the chain extender should dissolve completely in the GAP-diols and the mixture should be homogenous. The reaction mixture was then cooled to room temperature and an appropriate amount of isocyanate (either TDI or IPDI) (0.0063 M) was added. Stirring was continued under vacuum for another 30 min. In order to achieve a ratio of NCO/OH equal to unity, 0.0063 M of isocyanate was used. Dibutyl tin dilaurate (0.0005 M) and triethyl amine (0.0007 M) were then added to the mixture as a catalyst, and mixture left to complete the reaction in an oven at 60 ^{o}C for overnight. The final ETPEs were characterized by FTIR, TGA, DSC, and DMA. **Scheme 3.7** shows a representation for the synthesis of ETPEs based on the reaction of GAP-diols with isocyanate.

Chapter 3
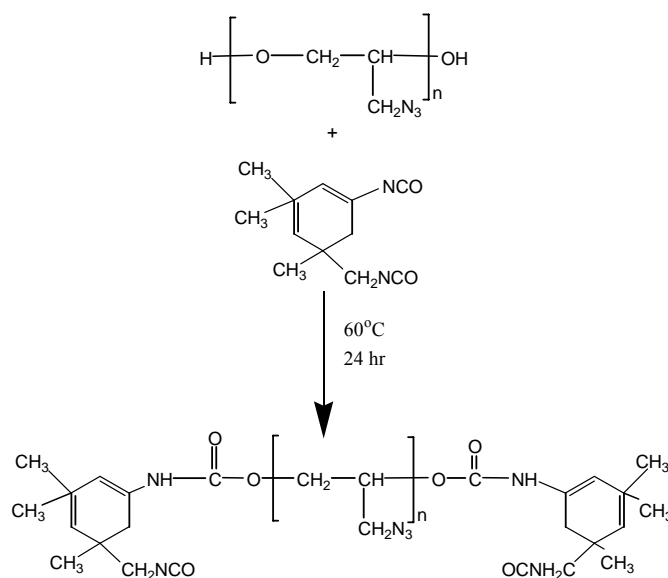
Scheme 3.7 Synthesis of energetic thermoplastic elastomers based on the reaction of GAP-diols with isophorone diisocyanate.

3.3 Results and discussion

This part includes a report about synthesis and characterizations of GAP-diols and energetic thermoplastic elastomres.

3.3.1 Synthesis and characterizations of hydroxyl terminated glycidyl azide polymer

The density of the GAP-diol was determined by using a pyknometer, and found to be about 1.28 g/cm^3, which is comparable with values reported in the literature [23]. Different analytical techniques such as GPC, UV spectroscopy, FTIR spectroscopy, proton and carbon NMR spectroscopy, DSC, and TGA were used to characterize the GAP-diols. The GPC profile of the GAP-diol is shown in **Figure 3.2** below. In the azidation reaction of PECH-diols with sodium azide, chlorine atoms were replaced by

Chapter 3

azide groups, which led to an increase in the molecular weight. Usually, the molecular weight of the GAP-diol was higher than the PECH-diols used in the azidation process. This could be attributed to the difference in the nature of azide groups as opposed to chloromethyl groups (hydrodynamic volume and interaction with polystyrene stationary phase). In any case, the polydispersity was not affected considerably by the azidation process. On the other hand, it is reported that high molecular weight poly(epichlorohydrin) (rubber) or poly(epichlorohydrin-co-ethylene oxide) azidation reactions lead to a decrease in molecular weight due to degradation of some PECH chains throughout azidation reaction [30]. This was not noticed in any of the experiments carried out in this study.
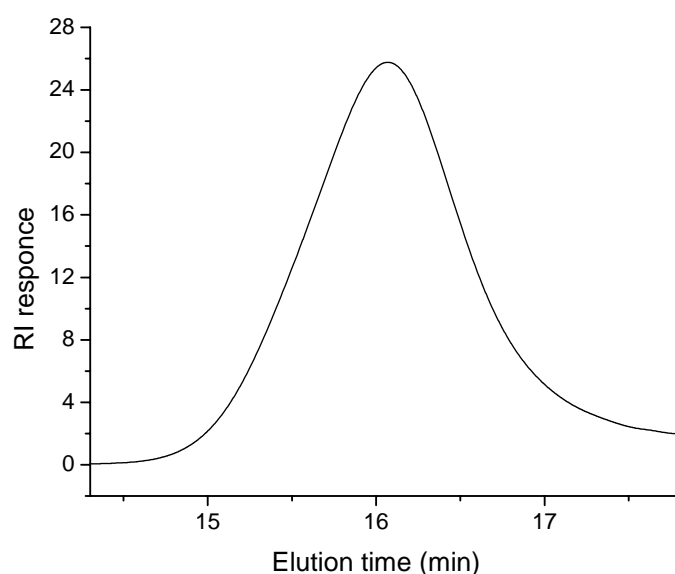
Figure 3.2 GPC trace of GAP-diol, $\overline{M_n}$ = 2000 and polydispersity 1.2.

The UV spectrum is shown in **Figure 3.3**. The UV spectrum shows absorption peak for GAP-diols at about 285 nm. This absorption could be attributed to the azide group, it was not observed in the UV spectrum of PECH-diols (see Figure 2.2).

Chapter 3
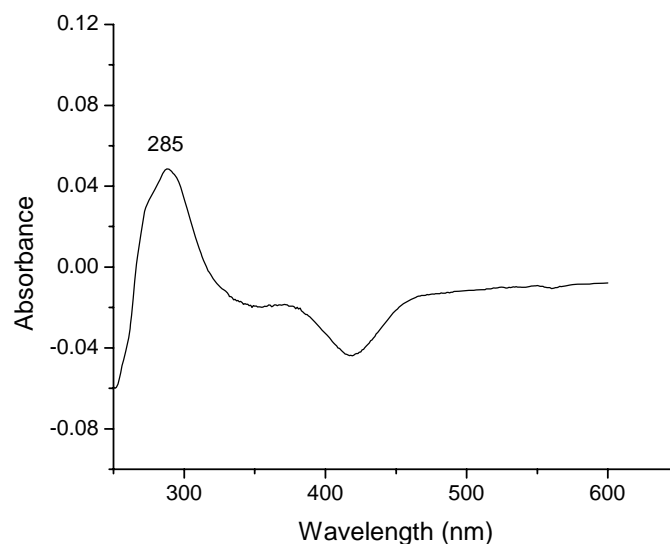
Figure 3.3 UV spectrum of GAP-diol. (Analysis conditions: dichloromethane as solvent and by using 1 mg/5 mL concentration).

The FTIR spectrum of the GAP-diol is shown in **Figure 3.4**. The most important characteristic peaks are the absorption peaks at about 1140 and 2100 cm^{-1}, which correspond to the polyether linkage group and azide groups, respectively. Absorption peaks at about 2850 and 3450 cm^{-1} are attributed to the methylene and terminal hydroxyl groups, respectively. In the IR spectrum, the disappearance of the peak at about 745 cm^{-1} and the formation of the peak at about 2100 cm^{-1}, attributed to the replacement of chlorine atoms of PECH-diols with the azide groups of GAP-diols. It has been reported that the azidation reaction slow after reaching a 90% conversion [23]. For this reason, it is preferable to carry out the reaction with an excess of sodium azide. Some of the azidation reactions did not reach complete conversion and the FTIR spectrum show the absorption of both chloromethyl and azide groups in the same spectrum.

Chapter 3
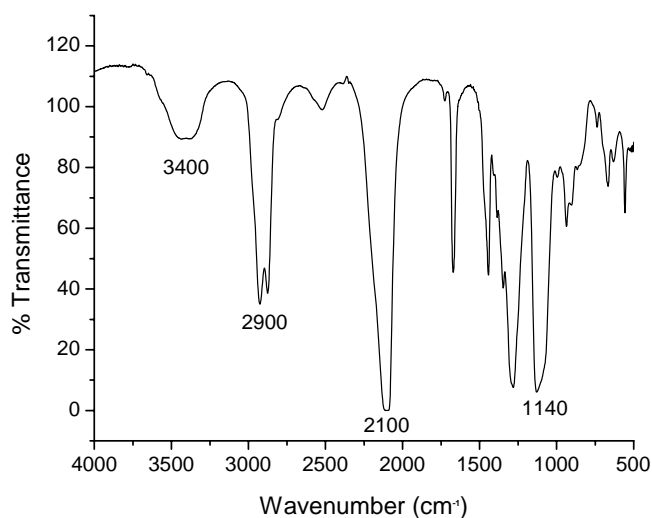
Figure 3.4 FTIR (NaCl) spectrum of GAP-diols.

These elastomers were characterized by ^{1}H-NMR, as shown in **Figure 3.5**. The most important feature of this spectrum is the signal at about 3.2 ppm, which is assigned to methylene protons of the pendent azidomethyl groups (CH_2N_3), and the signal at about 3.45-3.8 ppm, which is assigned to the main chain methylene and CH protons. The ^{13}C-NMR spectrum of GAP-diols is shown in **Figure 3.6**. The most important assignments on this spectrum are the signal at about 50-53 ppm, which is attributed to the azide groups. The absence of a signal at about 43-45 ppm, which is associated with the chloromethyl group of PECH-diols (see Figure 2.5), means that most of the chlorine atoms located on the chloromethyl pendant groups of PECH have been substituted with azide groups. The signal at about 69-71 ppm is associated with the polyether linkage (–O–$\underline{C}H_2$–). Solvent peak appears at 77 ppm and the signal at about 79 ppm is attributed to the (–HO–CH–). The rest of the assignments are indicated in the figure.

Chapter 3
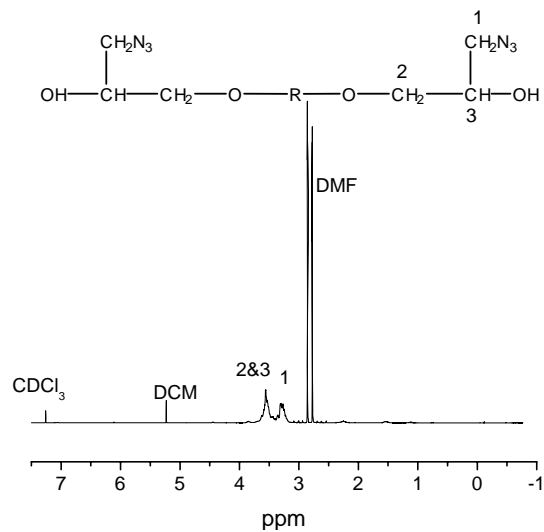
Figure 3.5 ^{1}H-NMR (CDCl$_3$) spectrum of GAP-diols (R is 1,4-butanediol).
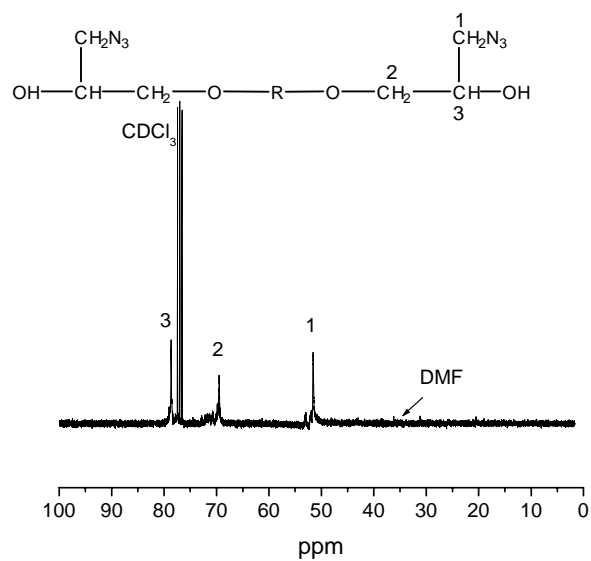
Figure 3.6 ^{13}C-NMR (CDCl$_3$) spectrum of GAP-diols(R is 1,4-butanediol).

GAP-diols are dark yellow liquids. Thermal behavior at low temperature represents an important feature for polymeric materials used in propellant formulation. The

Chapter 3

thermal analysis of GAP-diols was performed by DSC and **Figure 3.7** shows the results for a low temperature scan. The GAP-diols shows glass transition temperature at about -45 ^{o}C, which is in agreement with data in the literature [3, 9, 23].
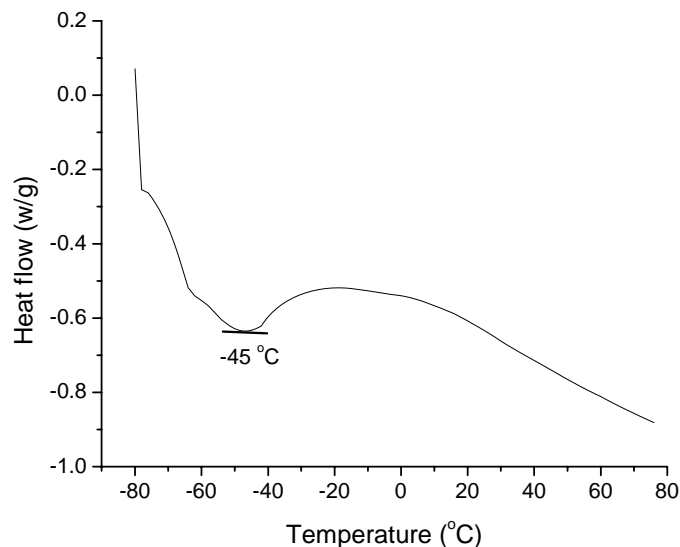
Figure 3.7 DSC thermogram of GAP-diols.

It is essential to study the decomposition behavior of polymeric propellant materials, especially in the case of such materials being used in space technology applications, where thermal decomposition of the propellant binders plays a crucial role in the combustion of the composite solid propellants. It was therefore necessary to study the thermal decomposition behavior of the GAP produced. The decomposition temperature of the GAP was determined from a DSC thermogram at high temperature. Results are recorded in **Figure 3.8**. The DSC scan of GAP shows a single exothermic peak in the temperature range 180-273 ^{o}C, with a maximum exothermic peak at about 242±5 ^{o}C. This result is in agreement with the literature, and the exothermic decomposition is attributed to the elimination of nitrogen by the scission of the azide bonds from the azide pendent groups of the glycidyl azide

Chapter 3

polymer [3, 9, 22]. On the other hand, another small degradation peak at 360 $^{\circ}$C could be attributed to the degradation of the polyether main chain of the GAP [31]. From the integration of the decomposition area the energy released was found to be about 1 500 J/g. This energy is higher than the data reported in the literature (see **Table 2.2**). This could be attributed to the effect of molecular weight on energetic properties [23].
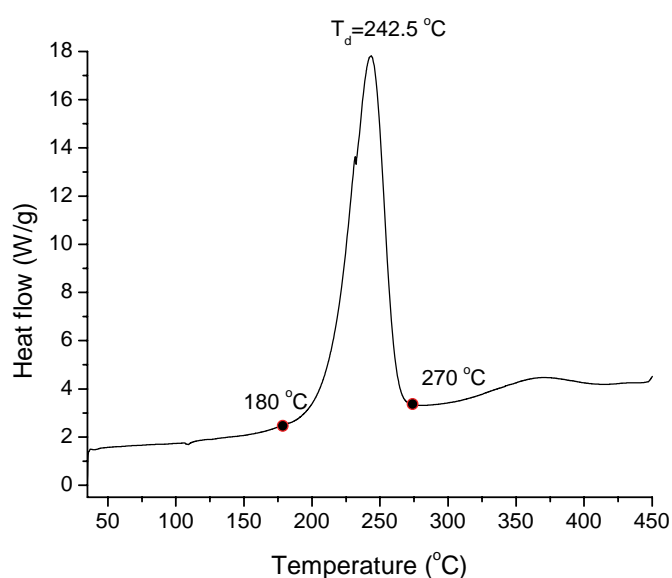
Figure 3.8 DSC thermogram of GAP-diols.

The decomposition of pure GAP-diols was also studied by using TGA. The typical TGA thermogram for GAP-diols is given in **Figure 3.9**, illustrating the determination of the characteristic temperatures. The TGA thermograms show that there were three decomposition stages. The first weight loss is due to residual and impurities from solvents and moisture. High moisture content could be attributed to the presence of hydroxyl groups. The second weight loss was about 66%. This weight loss could be attributed to the exothermic decomposition of the N_3 groups and decomposition of

Chapter 3

other parts from GAP associated with the elimination of azide groups. The last weight loss corresponds to the slow decomposition of the rest of the polymer (main polyether chain). The latter stage of weight loss occurs without any considerable heat liberation as there is no exothermic peak observed after the decomposition of the energetic group. The weight loss due to elimination of N_3 (66%) is comparable with literature. An earlier study of the thermal decomposition of GAP recorded a 40-65 wt.% loss [25, 32, 33].
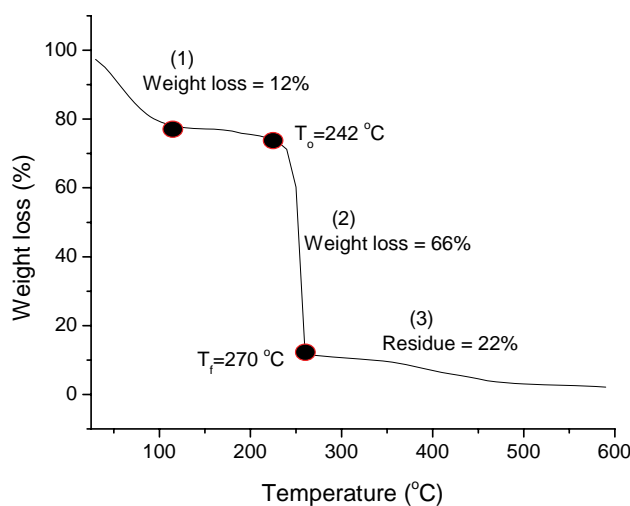
Figure 3.9 TGA thermogram of GAP-diols.

The spectroscopic and thermal analyses provide proof of the successful synthesis of GAP-diols by the azidation reaction of PECH-diols in DMF solvent. This product was used in later studies.

3.3.2 Synthesis of energetic thermoplastic elastomers

Hydroxyl terminated azido polymers were reacted with polyisocyanates via a urethane forming reaction to produce energetic thermoplastic elastomers. A binder can be formed with different mechanical properties by adjusting some parameters such as:

71

Chapter 3

type of curing agent, the curing reaction, and the ratio between reacting components. This will result in varying the cross-link density of the matrix, which will affect the mechanical properties such as strain, stress, and hardness. The curing process can be monitored with different techniques such as gel-time determination, viscosity and hardness measurements, FTIR spectroscopy and DSC. In this study, FTIR used to examine the investigate formation of ETPEs and different type of isocyanate namely isophorone di-isoyanate, toluene diisocyante, with different NCO/OH ratio was used. The affect of above the parameters on the thermomechanical properties of the final binder were studied by using DMA.

3.3.2.1 Spectroscopic analysis of energetic thermoplastic elastomers

FTIR spectrometry was used to study the formation of urethane linkages and **Figure 3.10** shows the spectrum of ETPEs produced by using IPDI as a curing agent. The spectrum shows the most important features of the GAP segment in the peaks $2100cm^{-1}$ and $1100cm^{-1}$, which are attributed to the azido group and polyether linkage, respectively. On the other hand, the thermoplastic segment (urethane) is shown in the absorption peaks at about $1726cm^{-1}$ and $3300cm^{-1}$, which are attributed to the urethane linkage and NH vibrations, respectively. The disappearance of the NCO stretching band at about $2270cm^{-1}$ and the presence of band at about $1726cm^{-1}$ provides proof of polyurethane formation between the GAP-diols and IPDI [9, 34]. The final rubbery product was a dark yellow color.

72

Chapter 3
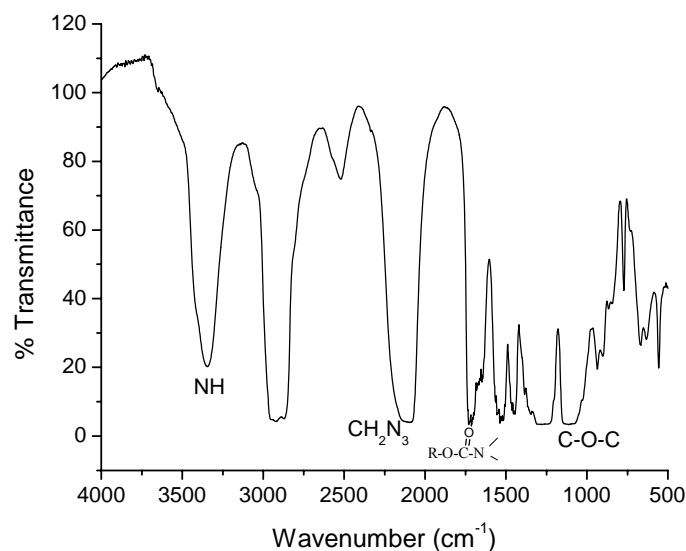
Figure 3.10 FTIR spectrum of energetic thermoplastic elastomers produced by using isophorone diisocyanate.

3.3.2.2 Thermo-mechanical analysis of energetic thermoplastic elastomers

DSC was used to study the effect of using different isocyanates on the glass transition temperature of the final binder. **Figure 3.11** shows the thermogram of ETPEs. DSC analyses shows the same results for two different binders and two glass transition temperatures were detected. The first corresponds to GAP-diols at about -37 $^{\circ}$C and the second to the thermoplastic part (urethane) at about abut 21 $^{\circ}$C. On the other hand, the ETPEs show exothermic decomposition at about 250 $^{\circ}$C and there was variation in the energy released obtained based on the integration for decomposition area. The energy released was affected by the NCO/OH ratio, and it was in the range 1400-1645 J/g. Variation in the energy released could be attributed to the difference in the length of hard segment to the energetic (soft) part.

73

Chapter 3
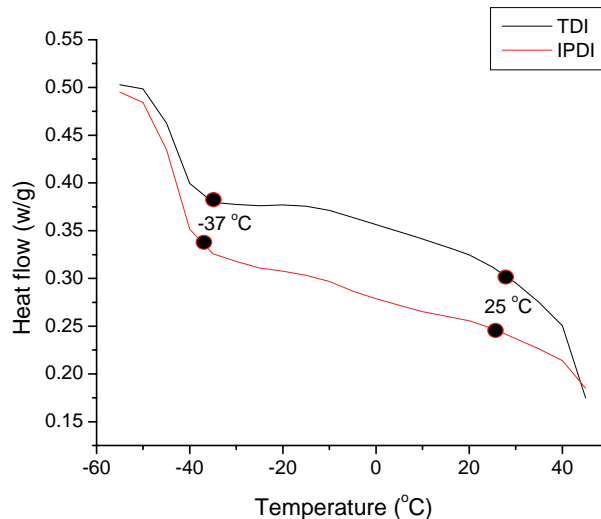
Figure 3.11 DSC analysis of energetic thermoplastic elastomers yield from the reaction of toluene diisocyante and isophorone diisocyanate with hydroxyl terminated glycidyl azide polymer by using NCO/OH ratio 1.

DMA was used to study the thermomechanical character of ETPEs, **Figure 3.12** and **Figure 3.13** shows the DMA analysis of the binder produced by two different isocyante and with a NCO/OH ratio of 1. The first tan δ maximum for two different binders did not show any significant difference. The tan δ maximum of the binder produced by reaction with IPDI was about -12 $^{\circ}$C, whereas the tan δ maximum of the binder produced by reaction with TDI was about -10 $^{\circ}$C, but tan δ peak of IPDI was narrow compared to TDI. On the other hand, the difference in storage modulus between the two binders was more pronounced, where the binder based on TDI showed a higher storage modulus compared to the binder produced from IPDI. These results could be attributed to differences in the structure of the isocyanate. TDI is reported to produce a stiffer binder than IPDI [31]. In contrast, when the NCO/OH ratio was increased to 2 the DMA analysis showed a shift of tan δ from -12 $^{\circ}$C to

Chapter 3

about 20 ^{o}C in the case of IPDI and from -10 ^{o}C to about 5 ^{o}C in the case of TDI. Also, tan δ exhibits broadness when the high ratio of curing agent is used. This could be attributed to high concentration of hard segment, cross-linking, or un-homogenous distribution of molecular weight. The storage modulus also changed from a sharp decrease (in the case of NCO/OH equal unity) to a smooth decrease, but the start of the curve was not affected noticeably.
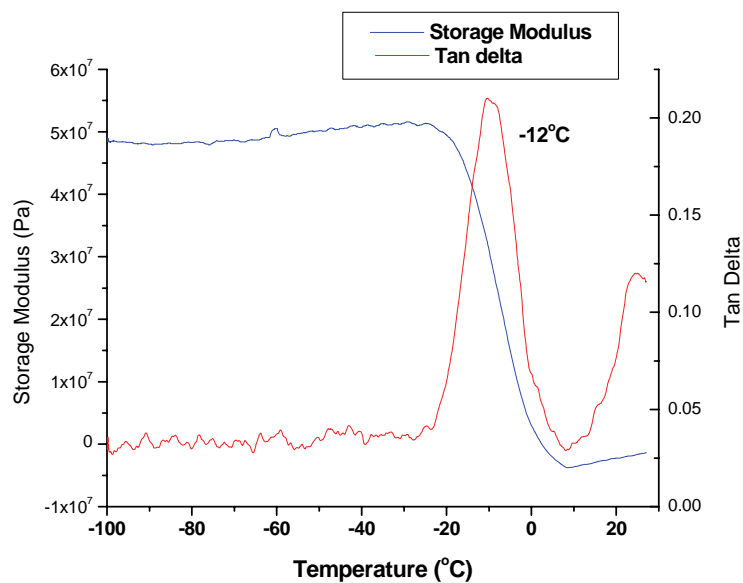
Figure 3.12 DMA measurements of energetic thermoplastic elastomers obtained from the reaction of isophorone diisocyanate with hydroxyl terminated glycidyl azide polymer (binder prepared by using NCO/OH equal unity).

Chapter 3
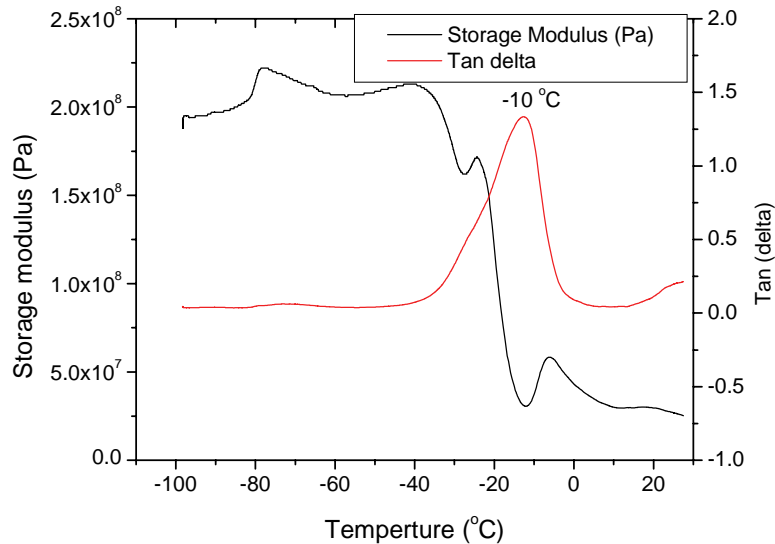
Figure 3.13 DMA measurements of energetic thermoplastic elastomers obtained from the reaction of toluene diisocyante with hydroxyl terminated glycidyl azide polymer (binder prepared by using NCO/OH equal unity).

Thermogravimetric analysis of ETPEs produced from the reaction of GAP-diols with IPDI is shown in **Figure 3.14**. There were two degradation steps, the first degradation started at about 190 ^{o}C. It is attributed to the decomposition of N_3 groups of elastomer segment and other part from the binders associated with this decomposition. There was about 35% weight loss noticed in this step. The second degradation step starts at about 275 ^{o}C. It is attributed to the thermoplastic (urethane) segment and about 40% weight loss was recorded in this step.

The formation of ETPEs was proved by using FTIR analysis. Themomechanical analysis was studied by DMA and a higher stiffness found in the case of TDI curing agent than IPDI. Also, TGA analysis was showed two degradation steps corresponding to elastomer and thermoplastic moieties.

Chapter 3
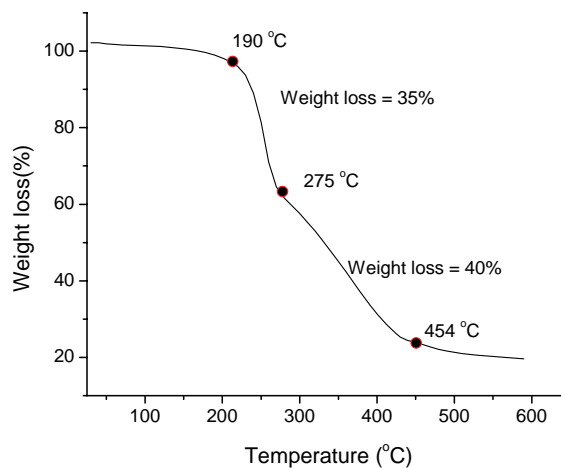
Figure 3.14 TGA thermogram of energetic thermoplastic elastomers yield from reaction of isophorone diisocyanate with hydroxyl terminated glycidyl azide polymer, binder prepared by using NCO/OH equal unity.

3.4. Summary

This chapter described the synthesis and characterization of glycidyl azide polymer with hydroxyl terminal groups. This polymer was prepared by the azidation reaction of hydroxyl terminated poly(epichlorohydrin). The GAP-diols which were produced had molecular weights of 3 000-4 000 g/mol and polydispersity of 1.2-1.4, as determined by GPC. The UV spectrum showed a weak single absorption for GAP at about 285 nm, and FTIR analysis confirmed the presence of an azido group in the elastomer backbone by absorption at about 2100 cm^{-1}. Proton and carbon NMR was used to study the microstructure of GAP-diols. This signal at about 53 ppm was the proof of the presence of azide groups. Thermal analysis of elastomers was studied by DSC. There was a single glass transition temperature at about -45 $^{\circ}$C and the decomposition took place at about 245 $^{\circ}$C. TGA analysis shows two main

77

Chapter 3

degradation steps corresponding to the decomposition of the azide unit and degradation of the polyether chain. GAP with hydroxyl terminated groups was used to prepare energetic thermoplastic elastomers based on the reaction with two different isocyanates namely, isophorone diisoyanate and toluene diisocyanate. FTIR was used to characterize the ETPEs. The disappearance of the NCO stretching band at 2270 cm^{-1} and appearance of a band at 1725 cm^{-1} provides proof for polyurethane formation between GAP-diols and IPDI. DMA used to investigate the effect of NCO/OH ratio and higher ratio was found to be stiffer as can be seen from Tan δ results.

Chapter 3

3.5 References

1. Provatas A., Energetic Polymers and Plasticisers for Explosive Formulations-A Review of Recent Advances 2000, www.dsto.defence.gov.au/corporate/reports/DSTO-TR-0966.**pdf** (accessed on 15/6/2004)

2. Akhavan J., Burke T. C., Poropllents, Explos, Pyrotechn 1992, 17, 271.

3. Agrawal J. P., Prog. Energy Combust Sci 1998, 24, 1.

4. Boyars C., Klager K., Propellants Manufacture, Hazards, and Testing. Advances in chemistry series, American Chemical Society, 88, 1969.

5. Camp A. T., Nitrocellulose Plastisol Propellants, Propellants Manufacture, Hazards, and Testing Conference, American Chemical Society 1969, Vol 88, 29.

6. Chem F., Duo Y., Luo S., Lou Y., Tan H., Poropllents, Explos, Pyrotechn 2003, 28(1), 7.

7. O Schwarz's, Polymer Materials Handbook, Natal Witness Printing and Publishing Company (Pty) Ltd 1995, 86.

8. Packham D. E., Handbook of Adhesion, Longman Group 1992, 143.

9. Gaur B., Lochab B., Choudhary V., Varma I. K., J. Macromol. Sci. Polym. Rev 2003, C43(4), 505.

10. Seymour, Carraher's, Polymer Chemistry, Fifth Edition, Marcel Dekker, Inc. 2000, 463.

11. Volk F., Bathelt H., Poropllents, Explos, Pyrotechn 1997, 22, 120.

12. Durgapal U. C., Dutta P. K., Mishra S. C., Pant J., Propellant Explosives Pyrotechnics 1995, 20, 64.

13. Terence J. K., Zachary M. B., Anthony V. C., Polymer 1998, 40, 65.

Chapter 3

14. Akhavan J., Kronfli E., Waring S.C., Polymer 2004, 45, 2119.

15. Akhavan J., Koh E., Waring S., Kronfli E., Polymer 2001, 42, 7711.

16. Cunliffe A. V., Desai H. J., Lewis T., Millar R. W., Paul N. C., Stewart M. J., Amass A. J., Polymer 1996, 37(15), 3471.

17. Diaz E., Brousseau P., Ampleman G., Prud'homme R. E., Poropllents, Explos, Pyrotechn 2003, 28(3), 101.

18. Oyumi Y., Inokami K., Yamazaki K., Matsumoto K., Poropllents, Explos, Pyrotechn 1995, 19, 180.

19. Kroeze E., Brinke G. T., Hadziioannou G., Macromolecules 1995, 28, 6650.

20. Kawasaki H., et al., Poropllents, Explos, Pyrotechn 1997, 22, 87.

21. Jaykrishnan A., Sunny M. C., Rajan M. N., J. Appl. Polym. Sci 1995, 56, 1187.

22. Mohan Y. M., Raju M. P., Raju K. M., J. Appl. Polym. Sci 2004, 93, 2157.

23. Frankel M. B., Grant L.R., Flanagan J. E., J. Propul. Power 1992, 8, 560.

24. Ampleman G., Maris A., Desilets S., Beaupre F., Manzara T., Synthesis and Production of energetic copolyurethane Themropastic Elastomers Based on Glycidyl Azide Polymer, 29th International ICT Conference 1998.

25. Selim K., Ozkar S., Yilmaz L., J. Appl. Polym. Sci 2000, 77, 538.

26. Schreuder-Gibson H. L., Rubber World 1990, 203(2), 34.

27. Provatas A., Energetic Materials 2003, 21, 237.

28. Drees D., Loffel D., Messmer A., Schmid K., Poropllents, Explos, Pyrotechn 1999, 24, 159.

29. Wingborg N., Eldsater C., Poropllents, Explos, Pyrotechn 2002, 27, 314.

30. Bul V. T., Ahad E., Rhaume D., Raymond M. P., J. Appl. Polym. Sci 1996, 62, 27.

31. Eroglu M. S., Hazer B., Guven O., Baysal B. M., J. Appl. Polym. Sci 1996, 60, 2141.

Chapter 3

32. Mohan Y. M., Raju M. P., Raju K. M., Int. J. Polymer. Mater 2005, 54, 651.

33. Erglu M. S., Polym. Bull 1998, 41, 69.

34. Hesse M., Meier H., Zeeh B., Spectroscopic Methods in Organic Chemistry, Georg Thieme Verlag 1997, 29-45.

Chapter 4

Synthesis and characterization of poly(methyl methacrylate-*b*-epichlorohydrin) and poly(methyl methacrylate-*b*-glycidyl azide) copolymers using nitroxide-mediated polymerization

Chapter 4

Synthesis and characterization of poly(methyl methacrylate-*b*-epichlorohydrin) and poly(methyl methacrylate-*b*-glycidyl azide) copolymers using nitroxide-mediated polymerization

Abstract

Thermoplastic elastomer binders were synthesized using a technique based on the use of a macro-azo-initiator (MAI). 4,4' Azobis (4-cyanopentanoyl chloride) (ACPC) was prepared from the chlorination reaction of ACPA, then hydroxyl-terminated poly(epichlorohydrin) and glycidyl azide polymer were polycondensed with ACPC to prepare MAI containing sessile –N=N– units of ACPC. The formation of the macro-azo-initiator was confirmed by FTIR and NMR. This MAI was used in the free radical polymerization of methyl methacrylate (MMA) to yield poly(methyl methacrylate-*b*-epichlorohydrin) (PMMA-PECH) and poly(methyl methacrylate-*b*-glycidyl azide) (PMMA-GAP) copolymers. Gel permeation chromatography (GPC) was used to determine the molecular weight of the block copolymers and conversions were determined gravimetrically. The block copolymers were characterized on the basis of infrared absorption and proton NMR spectroscopy. Thermal properties of the block copolymers were investigated with thermogravimetric analysis (TGA) and differential scanning calorimetry (DSC). Thermal analysis of the block copolymers showed a single broad glass transition temperature due to the miscibility of the two different segments in each other, and two clear degradation temperatures.

83

Chapter 4

4.1 Introduction and objectives

The introduction includes a general description of a free radical polymerization and its kinetics. A new trend in applying controlled/living free radical polymerization methods is reported with more focus on the nitroxide mediated polymerization (NMP).

4.1.1 Free radical polymerization

Free radical polymerization is one of the most common techniques used for polymer synthesis [1, 2]. Some commercially important polymars prepared by free radical polymerization include poly(acrylonitrile), poly(butadiene), poly(vinyl acetate), poly(vinly butyral), and poly(vinyl chloride). This type of polymerization is limited to monomers containing a vinyl group. These monomers range from small molecules to macromonomers. About 60% of all polymers are prepared by radical polymerization, but many aspects of this process are still not fully understood [2]. Advantages of radical polymerization are (a) it can be used with a large variety of monomers; (b) it can be used successfully with a wide range of functional groups; (c) it can be used under various reaction conditions (bulk, solution, emulsion, mini-emulsion, suspension); (d) it is insensitive to small traces of impurities such as oxygen, metal ions and water; and (d) it is simple to implement and inexpensive in relation to competitive technologies.

In contrast, the main drawback of free radical polymerization is that the reaction is not enantioface selective. The general mechanism for free radical vinyl polymerization utilizing an initiator that creates radicals by homolytic dissociation is presented in **Scheme 4.1**. The essential features of this mechanism are the initiation and propagation steps, which involve radicals being added to the double bond, and a termination step, which involves disproportion or combination between two growing chains.

Chapter 4

Initiation:

initiator-derived radical
primary radical
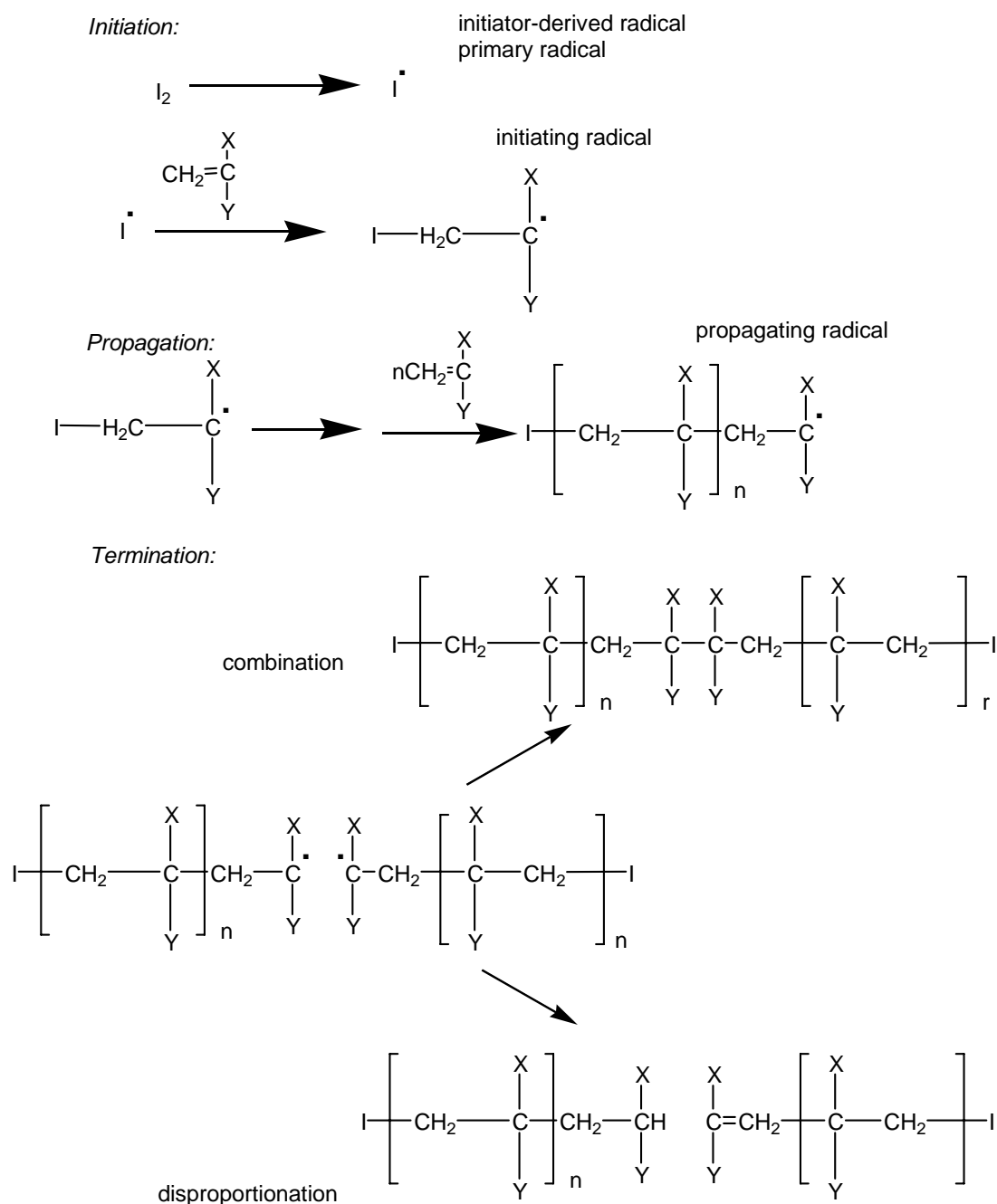
Scheme 4.1 Reaction mechanism for the classic free radical polymerization of vinyl monomer, initiated by homolytic dissociation of initiator [3].

Chapter 4

4.1.1.1 Initiation

Initiation is defined as a series of reactions that commence with the generation of primary radicals and culminates in the addition of the monomer to the carbon-carbon double bond so as to form initiating radicals. Initiation involves the hemolytic dissociation of an initiator molecule to form two radicals capable of initiating polymerization. The most common initiators are the azo or peroxy compounds such as 2,2' azobisisobutyronitrile (AIBN) **(1)**, benzoyl peroxide (BPO) **(2)**, and di-*t*-butyl peroxyoxalate (DBPOX) **(3)**.
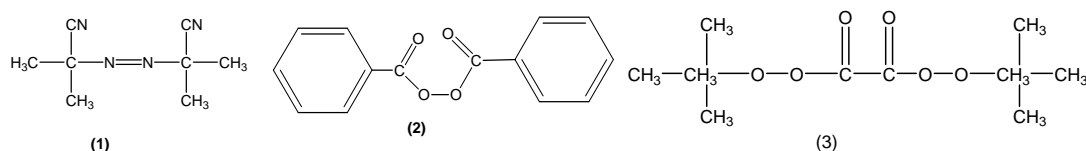
The rate of decomposition of initiators usually follows first-order kinetics and it is dependent on the solvent used and the temperature of polymerization. Decomposition can be described by an Arrhenius equation. Peroxides are commonly used either as thermal initiators or as a component in a redox system. Peroxides are photochemically reactive, but poor light absorption characteristics limit their applications as photoinitiators [3]. Initiators produce radicals by different mechanisms; typical radical producing reactions are [2]:

1. *Thermal decomposition* can be usefully applied to organic peroxides or azo compounds because when they are heated they form two phenyl radicals, with the loss of CO_2.

2. *Photolysis* is applicable to metal iodides, metal alkyls, and azo compounds, which are decomposed by radiation at a wavelength of 360 nm.

3. *Redox reaction*, an example of which the reaction between the ferrous ion and hydrogen peroxide in solution, to produce hydroxyl radical.

4. *Persulphates* are useful for emulsion polymerization; decomposition occurs in the aqueous phase and the radical diffuses into a hydrophobic, monomer containing droplet.

5. *Ionizing radiation*, such as α, β, γ, or X-rays, can also be used to initiate polymerization.

4.1.1.2 Propagation

The propagation step of radical polymerization comprises a sequence of radical additions to carbon-carbon double bonds. It follows the initiation step and a monomer is sequentially added to the growing polymer chain via the process of electron transfer. The radicals are continuously generated by the dissociation of the initiator. The rate of propagation is proportional to the concentration of the monomer and the square root of the concentration of the initiator. Propagation is temperature dependent, according to the Arrhenius equation [2].

4.1.1.3 Termination

In theory, a chain could continue to propagate until all the monomer in the system has been consumed, but free radicals are a particularly reactive species and interact very quickly to form inactive covalent bonds. Termination of free radical polymerization can take place mainly by two different mechanisms. The first mechanism occurs when two macroradicals combine. The second mechanism involves disproportionation. There are other mechanisms that also lead to termination, such as transfer of the active center to another molecule, which may be a solvent, an initiator, or a monomer; and interaction with impurities (like oxygen) or inhibitors.

Finally, radical polymerization is one of the most used processes for the commercial production of high-molecular weight polymers, but it has some notable limitations with respect to the degree of control that can be asserted over the macromolecular structure, in particular, the molecular weight distribution, composition, and architecture. Therefore the use of living/controlled free radical polymerization is required.

Chapter 4

4.1.2 Living/controlled free radial polymerization

Living or controlled free radical polymerization has played an important role in recent progress in macromolecular development. This is exemplified by the synthesis of new polymers with well-defined chemical structures (blocks, stars or other complex architecture), control of the molecular weight (a linear increasing trend of molecular weight with conversion), and achieving a low polydispersity index. Living polymerization has also been used to prepare a range of materials like novel surfactants, dispersants, coatings, adhesives, biomaterials, membranes, drug delivery media, and materials for microelectronics [4].

Living polymerization systems occur if there is a dynamic equilibrium between active and dormant species as a result of a rapid, reversible termination or reversible degenerative chain transfer reaction. The propagation and reversible termination should be much faster than any irreversible termination. Literature reports many radical polymerization methods that exhibit controlled or living characteristic, such as (I) dithiocarbamate iniferters [5-7], (II) a nitroxide-mediated process [8], (III) a transition metal complex-dediated atom transfer radical polymerization (ATRP) [9], and (VI) the reversible addition-fragmentation chain transfer (RAFT) process [4].

4.1.2.1 Dithiocarbamate photoiniferters

Photopolymerization has some advantages over thermally initiated polymerization. This is evidenced in the rapid growth of radiation curing as an industrial process, which depends on the use of photoinitiators, which can be used in controlled radical reactions and are defined as being substances that have the ability to convert physical energy of an incident light beam into chemical energy by forming reactive radical intermediates. The use of sodium *N,N'* diethyl dithiocarbamate (**4**) derivatives as so-called photoiniferters during radical polymerization reactions has been reported [10]. The term iniferter has first coined by Otsu, meaning substances that act as initiator, transfer agent and terminator in radical polymerization reactions [11].

Dithiocarbamate is an example of such a photoiniferters and will be discussed in more detail in Chapter 6.

$$CH_3-CH_2$$
$$CH_3-CH_2 \diagdown N-C-SNa$$

(4)
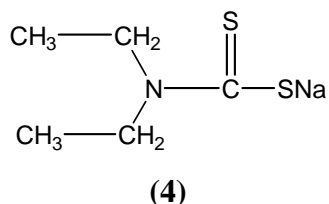
4.1.2.2 Atom transfer radical polymerization

Atom transfer radical polymerization (ATRP) provides considerable control over radical polymerization with common vinyl monomers. This technique is based on a reversible exchange between a low concentration of growing radicals and a dormant species. Reactivation of the dormant species allows the polymer chains to grow and deactivate again. ATRP has been successfully applied for the controlled polymerization of styrene, (meth)acrylates, (meth)acrylamides, acrylonitrile, and 4-vinylpyridine [12].

4.1.2.3 Reversible addition-fragmentation chain transfer

Rizzardo and co-workers were the first to report reversible addition-fragmentation chain transfer (RAFT) [3]. RAFT appears to offer advantages above other controlled polymerizations since it is applicable to a wide range of monomers and can be performed in a wide variety of solvents (including water) under a broad range of experimental conditions. The basic structure of the transfer agent used in the RAFT process is shown in **Figure 4.1**. Z refers to the stabilizing group, and R refers to the leaving group. The Z-group should be able to activate the dithioester double bond for fast addition of the propagating polymeric radicals and the R group should be compatible with the monomer that needs to be polymerized. It should also be a good leaving group, capable of reinitiating polymerization [4].
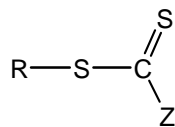
Figure 4.1 The basic structure of a RAFT agent.

4.1.2.4 Nitroxide-mediated polymerization

Nitroxide-mediated polymerization (NMP) is another form of controlled radical polymerization (CRP). There are two methods in preparing copolymers based on using NMP. The first method depends on the polymer being synthesized entirely by using NMP. The second method is based on transformation from other living polymerization techniques (anionic, cationic, ring-opening, etc.) to NMP by functionalization of a macromolecule, which can be used as a macro-azo-initiator (MAI). Utilization of a macro-azo-initiator for the synthesis of a block copolymer via a radical process is considered a very useful technique for many reasons. A block copolymer can be easily synthesized by conventional radical polymerization; not only block copolymers composed of addition polymer segments but also those of addition polymers and various oligomers segments can be synthesized; and the block efficiency of MAI is reasonably high [3].

Synthesis of block copolymers, using a MAI, can be carried out by two methods [13]. In the first type, a MAI having a thermally labile azo unit in every repeating unit is synthesized, and then a two-step polymerization of different monomers is carried out to yield block copolymers composed of the different addition polymer segments. In the second type, a MAI composed of oligomers or pre-polymers linked with thermally labile azo units is synthesized, and then a one-step polymerization of a monomer is carried out to give a block copolymer of the pre-polymers and additional polymer segments. **Scheme 4.2** shows a schematic representation of the two different types of methods for synthesis of block copolymers using MAI. In this study, the second type of MAI will be utilized.

Nitroxide-mediated radical polymerization is known as a pseudo living free radical polymerization technique. Georges *et al.* and Moad *et al.* [8, 14], reported that using

various nitroxides such as 2, 2, 6, 6-tetramethyl-1-piperidinyloxy (TEMPO) to promote control over radical based polymerization. Yuruk *et al.* [15], reported the synthesis of a block copolymers containing polystyrene and poly(ethylene oxide) or poly(propylene oxide) based on macro-azo-carbamate as an initiator. Akira and Susumu [16], reported the synthesis of polyethyleneglycol-polystyrene block copolymers based on using azobiscyanopentanoic acid as initiator.

Macroinitiaor
Type 1

Macroinitiator
Type 2

$-(R-X-)_m$

$(R-AAAA-R-X)-_m$

radical polymerization
of monomer A (1st step)

radical polymerization
of monomer B

one step

$-(R-AAAAA-R-X)_m$

radical polymerization
of monomer B (2nd step)

$-(R-AAAAA-R-BBBBB-X)_m$
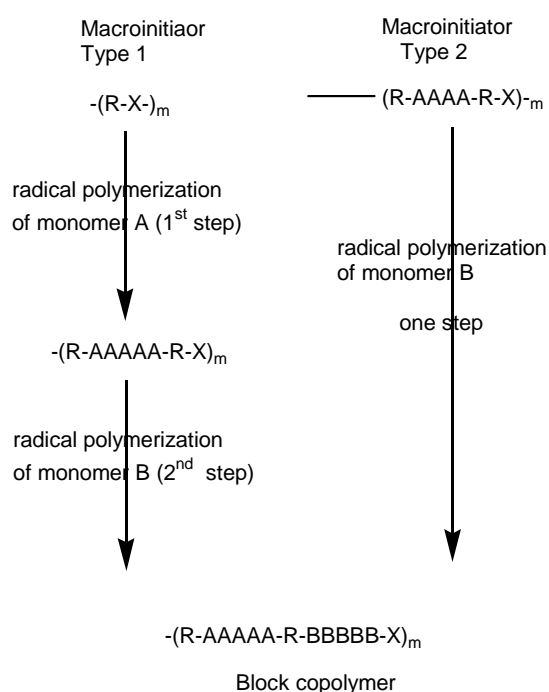
Block copolymer

Scheme 4.2 Schematic representation of the two types of methods used to synthesize of block copolymers using MAI (X is an active site for scission and R is aliphatic or aromatic hydrocarbons). Scheme adopted from [13].

Generally, controlling radical polymerization with nitroxide radicals has been shown to be an extremely useful tool for synthesizing polymers with low polydispersity indices (PDI < 1.3) and nitroxides are used mostly for controlling styrene polymerizations [12]. Davis and Matyjaszewski [17], reported in their review that nitroxide-mediated polymerizations have been successfully used to prepare

copolymers of styrene-based monomers but attempts to incorporate other monomers have been difficult. They attributed this to the fact that radicals generated by the thermal self-initiation reaction of styrene are required to moderate the rate of polymerization by consuming the excess of nitroxide produced by termination. They found that when the ratio of styrene in the monomer feed is high, copolymerization with non-styrene based monomers is possible, but if the styrene feed level decreases then the rate of polymerization decreases and then co-monomer consumption is incomplete [17]. Burguiere *et al*. [18], reported that polymerization of methacrylate with nitroxides did not proceed in a controlled fashion. This could be attributed to the ratio of the rate of decomposition of the chain end to the rate of recombination prevented in a controlled reaction. They concluded that the only way to overcome this deficiency would be to alter the structure of the nitroxide to such an extent that the chain end functionality is maintained. Baumert and Mulhaupt [19], reported on the synthesis of copolymers of styrene with acetonitrile (AN), using 4,4'-azobis(4-cyanopentanecarboxylic acid) as an initiator.

On the other hand, Cai *et al*. [20], reported the synthesis of random copolymers of styrene and methyl methacrylate with a hydroxyl group at one end and a carboxyl group at another, using 4,4'-azobis(4-cyanovaleric acid) and 4-hydroxyl-2, 2, 6, 6-tetramethyl-1-piperidinyloxy. The latter copolymers were deposited on the surface of a silicon wafer by the reaction between the hydroxyl end group of the copolymer and the wafer. They found that polymerization proceeds in a controlled fashion and with low polydispersity index (<1.3), even at a low styrene content in the monomer feed. Nitroxide-mediated polymerization could be considered as an easy and effective method for the synthesis of block copolymers.

Generally, there are two classes of azo-compound namely, the dialkyldiazenes **(5)** and the dialkyl hyponitrites **(6)**.

$$R—N{=}N—R' \qquad\qquad R—O—N{=}N—O—R'$$
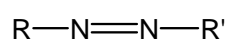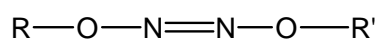
$$\textbf{(5)} \qquad\qquad\qquad\qquad\qquad \textbf{(6)}$$

Dialkyldiazenes can be decomposed thermally or photochemically and used as initiators for the radical polymerization. The most commonly encountered are the azonitriles, these include 2,2'-azobis (2-methylpropanenitrile), which is more commonly known as isobutyronitrile or (AIBN) (**1**) [4].

4,4'-Azobis (4-cyanovaleric acid) (**7**) is considered as a water-soluble azo compound. It is decomposed in benzene or toluene solvent in a temperature range from 37-105 $^{\circ}$C with an activation energy of about 131.7 kJ mol^{-1} [21].
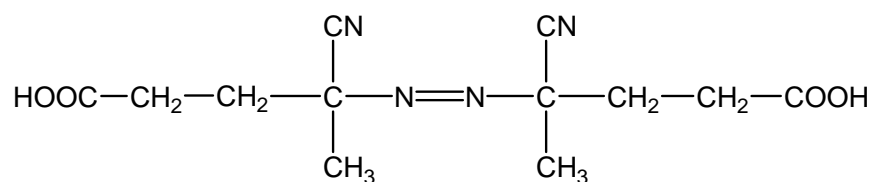
(**7**)

The azo compound's structure affects their efficiency to generate radicals and it shows a λ_{max} in the range 350-370 nm. Azo compounds are therefore potential photoinitiators. As a consequence, it is very important to avoid exposing a polymerization mixture to excessive light during its preparation, when dialkyldiazens are used as thermal initiators [3,21].

The hyponitrites (**6**), esters of hyponitrous acid (HO-N=N-OH), are low temperature sources of alkoxy or acyloxy radicals. However, the utilization of hyponitries as initiators of polymerization is very limited due to difficulties in synthesis and commercial availability [3, 21].

4.1.3 Thermoplastic elastomers

Thermoplastic elastomers (TPEs) such as styrenic block copolymers are used in different applications such as coatings, adhesions, and sealants. On the other hand, the polyurethane/elastomer, polyester/elastomer, and polyamide/elastomer block copolymers are used in different applications such as body implants, and the replacement of glass bottles for use in the medical environment [22]. Thermoplastic

elastomers are copolymers of the type ABA or AB, where A and B are the hard and the soft segment, respectively. An advantage of thermoplastic elastomers is that it allows rubber-like articles to be produced by rapid processing techniques developed by the thermoplastics industry [22]. Thermoplastic elastomers can be processed by conventional thermoplastic processes (such as extrusion and molding) and in their final state have performance properties similar to those of thermosets. TPEs reduce waste disposal problems because they can be recycled many times without significant loss of properties [22]. This type of block copolymer has the potential to exhibit a wide variety of new physical or chemical characteristics depending on the combination of the natures of the polymer segments chosen. PMMA-PECH block copolymers can be used as TPEs and in many different applications, such as adhesives and paint.

Energetic thermoplastic elastomers are applied in different advanced applications such as air bag system, aerospace and propellant formulations [23]. Energetic binders based on cyclic ethers (oxirane, oxetane derivatives) have advantages over inert binders such as hydroxyl terminated polybutadiene (HTBP). They are considered as promising candidates for energetic binders in future composite propellants [24]. Materials that have the ability to liberate large amounts of H_2, N_2, CO, and gaseous hydrocarbons on burning are needed for the propellant formations. Conventional binders used in propellants depend on the curing of elastomers with the isocyanate throughout urethane reaction, with the disadvantage of toxic HCN evolution, presence of moisture, and difficulty in controlling the curing reaction [25]. These parameters make it difficult to achieve reproducibility in the final product properties from batch to batch. This could lead to a high dissimilarity in the final product properties. Modification of these polymer properties either by changing the backbone structure or by copolymerization with other monomers represents a suggested solution for these problems [25]. Eroglu *et al.* [26], reported the synthesis of a block copolymer of styrene and vinyl acetate with poly(epichlorohydrin) and poly(glycidyl azide) using

4,4'-azobis(4-cyanopentanoyl chloride) (ACPC) as a nitroxide-mediated polymerization. PMMA as hard segment characterized with high oxygen content, where GAP segment posses energetic decomposition and combination of both segments will form an excellent binder. Usually, ammonium nitrate (AN) is used as an oxidizing agent and as it crystallizes, it tends to affect the stability of the formulation. This problem could lead to the catastrophic rocket motor failure [25]. Alteration in the polymer structure could lead to a different interaction with the rest of formulation ingredients, which will affect the mechanical properties of the final product. Also, changes in the chemical composition of the binder will play a significant role in the combustion properties of the binder, which again will play a significant role in the final properties and performance of a formulation.

4.1.4 Objectives

The main objective of this part of the study was to prepare poly(methyl methacrylate-*b*-epichlorohydrin) (PMMA-*b*-PECH) and poly(methyl methacrylate-*b*-glycidyl azide) (PMMA-*b*-GAP) copolymers. This objective was achieved by two steps. In the first, 4,4'-azobis (4-cyanopentanoyl chloride) was synthesized by reaction of 4,4' azobis (4-cyanopentanoyl acid) with thionyl chloride. Hydroxyl terminated poly(epichlorohydrin) (PECH-diols) and glycidyl azide polymer (GAP-diols) were then reacted with 4,4'-azobis (4-cyanopentanoyl chloride) to yield a macro-azo-initiator. This macro-azo-initiator was used in the polymerization of methyl methacrylate (MMA) monomer to yield (PMMA-*b*-PECH) and (PMMA-*b*-GAP) copolymers.

4.2 Experimental

4.2.1 Materials

4,4' azobis (4-cyanopentanoyl acid) (purity >98%) was purchased from Fluka and used without further purification, as were thionyl chloride and sodium azide. PECH-

diols was produced from a cationic ring-opening polymerization under the following conditions: toluene as solvent; 1, 4-butanediol as initiator; borontrifluoride etherate (BF$_3$-etherate) as catalyst; and [ECH]/[Diol] = 50 (see also Chapter 2, Section 2.3.1). The GAP-diols was synthesized via nucleophilic substitution reaction of PECH-diols with sodium azide in dimethyl formamide (DMF), as described in literature [25, 28] (see also Chapter 3, Section 3.3.1). Dichloromethane (DCM) and chloroform were purified by following standard procedures. Methanol, Magnesium sulfate, and calcium choride were obtained from Saarchem. Methyl methacrylate was first washed with a 0.3 M KOH solution to remove inhibitor, distilled under reduced pressure, and then stored over molecular sieves (5A) in a refrigerator until use (preferably with in 1 week). All purified solvents and reagents were stored over molecular sieves.

4.2.2 Analytical equipments and methods

3.2.2.1 UV, FTIR, NMR, GPC, and DSC analyses

Equipment description and analysis methods applied for the UV, FTIR, NMR, GPC, and DSC are given in Chapter 2, Section 2.2.2. TGA equipment description and analysis method provided in Chapter 3, Section 3.2.2.

4.2.3 Experimental techniques

4.2.3.1 Synthesis of 4,4'-azobis (4-cyanopentanoic chloride)

A three-neck flask equipped with a dropping funnel and a condenser with a calcium chloride guard tube in the top was used for the synthesis of ACPC. (*Note*, the calcium chloride guard tube must be connected directly to the top of the fume hood in order to extract all toxic gases, such as SO and SO$_2$, generated from the reaction). Chlorination of the carboxylic acid to the acid chloride was performed using thionyl chloride, in dry dichloromethane as solvent. First, 4,4'-azobis (4-cyanopentanoic acid) (1.5 g, 5.35 mmol) was dissolved in 30 mL of freshly distilled dichloromethane and solution stirred for about 1 hr at room temperature. The reaction flask was then cooled in an ice bath and thionyl chloride (1.9 g, 16 mmol) was added dropwise to the

reaction flask using a dropping funnel. The reaction mixture was stirred at room temperature for 2 hr. Then the temperature was raised to 35 ^{o}C for another 12 hours. Solvent were removed under reduced pressure, using a rotary evaporator. The product was used in the next reaction. **Scheme 4.3** shows the proposed method for synthesis of ACPC.
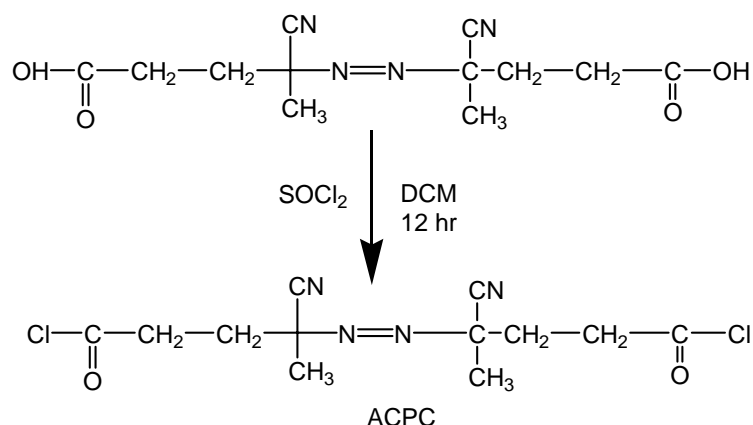
Scheme 4.3 Preparation of 4,4'-azobis (4-cyanopentanoic chloride) acid by the reaction of 4,4'-azobis (4-cyanopentanoic acid) with thionyl chloride.

4.2.3.2 Synthesis of poly(epichlorohydrin) macro-azo-initiator

The attachment of 4,4'-azobis (4-cyanopentanoic chloride acid) to poly(epichlorohydrin)-diols was achieved by an esterification reaction between the hydroxyl groups of the PECH-diol and the acid chloride groups of ACPC. A dry 250 mL round-bottomed flask, fitted with a magnetic stirrer and a reflux condenser with a calcium chloride guard tube was charged with PECH-diols (10 g, 5 mmol), triethylamine (5 mmol), and 100 mL of chloroform and stirred for about 1 hr at room temperature. The reaction flask was then cooled in an ice-water bath at -5 ^{o}C and ACPC (0.75 g, 2.5 mmol) in about 20 mL of chloroform was added dropwise by using dropping funnel. The reaction mixture was stirred for another 3 hours in the ice bath. The reaction mixture was then heated to 30-35 ^{o}C and left to stir overnight, in the dark. After that, the reaction mixture was filtered and washed with 15 wt% aqueous HCl. The organic layer was collected and dried over magnesium sulfate. Finally, the

PECH-macro-azo-initiator (PECH-MAI) was obtained by evaporating the solvent using a rotary evaporator (*Note*, in all steps the containers of the reaction mixture and product were protected from exposure to direct light as far as possible by covering the glassware with aluminum foil, in order to prevent photodegradation).   The product color changed from colorless to pale yellowish and an increase in its viscosity was noticed.   The macro-azo-initiator was stored in a refrigerator to avoid thermal decomposition. The yield of the reaction was about 80% and the final product was also characterized by using FTIR and NMR spectroscopy. **Scheme 4.4** shows the reaction used for the synthesis of PECH-MAI. There is a possibility that MAI will attach to both terminals of PECH or only one side. Therefore; it is expected to have more than one mixture of macro-azo-initiators not only what is presented in Scheme 4.4.

^{1}H-NMR (CDCl$_3$): δ= 1.25 ppm [CH$_2$ of 1, 4-butanediol], δ= 1.6 ppm [CH$_3$ of ACPC], δ= 2.3-2.7 ppm [CH$_2$ of ACPC], δ= 3.65-3.7 ppm due to protons of methylene, methane, and chloromethyl units of PECH. ^{13}C-NMR (CDCl$_3$): δ= 23 ppm [CH$_3$ of ACPC], δ= 26 ppm [CH$_2$ of 1,4-butanediol], δ= 51 ppm [CH$_2$ of ACPC], δ= 46 ppm [CH$_2$Cl of PECH], δ= 70 ppm [CH$_2$ of PECH] δ= 71 ppm [C of ACPC], δ= 78 ppm [CH of PECH], δ= 117 ppm [CN of ACPC], δ= 175 ppm [C=O of ACPC]. FTIR (NaCl): 2906 (s, CH$_2$, CH), 2866 (s), 1730 (s, C=O), 1752 (w), 1428 (s), 1341 (w), 1270 (s), 1130 (s, –C–O–C–), 975 (w), 745 (s, –CH$_2$Cl$_2$), 617 cm^{-1}(w).
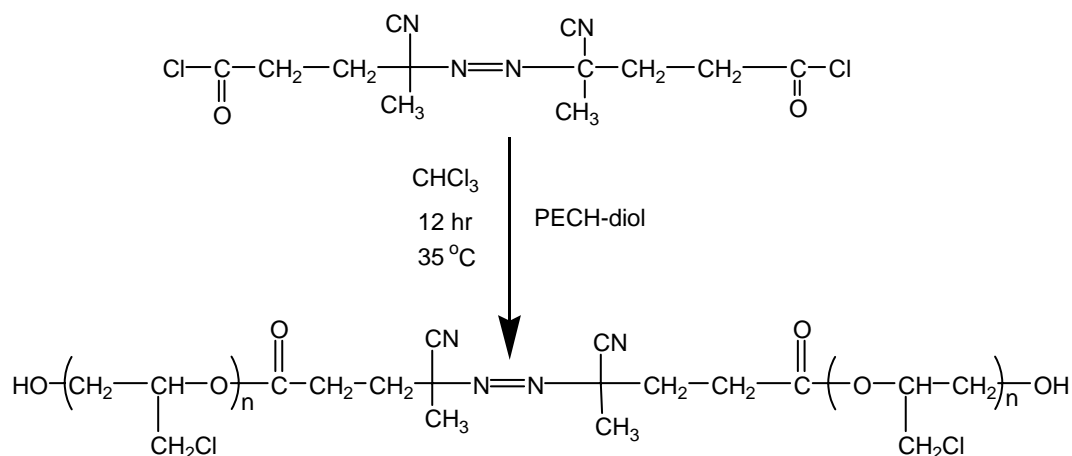
Scheme 4.4 Preparation of poly(epichlorohydrin)-macro-azo-initiator by the reaction of PECH-diols with 4,4'-azobis (4-cyanopentanoyl chloride).

4.2.3.3 Synthesis of glycidyl azide polymer macro-azo-initiator

Glycidyl azide polymer-maro-azo-initiator (GAP-MAI) was prepared using the same procedure similar to that used for the preparation of PECH-MAI. After the removal of the solvent by evaporation, the product color changed from slightly yellow to brown. **Scheme 4.5** shows the reaction for the synthesis of GAP-MAI. There is a possibility that MAI will attach to both terminals of GAP or only one side from diols. Therefore; it is expected to have more than one mixture of macro-azo-initiators not only what is represented in scheme 4.5. The yield of was about 82%.

^{1}H-NMR (CDCl$_3$): δ= 1.27 ppm [CH$_2$ of 1, 4-butanediol], δ= 1.66 ppm [CH$_3$ of ACPC], δ= 2.3-2.7 ppm [CH$_2$ of ACPC], δ= 3.2-3.9 ppm [CH, CH$_2$, CH$_2$N$_3$ of GAP].

^{13}C-NMR (CDCl$_3$): δ= 23 ppm [CH$_3$ of ACPC], δ= 26 ppm [CH$_2$ of 1,4-butanediol], δ= 51 ppm [CH$_2$ of ACPC], δ= 52-55 ppm [CH$_2$N$_3$], δ= 70 ppm [CH$_2$] δ= 71 ppm [C of ACPC], δ= 78-80 ppm [CH], δ= 117 ppm [CN of ACPC], δ= 175 ppm [C=O of ACPC]. FTIR (NaCl): 2906 (s), 2866 (s), 2100 (s, –CH$_2$N$_3$), 1730 (s,C=O), 1658 (s), 1440 (w), 1375 (s), 1285 (s), 1100 (s, –C–O–C–), 930 (w), 714 (w), 660 cm^{-1} (w).
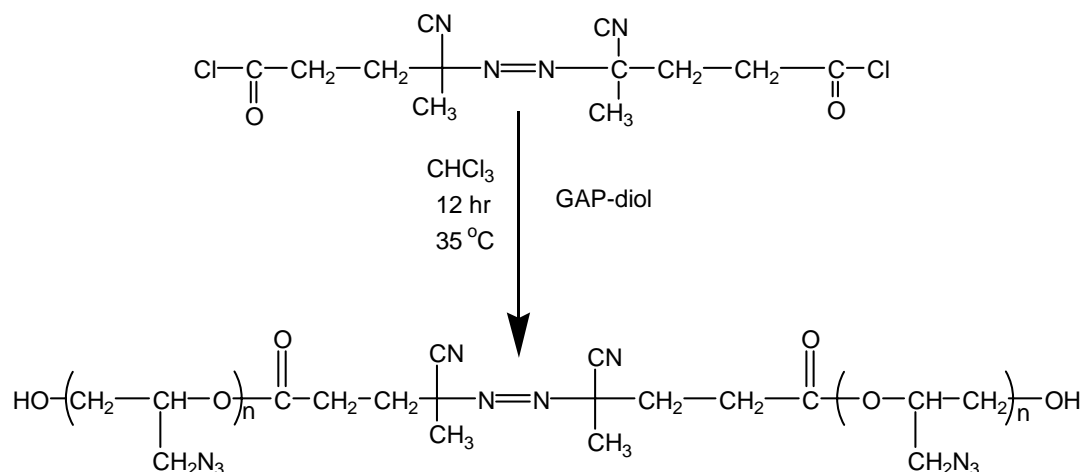
Scheme 4.5 Preparation of glycidyl azide polymer-macro-azo-initiator by the reaction of GAP-diols with 4,4'-azobis (4-cyanopentanoyl chloride).

4.2.3.4 Polymerization of methyl methacrylate in the presence of macro-azo-initiators

Polymerizations were performed in close ampoules. A mixture of macro-azo-initiator either PECH-MAI or GAP-MAI, MMA monomer, and toluene were placed in an ampoule and purged with nitrogen for about 10 min. After degassing, the ampoule was immersed in an oil bath at 80 $^\circ$C for a different period. The polymerization reaction was terminated by rapid cooling and the polymer was precipitated in methanol. Conversions were determined gravimetrically. The conversion samples were taken at a specific time via a syringe (2 mL) and poured into aluminum plates. The plates were left to dry in a fume hood, for over night to allow evaporating of the solvent. Then, the drying was completed in a vacuum oven at 40 $^\circ$C for 24 hours. **Scheme 4.6** shows the proposed reaction for the polymerization of MMA in the presence of macor-azo-initiator.
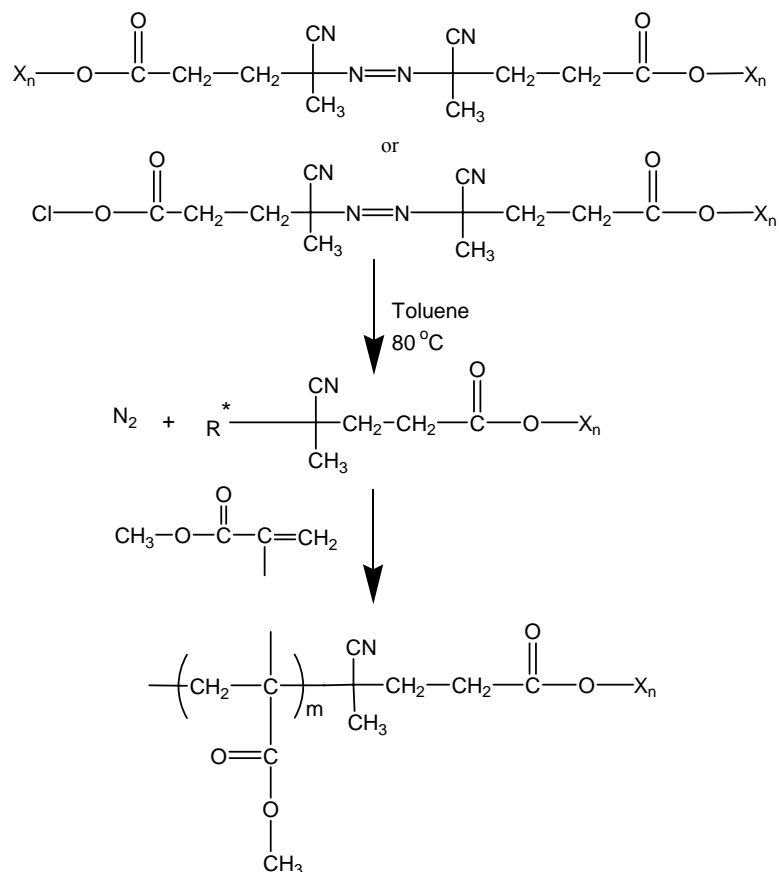
Scheme 4.6 Schematic representation of the polymerization of methyl methacrylate using a macro-azo-initiator, where X can be poly(epichlorohydrin) or glycidyl azide ealstomer.

4.3 Results and discussion

4.3.1 Poly(methyl methacrylate-*b*-epichlorohydrin)

This part includes results and discussion for the synthesis of poly(epichlorohydrin) - 4,4'-azobis (4-cyanopentanoyl chloride) as macro-azo-initiator, polymerization of methyl methacrylate in the presence of poly(epichlorohydrin)-macro-azo-initiator, and thermal analysis of poly(methyl methacrylate–*b*-epichlorohydrin).

4.3.1.1 Synthesis of poly(epichlorohydrin) - 4,4'-azobis (4-cyanopentanoyl
      chloride) as macro-azo-initiator

The attachment of ACPC to PECH-diol was achieved by means of an esterification reaction and **Figure 4.2** shows the FTIR spectrum of product. The absorption peak of an ester group is seen at about 1730 cm^{-1}. Chloromethyl and ether linkage groups of PECH appear at about 745 and 1120 cm^{-1}, respectively. This spectrum shows that ACPC is attached to the PECH through esterification of the OH group as can be seen from transmittance of OH group at about 3400 cm^{-1}. The peak becomes smaller and there is slight shift of the hydroxyl group peak.
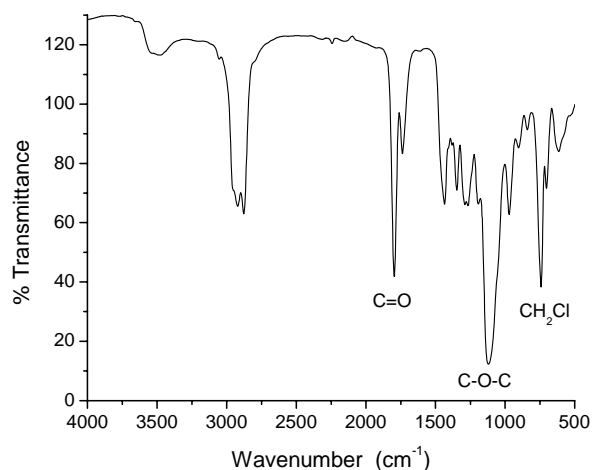
Figure 4.2 FTIR (NaCl) spectrum of poly(epichlorohydrin) after reaction with 4,4'-azobis (4-cyanopentalyl chloride) to obtained poly(epichlorohydrin)-macro-azo-initiator.

The ^{1}H-NMR spectrum of PECH-MAI is shown in **Figure 4.3**. The signals at about 1.26 and 2.3-2.7 ppm are attributed to the CH_3 and CH_2 groups of azobis cyanopentanoyl, respectively. The signal at about 1.6 ppm could be attributed to the 1, 4-butanediol and the signals at 3.6-3.8 ppm correspond to the CH_2, CH, and CH_2Cl of PECH. These results give further conformation that 4,4'-azobis (4-cyanopentanoyl chloride) was attached to the PECH-diols and formed the macro-azo-initiator. This

PECH-MAI was used after purification in the polymerization of MMA monomers to yield PMMA-*b*-PECH copolymers.
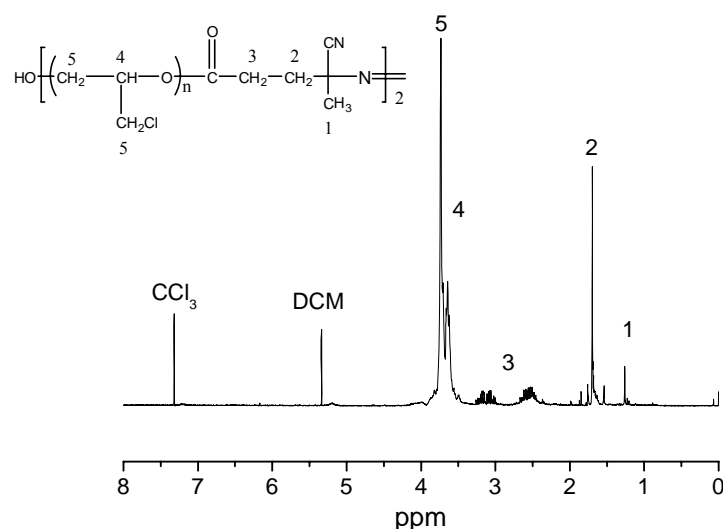
Figure 4.3 ^{1}H-NMR (CDCl$_3$) spectrum of poly(epichlorohydrin) after reaction with 4,4'-azobis (4-cyanopentalyl chloride) to obtained poly(epichlorohydrin)-macro-azo-initiator.

4.3.1.2 Polymerization of methyl methacrylate in the presence of poly(epichlorohydrin)-macro-azo-initiator

PECH-MAI was used in the solution polymerization of MMA to obtain block copolymers with PECH segments. The effect of using different amounts of PECH-MAI in the polymerization of MMA was studied and results are recorded in **Figure 4.4**. When a high concentration of PECH-MAI was used in the polymerization, the polymer yield increased. This could be attributed to the presence of a high number of initiation sites, which could increase the yield of polymerization. This result is in agreement with earlier finding of Eroglu *et al.* [28]. They found that the presence of a high macro-azo-initiator concentration in the polymerization of methyl methacrylate is directly proportional to a higher polymer yield.
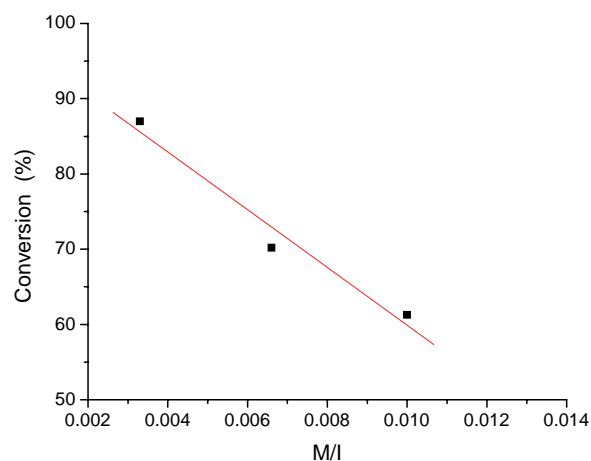
Figure 4.4 Effect of monomer-to-initiator mole ratio (M/I) used on the yield of polymerization. (Polymerization conditions: monomer MMA, 1 g; toluene as solvent, temperature 80 $^{\circ}$C, and reaction time 3 hr.)

The effect of the ratio of MAI to monomer used on the molecular weight and polydispersity was investigated and results are recorded in **Figure 4.5**. The more MAI is used, the lower the molecular weight will be, but polydispersity index did not change considerably. In all cases, the polydispersity index was less than 1.7. The highest molecular weight was about 35 000 g/mol and the lowest was about 20 000 g/mol. Low polydispersity and the change in the molecular weight with a change in the ratio of MAI to monomers gives an indication about the possibility to control the polymerization. This variation in the molecular weight will affect the physical and chemical properties of PMMA-*b*-PECH copolymers due to the different percentages of elastomers and thermoplastic segments.
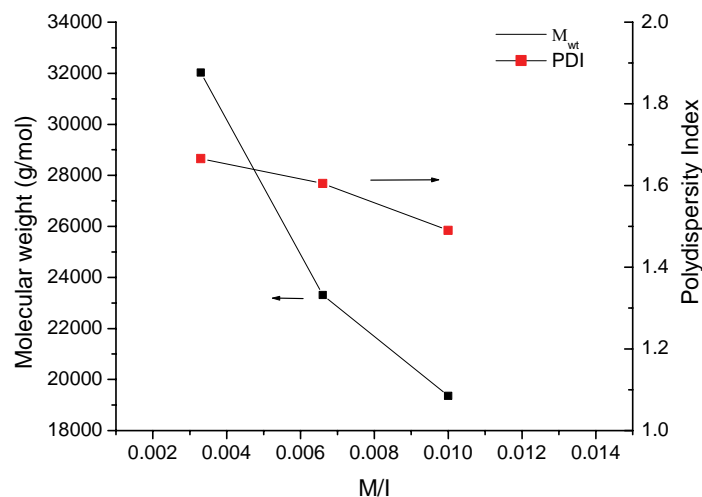
Figure 4.5 Effect of monomer-to-initiator ratio used in the polymerization on the molecular weight and polydispersity index of the final product obtained. (Polymerization conditions: toluene as solvent, temperature 80 ^{o}C, and reaction time 3 hr.)

The chromatograms of the product from the conversion plates and the product obtained from polymerization solution after being precipitated, washed several times with methanol are shown in **Figure 4.6**. These normalized chromatograms show that unreacted macro-initiator was removed, where (A) shows the PECH-MAI, (B) shows PMMA-*b*-PECH from the conversion plates, and (C) shows PMMA-*b*-PECH precipitated in methanol. The chromatograms show that the most of PECH-MAI was removed from the product by precipitation in methanol. The slight shoulder could be attributed to the cross-linked PECH-MAI or homo-PMMA.

The FTIR spectrum in **Figure 4.7** shows characteristic bands of the different polymer segments in the PMMA-*b*-PECH copolymers. Absorption at about 745cm^{-1} corresponds to the CH$_2$Cl in PECH segment, while the absorption band at about 1725cm^{-1} is attributed to the carbonyl group (C=O) of the PMMA segments.
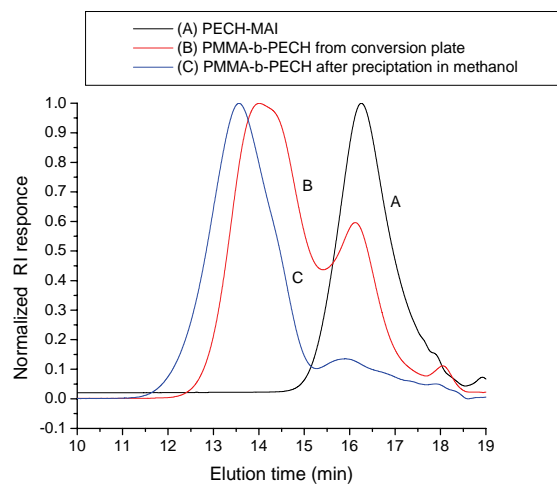
Figure 4.6 GPC profiles of (A) PECH-MAI, (B) PMMA-*b*-PECH copolymers from the conversion plates and (C) PMMA-*b*-PECH copolymers precipitated in methanol. (Polymerization conditions: [PECH-MAI]/ [MMA] = 0.0033, toluene as solvent, temperature 80 $^{\circ}$C, and reaction time 3 hr.)
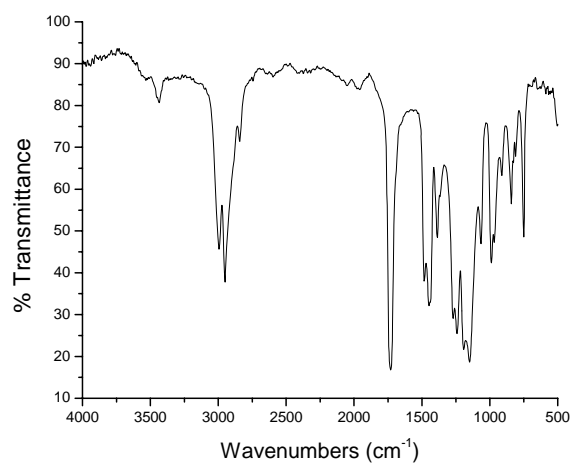
Figure 4.7 FTIR spectrum of poly(methyl methacrylate-*b*-epichlorohydrin) copolymers obtained by thermal polymerization of MMA in the presence of poly(epichlorohydrin)-macro-azo-initiator.

The ^{1}H-NMR spectrum of PMMA-*b*-PECH block copolymer is shown in **Figure 4.8**. The methoxy, methylene, and methyl proton signals due to PMMA segments appear

at about 3.6, 2.0-1.5, and 1.1-0.7 ppm, respectively. On the other hand, the small signal at about 4 and 1.7 ppm are attributed to the chloromethyl group and the methylene of PECH. The other assignments are indicated in the figure. The low intensity of the PECH peaks is attributed to high percentage of PMMA in the final product compared to the PECH elastomers.

Figure 4.9 shows the ^{13}C-NMR spectrum of PMMA-*b*-PECH copolymers. An important feature of this spectrum is absorption at about 177 ppm which is attributed to the carbonyl group of the PMMA segment. There is a small peak at about 45 ppm, which could be attributed to the chloromethyl group of PECH. The rest of the assignments are indicated in the figure.
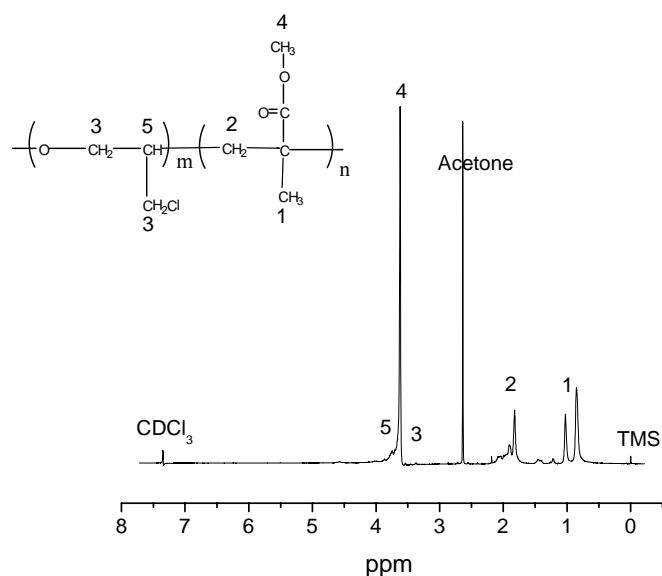
Figure 4.8 ^{1}H-NMR (CDCl$_3$) spectrum of poly(methyl methacrylate-*b*-epichlorohydrin) copolymers prepared by thermal polymerization of MMA in presence of poly(epichlorohydrin)-macro-azo-initiator.
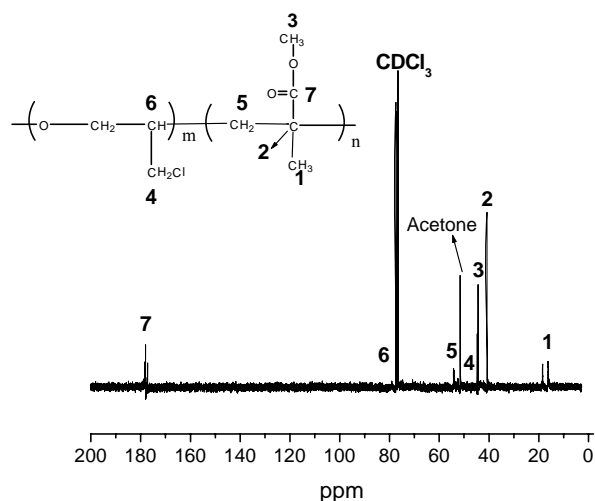
Figure 4.9 ^{13}C-NMR (CDCl$_3$) spectrum of poly(methyl methacrylate-*b*-epichlorohydrin) copolymers prepared by thermal polymerization of MMA in presence of poly(epichlorohydrin)-macro-azo-initiator.

4.3.1.3 Thermal analysis of poly(methyl methacrylate-*b*-epichlorohydrin)

Differential scanning calorimetry was used to determine the glass transition temperature of the block copolymers. **Figure 4.10** shows DSC analysis of the copolymer prepared using the macro-azo-initiator. There was no clear glass transition temperature (T$_g$) detected for the PMMA-*b*-PECH copolymers. Actually, it was very difficult to detect the glass transition temperature from the DSC of copolymer and a slight change can be seen at about 80 $^{\circ}$C, which is between the T$_g$ of two different segments. This could be attributed to the miscibility of two different segments with each other. This will be discussed in more details in the next chapter, when results of the thermal behaviour of different blend systems is presented (for more details see Chapter 5).
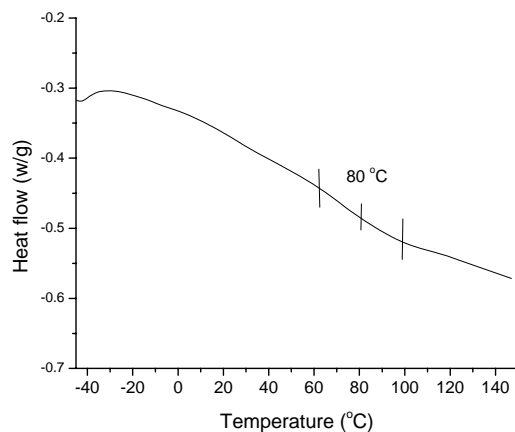
Figure 4.10 DSC thermogram of poly(methyl methacrylate-*b*-epichlorohydrin) copolymers.

TGA analysis of the PMMA-*b*-PECH copolymers showed two steps in the thermal degradation profile, as can be seen in **Figure 4.11**. The first degradation starts at about 136 ^{o}C up to about 298 ^{o}C, where about 10% of product degraded. This part of the degradation could be attributed to the PECH. The second degradation step starts at about 298 ^{o}C. This attributed to the PMMA main chains. Usually, the thermal degradation of pure PMMA has three distinctive steps [1]. The first is due to the decomposition of relatively weak head-to-head linkage, impurities, and solvents in the lattices. The second is due to the chain-end of PMMA, and the third is due to the PMMA main chain decomposition. The three degradation steps of pure PMMA are at about 167, 278, and 329 ^{o}C, respectively [1]. In pure PMMA the first decomposition weight loss usually does not exceed 2%, whereas in the case of PMMA-*b*-PECH copolymers there was about 13% weight loss. This could be attributed to the presence of PECH segment. This result provided further conformation for the presence of PECH segment on the polymer as high degradation in the first stage was noticed.
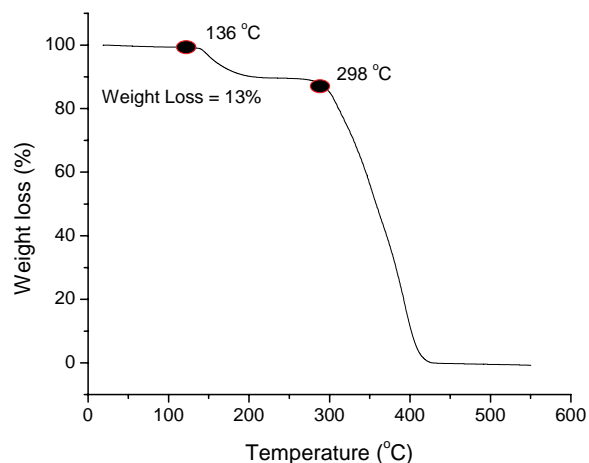
Figure 4.11 TGA analysis of poly(methyl methacrylate-*b*-epichlorohydrin) copolymers.

4.3.2 Poly(methyl methacrylate-*b*-glycidyl azide) copolymers

When GAP elastomers are attached to other polymers, the final product will possess an energetic nature due to the presence of N_3 group, which decompose exothermically above 200 ^oC [24]. This section describes the results for the synthesis of GAP-MAI, the polymerization of MMA in the presence of GAP-MAI, and the characterizations of PMMA-*b*-GAP copolymers as an energetic thermoplastic elastomer.

4.3.2.1 Synthesis of glycidyl azide- 4,4'-azobis (4-cyanopentanoyl chloride) as macro-azo-initiator

The success of the poly(condensation) reaction of GAP-diol with ACPC to the obtained GAP-MAI was confirmed by FTIR and NMR analyses. **Figure 4.12** shows the FTIR spectrum of GAP-MAI. The most important absorbance peaks appeared at about 1730 cm^{-1}, due to the carbonyl group from ACPC, and at about 2100 cm^{-1} due to the azide group. A decrease in the transmittance of the hydroxyl group at 3400cm^{-1} and a slight shift, after the reaction of GAP with ACPC, was also evident. The ^{1}H-NMR spectrum of GAP-MAI is shown in **Figure 4.13**. The signal at about 1.2 ppm is

attributed to the 1,4-butanediol. Signals of the protons methyl (CH_3) and methylene (CH_2) groups of the azobis cyanopentanoyl appear at about 1.6 and 2.5 ppm, respectively. Azide group protons peaks (CH_2N_3) and the methylene protons of the polyether chain appear at about 3.2-4 ppm. The rest of assignments are indicated in the figure.
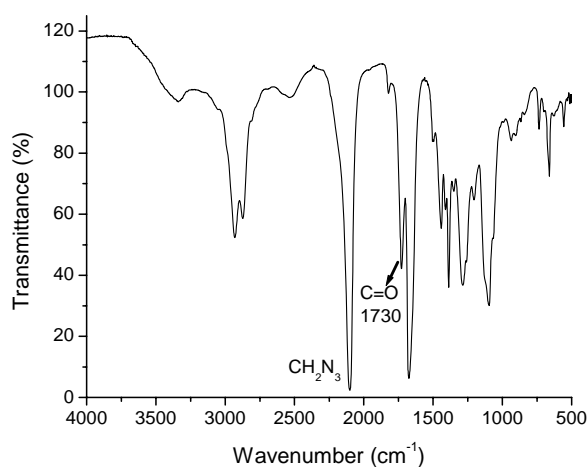
Figure 4.12 FTIR spectrum of glycidyl azide polymer after reaction with ACPC to yield glycidyl azide polymer-maro-azo-initiator.
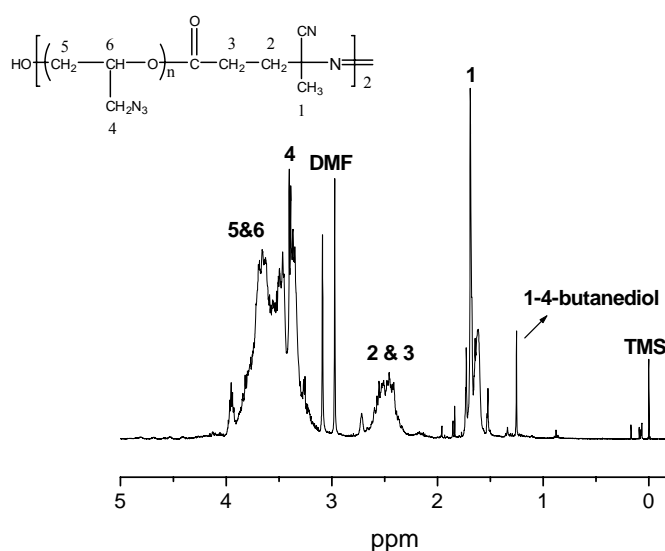
Figure 4.13 ^{1}H-NMR (CDCl$_3$) spectrum of glycidyl azide polymer-maro-azo-initiator.

The ^{13}C-NMR spectrum of GAP-MAI is shown in **Figure 4.14**. Peaks at about 52 and 116 ppm, were attributed to the azide group and carbonyl group of the azo compound, respectively. The peak at about 115 ppm was attributed to the CN of the azo compound. The rest of the assignments are indicated in the figure.
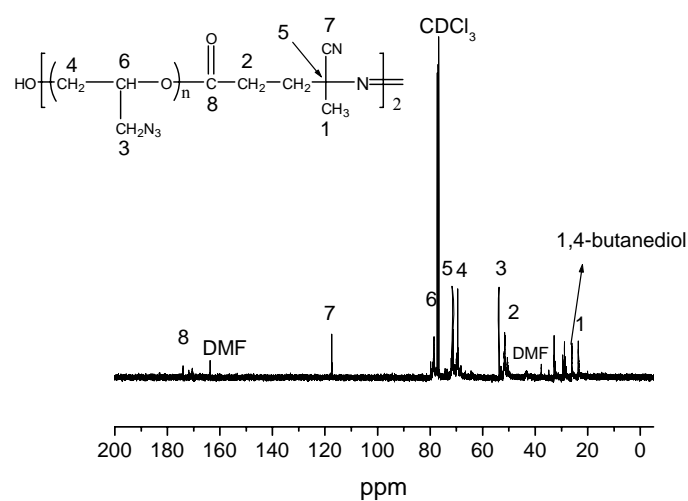
Figure 4.14 ^{13}C-NMR (CDCl$_3$) spectrum of glycidyl azide polymer-maro-azo-initiator.

FIIR and NMR data provided proof of the attachment of 4,4'-azobis (4-cyanopentanoyl chloride) (ACPC) to the GAP and the formation of MAI. GAP-MAI was used in the subsequent polymerization of MMA, the results of which are reported below.

4.3.2.2 Polymerization of MMA in the presence of glycidyl azide polymer-macro-azo-initiator

GAP-MAI was used in the solution polymerization of MMA to obtain block copolymers having a GAP segment. The effect of using different amounts of GAP-MAI in the polymerization of MMA was studied and the results are presented in **Figure 4.15**. When a high concentration of GAP-MAI was used in the

polymerization, the polymer yield increased. This could be attributed to the formation of a large number of initiation sites during the polymerization and therefore a higher yield. This result is in agreement with previously report results on the effect of using high concentrations of MAI in the polymerization of vinyl monomers [13].
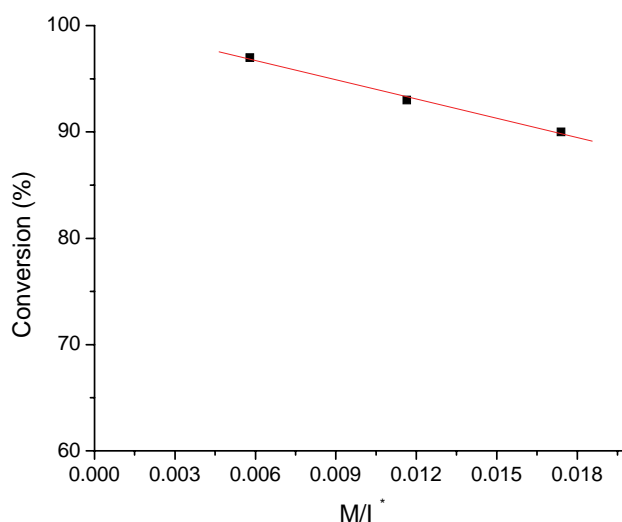
Figure 4.15 Effect of monomer-to-initiator mole ratio (M/I) used on the yield of polymerization. (Polymerization conditions: toluene solvent, temperature 80 ^{o}C, reaction time 3 hr.)

GPC chromatograms of polymers obtained with different mole ratio of M/I are shown in **Figure 4.16**. It is noticed that using a higher concentration of macro-azo-initiator in the polymerization shifts the GPC peak to higher retention times, which means lower molecular weight. This means that the use of a high macro-azo-initiator concentration, leads to a high number of polymer chains, shorter chains, and a higher yield of polymer. Furthermore, the macro-azo-initiator was removed from the product after precipitation in methanol. The slight shoulder could be attributed to homo polymer formed during the thermal polymerization.
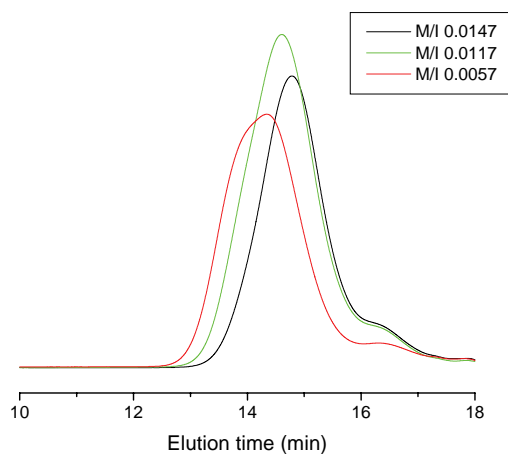
Figure 4.16 GPC chromatograms of poly(methyl methacrylate-*b*-glycidyl azide) copolymers obtained using different mole ratios of glycidyl azide polymer-maro-azo-initiator. (Polymerization conditions: toluene solvent, temperature 80 $^{\circ}$C, and reaction time 3 hr.)

The effect of the ratio of MAI to monomer used on the molecular weight and polydispersity index was investigated and the results are recorded in **Figure 4.17**. The more MAI is used, the lower the molecular weight will be, but polydispersity seems to increase slightly. The polydispersity index was less than 1.7, which gives an indication that polymerization proceeded in a controlled fashion. A similar trend of polydispersity index and M_{wt} was observed in the case of PMMA-*b*-PECH copolymers. The highest molecular weight was about 22 000 g/mol, and the lowest molecular weight was about 15 000 g/mol.
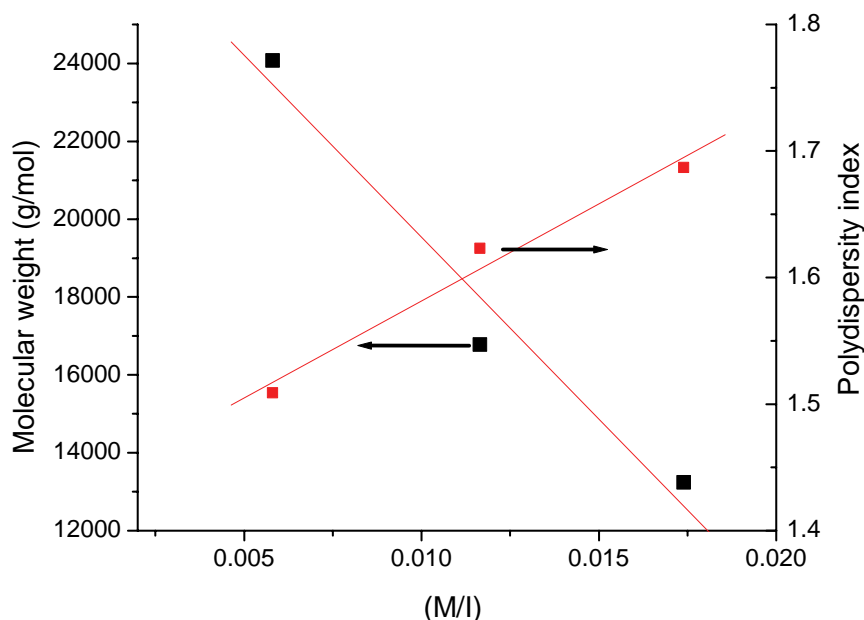
Figure 4.17 Effect of monomer-to-initiator mol ratio used in the polymerization on the molecular weight and polydispersity of final product obtained. (Polymerization conditions: toluene solvent, temperature 80 °C, and reaction time 3 hr.)

The final product of the polymerization was characterized after washing with methanol and drying. Characteristic bands of the different polymer segments in the block copolymer were observed in FTIR spectra. **Figure 4.18** shows the FTIR spectrum of PMMA-*b*-GAP copolymers. Absorption at about 2 100 cm^{-1} corresponds to the N$_3$ of the GAP segment, while the absorption band at about 1 725 cm^{-1} is attributed to the carbonyl group (C=O) of the PMMA segments. This result provides confirmation of the formation of energetic thermoplastic elastomers by using spectroscopy techniques.
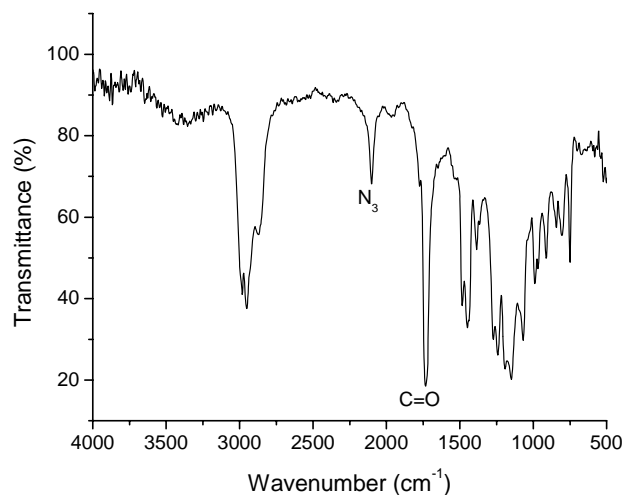
Figure 4.18 FTIR spectrum of poly(methyl methacrylate-*b*-glycidyl azide)
copolymers prepared by the thermal polymerization of MMA in the presence of
glycidyl azide polymer-maro-azo-initiator.

Figure 4.19 shows the ^{1}H-NMR spectrum of PMMA-*b*-GAP copolymers. The
methoxy, methylene, and methyl protons of PMMA segments appear at about 3.6,
2.0-1.5, and 1.1-0.7 ppm, respectively. The small peak at about 3.4 ppm is attributed
to the azido group of GAP. The rest of the assignments are indicated in Figure 4.19.
The ^{13}C-NMR spectrum of PMMA-*b*-GAP copolymers is shown in **Figure 4.20**. The
most characteristic peaks of this spectrum are the peaks at about 179 ppm, which are
attributed to the carbonyl group of PMMA segments. The small peak at about 55 ppm
could be attributed to the azido group of GAP. The rest of the assignments are
indicated in the figure.
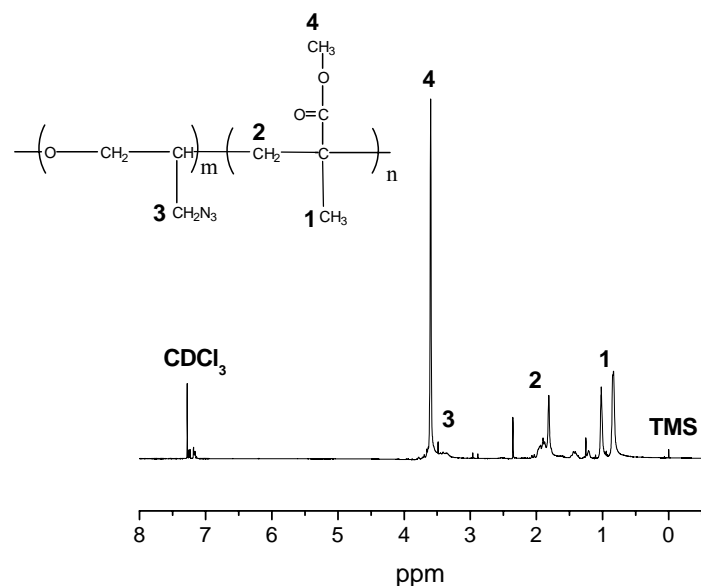
Figure 4.19 ^{1}H-NMR (CDCl$_3$) spectrum of poly(methyl methacrylate-*b*-glycidyl azide) copolymers prepared by thermal polymerization of MMA in presence of glycidyl azide polymer-maro-azo-initiator.
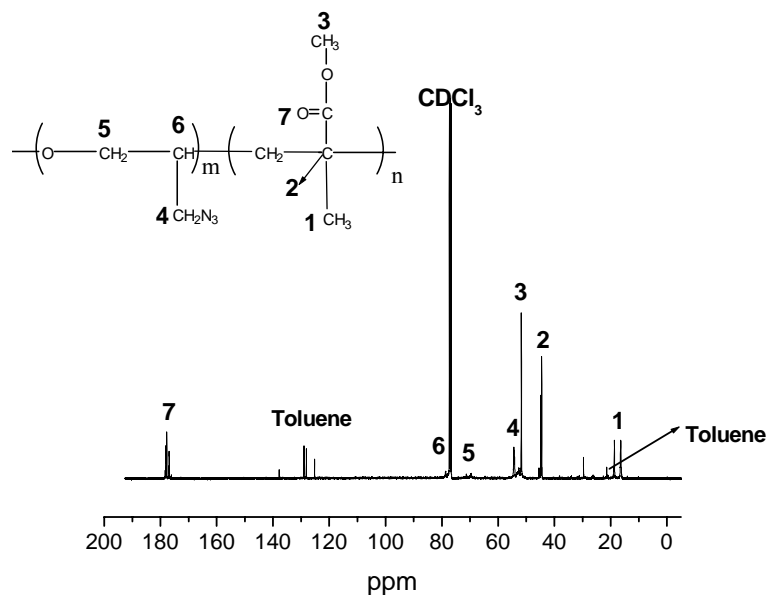
Figure 4.20 ^{13}C-NMR (CDCl$_3$) spectrum of poly(methyl methacrylate-*b*-glycidyl azide) copolymers prepared by thermal polymerization of MMA in the presence of glycidyl azide polymer-maro-azo-initiator.

4.3.2.3 Thermal analysis of poly(methyl methacrylate–*b*-glycidyl azide)

copolymers

Thermal behavior of energetic binder systems is crucial and affects the final formulation. In this work, DSC was used to determine the glass transition temperature of the block copolymers. **Figure 4.21** shows DSC analysis of PMMA-*b*-GAP copolymers. DSC analysis shows a broad glass transition temperature at about 70 ^{o}C. Small transitions at about –30 ^{o}C (GAP) and at about 110 °C (PMMA) can also be detected. It appears that the block copolymer causes some phase separation. It is expected to find two glass transition temperatures due to the two different segments (elastomer and thermoplastic). The appearance of a single T_g could be attributed to the miscibility of two different segments in the system. In the case of three T_gs, it would appear as if there is some miscibility, as well as some phase separation (partial miscibility). In order to clarify this point, the miscibility of two different pairs will be investigated by running thermal analysis (DSC) for blends prepared from different weight ratios of GAP/PMMA (for more details see Chapter 5).
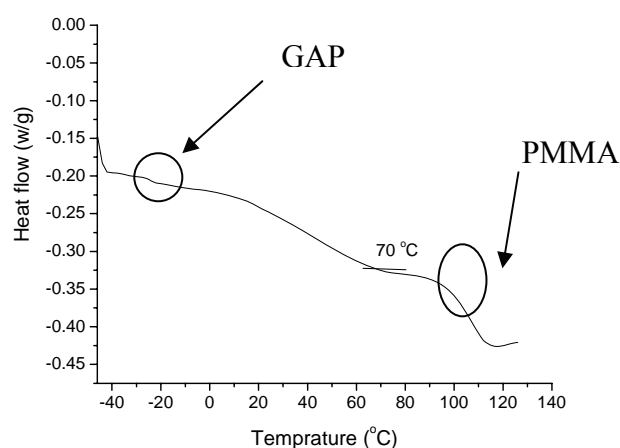
Figure 4.21 DSC thermogram of poly(methyl methacrylate-*b*-glycidyl azide) copolymer.

The decomposition behavior of energetic binders used in propellant formulations is very important and affects the final properties and performance. High temperature DSC analysis of PMMA-*b*-GAP copolymer shows an exothermic decomposition at about 250 $^{\circ}$C (maximum), as can be seen in **Figure 4.22**. This decomposition is attributed to the GAP segments in the copolymer. The figure shows that copolymer decomposition starts at about 175 $^{\circ}$C, which should be considered in order to avoid any explosion during the process. The maximum decomposition temperature of the azido group of GAP was at about 242 $^{\circ}$C (Chapter 3, Section 3.3.1, Figure 3.8). The block copolymer shows maximum decomposition at about 252 $^{\circ}$C, which is higher than that of the homo-GAP and the decomposition behavior was not homogenous, as was the pure GAP. This could be attributed to the effect of the hard segment (PMMA) on hindering the decomposition of the soft segment (GAP) or to the distribution of these energetic parts throughout the polymer chains. The energy released during the decomposition was about 213 J/g, which is lower than the energy released by energetic thermoplastic elastomers prepared based on the urethane reaction described in Chapter 3, Section 3.3.2.2.
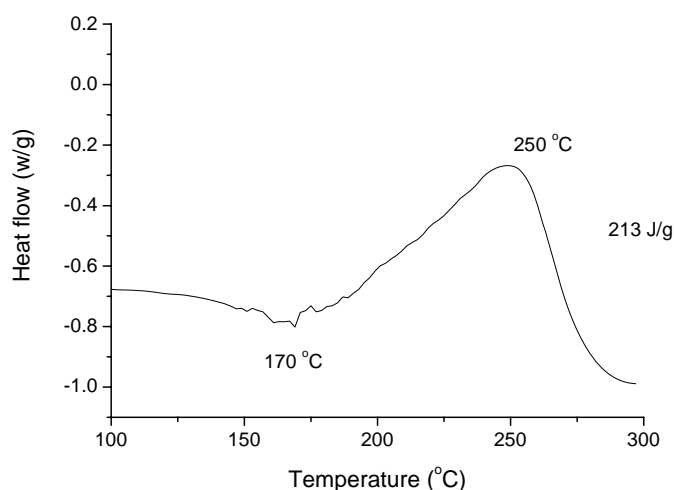
Figure 4.22 DSC thermogram of poly(methyl methacrylate-*b*-glycidyl azide) copolymer.

PMMA-GAP copolymer was carried by TGA and its thermal degradation showed two steps as can be seen in **Figure 4.23**. The first degradation starts from about 220 ^{o}C up to 350 ^{o}C, where about 35% of product is degraded. This part of the degradation is attributed to the decomposition of azide groups of GAP chains, impurities, and end chains of PMMA. Elimination of N_3 groups could be the major degradation source in this step. The first degradation of PMMA-GAP is higher than the first degradation step of PMMA-*b*-PECH by about 170%. This could be attributed to the exothermic decomposition nature of the energetic segment (azide groups), which could enhance the degradation of other parts from the copolymer. The second degradation could be attributed to the PMMA main chains. Thermal analysis results of DSC and TGA provide further confirmation of the presence of an azido group of energetic elastomers in the final binder system, as can be seen from the exothermic decomposition and degradation behavior at temperature about 200 ^{o}C.
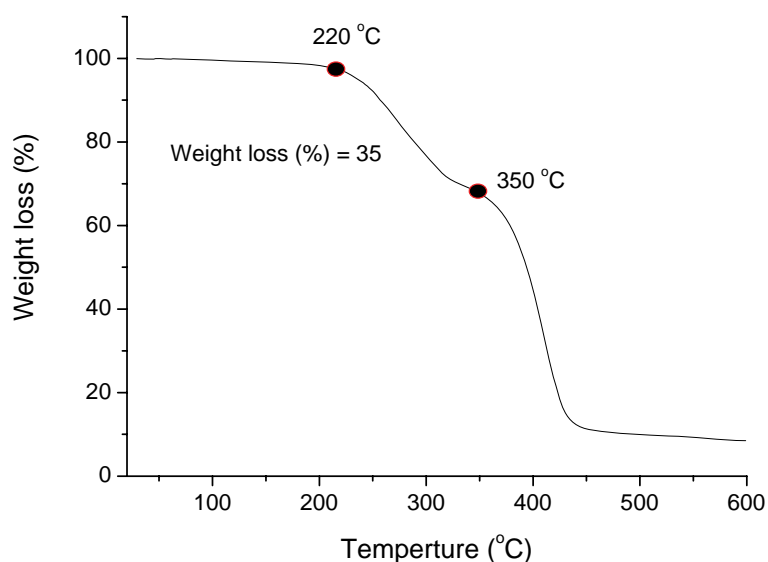
Figure 4.23 TGA analysis of poly(methyl methacrylate-*b*-glycidyl azide) copolymer.

4.4 Summery

Syntheses of macro-azo-initiators, namely poly(epichlorohydrin) macro-azo-initiator and glycidyl azide polymer macor-azo-inititoter, were achieved by a polycondensation reaction between terminated hydroxyl groups of elastomers and 4, 4'-azobis (4-cyanopentanoyl chloride), as proved by FTIR and NMR spectroscopy. These macro-azo-initiators were utilized in the thermal polymerization of methyl methacrylate monomer to yield PMMA-*b*-PECH copolymers as thermoplastic elastomers and PMMA-*b*-GAP copolymers as energetic thermoplastic elastomers. Utilization of high concentrations of macro-azo-initiator in the polymerization leads to a higher polymer yield and a lower molecular weight. Spectroscopic analysis by FTIR and NMR confirmed the presence of two different segments in the final binder. Thermal analysis showed that the copolymer has a broad, single glass transition temperature, which could be attributed to the miscibility of two different segments with each other. This miscibility will be investigated later by studying the behavior of a different blending system of PMMA, PECH, and GAP. Thermogravimetric analysis of the binders shows degradation in two different stages. In the case of PMMA-*b*-GAP copolymers, the degradation in the early stage (less than 300 $^{\circ}$C) was higher due to the decomposition of azide group. Finally, thermoplastic elastomers obtained from this work can be used in different applications. PMMA-*b*-PECH copolymer can be used in coating, sealing, nano-composite, and adhesives, where PMMA-*b*-GAP copolymer can be used in propellants, air bag system, and plastic bonded explosives (PBXs).

4.5 References

1. Brandrup J., Immergut E. H., Grulke E. A., Abe A., Bloch D. R., Polymer Handbook, 4th Edition, 1999.

2. Seymour, Carraher's, Polymer Chemistry, Fifth Edition, Marcel Dekker, Inc. 2000, 463.

3. Moad G., Solomon D. H., The Chemistry of Radical Polymerization, 1st Edition, Elsevier 2006.

4. Moad G., Rizzardo E., Thany S. H., Aust. J. Chem 2005, 58, 379.

5. Ishizu K., Khan R. A., Furukawa T., Furo M., J. Appl. Polym. Sci 2004, 91, 3233.

6. Sebenik A., Prog. Polym. Sci 1998, 23, 875.

7. Destarac M., Charmot D., Frank X., Zard S. Z., Macromol. Rapid Commun 2000, 21, 1035.

8. Georges, M. K., Veregin, R. P. N., Kazmaier, P. M., Hamer, G. K., Macromolecular 1993, 26, 2987.

9. Kajiwara A., Matyjaszewski K., Macromolecular 1998, 31, 3489.

10. Guan J., Yang W., J. Appl. Polym. Sci 2000, 77, 2569.

11. Otsu T., J. Polym. Sci. Part A: Polym. Chem 2000, 38, 2121.

12. Jenkins D. W., Hudson S. M., Chem Rev 2001, 101, 3245.

13. Takahashi H., Teda A., Nagai S., J. Polym. Sci. Part A: Polym. Chem 1997, 35, 69.

14. Moad G., Rizzardo E., Solomon D. H., Macromolecular 1982, 15, 909.

15. Yuruk H., Ozdemir A. B., J. Appl. Polym. Sci 1986, 31, 2171.

16. Akira U., Susumu N., J. Polym. Sci. Part A: Polym. Chem 1986, 24, 405.

17. Matyjaszewski K., Davis K. A., Statistical, Gradient, Block and Graft Copolymers by Controlled/Living Radical Polymerizations, Springer 2002, 15-19.

18. Burgnie' C., Dourger M. A., Charleux B., Vairon J. V., Macromolecular 1999, 32, 3883.

19. Baumert M., Mulhaupt R., Macromol. Rapid Commun 1997, 18, 787.

20. Jie C., Li X., Zhiqing M., Zhijun C., Yun L., Xiqun J., Rongshi C., J. Appl. Polym. Sci 2006, 102, 3118.

21. Denisov E. T., Denisova T. G., Pokidova T. S., Handbook of Free Radical Initiators, John Wiley & Sons, Inc. 2003, 303.

22. Holden G., Understanding Thermoplastic Elastomers, Hanser 2000, 1-13.

23. Agrawal J. P., Prog. Energy Combust Sci 1998, 24, 1.

24. Frankel M. B., Grant L. R., Flanagan J. E., J. Propul. Power 1992, 8, 560.

25. Gaur B., Lochab B., Choudhary V., Varma I. K., J. Macromol. Sci. Polym. Rev 2003, C43(4), 505.

26. Eroglu M. S., Hazer B., Guven O., Baysal B. M., J. Appl. Polym. Sci 1996, 60, 2141.

27. Frankel M. B., US Patent 1990, 4, 379, 894.

28. Eroglu M E., Hazer B., Guven O., Baysal B M., J. Appl. Polym. Sci 1998, 68, 1149.

Chapter 5

Determination of the miscibility of the hydroxyl terminated poly(epichlorohydrin), poly(glycidyl azide) and rubbery poly(epichlorohydrin) with poly(methyl methacrylate) and poly(styrene)

In "Principles of Polymer Chemistry" Paul Flory wrote:

The critical value of the interaction free energy is so small for any pair of polymers of high molecular weight that it is permissible to state as a principle of broad generality that *two high polymers are mutually compatible with one another only if their free energy of interaction is favorable, i.e., negative.*

Determination of the miscibility of the hydroxyl terminated poly(epichlorohydrin), poly(glycidyl azide) and rubbery poly(epichlorohydrin) with poly(methyl methacrylate) and poly(styrene)

Abstract

The phase behavior of blends of amorphous poly(methyl methacrylate) and poly(styrene)/ poly(epichlorohydrin) (PECH-diols), poly(glycidyl azide) (GAP-diols), and an amorphous rubbery poly(epichlorohydrin) (RPECH) blends was examined using various analytical techniques, such as differential scanning calorimetry (DSC), dynamic mechanical analysis (DMA), scanning electron microscopy (SEM), and Fourier transform infrared spectroscopy (FTIR). Blends showed a single broad glass transition temperature (T_g) from DSC or DMA results and the only phase separation identified was for RPECH blended with PS while two T_g values were detected. The effect of the halogenated pendent group (chloromethyl and azide) on the final properties of blends was evaluated. Results showed that the chloromethyl groups had a stronger intermolecular interaction than azide groups. Hydroxyl groups and low molecular weight play a vital role in enhancing miscibility through interaction with hydrogen bonding and plasticizing the hard polymer chains. The SEM micrographs of blends show compatibility of the two different phases with each other, without a distinguished phase separation.

Chapter 5

5.1 Introduction and objectives

In this section, the miscibility of the selected polymer blends and characterization tools used to study the miscibility of blends has been reported.

5.1.1 Polymer blends

New polymeric materials can be developed by using polymer blends. The term blend is usually reserved for a mixture of two or more polymers with a noticeable difference in their chemical composition and/or microstructure. Such blends show properties superior to any one of the component polymers alone. The manifestation of superior properties depends upon the miscibility of the homopolymer on the molecular scale [1, 2]. Usually, a compatible system of un-crystalline polymers forms transparent films even if the refractive indices of the components differ. A mixture will form a transparent film when the polymer molecules are dispersed; so well that, the dimensions of any segregated regions are smaller than the wavelength of light [3]. An important and determining aspect of the properties of a blend is the miscibility of their components. The miscibility of a blend of two homopolymers is usually generated from specific intermolecular interactions between the polymer components, which usually give rise to a negative free energy of mixing. Intermolecular interactions are usually considered to be the driving forces for miscibility and the important role they play in the miscibility of polymer blends has been demonstrated in different blend systems. The most common interactions presented in blends are: hydrogen bonds, π-electrons and ionic and dipole interactions, and charge-transfer complexes [2]. On the other hand, for random copolymer-homopolymer mixtures, miscibility can arise from the so-called "repulsion effect".

The miscibility of poly(epichlorohydrin) (PECH) rubber with several different polymers has been investigated by Fernandes *et al*. [4-6]. They reported that PECH is miscible with a series of linear aliphatic polyesters. Anderson and Rodriguez [7], reported that PECH and a commercial copolymer of poly(epichlorohydrin/ethylene oxide) rubber are compatible with PMMA and they found that blends of PMMA/PECH and PMMA/(ECH/EO) were miscible, based on the clarity of the films and the observation of a single glass transition over a wide composition range. Furthermore, PMMA shows miscibility with poly(vinyl chloride), as reported by many authors [8, 9]. This blend is considered as a type of rubber modification of glassy polymers, which reduces the brittleness of a glassy polymer and enhance the processing. The interaction between the chlorine moiety of PECH and PVC with the carbonyl group of PMMA is reported to be the main reason for the miscibility of these blends [1, 4, 8].

The method of blend preparation is a very important factor in determining the final homogeneity of blends. The preparation of blends from a solution is an easy method. The final homogeneity of blends depends on the effects caused by preparation parameters, like the type of solvent, the casting temperature, and the rate of solvent evaporation. It is therefore important to mention the type and method used in preparing blends. Various analytical tools can be used to study the miscibility of polymers blends and these are discussed in Section 5.1.1.1.

5.1.1.1 Analytical techniques used to determine the miscibility of polymer blends

Thermal analysis techniques are considered as the most widely used to ascertain the miscibility of polymer blends. This is based on the fact that an investigation of motional transitions in solid polymer blends can provide valuable information as to the phase state and morphology of the blend as a function of its composition. The glass transition temperature is considered as an easy indication of blend miscibility,

where the occurrence of two values for glass transition temperatures (T_g) is the evidence of phase separation. The most useful method for the determination of the glass transition in polymer blends has traditionally been differential scanning calorimetry (DSC). The latter offers many advantages for the investigation of thermal behavior in polymer blends and also its ease of use and simplicity in sample preparation and quantity. Dynamic mechanical thermal analysis is another valuable technique in studying the polymer blends and detecting (T_g) with more sensitivity than DSC.

As mentioned previously, incompatible polymer pairs show two different glass-transition temperatures, where if the mixing is complete on the molecular level (compatible blend) and a true solution is formed, the single glass transition will be shown [10]. From a thermodynamic view point, a miscible polymer should form a single phase. For this the Gibbs free energy of mixing ΔG_{mix} should be negative (**Equation 5.1**).

$$\Delta G_{mix} = \Delta H_{mix} - T\Delta S_{mix} \qquad \text{-----------------------} [5.1]$$

ΔH_{mix} and ΔS_{mix} are the enthalpy and entropy of mixing, respectively. In order to get negative heat of mixing it is necessary to find strong binary interactions between two polymer pairs [1, 3].

A few miscible blends such as butadiene-acrylonitrile copolymers with PVC and PVC in ethylene-vinyl acetate copolymers (EVA) have been found to exhibit a T_g versus composition dependency, which can be predicted by a simple Fox equation (**Equation 5.2**)

$$1/T_g = W_1/T_{g1} + W_2/T_{g2} \qquad \text{-----------------------} [5.2]$$

where W_1 and W_2 are the weight fractions for the blend components 1 and 2, respectively [1, 2]. Another equation which is most commonly used is the Gordon-Taylor equation (**Equation 5.3**), which was originally derived for random copolymers [1],

$$T_g = \frac{W_1 T_{g1} + k W_2 T_{g2}}{W_1 + k W_2} \quad \text{-----------------------[5.3]}$$

where

$$k = \frac{\Delta\alpha_2 V_2}{\Delta\alpha_1 V_1}$$

$\Delta\alpha_i$ is the change in cubic expansion coefficient of the *i*th component at its glass transition temperature, and V_i is its specific volume. In most instances k is used as an adjustable parameter. All of these equations have also been used to describe the glass transition of a random copolymer in terms of the glass transitions of the component homopolymers [1-3].

Many miscible polymer blends with strong intermolecular interactions present positive deviations, which cannot be modeled by the Fox equation [1]. The Gordon-Taylor equation can successfully describe the T_g behavior for miscible blends with positive or negative deviations if the parameter k is used as an adjustable parameter, provided that the specific interactions are not too strong [1]. On the other hand, broadening of the glass transition temperature (T_g) is usually attributed to equilibrium composition fluctuations, which become frozen into the glassy state on cooling and influence the range of temperatures over which molecular motions become active on subsequent heating [4, 6].

5.1.1.2 Spectroscopic analysis techniques for the miscibility of polymer blends

Although thermal methods are the most widely used for determining polymer miscibility, other methods such as spectroscopic techniques are applied in this field. The main use of spectroscopic analysis techniques is to investigate specific interactions between polar groups of the polymers, which are often responsible for the miscibility. FTIR and NMR spectroscopy are used in the characterization of the polymer blends and to study the interactions. FTIR spectroscopy in particular is very attractive because of the wide availability of Fourier transform infrared spectrometers and is widely used in characterization of polymer blends [2]. Frequency shifts and band broadening for some groups could be attributed to intermolecular chemical interactions and to changes in polymer-chain configurations. Many of the blends containing polymer with carbonyl groups (proton acceptor) appear to be sensitive to the presence of intermolecular interactions. Also, presence of hydroxyl groups as proton donors lead to the formation of interactions. The absorption peaks of moieties involving specific interactions in polymer blends shift compared to those of the pure polymer; on the other hand, if the blends are immiscible, no shift in the absorption wavelength is observed with composition changes. The shift in absorption is associated with the hydrogen bonding in the specific interaction. The importance of using IR in characterized associated polymer blends is that IR spectroscopy does not only give information about miscibility, but it identifies the actual moieties involved in the interactions. In addition, IR intensities are significantly more sensitive than IR frequencies as reported by some authors [1, 2]. However, the intensities change is very obvious with composition change.

5.1.1.3 Microscopy analysis techniques for the miscibility of polymer blends

Microscopy is unique in the characterization of the microstructural variations of polymer blend morphology. Examples of these techniques are basic visualization,

optical microscopy (OM), scanning electron microscopy (SEM), and transmission electron Microscopy (TEM). The large depth of field of the SEM makes it ideally suited for the examination of samples with a high degree of surface relief. SEM is used to study the internal structure of polymer blends. The best results are obtained when the internal phase is poorly bonded.

Poly(epichlorohydrin) is a linear amorphous elastomer exhibiting a glass transition temperature at about -25 ^{o}C[11]. Glycidyl azide polymer with hydroxyl terminate groups (GAP-diols) is produced from azidation of hydroxyl terminated poly(epichlorohydrin) (PECH-diols) [12]. Interesting observations of T_g effects during the preparation of PMMA-*b*-PECH and PMMA-*b*-GAP copolymers prompted an investigation into the miscibility of PECH-diols and GAP-diols with PMMA.

5.1.2 Objectives

The main aim of this study is to evaluate the miscibility of PMMA and polystyrene with a low molecular weight PECH and GAP. The miscibility of high molecular weight (rubbery) poly(epichlorohydrin) (RPECH) with two different thermoplastics was also investigated. It is also important to know the miscibility of PMMA with these elastomers in order to use these results as comparison for that obtained from PMMA-*b*-PECH and PMMA-*b*-GAP copolymers. The miscibility of polystyrene with rubbery PECH is also studied.

5.2 Experimental

5.2.1 Materials used

The following materials were used: standard homo-PMMA ($\overline{M_{wt}}$= 81 307 g/mol PDI=1.86, T_g= 105 ^{o}C) and high molecular weight rubbery PECH ($\overline{M_{wt}}$ = 537 439

g/mol, PDI= 4.36) was obtained from Aldrich. Homo-polystyrene ($\overline{M}_{wt}$ = 145 849 g/mol, PDI= 1.4) was prepared by anionic polymerization. Analytical grade THF was obtained from Saarchem. PECH-diols ($\overline{M}_{wt}$ about 2 000 g/mol) was prepared as described in Chapter 2, Section 2.2.3.1. GAP-diols ($\overline{M}_{wt}$ about 2 500 g/mol) was prepared as described in Chapter 3 Section 3.2.3.1.

5.2.2 Analytical equipment and methods

5.2.2.1 DSC analysis

For DSC instrument description see Chapter 2, Section 2.2.2.5. The experiments were performed as follows, under an N_2 atmosphere and at a heating rate of 10 ^{o}C/min:

1. First heating: sample heated from room temperature to 125 ^{o}C.
2. First cooling: sample cooled to -60 ^{o}C.
3. Second heating: sample heated from -60 ^{o}C to 125 ^{o}C.

The results reported in this work correspond to the second heating run.

5.2.2.2 DMA and FTIR analysis

Equepment description and analysis methods applied for the FTIR are given in Chapter 2 Section 2.2.2.2. DMA equipment description and analysis methods are provided in Chapter 3 Section 3.2.2.2.

5.2.2.3 SEM analysis

A scanning Electron Microscop was used to study the surfaces of the samples after the evaporation of the solvent. Imaging of the surfaces of the samples was accomplished using a Leo® 1430VP scanning electron microscope. Prior to imaging, the samples were sputter-coated with gold.

5.2.3   Experimental techniques

5.2.3.1 Preparation of blends

All blend samples were prepared by a solution-casting method.   Solutions of the blends 3.5% (w/v) were prepared in THF as solvent. The polymer (PMMA, PS, or RPECH) was slowly added, with stirring, to avoid the formation of lumps.   The solution was stirred in an oil bath at 50 ^{o}C, in the case of low molecular weight polymer, or 55 ^{o}C in case of rubbery elastomers.   The stirring was continued for 4 hours. The mixture was then poured into a glass plate and the solvent was allowed to evaporate slowly at room temperature, in a fume hood, for two days.   Finally, drying was completed in a vacuum oven at 40 ^{o}C for 24 hours.

5.3 Results and discussion

The results of the experiments are discussed in two parts.   The first part reports the results obtained from PMMA blends.   The second part presents the results of polystyrene blends.

5.3.1   PMMA blends

The results obtained from the blending of PMMA with (1) PECH-diols, (2) GAP-diols, and (3) RPECH are presented and discussed here.

5.3.1.1 PMMA/PECH-diols blend

Blends of PMMA with PECH-diols were optically transparent at room temperature. DSC thermograms exhibit single, composition-dependent T_g values.   There was however a considerable broadening of these transitions for both systems, particularly at intermediate compositions, with maxima at about 50 wt.% PMMA.   This

broadening makes the judgment of the T_g of the blends difficult; a mid point of this broadening was chosen as the T_g. **Figure 5.1** shows the thermograms of PMMA blend with PECH-diols for different weight ratios. The DSC thermogram shows a good miscibility between the two different segments; a single glass transition temperature is observed. The glass transition temperature of PMMA is reduced to about 60 ^{o}C by adding 20 wt% PECH. In contrast, blending 20 wt% PMMA with PECH increases the T_g of the elastomer to about -20 ^{o}C.
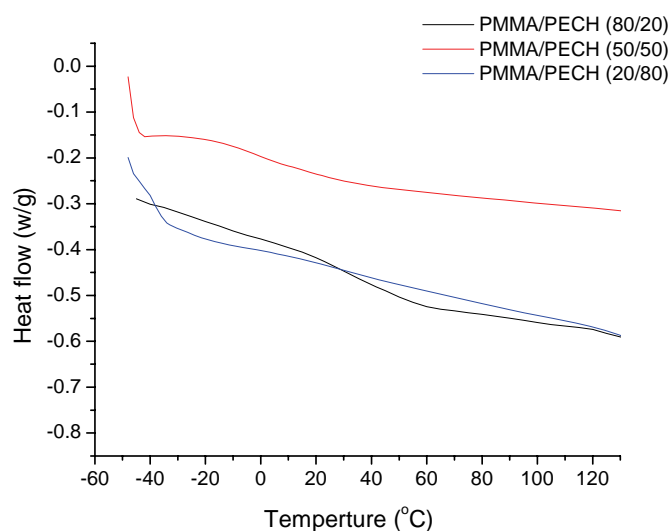
Figure 5.1 DSC thermograms of PMMA/PECH-diols blends of different weight ratios.

The miscibility of PMMA and PECH-diols could be attributed to the polarity of the different groups, such as the chloromethyl group, the hydroxyl group, polyether of PECH, carbonyl group of PMMA, and polyether linkage of PMMA and PECH. Further, the broadening in the glass transition temperature, especially when 1/1 weight ratio is used, could be attributed to the miscibility of different polymer chains in each other, which will decrease the possibility of identifying a sharp glass transition temperature (volume change).

Figure 5.2 shows the chemical structures of two different polymers, with an indication of the sites, where the interaction could take place. It is reported that PVC/PMMA forms a miscible blend due to specific interactions, of the hydrogen bonding type, between carbonyls (C=O) of PMMA and α-hydrogen of the (CHCl) groups of PVC [13]. It is also reported that poly(epichlorohydrin) forms a miscible blend with poly(vinyl acetate) due to hydrogen bonding between the α-hydrogen of PECH and the carbonyl of PVA [14]. Finally, the presence of hydroxyl groups, which can act as proton donors play an important role in the miscibility of PMMA/PECH blends, where the carbonyl group works as proton acceptor [15].
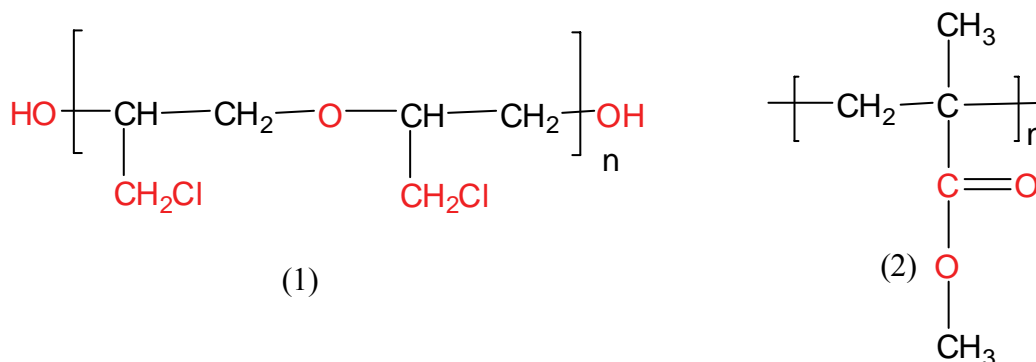
Figure 5.2 The chemical structures of, (1) PECH-diols and (2) PMMA.

The glass transition temperatures of the blends were obtained by using DSC analysis (experimental T_g), the Fox equation, and the Gordon-Taylor equation are shown in **Figure 5.3**. The glass transition of polymer blends exhibits negative deviations from the additivity law: $T_g = W_1 T_{g1} + W_2 T_{g2}$, where W_1 and W_2 is the weight fraction of component 1 and 2, respectively. T_{g1} and T_{g2} is the glass transition of component 1 and 2, respectively. It is reported that, positive deviations from a simple additivity means that two polymers have strong exothermic, which will lead to form a negative volume of mixing or densification [3, 10]. This will results in a higher T_g due to a

reduction in free volume [8]. In this blend system a negative deviation from additivity is formed. This could be attributed to the low molecular weight of PECH-diols compared to PMMA. Finally, it is probable that the PECH-diols acts as a compatible dilutent, where the blends show broad glass transition temperature. The results nonetheless confirm the formation of a homogeneous blend when PMMA is mixed with PECH-diols. Figure 5.3 shows the Gordon-Taylor equation with k = 1.4 (adjustment parameter) [1]. This value is relatively high, implying that the interaction between PECH-diols and PMMA is strong.
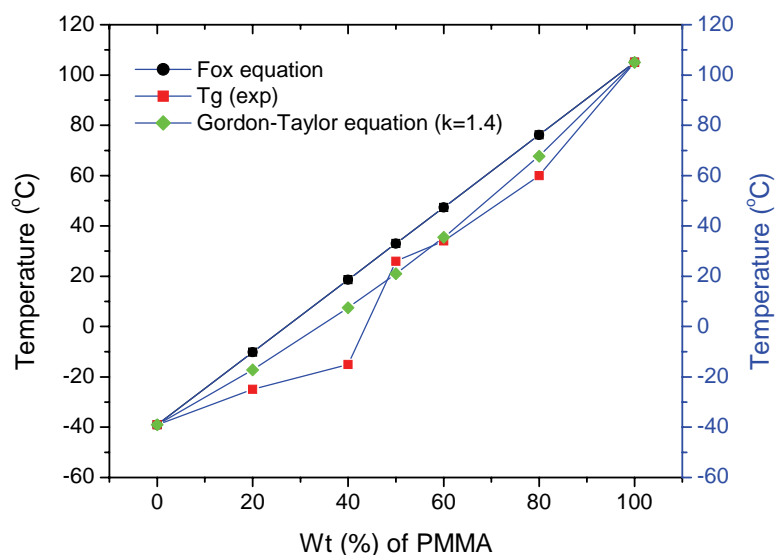
Figure 5.3 Variation of T_g as a function of PMMA content in PMMA/PECH-diols blends by using DSC measurement T_g (exp), Fox equation, and Gordon-Taylor equation (k=1.4).

DMA results for the PMMA/PECH-diols blend (1/1) are presented in **Figure 5.4**. The elastic portion of the complex modulus, E', is seen to decrease smoothly from a plateau value as the temperature is raised through the transition temperature and the

slight decrease in the start of the storage modulus could be attributed to the internal stress associated with sample preparation. There is no phase heterogeneity, which usually shows up as multiple plateaus in the E' versus temperature plot. Tan δ is also shown in Figure 5.4; there is the expected single peak at the mechanical transition temperature, with no evidence of a transition peak at lower temperature. Tan δ maximum was at about 27 °C. The broadness of tan δ could be attributed to the difference in the molecular weight between PMMA and PECH-diols.
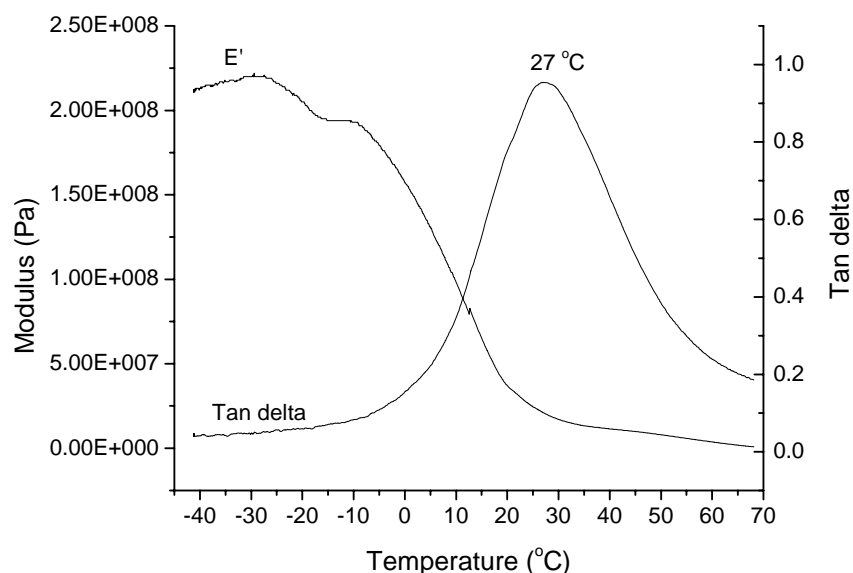
Figure 5.4 DMA analysis of PMMA/PECH-diols blend (1/1) wt. % ratio shows storage modulus (E') and tan δ as a function of temperature.

The FTIR spectra of PMMA/PECH blends are shown in **Figure 5.5**. FTIR spectroscopy provides information consistent with specific interactions between the two polymers, but it is not sensitive enough to provide more detailed information such

as how the strength of the interaction may vary as a function of blend composition and which part (chemical group) is related to this interaction [8].

(A)

(B)

(C)
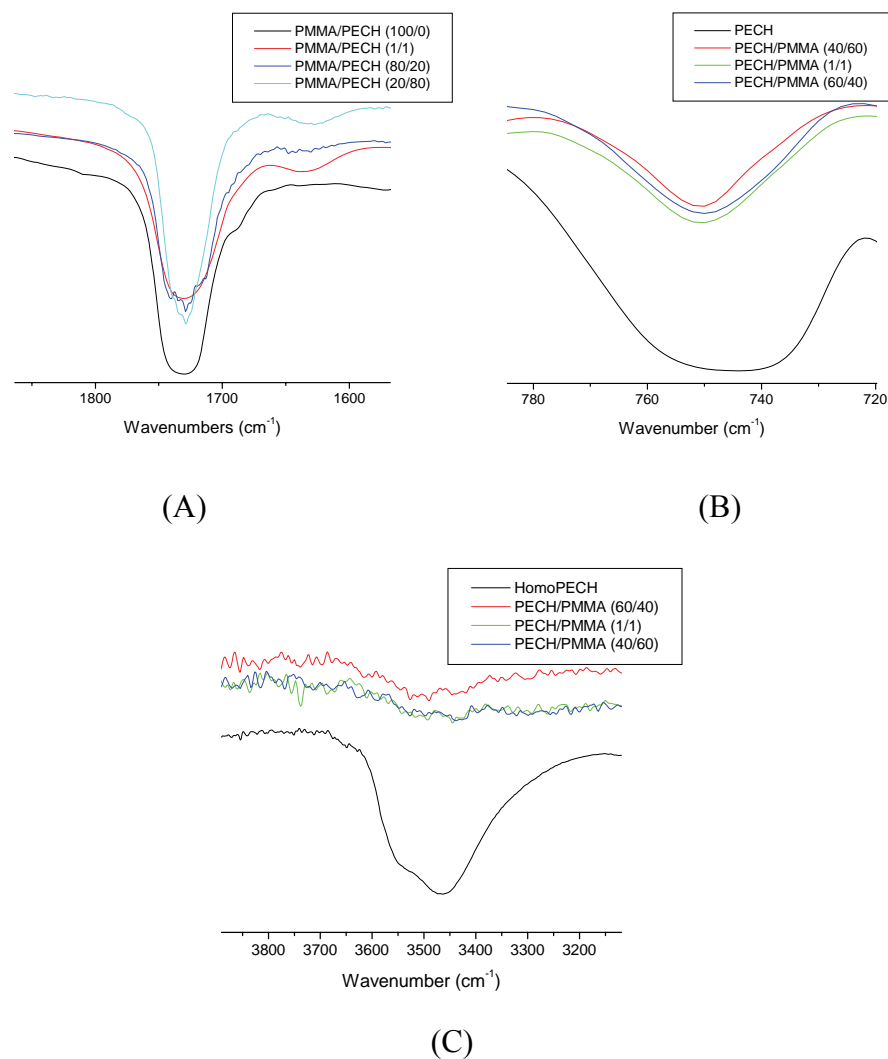
Figure 5.5 FTIR spectra for PMMA/PECH-diols blends, showing (A) carbonyl stretching, (B) chloromethyl group, and (C) hydroxyl group.

Slight changes and shifts for carbonyl group peaks were noticed when PMMA is blended with PECH-diols. Most of the carbonyl absorption peaks are located at about

1728 cm^{-1} for most of the blend compositions. There was however change in shape of the carbonyl group peak after blending with PECH-diols. At the same time, the chloromethyl group' peak was affected by the blending with PMMA. This could be attributed to the interaction of the chloromethyl group with the carbonyl group. The FTIR spectrum of PECH-diols shows the absorption of hydroxyl groups at about 3400cm^{-1}, which may be considered as being composed of two components: a broad band centered at 3466 cm^{-1}, attributed to hydrogen-bonded hydroxyl groups (self-associated), and a relatively narrow band at 3534 cm^{-1}, assigned to free (non-associated) hydroxyl groups [2, 16]. Nonetheless, interesting results are associated with the hydroxyl group, where blending of PMMA and PECH-diols almost diminishes the absorption of the OH group. This could be attributed to the interaction of a polar pendent hydroxyl group (proton donor) with the carbonyl group of PMMA (via formation of hydrogen-bonding interaction between PECH-diols and PMMA). Finally, FTIR analysis provides proof of intermolecular interaction between polymer pairs and its responsibility for the miscibility of PECH-diols and PMMA.

The scanning electron micrographs of PMMA/PECH-diols blend is shown in the **Figure 5.6**.
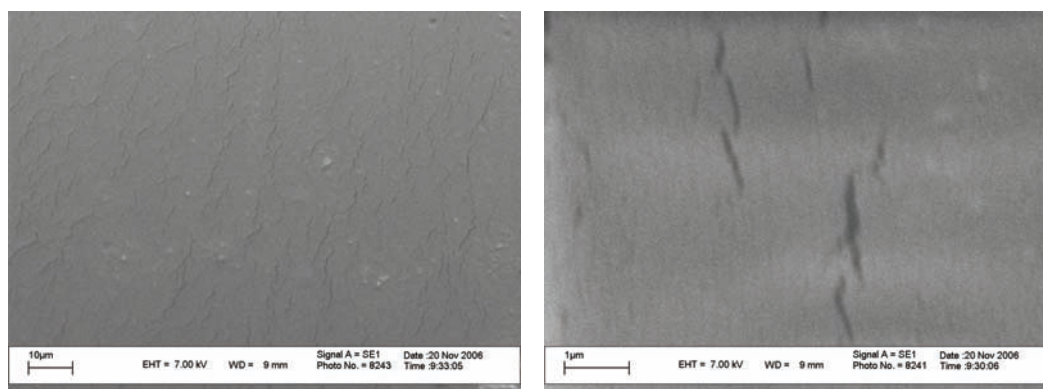
Figure 5.6 SEM micrographs of a PMMA/PECH-diols (1/1 wt %) blend.

The blends generally had a smooth surface. This could be attributed to the compatibility of two different segments with each other. Small micro-cracks were seen in the micrographs. These were attributed to the brittleness of PMMA or could be associated with the preparation of the blend films for analysis (during casting, or evaporation of the solvent). No clear explanation for the formation of these small micro-cracks can be offered here.

5.3.1.2 PMMA/GAP-diols blend

There are no previous reports on the blending PMMA with GAP-diols. This can be attributed to the special applications of GAP and its limited production as a commercial polymer, due to the high risk associated with its azide groups (exothermic decomposition), which make its transportation and handling difficult [13].

The DSC thermograms of PMMA blended with GAP-diols in different weight ratios are presented in **Figure 5.7**. The polymer blends form optically transparent films and a single glass transition temperature is observed. Also, the broadness of the glass transition is still observed in these blends. Usually polymers containing halogen groups, such as PVC, PECH, and PVF show miscibility with PMMA, which could be attributed to the interaction between halogens and carbonyl groups [8, 9, 13, 17, 18]. The glass transition temperature of the 20% GAP-diols and 80% PMMA blend was about 58 $^{\circ}$C, which is comparable to the 20% PECH-diols and 80% PMMA blend. On the other hand, a blend containing 20 wt% PMMA and 80 wt% GAP-diols shows T_g at about -38 $^{\circ}$C, which is lower than the glass transition temperature of the 80% PECH and 20% PMMA blend. This could be attributed to the difference in the interaction of two different pendent groups added to lower glass transition of GAP. By contrast, the glass transition temperature was difficult to identify when a mixture of same weight ratio between PMMA and GAP-diols was used (50% GAP and 50% PMMA blend). This phenomenon was noticed before, with the PECH-diols blend in

the same weight ratio see Section 5.3.1.1. Generally, the miscibility of PMMA and GAP could be attributed to the interaction between the azide pendent, and hydroxyl groups of GAP-diols and carbonyl groups of PMMA.
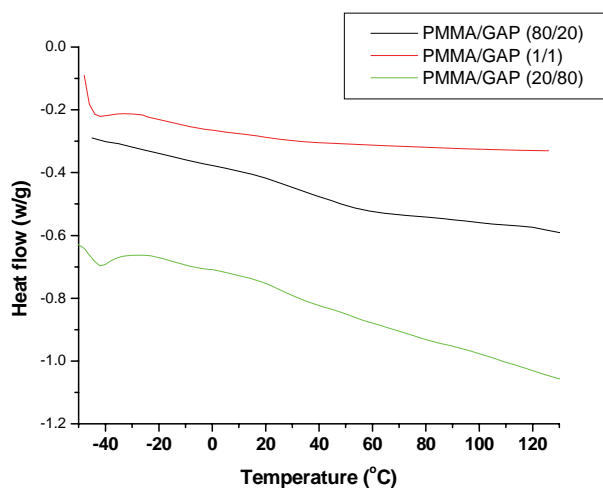
Figure 5.7 DSC thermograms of PMMA/GAP-diols blends of different weight ratio.

Figure 5.8 shows the chemical structures of the two different polymers, with an indication of the places where intermolecular interaction could take place. GAP-diols produced from azidation of PECH-diols by replacing chloromethyl groups with azide groups. Hence the results of this study could also provide a comparison of the effects of each group in the blend system.
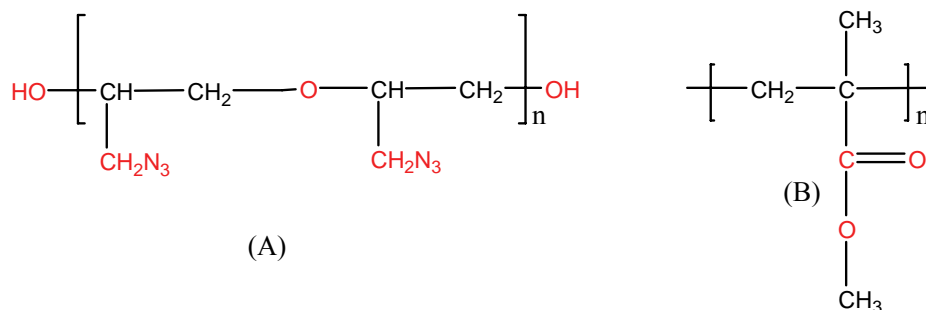
Figure 5.8 Chemical structure of two different polymers, (A) GAP-diols, and (B) PMMA.

The glass transition temperature of the blends, calculated by using the Fox and equations, and the experimentally obtained value (DSC analysis based on the mid point of broad T_g) are shown in **Figure 5.9**. PMMA/GAP-diols blends show a different trend in terms of the deviation from the additivity law compared to PMMA/PECH-diols blends and show two different trends for all the compositions. When a high concentration of PMMA was used in the blends (more than 50%) the additivity was negative. Where, using high weight concentration of GAP in the blend, the additivity is positive with the additivity law.
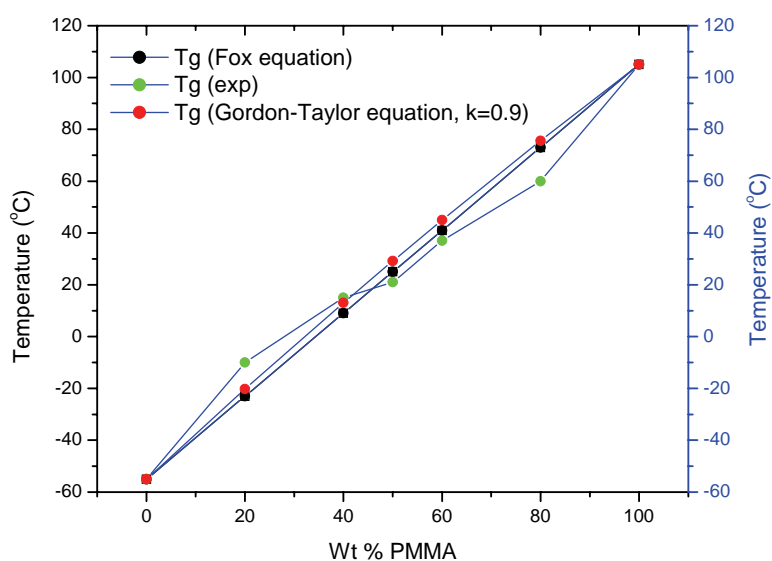
Figure 5.9 Variation of T_g as a function of PMMA content in PMMA/GAP-diols blends determined using DSC measurement, Fox equation, and Gordon-Taylor equation (k=0.9).

The similarities between the PMMA/PECH-diols and PMMA/GAP-diols blend systems (when 50 wt% PMMA) could be attributed to the low molecular weight of pre-polymer compared to the hard segments. On the other hand, there could be two reasons for the different behavior of the GAP blends to PECH. The first is the interaction of the azide group with the carbonyl groups of PMMA, and the second is the low glass transition temperature of GAP-diols compared to that of the PECH. In contrast, Gordon-Taylor's equation by using (k=0.9) is shown in Figure 5.9. The k value is lower than PMMA/PECH-diols blend, which could be attributed to the lower intermolecular interaction.

Dynamic mechanical analysis was used to study the PMMA/GAP-diols blend and the result is presented in **Figure 5.10**. The elastic portion of the complex modulus, E', is seen to decrease smoothly from a plateau value as the temperature is raised through the transition temperature. There was no phase heterogeneity, which usually shows up as multiple plateaus in the E' versus temperature plot. In Figure 5.10, Tan δ shows the mechanical transition temperature as a single peak and there was no evidence of the transition peaks at lower temperatures. The maximum of tan δ of PMMA/GAP-diols is about 45 $^\circ$C. This value is higher than tan δ of the PMMA/PECH-diols blend with the same weight ratio. The broadness of tan δ in case of the PMMA/GAP-diols blend is noticed, and it is greater than in the case of the PMMA/PECH-diols blend. The higher T_g in the case of PMMA/GAP-diols blends could be attributed to weak interaction of the azide groups with carbonyl groups, which will affect the miscibility of the final blend system.
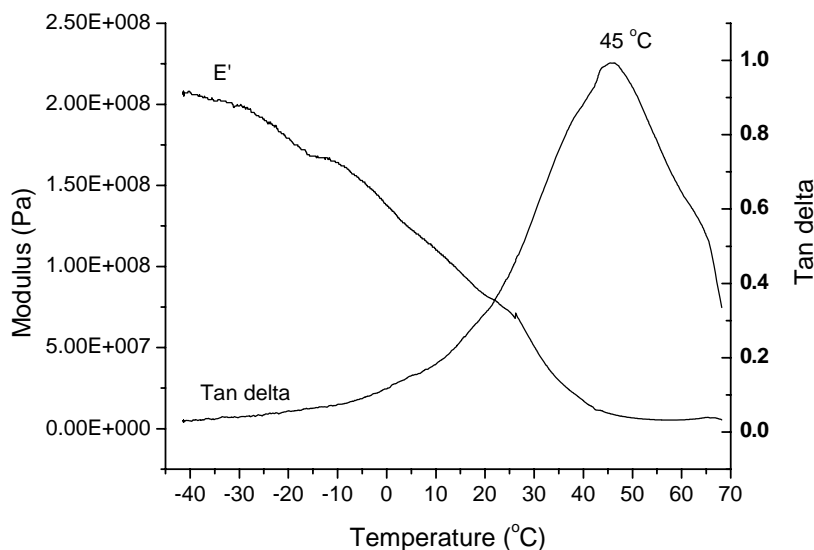
Figure 5.10 DMA analysis of PMMA/GAP-diols blend (1/1) wt. % ratio shows storage modulus (E') and tan δ as a function of temperature.

The FTIR spectra of PMMA/GAP-diols blends of different weight ratios, showing the carbonyl, azide, and hydroxyl peaks, are shown in **Figure 5.11.** The carbonyl group's peak shape and sharpness shows a clear change after blending with GAP-diols. This phenomenon was noticed previously with PECH-diols blends. Most of the carbonyl absorption peaks are seen to be located at about 1729 cm^{-1} for all blend compositions and any shift of the peak was negligible. However, as the GAP content increases; the carbonyl peak becomes narrower, which could be an indication of intermolecular interaction via the carbonyl group. On the other hand, the azide group's absorption is affected by blending with PMMA, as can be seen from the change in the shape of peak in Figure 5.11-B. This could be attributed to the interaction of the azide with the carbonyl group or to the low molecular weight of GAP-diols compared to that of the PMMA.
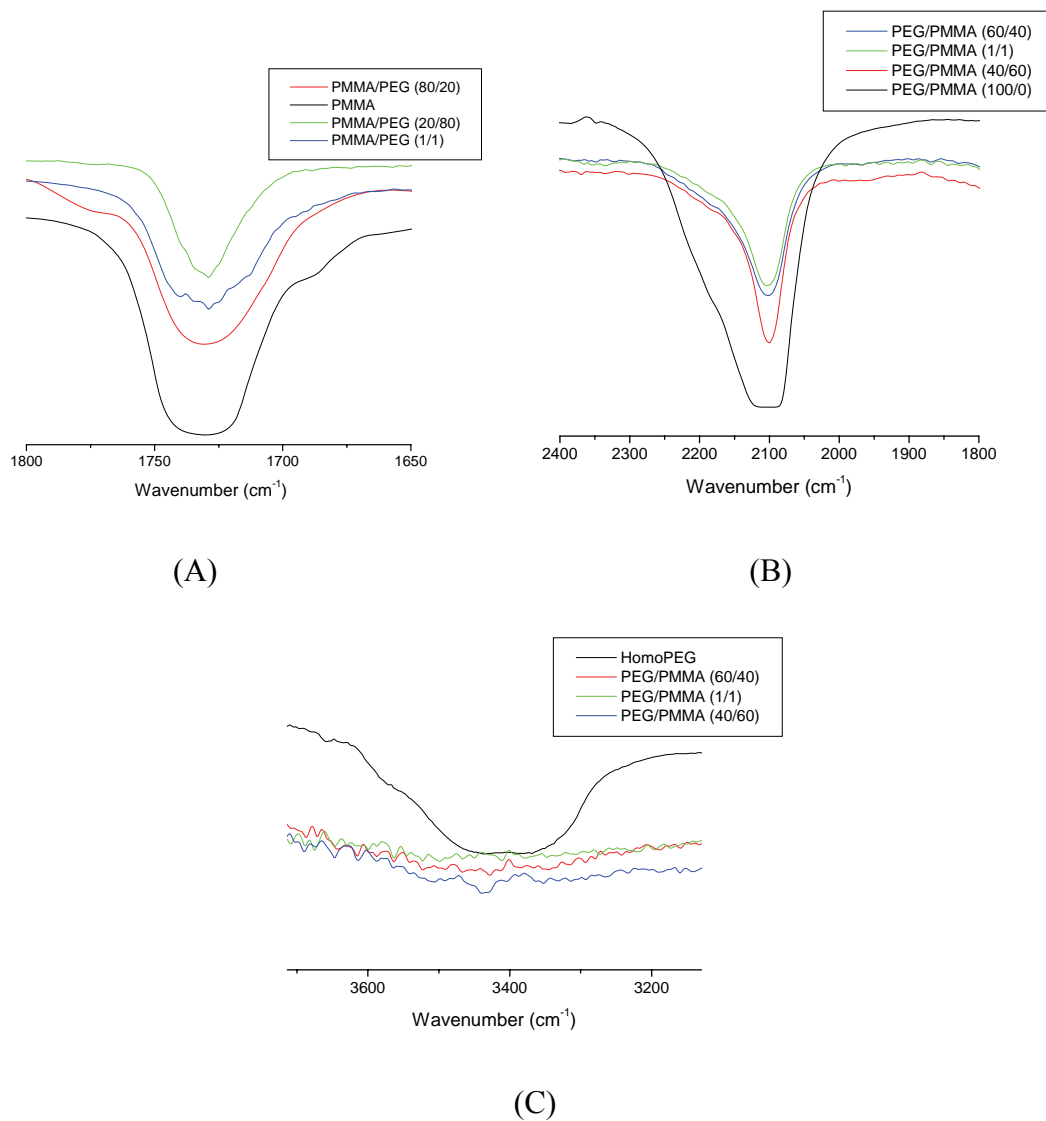
Figure 5.11 FTIR spectra for PMMA/GAP-diols blends showing (A) carbonyl stretching region, (B) azide group, and (C) hydroxyl group.

However, there is a similarity in the result for the hydroxyl group of the PECH-diols and GAP-diols blends, where blending diminishes the absorption of OH group similar

to what happened with the PECH-diols blends. This could be attributed to the interaction of the polar hydroxyl group with the carbonyl group of PMMA. Also, FTIR results show the interactions of the carbonyl, azide, and hydroxyl groups, which could be responsible for the formation of miscible blends.

The SEM images of PMMA/GAP-diols blend of the same weight ratios are shown in **Figure 5.12**. The micrograph shows a smooth surface with a mixture of little spots, which could be associated with the processing of blend. The smoothness of the blend could be attributed to the compatibility of the two different segments with each other. The small micro-cracks which were observed in the PMMA/PECH-diols blend were not found in the PMMA/GAP-diols blend.
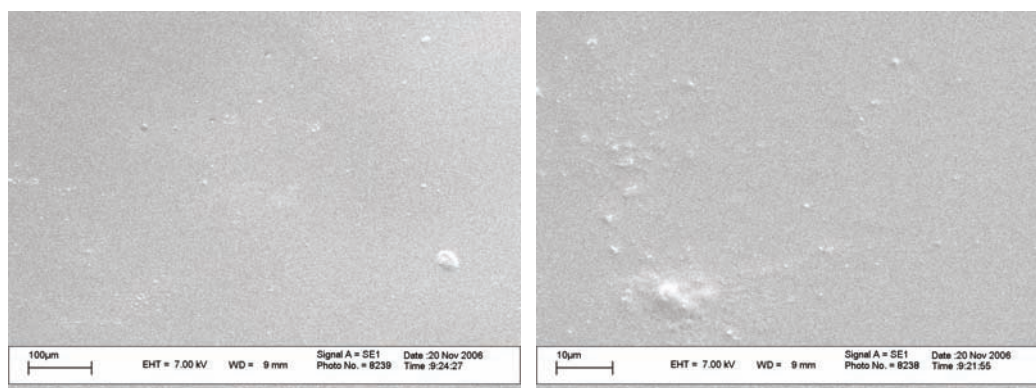
Figure 5.12 SEM micrographs of PMMA/GAP-diols (1/1 wt %) blend.

5.3.1.3 PMMA/rubbery poly(epichlorohydrin) blend

Blends of PMMA and rubbery poly(epichlorohydrin) were optically transparent at room temperature. DSC thermograms of these system exhibit single and composition-dependent T_g values, as can be observed in **Figure 5.13**. However, there was a considerable broadening of these transitions. The sharp glass transition temperature of PMMA ($T_g = 105$ ^{o}C) decreases by about 31% when a blend is made

from 25 wt % RPECH and 75 wt % PMMA. On the other hand, when a blend was made from 25 wt % PMMA and 75 wt % RPECH, the T_g value was about -10 ^{o}C. These results confirm the miscibility of two different polymer pairs and the dependence of the transition on the composition. The miscbility of PMMA/RPECH could be attributed to the interaction between the following groups: carbonyl, chloromethyl, and ether linkage [13].
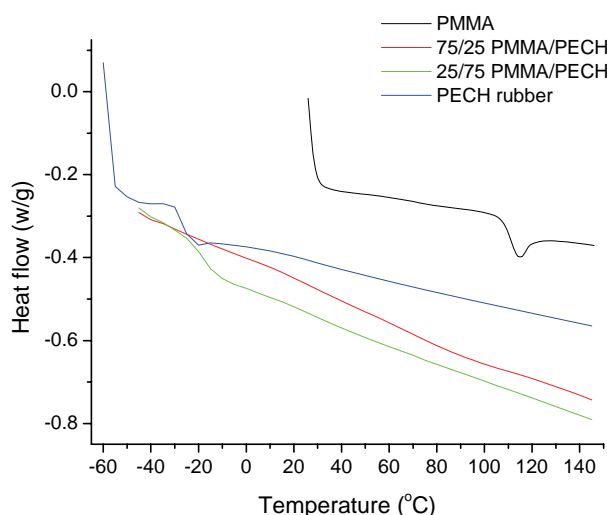
Figure 5.13 DSC thermograms of homo-PMMA, RPECH, and PMMA/RPECH blend of different compositions.

In conclusion, PMMA produces miscible blends with the PECH-diols, the GAP-diols, and RPECH. This miscibility is confirmed by the formation of optically transparent films, and by a broad, single glass transition temperature.   Miscibility can be attributed to the interaction between the carbonyl group of PMMA with the halogenated groups (chloromethyl and azide groups), and hydroxyl groups. The low molecular weight and plasticization effect of PECH-diols and GAP-diols also could

play roles in this interaction. Also, the miscibility appears to be independent from the molecular weight.

5.3.2 Polystyrene blends

Blends consisting of polystyrene with PECH-diols, GAP-diols, and high molecular weight rubbery poly(epichlorohydrin) were obtained by the same method followed for PMMA blends, using THF as solvent. Results of the study of these blends are presented here.

5.3.2.1 Blends of polystyrene with hydroxyl terminated poly(epichlorohydrin) and glycidyl azide polymer

The DSC thermograms of homo-polystyrene and blends of polystyrene with PECH-diols and GAP-diol of (1/1) wt% are shown in **Figure 5.14**. The thermogram of PS shows a very sharp glass transition temperature at about 110 ^{o}C. Blending of PS with GAP-diols reduces the T_g to about 65 ^{o}C, while blending of PS with the same amount of PECH-diols reduces the T_g to about 58 ^{o}C. However, it was very interesting to find the miscibility of the two different blends; this wasn't expected due to the difference in the polarity and nature of PS compared to PMMA. There are two possibilities for this miscibility: first, low molecular weight of pre-polymer work as a plasticizer for the polystyrene chains and inhibit formation of a sharp T_g or even phase separation, and the second, a strong interaction of halogenated groups of with the aromatic ring of PS. This speculation could be more pronounced in case of GAP-diols due to the presence of a small decline in the thermogram at about 110 ^{o}C (T_g of polystyrene), which wasn't seen in the case of PECH-diols. This could be attributed to the effect of the chloromethyl group (polarity) compared to the azide group or, in other words, strong interaction of chloromethyl groups with the aromatic ring compared to azide groups. This result leads to support a previous conclusion that was made in Section

5.3.1.2, namely that chloromethyl groups form stronger intermolecular interaction than azide groups.
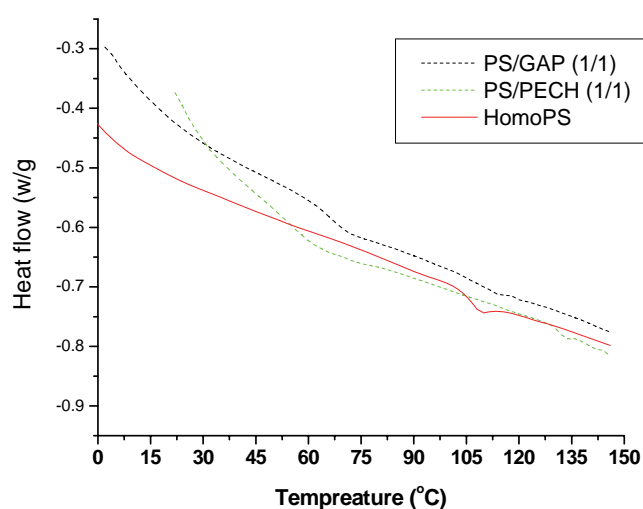
Figure 5.14 DSC thermograms of homo-polystyrene, (1/1) wt.% blend of PS/PECH-diols, and PS/GAP-diols.

5.3.2.2 Blend of PS and rubbery poly(epichlorohydrin)

Blends of polystyrene and high molecular weight rubbery PECH in different weight ratios were prepared using the casting method. Results of DSC analysis are shown in **Figure 5.15**. This blend shows two separate T_g values, which is different from the previous blends. The first T_g is close to the PS transition at about 110 $^{\circ}$C, and the second T_g is in the range -20 to -30 $^{\circ}$C, which is close to the RPECH transition. This could be an indication of the phase separation in this blend, which did not occur in the RPECH/PMMA blend or PS/low molecular weight pre-polymer. The phase separation (immiscibility) in the case of these blends could be attributed to the difference in the polarity of the two different segments and weak interaction between chloromethyl groups of RPECH and the aromatic ring. In any case, RPECH shows a

slight interaction or it functions as a weak plasticizer for the polystyrene chains, leading to decrease in its T_g slightly. This can be attributed to the effect of the chloromethyl group in the interaction with aromatics groups; this is a very weak interaction, compared to the interaction with a carbonyl group (PMMA). On the other hand, the difference in the miscibility of PECH-diols and RPECH with polystyrene could be attributed to the following: (1) low molecular weight elastomers work as plasticizer for PS chains, (2) the presence of hydroxyl groups in the case of PECH-diols, (3) chloromethyl groups provide less hindrance; and they move easily and interact, in the case of elastomers, and (4) strong intermolecular interaction between chloromethyl groups and carbonyl groups compared to an aromatic ring.
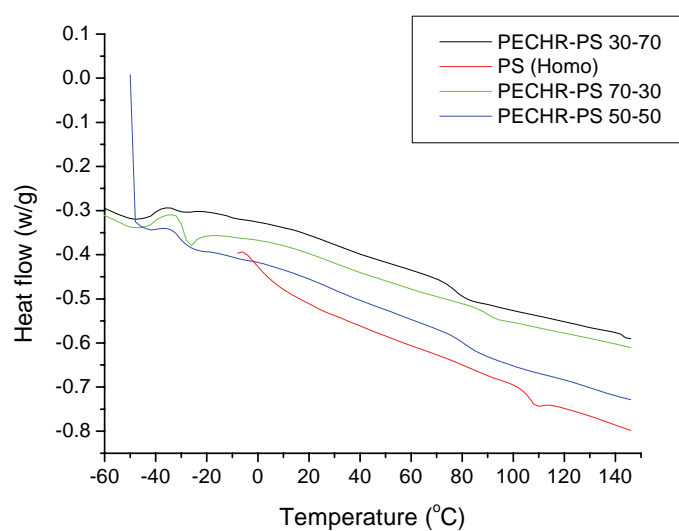
Figure 5.15 DSC thermograms of homo polystyrene, polystyrene/RPECH blends, homo rubbery PECH.

5.4 Summary

The miscibility of PMMA with PECH-diol, GAP-diol, and RPECH blends was investigated. Results obtained using different techniques showed that, PMMA produces a miscible blend when it is prepared by a casting method, using THF at 55 °C. The as-cast blend films present only one blend-composition dependent T_g, which means that the molecular mobility of the chains of each homopolymer are mutually affected. The FTIR results confirm the above finding. Most of the interaction between PMMA and low molecular weight polymers could be attributed to the hydrogen bonding through the carbonyl, chloromethyl, azide, and hydroxyl groups. SEM micrographs show smooth surfaces without any appearance of phase separation between two different polymers. There was however micro-cracks in the case of PMMA/PECH blend. The miscibility of polystyrene and PECH-diol, GAP-diol, RPECH blends were also investigated. PS showed miscible blends with both elastomers, which could be attributed to the halogenated groups and low molecular weight of elastomers (they work as plasticizers). The only immiscible blend that occurred in this work was in case of the polystyrene/RPECH blend, where two glass transition temperatures were detected. The most important findings from this study are the following: (1) chloromethyl groups show stronger interaction than azide groups with carbonyl groups, (2) the hydroxyl group of elastomers will enhance and motivate the miscibility of a blend system, (3) low molecular weight elastomers work as plasticizers, and (4) chloromethyl groups in low molecular weight elastomers have a stronger interaction than high molecular weight rubbery elastomers,

The results obtained from this study could be transferred to the industry in two different ways, firstly, replacement of PECH rubber by PECH-diol in a blended system with PMMA, which could be a reduction of materials and processing cost.

Secondly, PMMA/GAP blends could be used as a blended system in advanced applications such as propellant binder formulations and air bag system, where glass transition temperature could be controlled by alternating in the blend compositions.

5.5 References

1. Turi E. A., Thermal characterization of polymeric materials, 2nd Edition. Academic Press Limited 1997, Vol. 2, 748-755.

2. Garton A., Infrared Spectroscopy of Polymer Blends, Composites and Surfaces, Hanser 1992, 36-38.

3. Rudin A., The elements of polymer scinence and Engineering, 2nd Edition, Academic Press 1998, 445-460.

4. Fernandes A. C., Barlow J. W., Paul D. R., J. Appl. Polym. Sci 1986, 32, 5481.

5. Fernandes A. C., Barlow J. W., Paul D. R., J. Appl. Polym. Sci 1984, 29, 1971.

6. Fernandes A. C., Barlow J. W., Paul D. R., J. Appl. Polym. Sci 1986, 32, 6079.

7. Anderson C., Rodriguez F., Polym Mater Sci Eng 1984, 51, 609.

8. Shen S., Torkelson J. M., Macromolecules 1992, 25, 721.

9. Aouachria K., Belhanech N., Bensemra, Polym. Degrad. Stab 2006, 91, 504.

10. Manson J. A., Sperling L. H., Polymer Blends and Composites Plenum Press 1971, 86.

11. Xu F. Y., Chien J. C. W., Macromolecules 1994, 27, 277.

12. Matyjaszewski K., Cationic Polymerizations Mechanisms, Synthesis, and Applications, Marcel Dekker, INC 1996, 46.

13. Frankel M. B., Grant L.R., Flanagan J.E., J. Propul. Power 1992, 8, 560.

14. Kamira A., Naima B., Polym. Test 2006, 25(8), 1101.

15. El Shafee E., Polym 2002, 43, 921.

16. Rocco A. M., Moreira D. P., Pereira R. P., Daniel P. M., Robson P. P., Eur. Polym. J 2003, 39, 1925.

17. Hesse M., Meier H., Zeeh B., Spectroscopic Methods in Organic Chemistry, Georg Thieme Verlag 1997, 29.

18. Jaykrishnan A., Sunny M. C., Rajan M. N., J. Appl. Polym. Sci 1995, 56, 1187.

19. Garcia J. L., Koelling K. W., Seghi R. S., Polym 1997, 39, 1557.

Chapter 6

Synthesis and characterization of poly(epichlorohydrin-methyl methacrylate) and poly(glycidyl azide-methyl methacrylate) copolymers prepared using *N,N*-dithiocarbamate-mediated iniferters

Synthesis and characterization of poly(epichlorohydrin-methyl methacrylate) and poly(glycidyl azide-methyl methacrylate) copolymers prepared using *N,N*-dithiocarbamate-mediated iniferters

Abstract

Three different types of thermoplastic elastomers, poly(epichlorohydrin-methyl methacrylate), poly(epichlorohydrin-styrene), and poly(methyl methacrylate-glycidyl azide) copolymers were prepared using an *N,N*-diethyldithiocarbamate iniferter. The formation of poly(epichlorohydrin) and glycidyl azide polymer with pendent *N,N*-diethyldithiocarbamate groups as macro-photoiniferters were confirmed by using various spectroscopic techniques. The photopolymerization of methyl methacrylate and styrene monomers was investigated. Controlled radical polymerization of vinyl and acrlate monomers was confirmed by a linear increase in the molecular weight with conversion and a first-order time-conversion plots. The polydispersity index of products remained at 1.4-1.6 during polymerization. The copolymers were characterized by FTIR, ^{1}H-NMR, and ^{13}C-NMR, which proved the formation of two different segments in the final binders. Thermal analysis confirmed the presence of two different segments and different scanning calorimetry (DSC) showed a broad glass transition temperature (T_g) and an exothermic decomposition on the case of the glycidyl azide copolymers. Vacuum stability test was conducted and binder found to be most likely compatible with RDX according to Picatinny's arsenal test.

Keywords: Thermoplastic elastomers; poly(epichlorohydrin); methyl methacrylate; styrene, photopolymerization; dithiocarbamate; compatibility.

6.1 Introduction and objectives

The literature review will be divided into four parts. The first part will report on block and graft copolymers and their contribution to polymer science and the plastics industry. The second will focus on photopolymerization. The third will cover controlled/living free radical polymerization, with specific attention to iniferters, especially *N,N*-diethyl dithiocarbamate photoiniferters. The fourth will give a brief description in thermoplastic elastomers.

6.1.1 Block and graft copolymers

6.1.1.1 Block copolymers

The design and synthesis of materials with novel properties (structure-property relationship) is an important aspect of polymer chemistry. When only one species of monomer is used to build a macromolecule the product is called a homopolymer, normally referred to as a polymer. If the chains are composed of two types of monomer units, the material is known as a copolymer, and if three different monomers are incorporated in one chain, the materials are known as a terpolymer. Copolymers can be statistical, alternating, block, or graft [1-3].

Block copolymers are subjects of great interest, mainly from the practical viewpoint of material science, where quite often desired properties, such as mechanical properties, are not attainable by the properties of a single homopolymer. Most notably, block copolymers which consist of several types of monomer sequences are of a special interest because they combine the properties of the corresponding homopolymers without phase separation. On the other hand, thermodynamic incompatibility of the constituent blocks of copolymers leads to microphase

separations, with various phase morphologies, which often provide useful and unique properties not attainable in simple homopolymers or random copolymers.

The synthesis of block copolymers that have different combinations of components and molecular weight distributions has been a subject of interest. Controlled block copolymerization is accomplished using living anionic and cationic polymerization techniques. However, major drawbacks of the ionic processes are the monomer selectivity and rigorous synthetic requirements. In addition, anionic polymerization is limited to certain types of monomers and excludes monomers that polymerize by other mechanisms. The transformation approach in block copolymer synthesis, in which different propagation species are used, allows multiple combinations of monomers [1]. On the other hand, free radical polymerization is easy to perform, less susceptible to impurities and, more importantly, it can be applied to most of the vinyl monomers [2] (For more details on free radical polymerization, refer to Chapter 4, Section 4.1.1). Therefore, controlling polymer properties through the synthesis of various kinds of block copolymers is a continuing theme in both industry and in academic laboratories. Block copolymers are used in many different applications such as improving interfacial adhesion in various multiphase polymeric systems such as blends and laminate joints.

6.1.1.2 Graft copolymers

The synthesis of graft copolymers is another important aspect of polymer science. Graft copolymers can be described as having the general structure (**1**), where the main polymer backbone A, commonly referred to as the trunk polymer (main block), has branches of polymer chains B emanating from different points along its length. The chain extensions in the graft copolymers are at branch points along the chain and branch polymers are typically homo polymers.
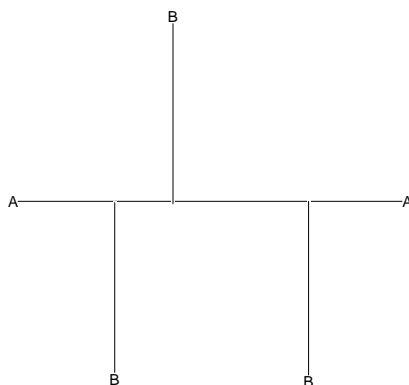
(1)

Various methods used in the synthesis of polymers have been proposed and used for synthesis of grafted copolymers, such as free radical, anionic, cationic, and condensation polymerizations. Vinyl graft copolymerization is the most popular method: it is usually described as the modification of a pre-existing polymer chain (trunk polymer), where polymer chains, comprised of different structural units from those of the trunk polymer are grown from the trunk polymer backbone. The basic method is shown in **Scheme 6.1**, and it is commonly referred to as a "grafting from" mechanism. It begins with the creation of free radical sites on the trunk polymer chain, where vinyl monomers can react with the radical to propagate into a new polymer chain that is covalently bonded to the trunk polymer.

This type of copolymerization methods offers the possibility of creating novel polymer systems that permanently combine the properties of both polymer chains. It is important to note that Scheme 6.1 does not show polymer B (homopolymer) generated during the free radical polymerization, which it is not chemically bonded to the trunk polymer A. Homopolymer can be produced during the course of the reaction in several ways, depending on the experimental conditions [3]. Living radical polymerization does not result in such well-defined architectures as obtained in living ionic polymerizations, but the greater versatility of free-radical

polymerization compared to ionic polymerizations somewhat compensates for this deficiency. Free-radical polymerization can be conducted over a wide temperature range, using a variety of solvents, and can be applied to a wide variety of monomers [4].
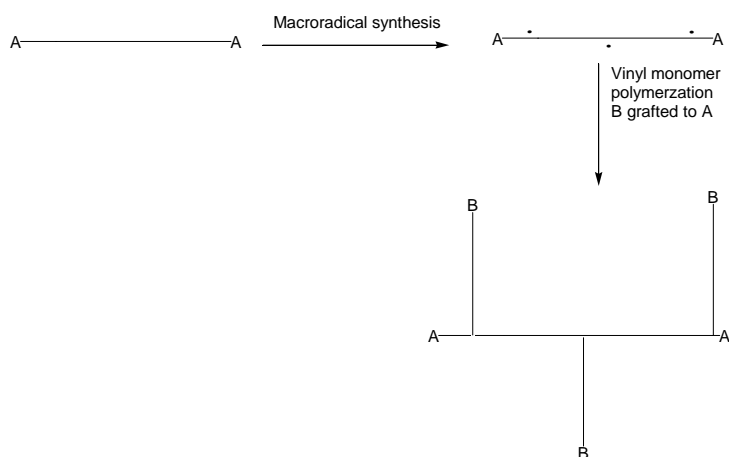
Scheme 6.1 General method of graft copolymerization of trunk polymer A, with vinyl monomer B by means of a free radical mechanism.

The main requirement in utilizing grafted copolymers in different applications is associated with a good understanding of both intramolecular and intermolecular characteristics and structure-property relationships. The major problem encountered in graft copolymerization (especially in a free radical polymerization system) is the simultaneous formation of a homopolymer. This presents difficulties especially because the separation of a homopolymer from the grafted derivative is often difficult, which creates problems with characterizing the graft derivative. Battaerd and Tregear stated the following: "In fact, homopolymer formation is the major reason for the lack of a widespread industrial development of graft copolymers" [5].

Graft copolymers have a variety of potential applications resulting from the wide range of properties available when different polymer chains are connected to form a

hybrid branched macromolecule. Grafted copolymers are used in the textile industry in order to improve fiber comfort, increase water uptake, and improve abrasion and flame resistance. Usually, hydrophilic monomers are used by grafting with fibers like cellulose. They are also used in composites, where interfacial adhesion plays a significant role in grafted polymers used for high-strength applications. As an example, the grafting of methyl methacrylate side chains onto butyl rubber (trunk polymer) has been performed in an attempt to improve interfacial compatibility, for possible use with other elastomers and plastics [6]. Grafted polymer materials are also used in medical applications, where the possibility exists to improve biocompatibility [3]. Further, grafted copolymers have proved themselves to be efficient compatibilizing agents for many different incompatible polymer mixtures [3, 6].

6.1.2 Photopolymerization

Photopolymerization has been used for a long time. An example of this is when Egyptian mummy cloth was soaked in lavender oil and dried by exposure to the sunlight.
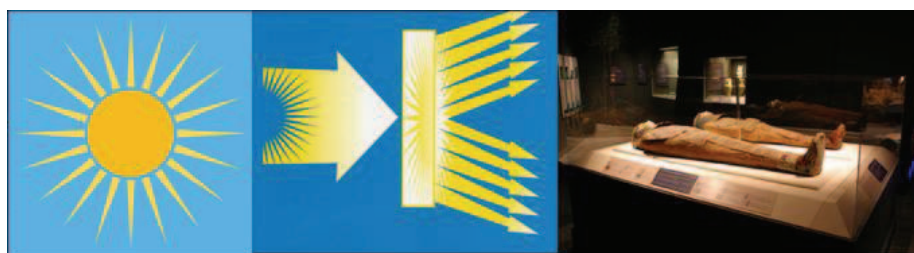
Figure 6.1 photopolymerization of Egyptian mummies cloth by using sunlight.

Today, photopolymerization is one of the most widely used processes for materials production. In 1995, a higher than 15% annual growths in the use of photopolymerization was predicted [7]. The worldwide market for UV-curable

systems approached $1 billion in 1995. However, the field is still relatively young and offers tremendous opportunities for creative scientists and engineers. This is evidenced in the rapid growth of radiation curing as an industrial process, which depends on the use of photoinitiators [7].

The growth in the applications of photopolymerization is driven by the advantages afforded by the use of light, rather than heat, to drive the conversion of monomer to polymer. Advantages of photopolymerization include solvent-free formulations, very high reaction rates at room temperature, spatial control of the polymerization, low energy input, and chemical versatility because a wide variety of monomers can be polymerized photochemically [7, 8]. Because of this unique set of advantages, photopolymerization has gained prominence recently for the pollution-free curing of polymer films as well as emerging applications in dental materials, conformal coating, electronic and optical materials, and rapid prototyping of three-dimensional objects [8]. Ultraviolet (UV)-induced polymerization is a desirable method for the surface modification of polymers for a number of reasons. The procedure is relatively simple, energy-efficient, and cost-effective, UV-induced polymerization is well suited for integration with other technologies such as microcontact printing and photolithography, to produce desired surface chemistry changes in well-defined two-dimensional regions on a surface [9]. Usually, applications of photopolymer technology can be classified into six general categories: electronic materials, printing materials, optical and electro-optical materials, fabrication of devices and materials, adhesives and sealants, and coatings and surface modifications [8]. In addition, photoinitiated vinyl polymerization is used in many techniques such as the curing of coatings on wood, metal, and paper, adhesives, printing inks, and photoresists.

Photopolymerization depends on using photoinitiators that usually absorb light in the ultraviolet-visible spectral range, generally 250-450 nm, and convert this light energy into chemical energy in the form of reactive intermediates, such as free radicals and

reactive cations, which subsequently initiate polymerization. Normally UV, visible (Vis) or infrared (IR) light are utilized to initiate photochemical reactions, but higher energy sources at shorter wavelength (e.g. electron-beam) have also been utilized. Photopolymer reactions can be categorized based on the chemical and physical processes utilized. The five categories are photopolymerization, photocrosslinking, photomolecular reactions, photodegradation, and photo/thermal reactions [7, 8].

As mentioned earlier, photopolymerization depends on using photoinitiators, which is generally divided into two classes according to the process by which the initiating radicals are formed. Compounds which undergo unimolecular bond cleavage upon irradiation as shown in **Scheme 6.2**, are termed Type 1 photoinitiators, examples of this type being the dithiocarbamate iniferters [7].

$$PI \longrightarrow PI^* \xrightarrow{\text{unimolecular reaction (fragmentation)}} R^{1\cdot} + R^{2\cdot}$$

photoinitiator   excited photoinitiator   free radicals
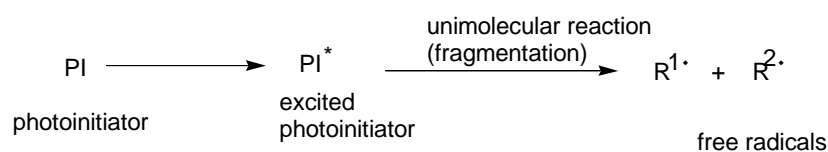
Scheme 6.2 Type 1 photoinitiator: unimolecular fragmentation [7].

In the second type of photoinitiator, the exited state photoinitiator interacts with a second molecule (a coinitiator) to generate radicals in a bimolecular reaction, as shown in **Scheme 6.3**. An example of Type 2 is benzophenone [7].

$$PI \xrightarrow{h\nu} PI^* + COI \xrightarrow{\text{bimolecular rection}} R^{1\cdot} + R^{2}$$

photoinitiator   excited photoinitiator   coinitiator
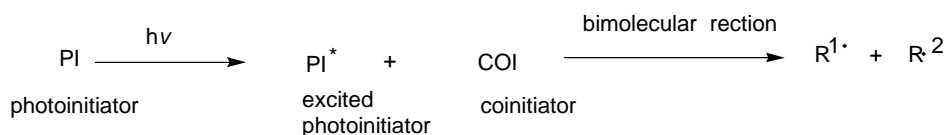
Scheme 6.3 Type 2 photoinitiator: bimolecular reaction [7].

6.1.3 Living/controlled radical photopolymerization

Living or controlled radical polymerization has helped pursue some of the main goals in macromolecular development, namely the synthesis of new polymers with well-defined chemical structures, and control of the molecular weight (a linear increase of molecular weight with conversion) and low polydispersity. In living polymerization systems there is a dynamic equilibrium between active and dormant species as a result of rapid, reversible termination or a reversible degenerative chain transfer reaction. The propagation and reversible termination should be much faster than any irreversible termination [4].

Literature reports several radical polymerization methods that exhibit controlled or living characteristic, such as (I) the use of dithiocarbamate iniferters [4, 10, 11]; (II) nitroxide-mediated processes [12]; (III) atom transfer radical polymerization (ATRP) [13]; and (IV) the reversible addition-fragmentation chain transfer (RAFT) process [2].

Quirk and Lee defined the characteristics of living polymerization as follows [4]:

1. Polymerization proceeds until all monomers have been consumed. Further addition of monomers results in continued polymerization.

2. The number average molecular weight ($\overline{M_n}$) is a linear function of conversion.

3. The number of polymer molecules is constant and independent of conversion.

4. The molecular weight can be controlled by the stoichiometry of the reaction.

5. Polymers with narrow molecular weight distribution are produced.

6. Chain-end functionalized polymers can be prepared in quantitative yields.

7. In radical polymerization, the number of active end groups should be 2, one from each end.

Controlled and living polymerization techniques provide several powerful tools for the synthesis of block and graft copolymers with well-defined structures. This is achieved by several techniques, such as (a) sequential monomer addition, (b) coupling reaction of living chains, and (c) reaction of end-functionalized polymers. In this study controlled polymerization techniques in which *N,N*-diethyl dithiocarbamate is used as photoiniferter was employed.

6.1.3.1 Iniferters

The concept of iniferters was first reported by Otsu *et al.* [14]. He also proposed the name "iniferter" (*ini*tiator-trans*fer* agent-*ter*minator) which means substances that act as initiator, transfer agent and terminator in radical polymerization reactions. Many radical initiators, such as peroxides, azo compounds, tetraphenylethane derivatives, and organic sulfur compounds, can serve as iniferters. Usually, organic sulfur compounds, such as alkyl or aryl sulfides and disulfides, have high chain transfer reactivity, and part of the thionyl radicals produced may undergo primary radical termination. It is reported that iniferters having the *N,N*-diethyl dithiocarbamyl (DDC) are excellent iniferters [15].

Most iniferters are basically organic sulfur compounds with low decomposition energy, where the bond dissociation energies of the relatively weak C-C bond are in the range of 85-65 kcal/mol in the wavelength range 300-440 nm, where the bond decomposition of C-S is in the range of 65-55 kcal/mol in wavelength range 440-495nm [7]. Consequently, under suitable conditions, the compounds are dissociated into reactive radicals and inert radicals. The latter serve as capping agents. Various vinyl monomers, such as styrene and methyl methacrylate, were polymerized using iniferters and polymerization proceeded via a living/controlled mechanism [16]. The evidence used to support this includes the low polydispersity of the products

(typically PDI ranging from 1.7 to 3), a linear increasing trend of molecular weight with the conversion, and the formation of a related block copolymer [17].

In their review, Otsu and Matsumoto reported that iniferters can be classified into two types: A-B and B-B type iniferters [15]. A-B type iniferters dissociate into different radicals when they are subjected to thermal or photochemical energy, as can be seen in **Equation 6-1**.

$$A\text{---}B \xrightarrow{\triangle \text{ or } h\nu} A^{\cdot} + B^{\cdot} \quad \text{-----------} [6\text{-}1]$$
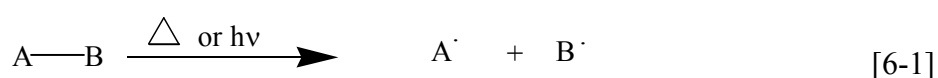
$A^{\cdot}$ is the reactive radical, which participates only in initiation and acts only as an initiator radical, and $B^{\cdot}$ is the less or non-reactive radical, which cannot enter initiation and acts as a primary radical terminator. Benzyl *N,N*-diethyl dithiocarbamate (BDC) and 1-phenylethyl *N,N*-diethyldithiocarbamate (StDC) are regarded as A-B type iniferters. When they dissociate they first form reactive benzyl or styrl radicals, which are involved in polymerization, and then the less reactive *N,N*-diethyldithiocarbamyl radicals, terminate the growing macroradical [4, 15]. **Scheme 6.4** shows the reaction for an A-B type iniferter. The iniferter thermally or photochemically dissociates at the weak bonds, and then monomer molecules are inserted by propagation, followed by a primary radical termination and/or chain transfer, to yield polymers. In addition, polymer chains will contain iniferter groups at the chain ends. These polymers may further act as the polymeric iniferters [18].
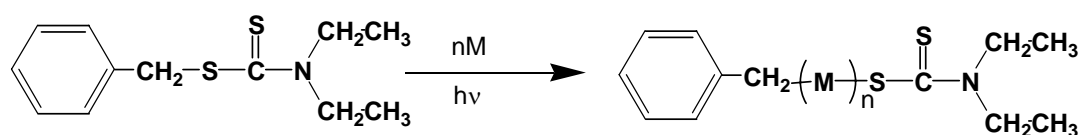
Scheme 6.4 Benzyl *N,N*-diethyl dithiocarbamate and photopolymerization of monomer (M) by using an A-B type photoiniferter.

A B-B type iniferter dissociates into two identical radicals as shown in **Equation 6-2**, Where B˙ can enter into both initiation and primary radical termination processes.

$$B\text{---}B \xrightarrow{\triangle \text{ or } h\nu} B\,{}^{\cdot} \; + \; B\,{}^{\cdot}$$ ------------------ [6-2]

Tetraethylthiuram disulfide (TD) is an example of a type B-B iniferter [4]. Polymer yield from these iniferters will have two dithiocarbamate fragments at α- and ω- chain ends, as a result of initiation and primary radical termination with dithiocarbamate radials (**Scheme 6.5**).

Scheme 6.5 Tetraethylthiuram disulfide and photopolymerization of monomer (M) by using a B-B type photoiniferter [4].

It is reported that A-B type iniferters are more useful than the B-B type for the more efficient synthesis of polymers with a controlled structure. In addition, the functionality of the iniferters can be controlled by changing the number of the A-B bonds introduced into an iniferter molecule, for example, B-A-B can be used as the binfunctional iniferter. Tetrafunctional, polyfunctional iniferters and gel-iniferters are

used for the synthesis of star polymers, graft copolymers, and multiblock copolymers, respectively [4, 19].

The living nature of iniferter polymerization depends on the reversible recombination of growing radicals with scavenging radicals. The best example of this type of system is polymerization with dithiocarbamate derivatives such as tetra-alkyl thiuram disulfide. The systems with thiuram disulfide as iniferter are usually characterized by an initial rapid growth and then a repetitive increase in molecular weight with conversion. In some cases, however, molecular weights do not increase linearly with conversion. The polymerization obeys first-order kinetics in the monomer, as often observed for steady-state conditions. Molecular weight distribution remains fairly constant but in most cases not below 2 [20].

6.1.3.2 Dithiocarbamate photoiniferters

N,N-dialkyl dithiocarbamates are known to undergo a reversible hemolytic cleavage under UV radiation, and promote a controlled polymerization [11]. The dithiocarbamate groups are known to act as photoinitiators in the free-radical polymerization of vinylic monomers. Dithiocarbamate photoiniferters have several advantages in radical polymerization, for example they can be used to prepare block copolymers using light for polymerization instead of heat. The main drawback of using dithiocarbamate photoiniferters in radical polymerization is the formation of polymers with high MWD copare to other controlled/living polymerization. in any case, MWD is also affected by the structure of the monomers used. Styrene and MMA and their derivatives can easily be polymerized by a living radical mechanism, but Vinyl acetate and Methyl acrylate are polymerized with a low or no living nature [16].

There are two different routes for the decomposition of S-S or C-S bonds in iniferters. One is thermal and the other is photochemical. The thermochemical bond strength of

the S-S bond in disulfides is known to be about 263 kJ/mol [21]. The decomposition of S-S or C-S bonds requires UV light of between 254 and 366 nm. For each case, the exact wavelength has to be determined from the UV absorption spectrum. Photochemical decomposition usually takes place at lower temperature that is easier to control [4].

When a macro-initiator with diethyl dithiocarbamate groups is subjected to UV radiation there are two possible mechanisms for the decomposition of the initiator: The first is a homolytic scission of the C-S bond between the pendant methylene carbon (indicated by the arrow marked **1** in **Scheme 6.6**) and the sulfur attached to it, the second is the scission of the bond between the sulfur and the carbon (indicated by the arrow marked **2** in Scheme 6.6). The decomposition of these groups depends on the bond length, bond energy, and the bond order of the individually activated bonds [4]. However, it appears as if the first of the above mechanisms is more generally accepted [4, 18].
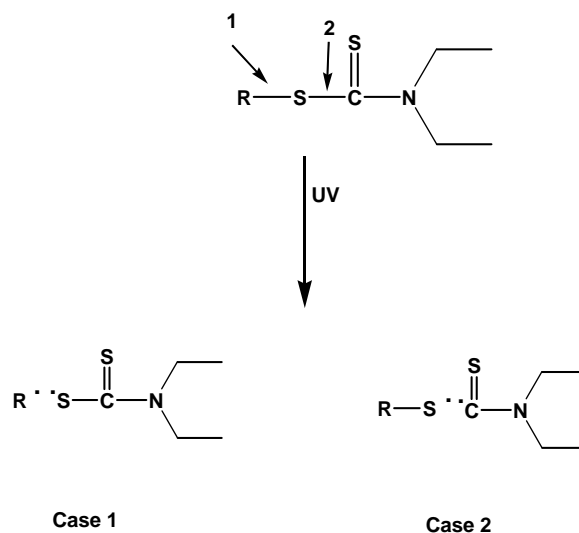
Scheme 6.6 Proposed reaction routes for the decomposition of dithiocarbmate photoiniferters after exposure to UV irradiation.

The nature of the two groups attached to the C=S double bond affect the polymerization. Destarac *et al*. [2], reported that a good iniferter must have two properties, firstly, the rate of addition to the (C=S) bond and fragmentation of the intermediate radical R should be rapid relative to propagation and, secondly the radical must reinitiate polymerization, preferably at a rate equal to that of the propagation in order to avoid any retardation [11]. On the other hand, it is reported that dithiocarbamate has the lowest rate of addition and chain transfer coefficients, which is attributed to the interaction between the N and the C=S double bond. Dithiobenzoates has the highest rate of addition and chain transfer coefficients, which is attributed to the benzyl ring of dithiobenzoate.

Photoiniferters such as *N,N*-diethyl dithiocarbamate can be used directly or as moieties attached to, inter alia, polymers. Most of the photoiniferters are difficult to use directly in large-scale applications because of limitations such as poor storage stability, bad odour, and incompatibility with monomers. One of the solutions to these problems could be the attachment of photoinitiators to the polymeric species, which could be decomposed in the presence of light. Polymeric photoinferters have low volatility and do not suffer from initiator migration effects. The low volatility should also reduce odour problems. Polymeric photoiniferters can be used as precursors to block and graft polymerization reactions. Several examples of the use of diethyl dithiocarbamate in this type of application have been reported [16, 22, 23]. As an example, the synthesis of a photoinitiator from 3-chloro-1,2-propanediol via the nucleophilic substitution of the chlorine atom by photoactive sodium diethyl dithiocarbamate [24].

6.1.3.3 Preparation of block copolymers using diethyl dithiocarbamate photoiniferters

When the iniferter technique is used in radical polymerization the polymer product will have the same functionality as the iniferter. Therefore various AB and ABA block copolymers consisting of PS, PMMA, and PVA were synthesized by using monofunctional iniferters such as benzyl *N,N*-diethyl dithiocarbamate and difunctional photoiniferters such as p-xylylene bis(*N,N*-diethyl dithiocarbamate) [18]. Qin *et al*. [25, 26], reported on the synthesis of poly(vinyl acetate-*b*-styrene-*b*-vinyl acetate) and poly(styrene-*b*-methyl methacrylate-*b*-styrene) as ABA triblock copolymers utilizing diethyl 2,3-dicyano-2,3-di(p-*N,N*-diethyl dithiocarbamymethyl) phenylsuccinate as a multi-functional iniferter. The results confirmed controlled polymerization and the polydispersity index was less than 1.9. Another method by which produces block copolymer is based on terminating the end groups of the first segment or polymer with a photoiniferter (usually done by modification of the polymer end groups) and then utilizing the latter as a macro-initiator for vinyl monomers, to yield block copolymers [27].

6.1.3.4 Graft copolymers prepared using diethyl dithiocarbamate photoiniferters

Graft copolymers can be obtained by using living free-radical polymerization. This task can be achieved by modifying conventional polymers to form macroinitiators for living graft polymerization. The grafting of conventional polymers proceeds in two steps: the first step is the synthesis of a macroinitiator from the trunk polymer and the second is the grafting of a second monomer onto the macroinitiator [4].

Photoiniferters can be used to synthesize graft copolymers via different techniques. One of the advantages of using photoiniferters in the synthesis of a grafted copolymer is the reduction of the amount of homopolymer generated during polymerization, when polymerization runs at low temperature. There are two ways to make a grafted

copolymer based on a DDC photoiniferter. In the first method the DDC photoiniferter has a polymerizable double bond, i.e., a monomer iniferter, which is successively used as both monomer and iniferter, to yield macromonomers and grafts. An example of this type is 4-vinylbenzyl *N,N*-diethyl dithiocarbamate (**2**), a monomer-iniferter, which is used for the synthesis of graft and cross-linked polymers [28].

(**2**)
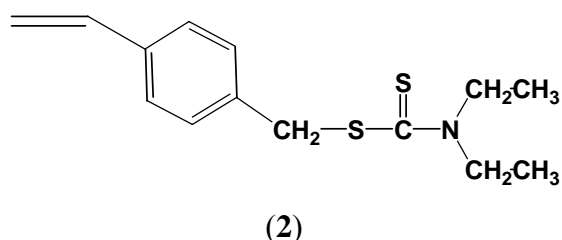
The second method is based on adding the DDC groups to the side group of the polymer. An example of this is when PVC-based polymeric iniferters bearing the DDC moieties on the side chain yield graft copolymers [4]. Graft copolymerization from PS modified with the DDC moiety have also been reported [29]. These copolymers have been applied to biomedical uses, including polymeric materials for catheters [15]. In addition, polymers with a dithiocarbamate photoiniferter group in a side-chain end were also synthesized. For example, when poly(vinyl chloride) was reacted with sodium dithiocarbamate in dimethylformamide (DMF), a polymer with 15 wt% DDC pendant group (**3**) was prepared, which was then used as a photoiniferter for preparing new antithrombogenic heparized polymers, which were commercialized [23].

(**3**)
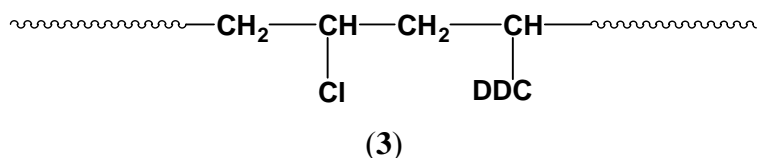
These iniferter techniques have been used for the surface grafting of hydrophilic monomers onto hydrophobic polymer surfaces. Photoiniferters also used to modify solid surfaces and nano-particles by graft polymerization with different types of polymers, which is a versatile and effective technique for tailoring surface chemistry and properties [9].

6.1.3.4 Thermoplastic elastomers

The emergence of thermoplastic elastomers (TPEs) is another important development in the field of polymer science and technology. TPEs material poses the elasticity of a rubber, under ambient conditions, and the thermoplasticity and processiblity of a plastic. TPEs consist of hard and soft segments. The hard segment gives the thermoplastic behavior to the copolymer, where the soft segment gives the elastomeric behavior. Thermoplastic elastomers are used in different applications such as sealants, adhesives; coatings etc. and they can be processed by conventional thermoplastic processes such as extrusion and molding. Also, it has the possibility to be recycled many times, which reduces waste disposal [30]. TPEs can be block or graft copolymers, where the latter have a variety of potential applications resulting from the wide range of properties available when different polymer chains are connected to form a hybrid branched macromolecule as mentioned previously in this document [30].

6.1.4 Objectives and work plan

The main objective of this study is to synthesize thermoplastic elastomers and energetic thermoplastic elastomers (ETPE) by utilizing controlled free radical polymerization. This was achieved by synthesize of macro-photoinitiators based on the grafting of *N,N* diethyl dithiocarbamate onto PECH and GAP. Those macro-photoinitiators were then used to initiate light induced free radical polymerization of

vinyl and acrylate monomers, when it is subjected to UV light. It is reported that PECH has good properties such as excellent oil resistance, heat aging resistance, and good air retention [31]. Finally, **Figure 6.2** is a schematic layout of the proposed work and various materials prepared.
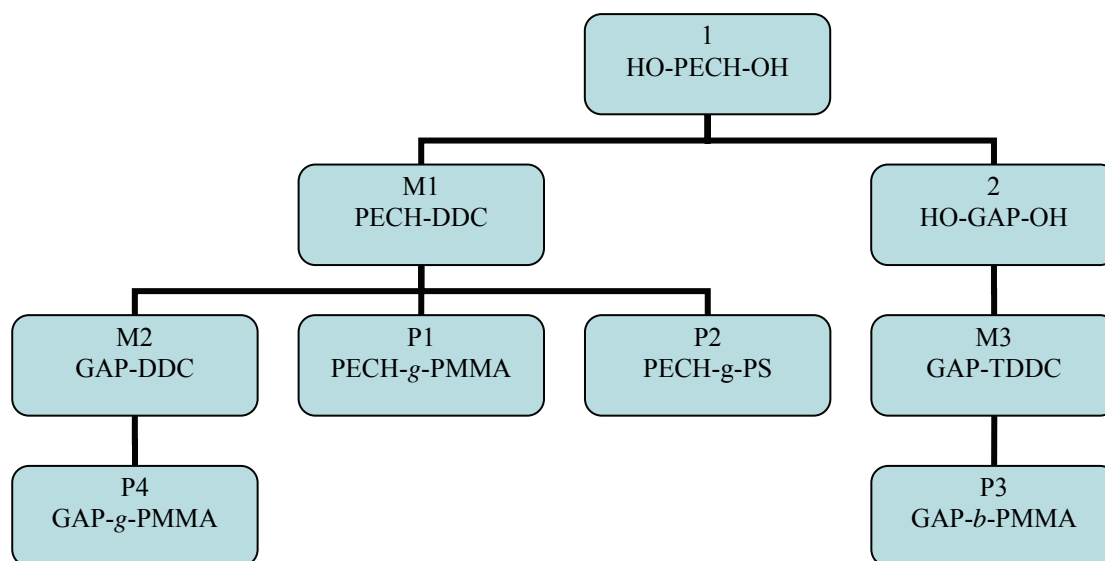
Figure 6.2 Schematic representations of different macro-initiators and copolymers to be prepared during this study.

1: Hydroxyl terminated poly (epichlorohydrin)

2: Hydroxyl terminated glycidyl azide polymer

M1: *N,N*-diethyl dithiocarbamate poly(epichlorohydrin) (macro-initiators)

M2: *N,N*-diethyl dithiocarbamate glycidyl azide polymer (macro-initiators)

M3: *N,N*-diethyl dithiocarbamate terminated glycidyl azide polymer (macro-initiators)

P1: Poly (epichlorohydrin-methyl methacrylate) graft copolymer

P2: Poly (epichlorohydrin-styrene) graft copolymer

P3: Poly (glycidyl azide-methyl methacrylate) block copolymer

P4: Poly (glycidyl azide-methyl methacrylate) graft copolymer

6.2 Experimental

6.2.1 Materials

Sodium *N,N'*-diethyl dithiocarbamate, sodium azide, and chloro acetic acid were obtained from Aldrich and used without further purification. Magnesium sulfate was obtained from Saarchem. Hydroxyl terminated poly(epichlorohydrin) elastomer (PECH-diol) was prepared by using a cationic ring-opening polymerization method (as described in Chapter 2, Section 2.2.3.1). Hydroxyl terminated glycidyl azide polymer elastomer (GAP-diol) was obtained by an azidation reaction of PECH-diol with sodium azide in DMF solvent (for more details see Chapter 3, Section 3.2.3.1). Toluene and dichloromethane were obtained from Saarchem and purified by following standard procedures. Methanol and ethanol (absolute) were used as has been received from Saarchem. MMA and styrene were first washed with a 0.3 M KOH solution to remove inhibitors and then distilled under reduced pressure. Monomers were stored over molecular sieves (5A) in a refrigerator and used within 1 week. All purified solvents and reagents were stored over molecular sieves.

6.2.2 Analytical techniques

6.2.2.1- UV, FTIR, NMR, GPC, DSC, and TGA analysis

The equipment and analytical methods used for the UV, FTIR, NMR, GPC, and DSC analysis are described in Chapter 2 Section 2.2.2. A description of the TGA equipment and the analysis method used is described in Chapter 3 Section 3.2.2.

6.2.2.2- Vacuum thermal stability test

The vacuum thermal stability test is described by RSA-MIL-STD-154. 2.5 g of each component and a mixture of the two components were used in the test and three thermal stability values obtained:

- The thermal stability value for the explosive formulation (reading V_A).
- The thermal stability value for the material the explosive formation will be in contact with (reading V_B).
- The thermal stability value or a mixture of the explosive sample and the material it will be in contact with (reading V_C).

The reactivity (Re) is then calculated by the following **Equation 6-3** and Table 6.1 shows the acceptance criterion for the vacuum themal stability test.

$$\text{Re} = V_c - (V_A + V_B) \dots\dots\dots\dots\dots[6\text{-}3]$$

Table 6.1 The acceptance criterion for the vacuum thermal stability test.

Grade of reactivity	Insignificant	Very Slight	Slight	Moderate	Excessive
	Re < 1,0	1,0 ≤ Re < 2,0	2,0 ≤ Re < 3,0	3,0 ≤ Re < 5,0	Re ≥ 5,0

6.2.3 Experimental techniques

These sections describe the experimental techniques used in the preparing of the macro-initiators and polymerize MMA and styrene monomers in the presence of different types of macro-initiators.

6.2.3.1 Preparation of *N,N*-diethyl dithiocarbamate-poly(epichlorohydrin)

N,N-diethyl dithiocarbamate-poly(epichlorohydrin) was synthesized by refluxing PECH-diol (2 g) with an equal mass of sodium diethyl dithiocarbamate for about 18 hours in an absolute ethanol (**Scheme 6.7**). On completion of the reaction, the sodium chloride formed during the reaction was filtered off, and the solvent was removed under vacuum. The viscous product was dissolved in dichloromethane and unreacted

sodium *N,N*-diethyl dithiocarbamate was removed by filtration. The organic solution was transferred to a separating funnel and washed three times with distilled water in order to dissolve all unreacted salts. The product was isolated from the dichloromethane by vacuum distillation and dried under vacuum overnight at room temperature. The yield was about 80%. The product was characterized by UV, FTIR, and NMR spectroscopy, as well by GPC.

^{1}H-NMR (CDCl$_3$): δ= 1.2 ppm [CH$_3$ of DDC], δ= 1.54 ppm [CH$_2$ of 1, 4-butanediol], δ= 3.1ppm [hydroxyl group proton of PECH], δ= 3.37-3.8ppm [CH$_2$Cl and CH$_2$ of PECH], δ= 3.95ppm [CH$_2$ of DDC], δ= 4.44ppm [CH of PECH].

^{13}C-NMR (CDCl$_3$): δ= 11.37 ppm [CH$_3$ of DDC], δ= 26.5, 75 ppm [CH$_2$ of the butane diol], δ= 34 ppm [CH$_2$ linked between PECH and DDC], δ= 38-46 ppm [CH$_2$Cl of PECH], δ= 48 ppm [CH$_2$ of DDC], δ= 68-72 ppm [–O–CH$_2$– of PECH], δ= 79-80 ppm [CH of PECH] and δ= 195 ppm [C=S of DDC].

FTIR (NaCl): 3406 (s, –OH), 2906 (s, –CH$_2$), 2866 (s, –CH), 1640 (s, C=S–N), 1485 (w), 1420 (w), 1355 (w), 1270 (w), 1200 (w), 1108 (s, –O–), 908 (w), 830 (s), 744(s, CH$_2$Cl), 700 (s), 570 (w) cm^{-1}. UV spectrum shows two peaks at about 251 nm (–S–C(=S)–) and 280 nm (–C(=S)–N).

Scheme 6.7 The reaction of hydroxyl terminated poly(epichlorohydrin) with sodium diethyl dithiocarbamate to produce *N,N*-diethyl dithiocarbamate-poly(epichlorohydrin) (R is 1, 4-butanediol).

6.2.3.2 Preparation of *N,N*-diethyl dithiocarbamate-glycidyl azide polymer

N,N-diethyl dithiocarbamate-poly(epichlorohydrin) (Section 6.2.3.1) was used in the synthesis of *N,N*-diethyl dithiocarbamate-glycidyl azide polymer (GAP-DDC) by replacing chloromethyl groups with azide groups via an azidation reaction in DMF as solvent. The following is a description of the typical experimental method: *N,N*-diethyl dithiocarbamate-poly(epichlorohydrin) (2 g) in DMF (80 mL) was placed in a two necked flask with the mixture heated to 50 °C for 2 hours. Sodium azide (2 g) was then slowly added to the mixture and the temperature increased to 60 °C. The reaction mixture was allowed to stir for 24 hr before allowing it to cool to room temperature. (*Note*: heating the reaction mixture to a high temperature was avoided in order to prevent degradation of diethyl dithiocarbamate pendant groups.) The

polymer solution was diluted with dichloromethane and the unreacted sodium azide and the sodium chloride formed during the reaction removed by filtration. The solution was transferred to a separating funnel and washed with water to extract the DMF. The organic layer at the bottom of the separation funnel was collected. This layer was then washed several times with water (minimum 3 times). The polymer solution in dichloromethane was dried over magnesium sulfate overnight. The polymeric product was isolated by removing the solvent by vacuum distillation. The yield was about 78%. The product was characterized by UV, FTIR, and NMR spectroscopy, as well as by GPC. The proposed reaction mechanism for the preparation of GAP grafted with *N,N*-diethyl dithiocarbamate can be seen in **Scheme 6.8** below. (*Note:* no brine was used to reduce the foam generated during the separation, as salt water could destroy the carbon sulfur bond.)

^{1}H-NMR (CDCl$_3$): δ= 1.2 ppm [CH$_3$ of DDC], δ= 1.54 ppm [CH$_2$ of 1, 4-butanediol], δ= 3.37-3.8 ppm [CH$_2$N$_3$ and CH$_2$ of GAP], δ= 3.95 ppm [CH$_2$ of DDC], δ= 4.44 ppm [CH of GAP].

^{13}C-NMR (CDCl$_3$): δ= 11.37 ppm [CH$_3$ of DDC], δ= 26.5 ppm [CH$_2$ of 1,4-butanediol], δ= 34 ppm [CH$_2$ linked between GAP and DDC], δ= 46 ppm [residual CH$_2$Cl$_2$ of GAP], δ= 50-54 ppm [CH$_2$N$_3$ of GAP], δ= 48 ppm [CH$_2$ of DDC], δ= 70-72 ppm [–O–CH$_2$– of GAP], δ= 79-80 ppm [CH of GAP] and δ= 195 ppm [C=S of DDC].

FTIR (NaCl): 3406 (s, –OH), 2906 (s, –CH$_2$), 2866 (s, –CH), 2100 (s,CH$_2$N$_3$), 1677 (s), 1450 (w), 1275 (s, –C=S–N), 1108 (s, –O–), 925 (w), 660 (s), 555 (s) cm^{-1}.

The UV spectrum shows two absorptions at 251 nm (–S–C(=S)–) and 280 nm (–C(=S)–N).
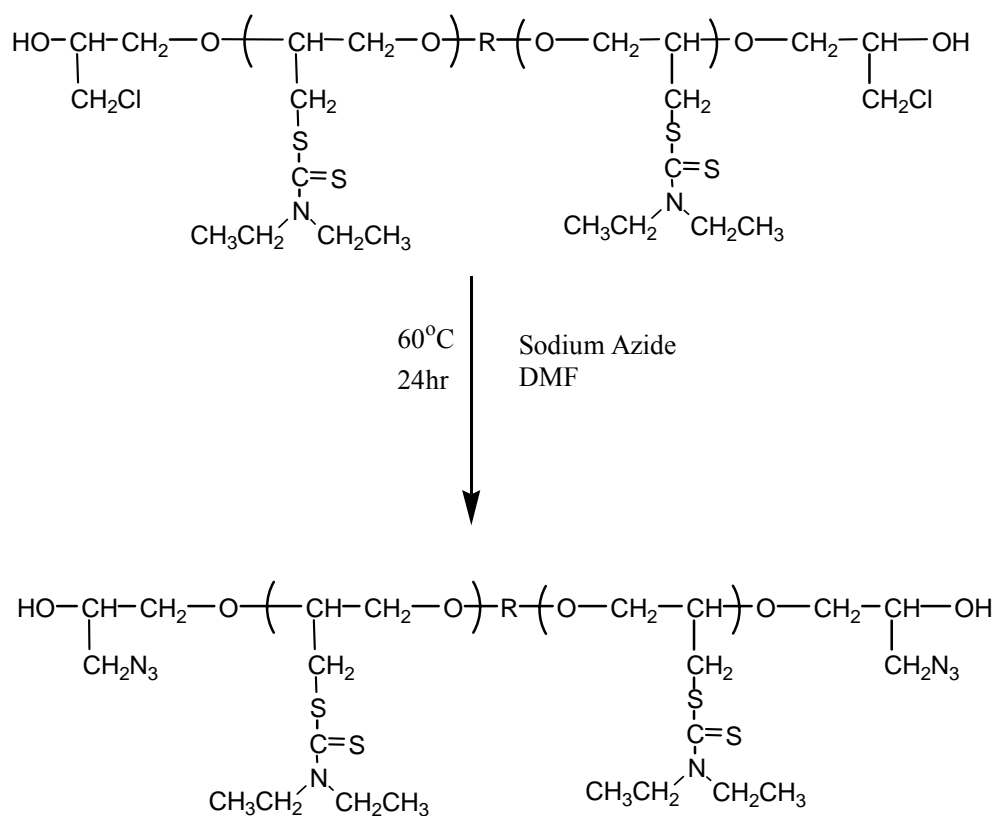
Scheme 6.8 Proposed reaction mechanism for the synthesis of *N,N*-diethyl dithiocarbamate-glycidyl azide polymer photoinitiators by the reaction of *N,N*-diethyl dithiocarbamate-poly(epichlorohydrin) photoinitiators with sodium azide in DMF (R is 1, 4-butanediol).

6.2.3.3 Preparation of *N,N*-diethyl dithiocarbamate terminated glycidyl azide polymer

N,N-diethyl dithiocarbamate terminated glycidyl azide polymer (GAP-TDDC) was prepared in two steps. First, GAP-diol was reacted with chloroacetic acid in a toluene solution. This reaction was based on the esterification reaction of the OH groups in

the GAP-diol. The following equipment was used: a dry 250 mL two necked flask fitted with a magnetic stirrer, a dropping funnel, and a reflux condenser with a calcium chloride grade tube. The flask was charged with GAP-diol (2 g, 1.3 mmol), triethyl amine (3.3 mmol), and toluene (100 mL) the mixture stirred for about 1hour at room temperature. Then, chloro acetic acid (0.24 g, 2.6 mmol) in toluene (20 mL) was added dropwise to the reaction mixture using a dripping funnel. The reaction mixture was stirred for about 1 hour at room temperature then refluxed for another 4 hours. After it had cooled to room temperature it was filtered through a filtering paper. The filtrate was washed with an aqueous solution 15 wt% HCl and the organic layer was dried over magnesium sulfate. Finally, the organic layer was collected in a round bottom flask and the solvent was removed under a reduced pressure. The attachment of DDC to GAP was based on nucleophilic substitution of terminal Cl groups with sodium *N,N*-dithiocarbamate in ethanol, as described previously in the method followed to prepare diethyl dithiocarbamate terminated glycidyl azide polymer. **Scheme 6.9** shows a schematic representation of the preparation of GAP-TDDC.
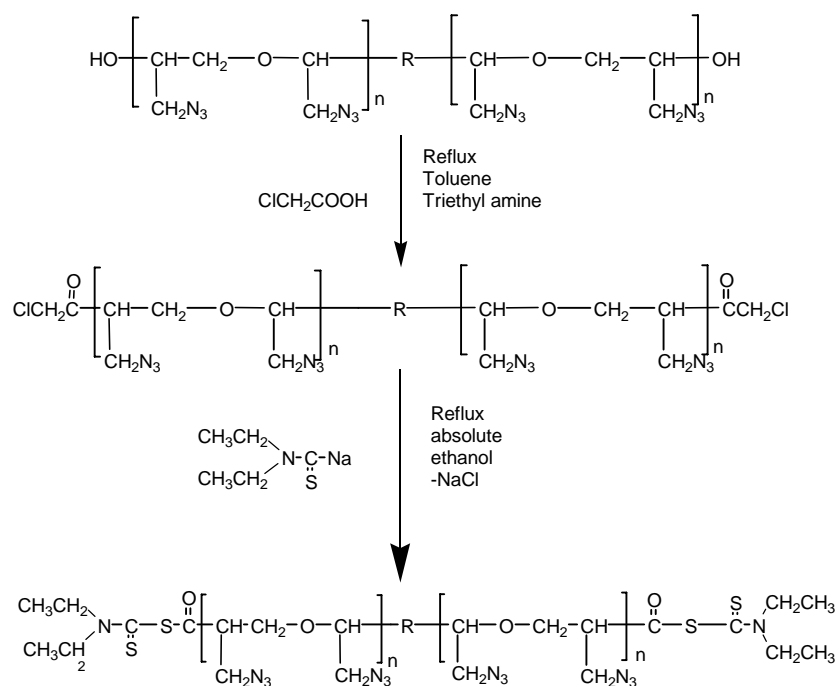
Scheme 6.9 Schematic representation of the preparation of *N,N*-diethyl dithiocarbamate terminated glycidyl azide polymer (R is 1,4-butanediol).

6.2.3.4 Photopolymerization in the presence of a macro-initiator

Photopolymerization reactions were carried out in toluene as solvent. A mixture of predetermined quantities of MMA or styrene (monomer) and PECH-DDC or GAP-DDC (macro-initiators) was placed in a Pyrex tube. The tube and contents were purged with nitrogen for about 15 minutes prior to irradiation. The reaction tube was exposed to ultraviolet radiation. A photo-reactor (Q-U-V Accelerated Weathering Tester) equipped with a cooling system and 15 Philips 8 W/06 lamps, emitting light nominally at $\lambda > 300$ nm, was used for this reaction. The temperature of the photo-reactor was maintained at 36 $^{\circ}$C. After polymerization for a given time, the

conversion of the polymerization reaction was determined gravimetrically. The conversion samples were taken at a specific time via a syringe (2mL) and poured into an aluminum dish. The dish was left to dry in a fume hood overnight to allow evaporation of the solvent. The final product was isolated by precipitation in methanol in order to remove all unreacted macro-initiator, and then dried under reduced pressure. **Scheme 6.10** shows the proposed reaction of polymerization of MMA in the presence of PECH-DDC to yield PECH-*g*-PMMA. **Scheme 6.11** shows the representation for the synthesis of GAP-*b*-PMMA.
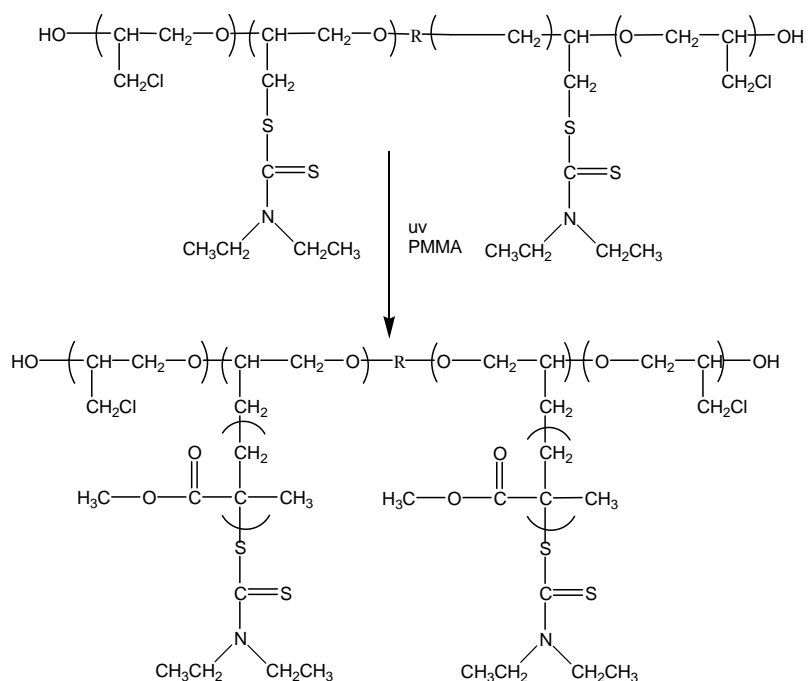
Scheme 6.10 Proposed mechanism for the synthesis of poly(epichlorohydrin-methyl methacrylate) graft copolymer (R is 1,4-butanediol).
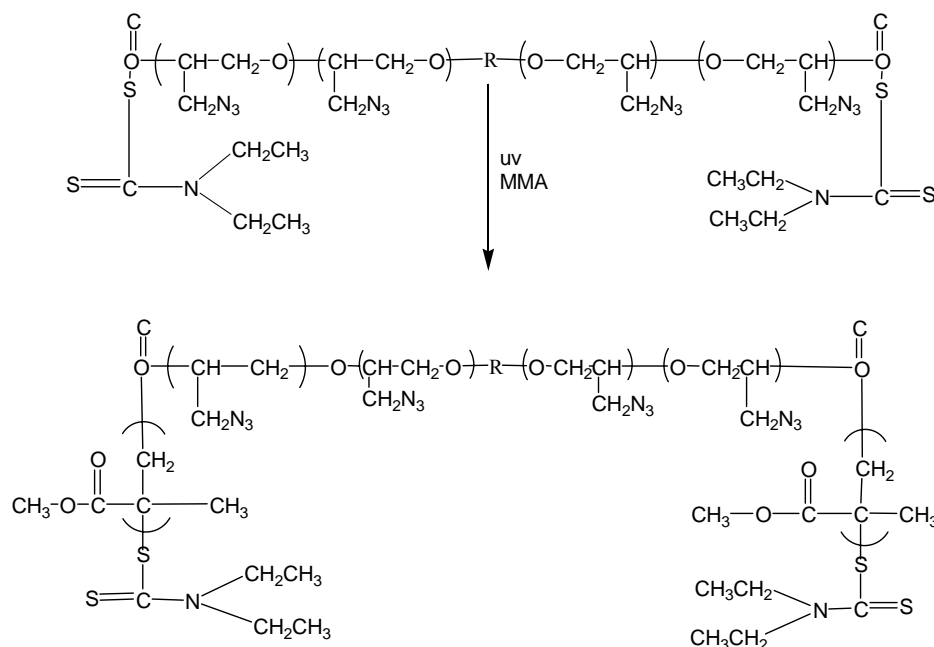
Scheme 6.11 Proposed mechanism for the synthesis of poly (glycidyl azide-methyl methacrylate) block copolymer (R is 1,4-butanediol).

6.3 Results and discussion

This part will be divided for three sections. The first section will cover the synthesis and characterization of the macro-iniferters, *N,N* dithiocarbamate-poly(epichlorohydrin), *N,N*-diethyl dithiocarbamate-glycidyl azide polymer and *N,N*-diethyl dithiocarbamate terminated glycidyl azide polymer. The second describes the synthesis and characterization of poly(epichlorohydrin-graft-methyl methacrylate) (PECH-*g*-PMMA) and poly(epichlorohydrin-graft-styrene) (PECH-*g*-PS) copolymers. The third describes the synthesis and characterization of poly(glycidyl azide-graft-methyl methacrylate) (GAP-*g*-PMMA), and poly(glycidyl azide-block-methyl methacrylate) (GAP-*b*-PMMA) copolymers.

6.3.1 Synthesis of macro-iniferters

Three different types of macro-iniferters were prepared, namely *N,N*-diethyl dithiocarbamate-poly(epichlorohydrin), *N,N*-diethyl dithiocarbamate-glycidyl azide polymer, and *N,N*-diethyl dithiocarbamate terminated glycidyl azide polymer.

6.3.1.1 *N,N*-diethyl dithiocarbamate-poly(epichlorohydrin) macro-iniferter

The attachment of diethyl dithiocarbamate to poly(epichlorohydrin) was achieved via nucleophilic substitution of chlorine moieties with sodium diethyl dithiocarbamate. Precipitation of sodium chloride as a white salt during the reaction indicated the formation of PECH-DDC. The successful synthesis of PECH-DCC was confirmed by FTIR, UV, and NMR analyses. The UV spectrum of PECH-DDC is shown in **Figure 6.3.** The UV spectrum of PECH-DDC has strong absorption bands at about 251 and 280 nm, which attributed to the –S–C(=S)– and –C(=S)–N groups, respectively [24, 32]. The UV spectrum of PECH does not show absorption peaks in this region. UV adsorption was also used to determine the extent of the substitution. The UV spectrum of the purified macro-initiator shows an increase in the adsorption with increasing reaction time. This could be attributed to the increased quantity of grafted thio compounds groups. A similar result was obtained when sodium diethyl dithiocarbamate reacted with PVC to prepare macro-initiators, and when 3-chloro-1,2-propane diol reacted with sodium diethyl dithiocarbamate to prepare diethyl dithiocarbamate-(1,2)-propane diol [4, 24]. The FTIR spectra of PECH (Chapter 2, Section 2.3.1.1) and PECH-DDC pendent groups were compared: characteristic peaks due to the –SC(=S)N and –C(=S)–N groups appearing at 915, 985, 1415 cm^{-1} and 1205, 1271, 1480, 1644 and 3400 cm^{-1}, respectively, could be assigned [9, 22, 28, 24, 28, 32]. While some of these peaks might overlap with some of the PECH homopolymer peaks, several are distinctive (e.g. at 1644 cm^{-1}) [33]. **Figure 6.4** shows the FTIR spectrum of PECH-DDC.
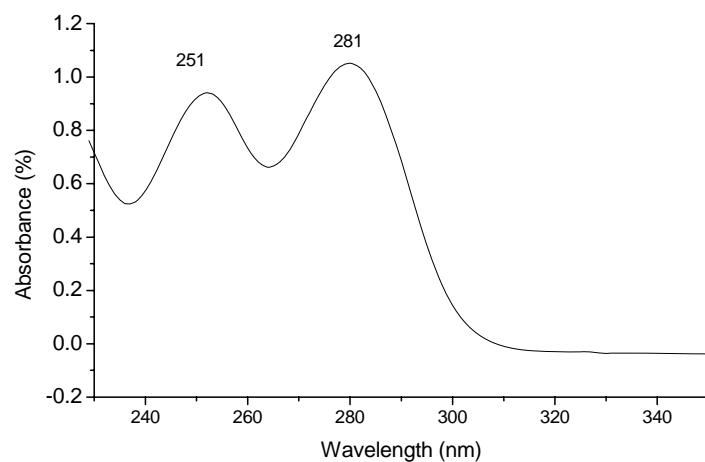
Figure 6.3 UV absorption spectrum of poly(epichlorohydrin) with diethyl dithiocarbamate pendant groups. (Concentration 1 mg/mL, dichloromethane used as solvent)
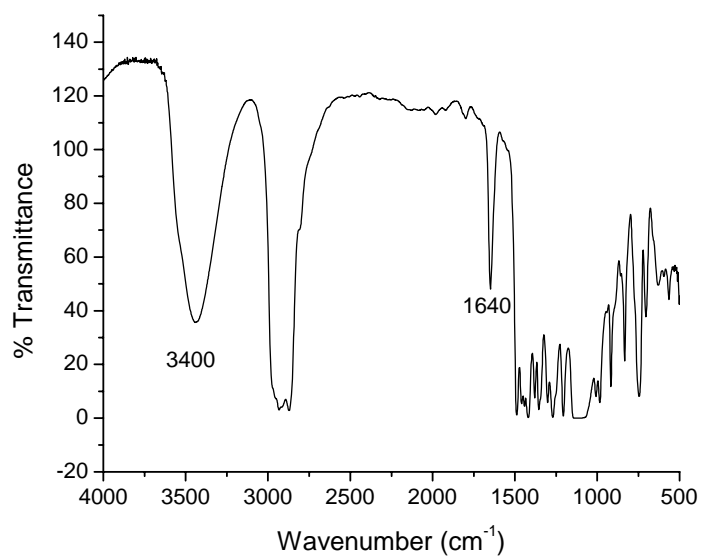
Figure 6.4 FTIR spectrum of poly(epichlorohydrin) with diethyl dithiocarbamate pendant groups.

The ^{1}H-NMR spectrum of PECH-DDC is shown in **Figure 6.5**. The most important peaks are those of the methyl protons of DDC (δ= 1.22-1.35 ppm, denoted 1), the methylene protons of diols (δ= 1.58 ppm, denoted 2), the chloromethyl protons of PECH (δ= 3.2-3.7 ppm, denoted 4), and the methylene protons of DDC (δ= 3.9 ppm, denoted 6). The ^{13}C-NMR spectrum of PECH-DDC is shown in **Figure 6.6**. The most important peaks are those of the methyl carbon of DDC (δ=10 ppm, denoted 1), the methylene carbon which links PECH to DDC (δ=33 ppm, denoted 3), the methylene carbon of DDC (δ=50 ppm, denoted 6), and the carbon sulfur double bond of DDC (δ=195 ppm, denoted 11).
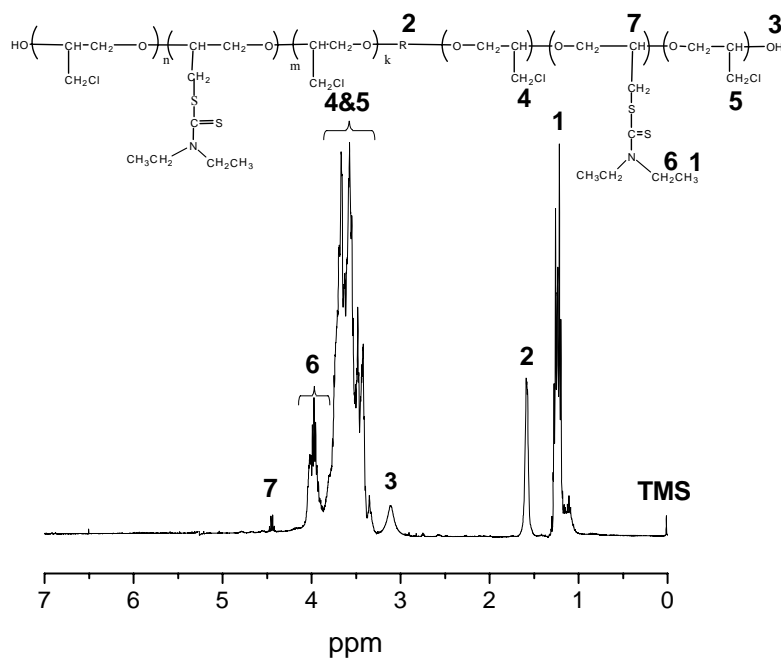
Figure 6.5 ^{1}H-NMR (CDCl$_3$) spectrum of poly(epichlorohydrin) with diethyl dithiocarbamate pendant groups (R is 1,4-butandiol).
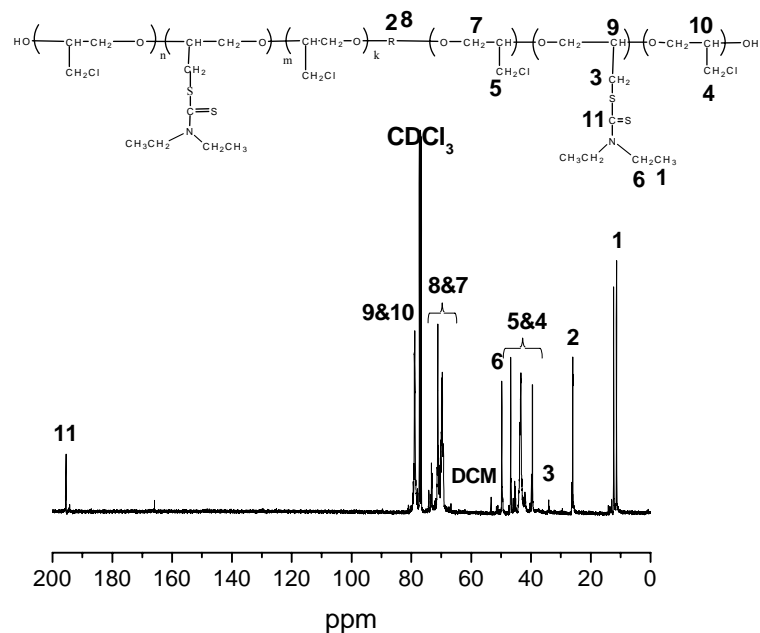
Figure 6.6 ^{13}C-NMR (CDCl$_3$) spectrum of poly(epichlorohydrin) with diethyl dithiocarbamate pendant groups(R is 1,4-butandiol).

The GPC of PECH before and after the attachment of DDC are shown in **Figure 6.7**. There is an increase in molecular weight of PECH after reaction with *N,N*-diethyl dithiocarbamate; the elution time shifts from 19.1 to about 18.2 min. The molecular weight of PECH-DDC is about 1172 g/mol, while the PDI did not change. The GPC profiles of PECH before and after the attachment of DDC indicate that the molecular weight increased by about 18%, due to the replacement of chloromethyl groups with diethyl dithiocarbamate. No reduction in molecular weight was noticed and the polydispersity index did not change with reaction between PECH and sodium dithiocarbamate. This is an indication that no cross-linking occurred.

The combination results of the FTIR, UV, NMR and GPC confirmed the successful preparation of diethyl dithiocarbamate-poly(epichlorohydrin) as macro-photoinitiator. This macro-iniferter will be used in the next step as photo initiator in the

polymerization of MMA and styrene monomers in order to produce PECH-*g*- PMMA and PECH-*g*-PS copolymers, respectively.
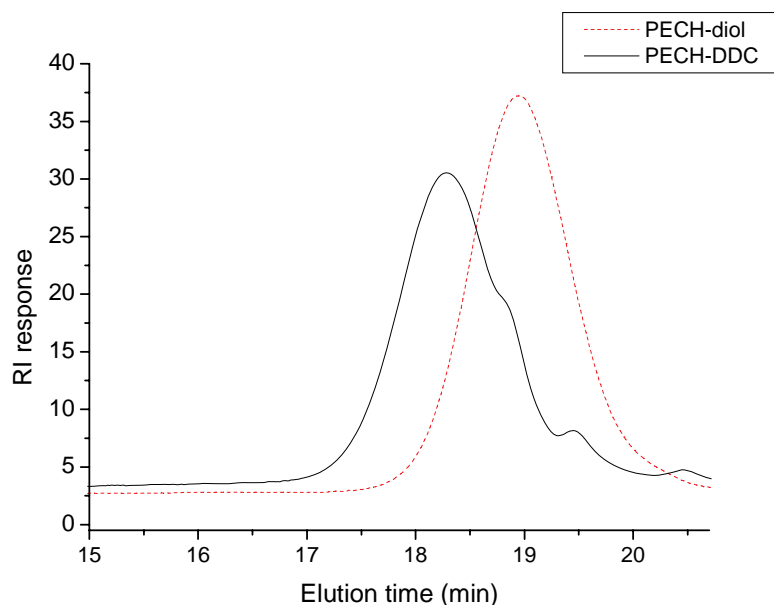
Figure 6.7 GPC traces of poly(epichlorohydrin) and poly(epichlorohydrin) with diethyl dithiocarbamate pendant groups.

6.3.1.2 *N,N*-diethyl dithiocarbamate-glycidyl azide polymer macro-iniferter

N,N-diethyl dithiocarbamate was attached to glycidyl azide polymer via two different mechanisms. The first reaction was based on the azidation reaction of diethyl dithiocarbamate-poly(epichlorohydrin) to yield *N,N*-diethyl dithiocarbamate-glycidyl azide (GAP-DDC). The second was based on the esterification of hydroxyl groups of GAP-diol with chloroacetic acid, to be reacted later with sodium diethyl dithiocarbamate via a nucleophilic substitution reaction, to yield *N,N*-diethyl dithiocarbamate terminated glycidyl azide (GAP-TDDC).

6.3.1.2.1 Synthesis of *N,N*-diethyl dithiocarbamate-glycidyl azide polymer

The azidation reaction of PECH-DDC was achieved via the reaction of PECH-DDC with sodium azide in DMF to yield GAP-DDC. Usually, the use of a polar aprotic solvent such as dimethylformamide (DMF), dimethyl sulphoxide (DMSO), and dimethylacetamide (DMA) gives complete conversion of poly(epichlorohydrin) to a GAP-diol in a shorter period than in aqueous solvents [34]. Some authors reported a mixture of different solvents in the azidation reaction [35]. Ahad *et al*. [36], reported that DMSO is the preferred solvent due to the high quality of the final product. However, removal of these solvents presents a problem in the synthesis of GAP. First, it is difficult to remove solvents from the final product, even with using reduced pressure and higher temperatures. The latter is not feasible due to the thermal instability of GAP.

For this reason, an organic/aqueous system was used to extract the polar solvent from the reaction mixture. An organic/aqueous system based on using dichloromethane or chloroform as diluents for the reaction mixture, and then adding an aqueous phase such as water or methanol to the mixture, which will extract the polar solvent. The two layers did not separate very well, and as a result complete separation took several hours. In addition, generation of foam in the separating funnel made the separation process more difficult (adding brine solution helps to reduce the amount of foam generated). In this study the reaction temperature did not exceed 60 $^{\circ}$C and brine was not used in the separation of products (in order to avoid degradation of dithiocarbamate pendent groups).

Figure 6.8 shows the FTIR spectrum of GAP with DDC pendent groups. The conversion of PECH-DDC to GAP-DDC can be easily monitored by IR spectroscopy, by following the disappearance of the absorption band at about 748 cm^{-1} (attributed to –CH$_2$Cl) and the appearance of the azido groups band at about 2099 cm^{-1}. In our

case, the absorption band at about 748 cm^{-1} did not completely disappear due to the proximity of the absorption of DDC group at about 735 cm^{-1}, whereas the formation of the 2099 cm^{-1} band gave clear evidence of the presence of azide groups.   As the azidation reaction was run at a low temperature, the chloromethyl groups might not be completely converted to azide groups. Confirmation of the presence of azide peaks, either in the FTIR or NMR spectra gives clear evidence of the formation of GAP-DDC as macro-iniferters.
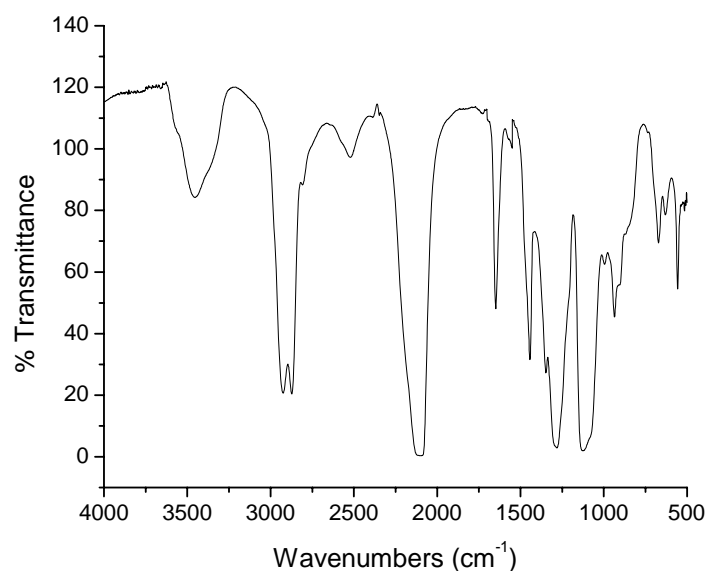
Figure 6.8 FTIR spectrum of glycidyl azide polymer with diethyl dithiocarbamate pendant groups.

The UV spectrum of GAP-DDC is shown in **Figure 6.9**. There are absorption peaks at about 251 and 281 nm, which can be attributed to the –S–C=S and S=C–N groups, respectively [24, 32].   On the other hand, the UV spectrum of GAP shows weak absorption at 280 nm compared to the GAP-DDC. The absorption at 280 nm is attributed to the azide groups (Chapter 3, Section 3.3.1) [37].
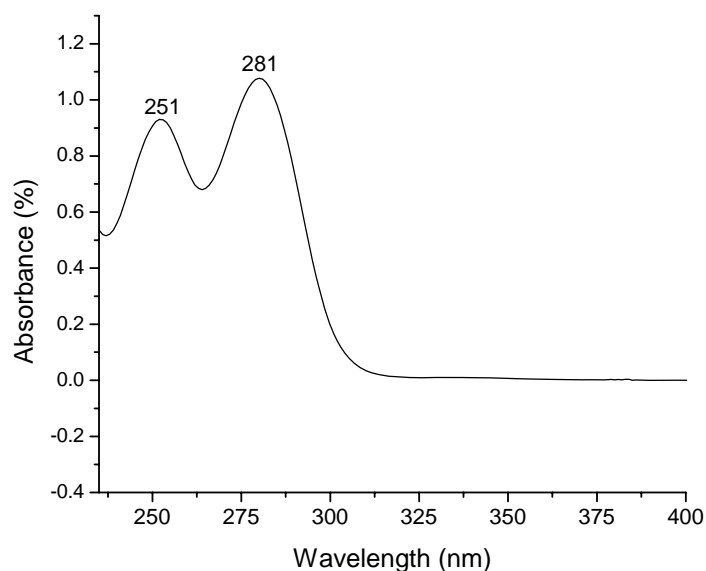
Figure 6.9 UV spectrum of glycidyl azide polymer with diethyl dithiocarbamate
pendant groups. (Concentration 1 mg/mL, dichloromethane used as solvent).

The ^{13}C-NMR spectrum of GAP-DDC is shown in **Figure 6.10**. The most important
peaks in the spectrum are peaks for the methyl carbon of DDC (δ= 10-12 ppm,
denoted 1), the methylene carbon that links GAP to DDC (δ= 27 ppm, denoted 2), the
methylene carbon of DDC (δ= 50 ppm, denoted 3), the azide group of GAP (δ= 50-55
ppm, denoted 4), the methylene of GAP (δ= 70 ppm, denoted 5), the ethyle of GAP
(δ= 79 ppm, denoted 6), and the carbon sulfur double bond of DDC (δ= 198 ppm,
denoted 7). The weak signal at about 44-46 ppm could be attributed to unconverted
chloromethyl groups.
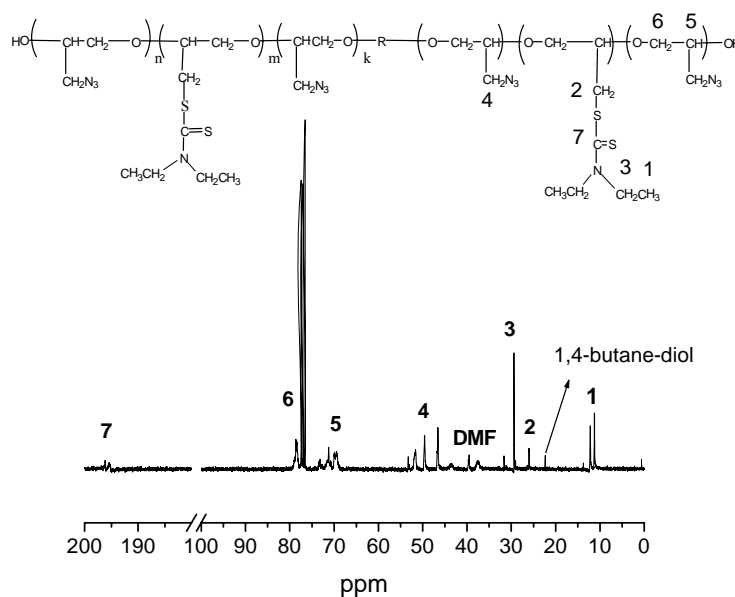
Figure 6.10 ^{13}C-NMR (CDCl$_3$) spectrum of glycidyl azide polymer with diethyl dithiocarbamate pendant groups (R is 1,4-butanediol).

Spectroscopic results confirmed the formation diethyl dithiocarbamate-glycidyl azide polymer as macro-iniferter. This compound was used as a photo-initiator in the graft copolymerization of MMA (see Section 6.3.4.2).

6.3.1.2.2 Synthesis of *N,N*-diethyl dithiocarbamate terminated glycidyl azide polymer

The FTIR spectrum of GAP after reaction with chloroacetic acid is shown in **Figure 6.11**. The attachment of chlorine atoms to the terminal end of GAP can be seen from the appearance of peaks at about 748 and 1763 cm^{-1}, which is attributed to the chloromethyl group and carbonyl group, respectively. In addition, the spectrum shows the absorption of azide groups at about 2100 cm^{-1}. This result shows that the esterification reaction proceeds successfully and that most of the OH terminal end groups were replaced by chlorine atoms. These chlorines were to be used later in the

reaction with sodium dithiocarbamate. **Figure 6.12** shows the FTIR spectrum of chlorine terminal GAP, after reaction with sodium dithiocarbamate. The most interesting feature in this spectrum is the shift of the chloromethyl peak at 745 cm^{-1}, which could be attributed to the reaction of chlorine atoms with DDC. The absorption at about 1630 cm^{-1} is attributed to the dithiocarbamate. The weak absorption at about 3400 cm^{-1} could be also attributed to the dithiocarbamate [38].

UV analysis of GAP-TDDC further confirmed the presence of DDC groups on the GAP. The absorption peaks at about 251 and 281 nm, which are attributed to the –S–C=S and S=C–N groups, respectively [24, 32]. GAP-TDDC will be used in MMA polymerization to prepare GAP-PMMA block copolymer (see Section 6.3.4.2).
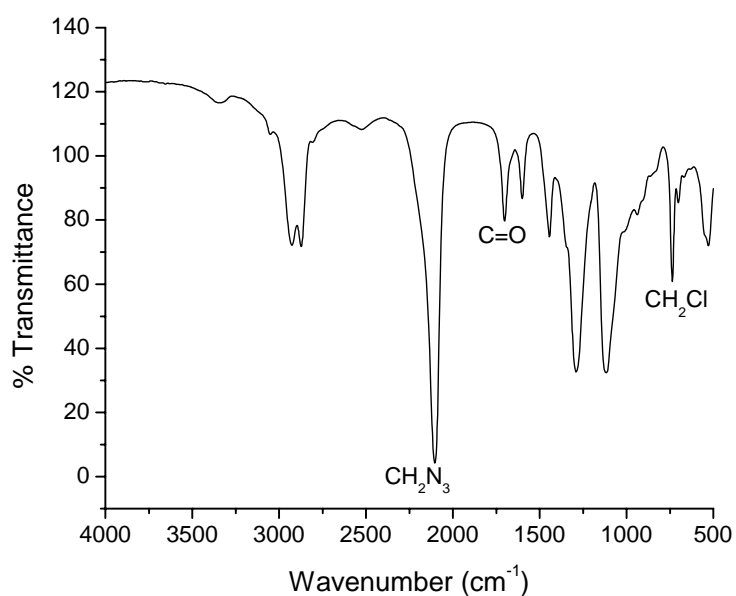
Figure 6.11 FTIR spectrum of chloro-terminated glycidyl azide polymer, after reaction of hydroxyl terminated glycidyl azide polymer with chloroacetic acid and esterification of OH groups.
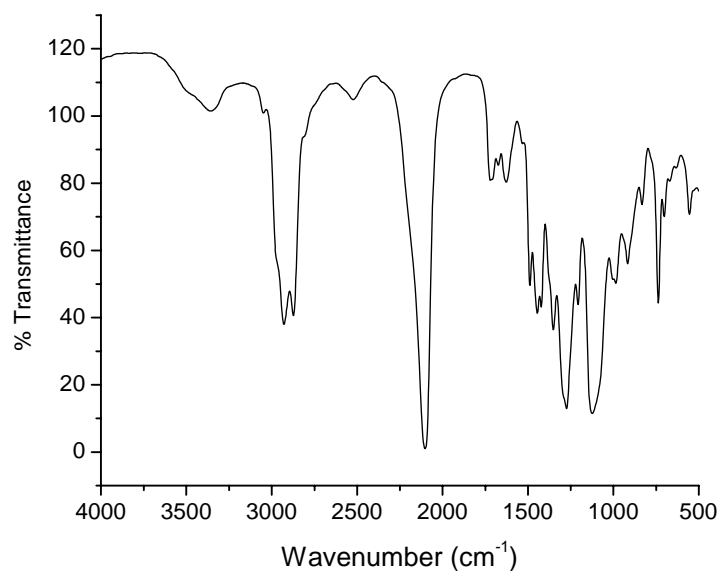
Figure 6.12 FTIR spectrum of diethyl dithiocarbamate terminated glycidyl azide
polymer.

6.3.2 Synthesis of poly(epichlorohydrin-methyl methacrylate) graft copolymer

Very recently, Cakmak and Baykara reported the synthesis of PECH-*g*-PMMA
copolymer by a combination of cationic and atom transfer radical polymerization [39]
and Tasdelen *et al*. [40], reported the synthesis of the block-graft copolymer,
poly(epichlorohydrin-*b*-styrene)-*g*-poly(methyl   methacrylate)   (PECH-*b*-St)-*g*-
PMMA) by a combination of activated monomer (AM), nitroxide mediated
polymerization (NMP) and atom transfer radical polymerization (ATRP) methods. In
this study, photoirradiation of PECH-DDC in the presence of MMA monomer
produced PECH-*g*-PMMA copolymer, according to the reaction depicted in **Scheme
6.10**.   As mentioned previously, when a macro-photoinitiator with diethyl
dithiocarbamate groups is subjected to UV radiation the phtotoinitiators will
decompose to generate radicals as illustrated in **Scheme 6.12**.
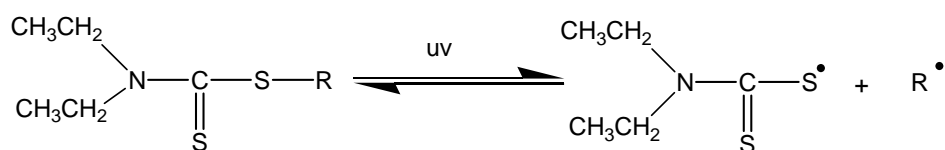
Scheme 6.12 Mechanism of the photo-induced dissociation of diethyl dithiocarbamate.

The decomposition of these groups depends on the bond length, bond energy and the bond order of the individual activated bonds. The iniferter photochmically dissociates into a carbon-centered radical R· and a sulfur-centered radical Et_2NSCS·.

The R· radical is reactive and initiates polymerization. The Et_2NSCS· radical with low reactivity, mainly reacts with the growing radicals RM_n· to form dormant covalent species, which can again photochemically dissociate. It is expected that a polymer terminated by *N,N*-diethyl dithiocarbamyl (Et_2NCSS) is suitable for further block copolymerization with other vinyl or acrylate monomers.

The photopolymerization of MMA was carried out in toluene and samples were taken at various UV irradiation times. As a reference, the thermally initiated polymerization of MMA in the absence of photoiniferter was also carried out. **Figure 6.13** shows the UV spectra of two PMMA samples. Spectrum (A) is that of PMMA obtained from the thermal polymerization of MMA monomers without photoiniferter. Spectrum (B) is that of PMMA obtained by photopolymerization of MMA monomers in the presence of diethyl dithiocarbamate-poly(epichlorohydrin) macroinitiators. PMMA polymerized in the presence of macroinitiators shows strong UV absorption peaks at about 280 nm, which could be attributed to the S=C–N group. This absorption peak were absent for the PMMA obtained by the thermal polymerization reaction. This provides proof that PMMA chains are terminated with DDC groups.
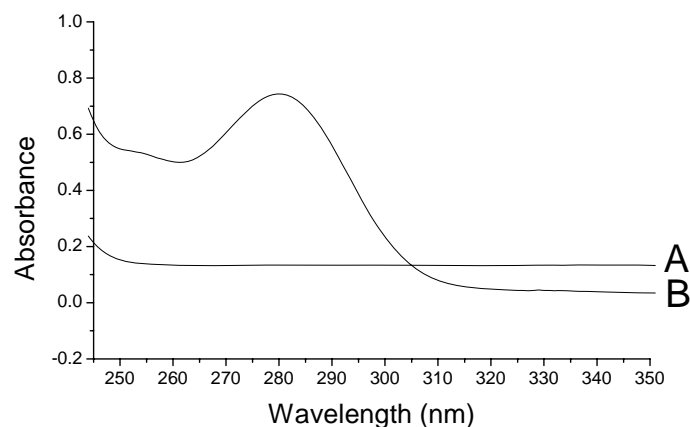
Figure 6.13 UV absorption spectra of poly(methyl methacrylate) (A) obtained by thermal polymerization, and (B) obtained by photopolymerization initiated by PECH-DDC. (Dichloromethane used as solvent, concentration 0.2 mg/mL.)

The effect of the reaction time on the photopolymerization of MMA was examined. **Figure 6.14** illustrates a typical GPC profile of these polymerizations series; all the GPC curves show a unimodal distribution. Two peaks appear in the GPC profile, the first peak corresponds to the dithiocarbamate-poly(epichlorohydrin) (retention time about 18.4 min) and the second to the PECH-*g*-PMMA copolymer (retention time 14.8 min and less). The decrease of the height of the PECH-DDC peak and the increase in the height of the PECH-*g*-PMMA peak, as well as the shift to shorter retention time of the latter as the reactions progress, suggests that the polymerization proceeded via a controlled radical polymerization mechanism. The consumption rate of PECH-DDC during the first part of the reaction (first 8 hours) appears to have been much higher than in the last 15 hours. This could be due to viscosity effects. As polymerization proceeds, the viscosity increases and this could adversely affect the overall reaction rate. In addition, as polymerization proceeds more DDC groups will

be consumed, which will reduce the initiation rate and cause a reduction in the conversion rate.
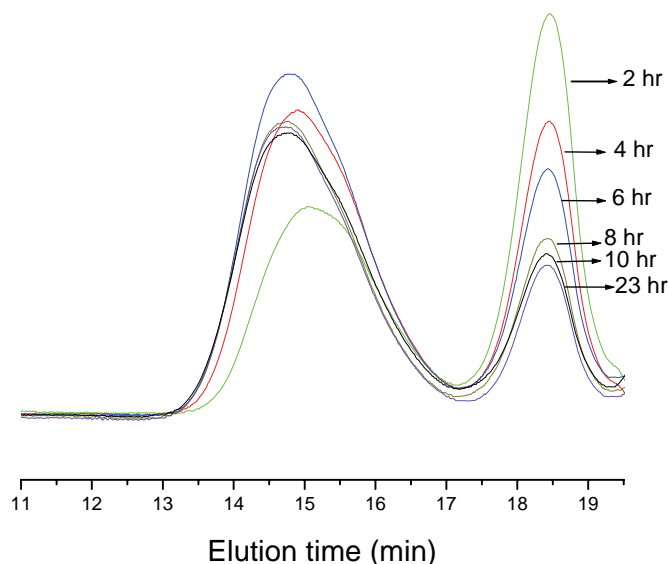
Figure 6.14 GPC traces of photopolymerization of MMA in toluene initiated by PECH-DDC. (Polymerization conditions: [PECH-DDC]/[MMA] = 0.0167.)

The GPC traces of PECH-*g*-PMMA, using UV and RI detectors, are shown in **Figure 6.15**. These chromatograms are of the final polymerization product; after all the unreacted PECH-DDC was extracted. The overlap of the two peaks (UV and RI) indicate that the unreacted material (macro-initiators) had been successfully removed, and that the only material still present is PECH-*g*-PMMA. In addition, superimposition of the two peaks indicates that most of the PMMA chains have DDC groups. The deviation of the UV peak from the RI peak at higher retention time could be attributed to some high molecular weight homo-PMMA being generated during the polymerization due to the effect of UV light. As has been mentioned, running polymerization without macro-photoiniferters will generate a small amount of high molecular weight PMMA.
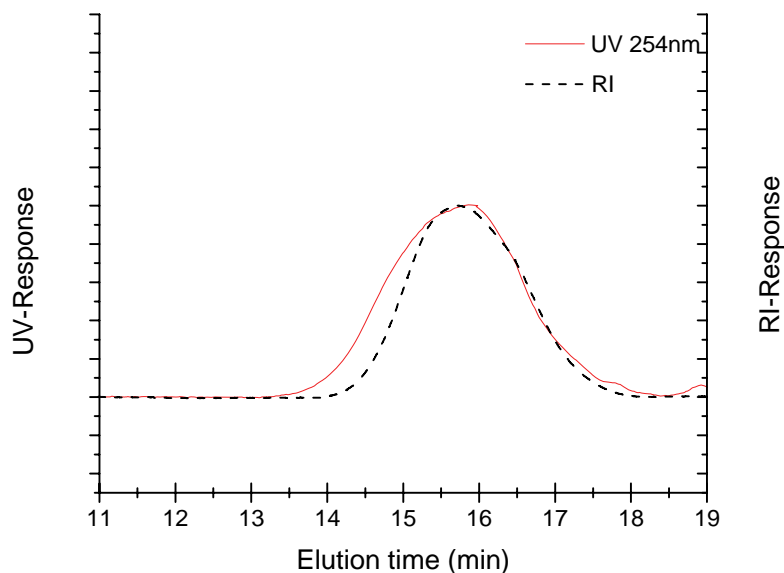
Figure 6.15 GPC traces of poly(epichlorohydrin-*g*-methyl methacrylate) copolymers produced from the photopolymerization of MMA initiated by PECH-DDC. (Polymerization conditions: [PECH-DDC]/[MMA]= 0.0167)

To better understand the mechanism of initiation and propagation, a first-order time-conversion plot for this polymerization system was performed. Conversion was obtained by gravimetric measurements. The first-order time-conversion plot is shown in **Figure 6.16**. The conversion after 2 hours of radiation was about 6.5%, and running the reaction for another 22 hr conversion only increased it to about 75%. While an increase in the molecular weight with an increase in the conversion was noticed, there is a deviation from linearity regarding the rate of molecular weight increase as the conversion increases. It appears, therefore, as if there is a decrease in reaction rate as the conversion increases, which could be an indication of the slow decrease of the active concentration [10]. The reason for this is not clear, although possible explanations could be: (a) the synthesis of PECH-*g*-PMMA, which will

increase the viscosity of the mixture, leading to a decrease in the reaction rate, or (b) decomposition of diethyl dithiocarbamate during the first period of the reaction. The latter should lead to an increase in polydispersity, which is not evident (Figure 6.17).
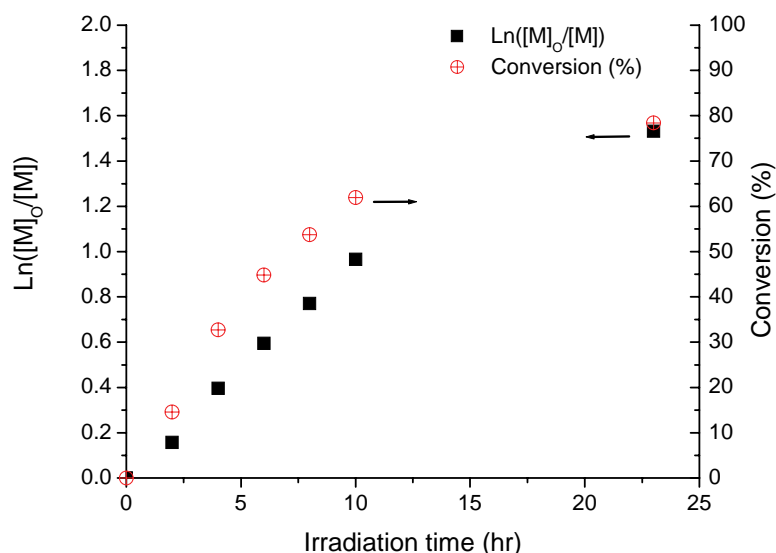
Figure 6.16 First-order time-conversion plots for the photopolymerization of MMA in toluene initiated by PECH-DDC. (Polymerization conditions: [PECH-DDC]/[MMA] = 0.0167.)

The effect of the reaction time on the number average molecular weight and polydispersity index of PMMA are shown in **Figure 6.17**. There is a considerable increase in the number average molecular weight with the reaction time. The polydispersity index remained in the range 1.48-1.64. This indicates that polymerization proceeds in a reasonably controlled fashion. In addition, the relatively high polydispersity of the final product could be attributed to the low rate of addition and chain transfer coefficients of dithiocarbamate. This could be attributed to the interaction between the N and the C=S double bond [2]. On the other hand, there was

a slight increase in the polydispersity index of the resulting polymers, which increased with the reaction time (as shown in the figure).

It is worth mentioning that running the photopolymerization of MMA without using photoiniferter yielded very little polymer. The molecular weight and polydispersity of the products were however high, compared to the products of the polymerization with macro-iniferters. This could be attributed to the absence of capping agents for propagating chains. Therefore, these chains are capable of obtaining a higher molecular weight of PMMA. These results are in agreement with those in a previous report describing the homopolymerization of PMMA with benzyl diethyl dithiocarbamate [17].
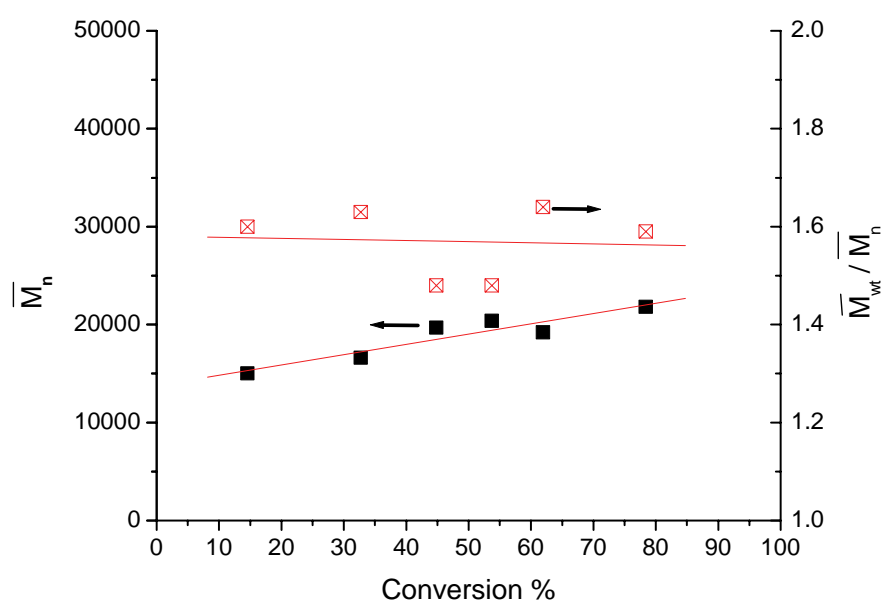
Figure 6.17 Plots of $\overline{M}_n$ and $\overline{M}_{wt}/\overline{M}_n$ versus conversion for the photopolymerization of MMA in toluene initiated by PECH-DDC. (Polymerization conditions: [PECH-DDC] /[MMA] = 0.0167.)

The effect of the stoichiometry ratio on the molecular weight of copolymers was investigated. An increase in the amount of the macro-iniferter compared to monomer (mole ratio) in the reaction mixture yielded polymer with a low molecular weight. This could be attributed to the high number of propagation sites when more macro-initiator was used, which will lead to generation of more chains with lower molecular weight. It is reported that the molecular weight controlled by the stoichiometry of the reaction is one of the other characteristics of living/controlled radical polymerization [2]. The composition and molecular weight of the block copolymers can be regulated by careful choice of the monomer/macro-iniferter ratio and the extent of polymerization.

The grafted copolymer obtained from the photopolymerization was characterized by FTIR and NMR. **Figure 6.18** shows the FTIR spectrum of the PECH-*g*-PMMA copolymer. Characteristic peaks of PMMA at 1724 cm^{-1} (C=O) and of PECH at 740cm^{-1} (CHCl$_2$) can be clearly seen.
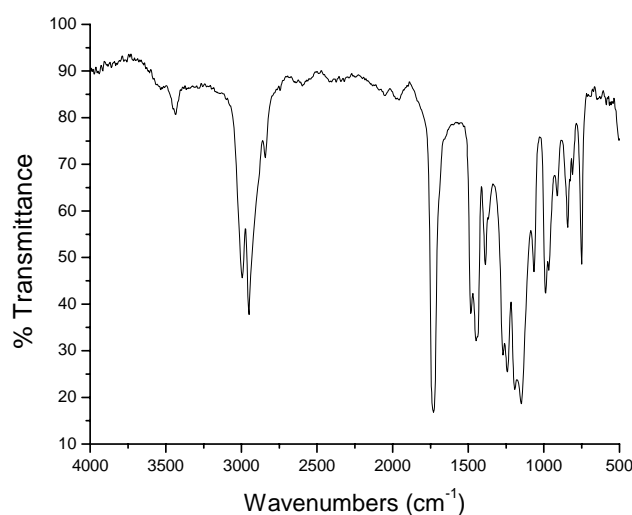
Figure 6.18 FTIR spectrum of PECH-*g*-PMMA copolymer prepared by the photopolymerization of MMA in the presence of PECH-DDC as macro-iniferter.

The structure of the grafted copolymer was analyzed by ^{1}H-NMR as shown in **Figure 6.19**. The peaks at about 3.6, 2.0-1.5, and 1.1-0.7 ppm correspond to the methoxy, methylene, and methyl protons of the PMMA segment, respectively. The peaks at about 4 and 1.7 ppm are attributed to the protons of the chloromethyl group, and the methylene of the PECH backbone, respectively. Other assignments are indicated in the figure.

Figure 6.20 shows the ^{13}C-NMR spectrum of PECH-*g*-PMMA and the assignments. The ^{13}C-NMR spectrum shows the characteristic peaks of two different segments. The carbonyl groups of PMMA are responsible for the peak at about 177 ppm and the chloromethyl groups for the peak at about 46 ppm.
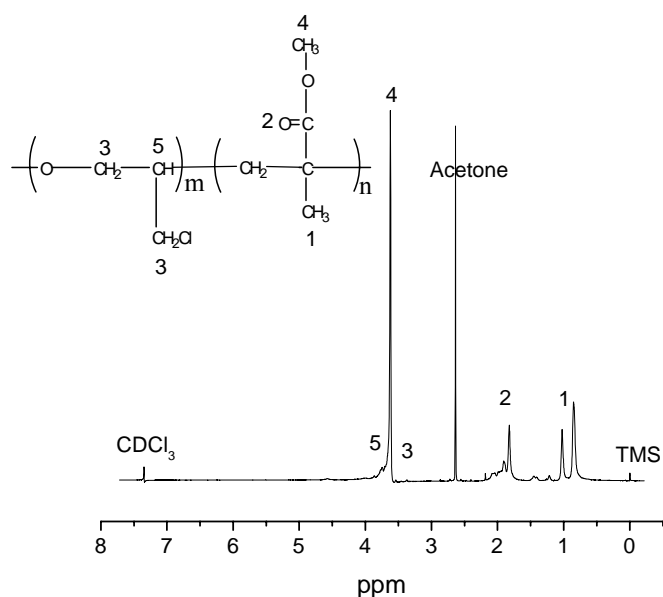
Figure 6.19 ^{1}H-NMR (CDCl$_3$) spectrum of PECH-*g*-PMMA prepared by the photopolymerization of MMA in the presence of PECH-DDC as macro-iniferter.
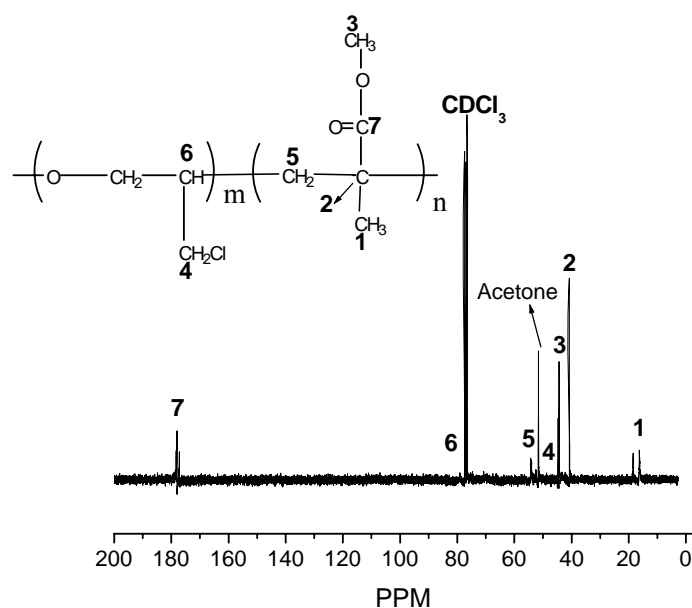
Figure 6.20 ^{13}C-NMR (CDCl[3]) spectrum of PECH-*g*-PMMA prepared by photopolymerization of MMA in the presence of PECH-DDC as macro-iniferter.

The thermal behavior of a copolymer gives an indication of the presence of the two different segments. Each segment will contribute to the thermal properties of the final product. The thermal behavior of the product of the photo-polymerization reaction was tested after precipitation in methanol and removal of unreacted macro-initiators. **Figure 6.21** shows the DSC thermogram of PECH-*g*-PMMA copolymer. The graft copolymer shows a glass transition temperature at about 75 ^{o}C, which is between the T$_g$ of the two homopolymers. There was also a slight discontinuity in the thermogram at low temperature (about -23 ^{o}C) and also at about 105 ^{o}C, which could be attributed to the glass transition of PECH and PMMA, respectively. For a typically grafted copolymer, the different glass transition temperatures representing those of the corresponding homopolymers are expected [36].
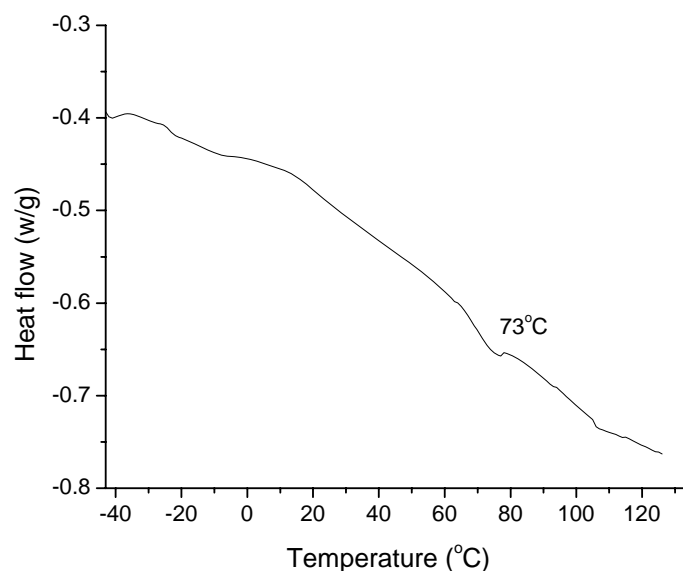
Figure 6.21 DSC thermogram of PECH-*g*-PMMA copolymer.

The two additional glass transitions observed here are indicative of the lack of miscibility of the PECH and PMMA segments which is in apparent contradiction to that which has been found previously (Chapter 5, Section 5.3.1). On the other hand, the comparison between the PECH-*g*-PMMA copolymer obtained when using PECH macro-azo-initiators (Chapter 4, Section 4.2.3.4) and the PECH-*g*-PMMA copolymers obtained from photopolymerization in the presence of PECH-DDC shows a greater effect on the soft segment in the graft copolymer than in the block copolymer. This observation is based on the sharp glass transition temperature of the grafted copolymer (Figure 6.21) compared to block copolymer (Chapter 4, Section 4.2.3.4). The finding could be attributed to the high segments of PMMA in the block copolymer or percentage of homo-PMMA, which is expected to be higher in the case of thermal polymerization than photopolymerization. This is another advantage of using the photopolymerization method in the synthesis of these copolymers. Hence the synthesis of copolymers via macro-iniferters is run at low temperatures, with few

side reactions, and leads to homopolymer formation. Therefore, depending on the choice of monomer, an iniferter tailor-made block copolymer can be obtained, e.g. hard-soft, amphiphilic, etc. and the block length can be adjusted by varying the monomer and iniferter concentrations. A relatively high polydispersity index is the drawback of this method.

The thermal degradation of the PECH-*g*-PMMA copolymer was studied by using TGA. TGA results are shown in **Figure 6.22**. The first degradation takes place at about 275-365 $^{\circ}$C, where about 55% of the product is degraded. This part of the degradation could be attributed to the PECH elastomers. The second degradation step starts after 365 $^{\circ}$C, it can be attributed to the PMMA main chains. At the beginning of the thermal degradation there is about 5% loss, which can be attributed to solvents and impurities. This analysis shows different degradation behavior of PECH-*g*-PMMA copolymer compared to PECH-*g*-PMMA copolymer obtained by using 4,4' azobis (4-cyanopentanoyl chloride) (ACPC) (Chapter 4, Section 4.2.3.4). The first degradation step in PECH-*g*-PMMA was at about 136 $^{\circ}$C through to 288 $^{\circ}$C and the weight loss was about 13%, where the second degradation step in the block copolymer was very sharp and about 85% of the sample degraded in this step. The difference in the thermal degradation could be attributed to the difference in the microstructure and arrangement of copolymer segments. It is expected that in the case of the graft copolymer the soft segments (PECH) have a more pronounced effect on the final polymer properties compared to the block copolymer. This conclusion is based on the results obtained from DSC and TGA techniques only.
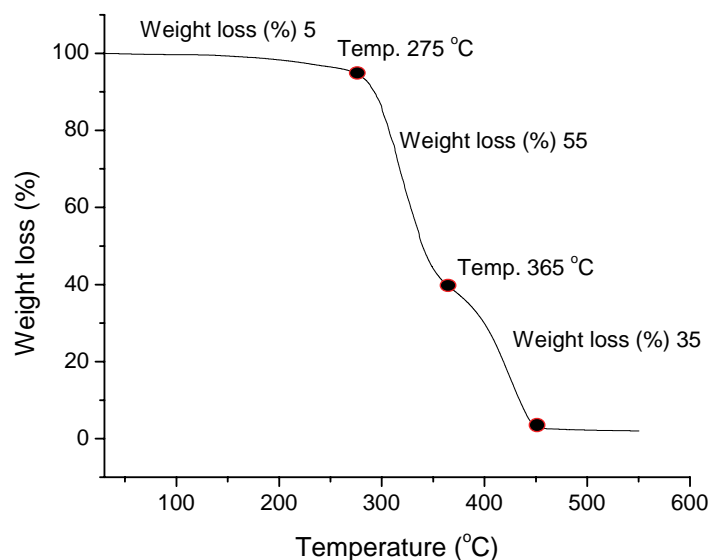
Figure 6.22 TGA analysis of PECH-*g*-PMMA copolymer.

6.3.3 Synthesis of poly(epichlorohydrin-styrene) graft copolymer

Macro-iniferters based on PECH-DDC can be utilized in photopolymerizations of vinyl monomers and the following is another example of grafted copolymers obtained, where photoirradiation of PECH-DDC in the presence of styrene monomers produce a PS-*g*-PECH copolymer. The effect of the reaction time on the polymerization reaction was examined and **Figure 6.23** illustrates the typical GPC profiles of these polymerizations series. Two peaks appear in the GPC profile, the first one corresponding to the dithiocarbamate-poly(epichlorohydrin) macro-initiators (retention time about 18.4 min) and the second one corresponding to the poly(epichlorohydrin-*g*-Styrene) copolymer (retention times 15.5 minutes or less). The shift to shorter retention time of the latter, as the reaction progresses suggests that the polymerization proceeded through a controlled radical polymerization mechanism.
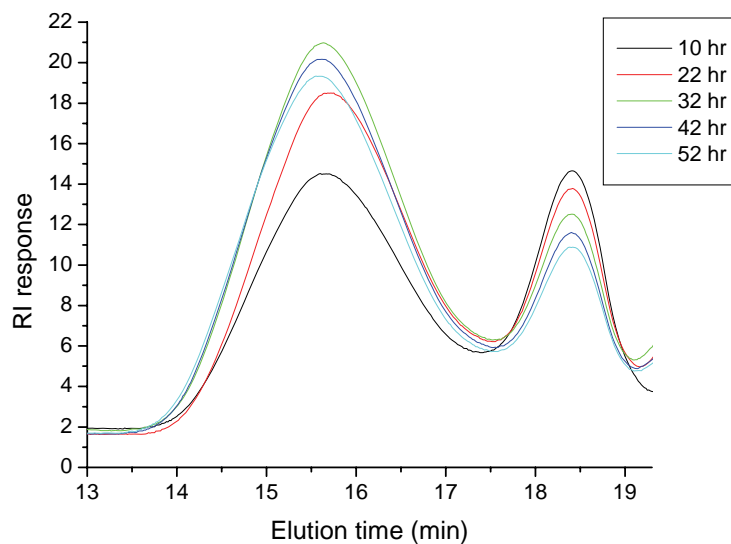
Figure 6.23 GPC traces of photopolymerization of styrene in toluene initiated by
PECH-DDC. (Polymerization conditions: [PECH-DDC]/ [Styrene] = 0.022).

The first-order time-conversion plot for this polymerization system was obtained and
conversion was estimated by gravimetric measurements. The first-order time-
conversion plot is shown in **Figure 6.24**. Linear increase of conversion with time
indicates that the polymerization proceeded throughout in a controlled fashion.
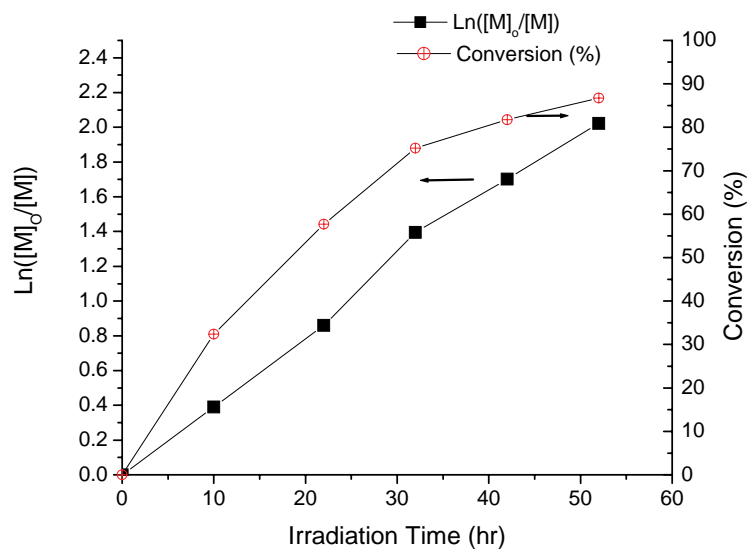
Figure 6.24 First-order time-conversion plot for the photopolymerization of styrene in toluene initiated by PECH-DDC. (Polymerization conditions: ([PECH-DDC]/ [styrene] = 0.022.).

The effect of the reaction time on the molecular weight and polydispersity of PECH-*g*-styrene copolymer is demonstrated in **Figure 6.25**. There is an increase in the molecular weight with the reaction time. The polydispersity index remained in the range of 1.4-1.6. This indicates that polymerization proceeds in a reasonably controlled fashion. The molecular weight of polystyrene graft copolymers did not exceed 20000 g/mol and the lower molecular weight of a PECH-PS graft copolymer compared to a PECH-PMMA graft copolymer could be attributed to higher mole ratio of macro-iniferters in the polymerization.
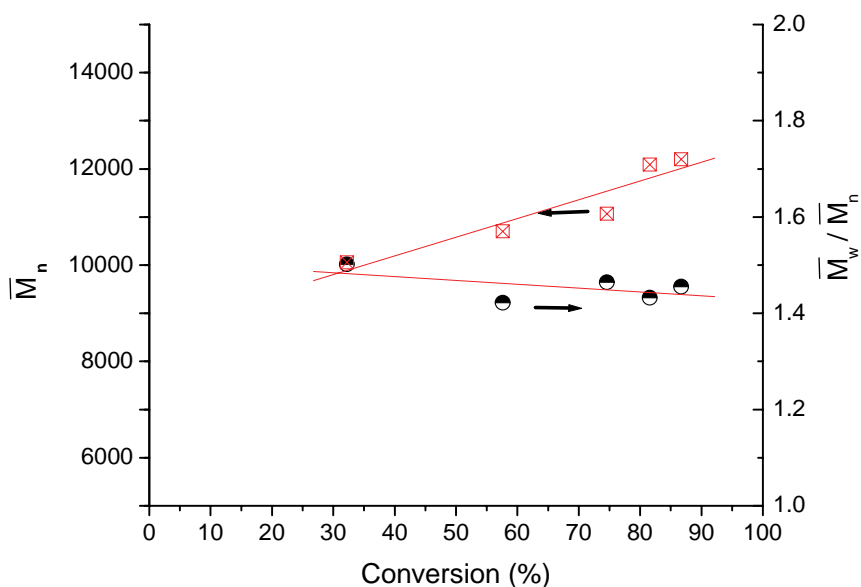
Figure 6.25 Plot of $\overline{M_n}$ and $\overline{M_{wt}}/\overline{M_n}$ against conversion for the photopolymerization of styrene in toluene initiated by PECH-DDC. (Polymerization conditions: [PECH-DDC]/[styrene] = 0.022.) .

The grafted copolymer was studied using spectroscopic techniques such as FTIR and NMR. **Figure 6.26** shows the FTIR spectrum of PECH-*g*-PS copolymer. The characteristic peak of the PS segment at about 1600 cm^{-1} corresponds to the aromatic bonds C=C. The characteristic peaks of the PECH segment are at about 745 and 1100 cm^{-1}, is attributed to the chloromethyl groups and polyether linkage, respectively. **Figure 6.27** shows the ^{13}C NMR spectrum of PECH-*g*-PS copolymer. The ^{13}C-NMR spectrum shows the characteristic intensities of two different segments: the peak of the carbons of the aromatic ring of PS appears at about 125 ppm and the peak of the chloromethyl groups of PECH appear at about 46 ppm.
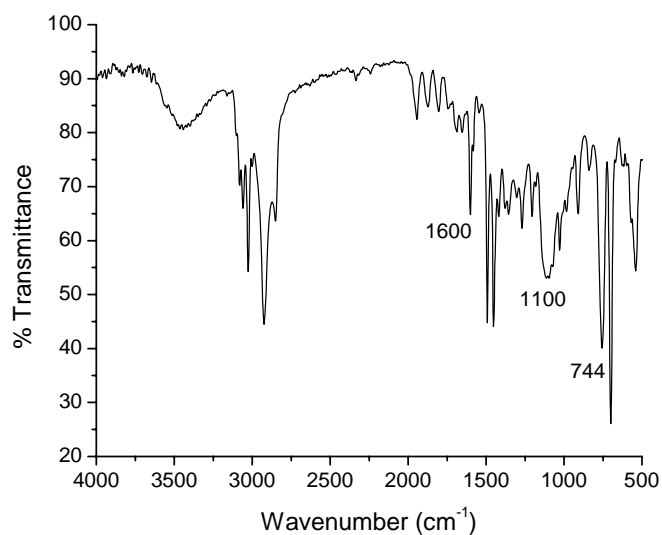
Figure 6.26 FTIR spectrum of PECH-*g*-PS obtained by photopolymerization of styrene monomer in the presence of PECH-DDC as macro-iniferter.
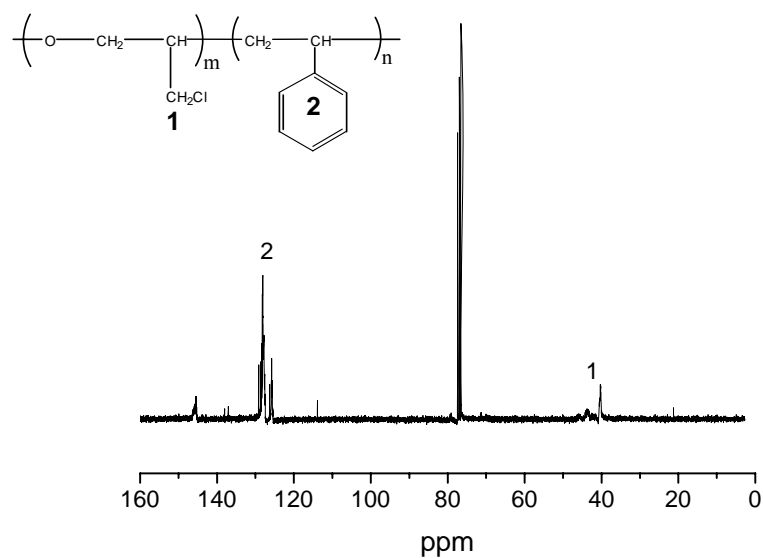
Figure 6.27 ^{13}C-NMR (CDCl$_3$) spectrum of PECH-*g*-PS obtained by photopolymerization of St monomer in the presence of PECH-DDC as macro-iniferters.

Spectroscopic analyses proved the formation of PECH-*g*-PS copolymer by the presence of intrinsic peaks of two different segments. A study of the polymerization kinetics showed that the reaction proceeds in a controlled fashion: as an increase in the conversions and molecular weight with slight effect on polydispersity. These results give an example about the possibility to utilize PECH-DDC macro-initiators in the polymerization of other vinyl monomers to produce further types of copolymers. These products could be considered as thermoplastic elastomers and used in different applications such as sealant, adhesives, and coatings. In this study, the focus will be on the polymerization of MMA to be utilized as a hard segment (thermoplastic) in energetic thermoplastic elastomers (energetic binder). This is due to a high oxygen content of this polymer, which could enhance the final properties of the energetic binder. In addition, PMMA burns with a bright flame, where polystyrene burning is characterized by yellow flame with a lot of smoke. This could give a further advantage for PMMA compared to polystyrene in propellant formulations [41].

6.3.4 Synthesis of poly(glycidyl azide-methyl methacrylate) copolymer

This part will be divided into two sections. The first section covers the results of GAP-*g*-PMMA copolymer obtained from photopolymerization of MMA monomer in the presence of diethyl dithiocarbamate-GAP. The second covers results of the GAP-*b*-PMMA copolymer obtained from photopolymerization of MMA monomer in the presence of diethyl dithiocarbamate terminated glaycidyl azide polymer. The reaction mechanism for the syntheses of the two different types of copolymer is the same and depends on photopolymerization based on DDC groups from GAP-DDC. The dissociation of DDC groups depends on different factors, such as the bond length, bond energy and the bond order of the individual bonds. This decomposition will lead to the formation of two types of different radicals, one is reactive for polymerization and the second is a resistance radical, which will participate in only

the termination reaction. This will lead to a copolymer comprising PMMA and GAP segments. In order to remove all unwanted products, the polymer obtained was re-precipitated several times (from methanol and THF) in order to remove all unreacted GAP-DDC macro-initiators.

6.3.4.1 Synthesis of poly(glycidyl azide-methyl methacrylate) graft copolymer

The successful synthesis of GAP-DDC was proved by UV, FTIR and NMR spectroscopy. Here, the focus is on utilizing GAP-DDC as macro-photoinitiator for the polymerization of MMA that will yield GAP-*g*-PMMA graft copolymer. The photopolymerization of MMA in toluene was carried out and samples were taken at various UV irradiation times. **Figure 6.28** shows the GPC profile as polymerization proceeds.
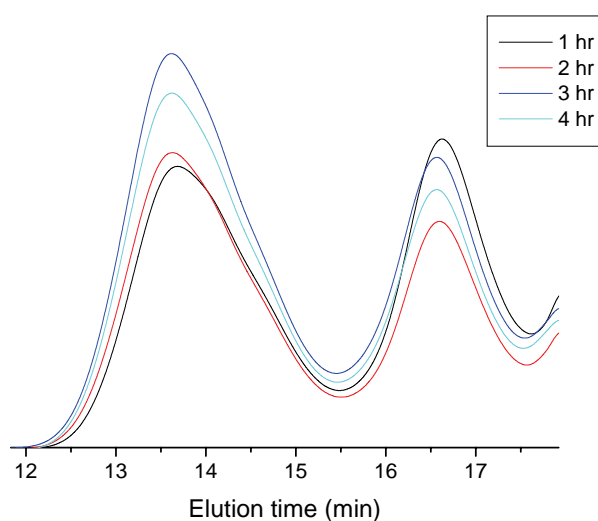
Figure 6.28 GPC traces of photopolymerization of MMA in toluene initiated by GAP-DDC. (Polymerization conditions: [GAP-DDC]/[MMA] = 0.014.).

Two separate peaks appear, one corresponding to the GAP-DDC (retention time about 16.8 min) and the other corresponding to the GAP-*g*-PMMA copolymer (retention

time 14 min or less) formed during the reaction. The slight shift in the retention time of the copolymer peaks as the polymerization proceeds gives an indication that the polymerization preceded in a controlled fashion. A first-order time-conversion plot for this polymerization system can be seen in **Figure 6.29**. Conversion was obtained by gravimetric measurements.
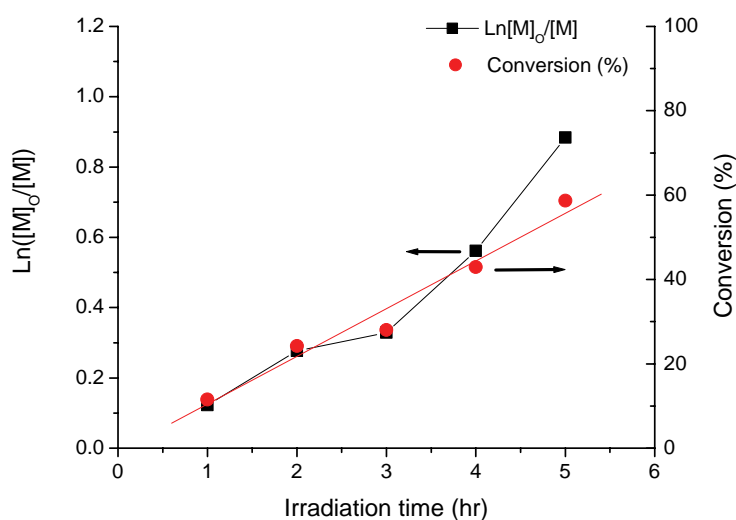
Figure 6.29 First-order time-conversion plots for the photopolymerization of MMA in toluene initiated by GAP-*g*-DDC. (Polymerization conditions: [GAP-DDC]/[MMA] = 0.014.).

The conversion after 1 hour of radiation was about 5%, and after running the reaction for another 4 hours there was only a 45% increase in the conversion. It appears, therefore, as if there is a decrease in reaction rate as the conversion increases. Also, there is a deviation from linearity in the last two samples. This is probably a result of the increase in the viscosity of the reaction mixture, rather than a decrease in the active species concentration, as no considerable change with polydispersity index as the reaction proceeded. This phenomenon was also observed in the polymerization of MMA with PECH-DDC. It is also worth noticing that PECH-DDC macro-initiators

give a higher polymerization yield compared to GAP-DDC. This could be attributed to the effect of the azide group of GAP-DDC in mediating the polymerization.

Figure 6.30 shows the plots of $\overline{M_n}$ and $\overline{M_{wt}}/\overline{M_n}$ against conversion for the photopolymerization. There is a considerable increase in the molecular weight within the first 1 hour of the reaction. As polymerization preceded after that he molecular weight did not change considerably, and polydispersity index remained in the range 1.5-1.6. The polydispersity index was almost constant in the last two samples and there was a very slight decrease of the molecular weight, which could be attributed to the UV degradation of polymer chains. The molecular weight of GAP-*g*-PMMA copolymer was comparable to the molecular weight of PECH-*g*-PMMA copolymer. Results show that polymerization proceeds in a reasonably controlled fashion, especially in the early period of the reaction.
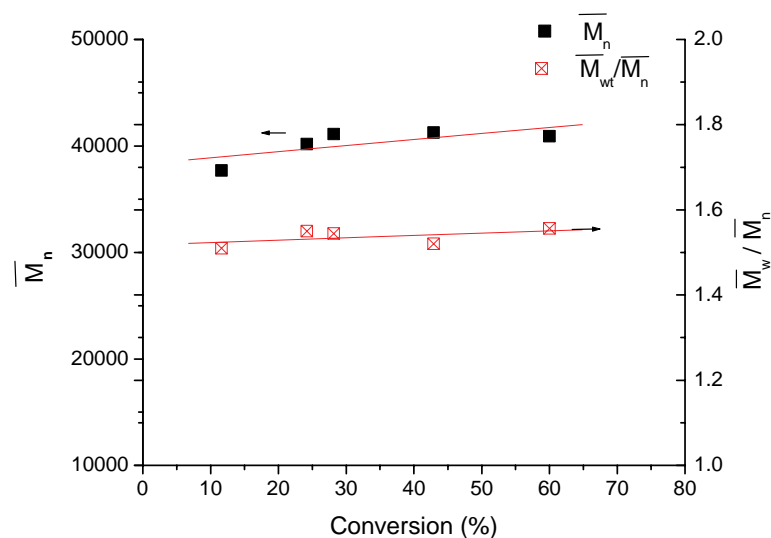
Figure 6.30 Plots of $\overline{M_n}$ or $\overline{M_{wt}}/\overline{M_n}$ against conversion for the

photopolymerization of MMA in toluene initiated by GAP-DDC. (Polymerization

conditions: [GAP-DDC]/ [MMA] = 0.014.).

The grafted copolymer was characterized by using UV, FTIR, and NMR. The UV spectrum shows a single absorption for the GAP-*g*-PMMA copolymer at about 280nm, which corresponds to the S=C–N group. **Figure 6.31** shows the FTIR spectrum of GAP-PMMA graft copolymer. The FTIR spectrum shows the characteristic peak of the PMMA segment at about 1730 cm^{-1} which corresponds to the carbonyl group. The characteristic absorption peaks of the GAP segment are observed at about 2100 and 1100 cm^{-1}, which is attributed to the azide groups, and polyether linkage, respectively.
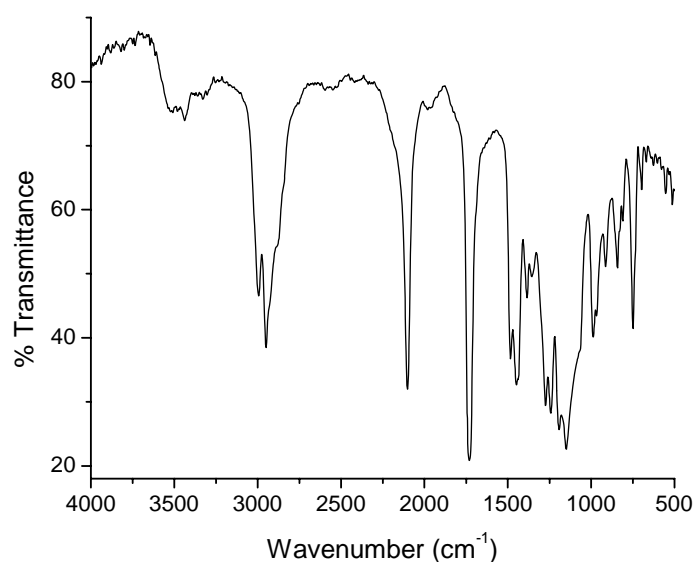
Figure 6.31 FTIR spectrum of GAP-*g*-PMMA copolymer obtained by photopolymerization of MMA in the presence of GAP-DDC.

The ^{13}C-NMR spectrum of GAP-*g*-PMMA copolymer is shown in **Figure 6.32**. The most characteristic peaks in this spectrum are at about 179 ppm, which are attributed to the carbonyl group of PMMA segments. On the other hand, the small peak at about 55 ppm is attributed to the azido group of GAP.
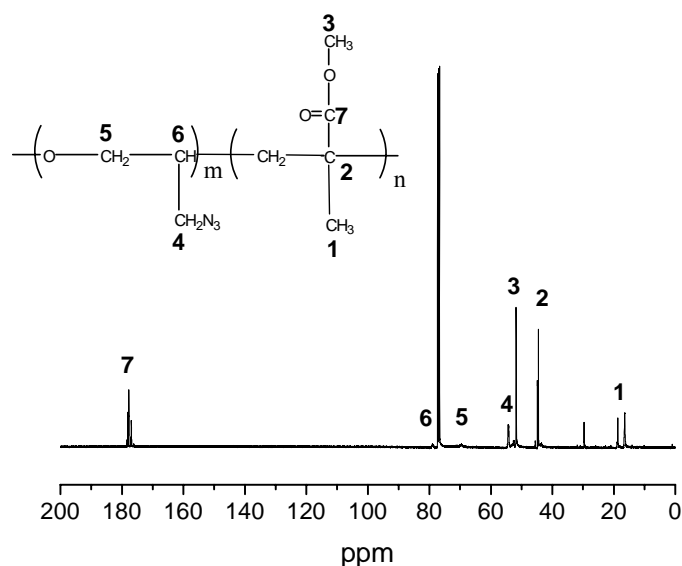
Figure 6.32 ^{13}C-NMR (CDCl$_3$) spectrum of GAP-*g*-PMMA copolymer obtained by photopolymerization of MMA in the presence of GAP-DDC.

GAP-*g*-PMMA copolymer is an energetic thermoplastic elastomer proposed and can be used for propellant and ammunition applications. Thermal behavior at low temperature is an important parameter for polymeric materials that will be used in propellant formulations. Thermal analysis of GAP-*g*-PMMA copolymer was performed using DSC and **Figure 6.33** shows the result of a low temperature scan. The thermogram clearly shows a broad glass transition temperature at about 75 $^{\circ}$C. This T$_g$ is located between the T$_g$ values of the two different homopolymer. There was also slight decline in the thermogram at low temperature (about -35 $^{\circ}$C) and at about 105 $^{\circ}$C. A single glass transition temperature could be attributed to the miscibility of two different segments with each other, which has been proved previously (Chapter 5, Section 5.3.1.2). Also, similarity in the T$_g$ of PECH-PMMA and GAP-PMMA graft copolymer was noticed, which could be attributed to the structural arrangement of copolymers and the same effect from the elastomeric part.

On the other hand, the T_g of GAP-*b*-PMMA obtained from the thermal polymerization of MMA in the presence of macro-azo-initiators (Chapter 4, Section 4.3.2) was higher than that of GAP-*g*-PMMA. This could be attributed to the structural arrangement or presence of a high percentage of PMMA homopolymer in the case of thermal polymerization, which will shift the T_g to higher temperature.
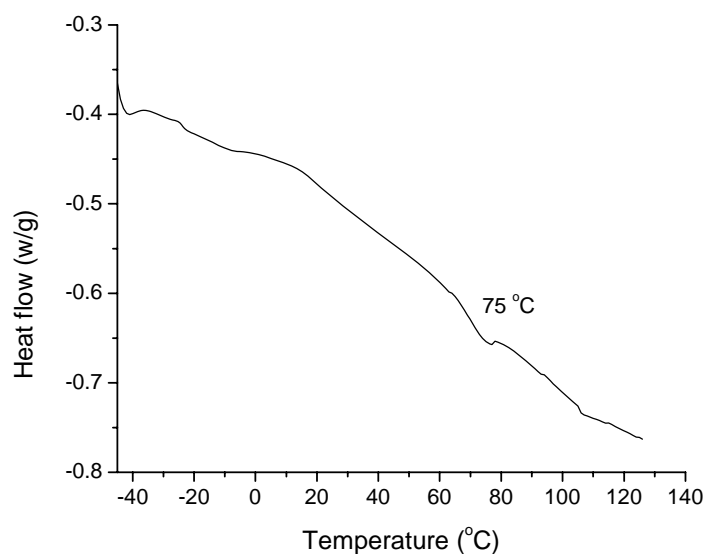
Figure 6.33 DSC thermogram of GAP-*g*-PMMA copolymer.

The thermal decomposition behavior of energetic binder systems represents another significant aspect and it is essential to study the decomposition behavior of potential polymeric propellant materials, especially when such materials are to be applied in space technology applications, where thermal decomposition of the propellant binders plays a crucial role in the combustion of the solid propellants and the final performance. Hence, it was essential to study the thermal decomposition behavior of the GAP-*g*-PMMA copolymer produced.

The decomposition temperature of the GAP-*g*-PMMA copolymer was determined by recording DSC thermogram at high temperature. Results are shown in **Figure 6.34**.

The DSC scan of GAP-*g*-PMMA shows an exothermic decomposition peak in the temperature range 160-295 ^{o}C, with a maximum exothermic peak at about 240 ^{o}C. The other interesting feature is the decomposition interruption of the grafted copolymer at about 200 ^{o}C. This was attributed to the structure of the copolymer and the arrangement of polymer chains. The energy released from the decomposition of GAP-*g*-PMMA copolymer was about 295 J/g.
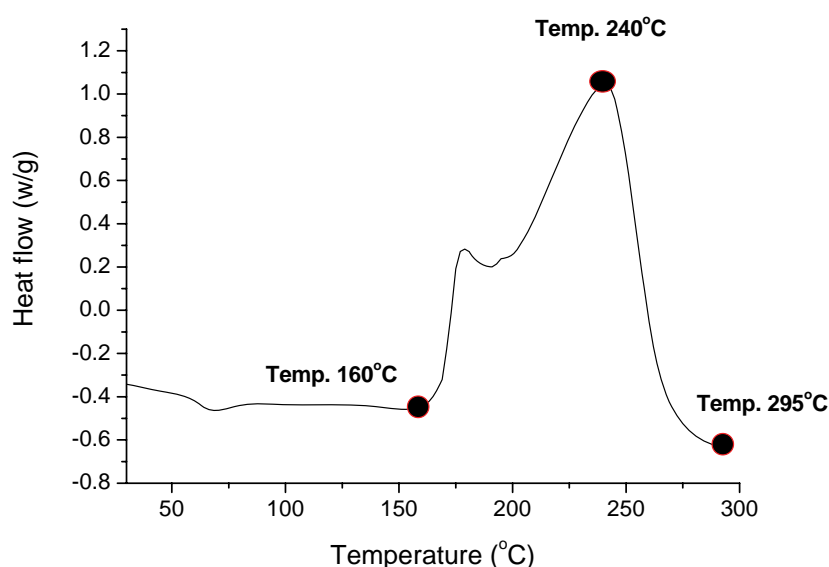
Figure 6.34 DSC thermogram of GAP-*g*-PMMA copolymer obtained by photopolymerization of MMA in presence of GAP-DDC.

The thermal degradation of GAP-*g*-PMMA copolymer was studied by using TGA. Results are shown in **Figure 6.35**. The first degradation is at about 214-321 ^{o}C, where about 40% of product was degraded. This part of the degradation could be attributed to the GAP elastomers, whose azide groups will decompose in this temperature range. The second degradation step starts above 321 ^{o}C and about 50% of weight loss occurs, which is attributed to the PMMA main chains. There was about 4% weight loss in the initial thermal analysis, attributable to solvents and

impurities. There is a similarity in the degradation behavior of the PMMA-*b*-GAP copolymer produced from macro-azo-initiators (Chapter 4, Section 4.3.2) and GAP-*g*-PMMA. This was attributed to the exothermic decomposition of azido groups in the two different copolymers.
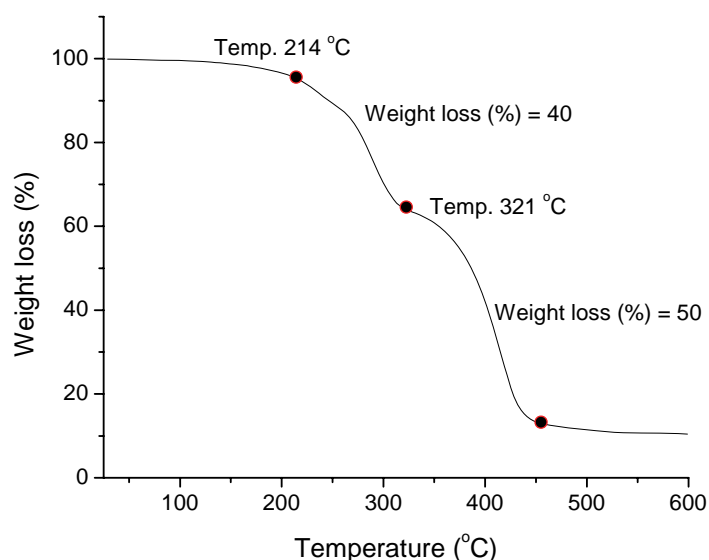
Figure 6.35 TGA analysis of GAP-*g*-PMMA copolymer obtained by photopolymerization of MMA in the presence of GAP-DDC.

6.3.4.2 Synthesis of poly(glycidyl azide-methyl methacrylate) block copolymer

Photoirradiation of MMA monomers in the presence of GAP-TDDC yields GAP-*b*-PMMA copolymer. The photopolymerization of MMA in toluene was carried out and samples were taken after various UV irradiation times. The effect of the reaction time on the polymerization of MMA was examined. **Figure 6.36** illustrates the typical GPC profiles of these polymerizations series. A slight shift in the GPC profiles to lower the retention time, as polymerization proceeds, was noticed. This was attributed to the increase in the molecular weight of block copolymers.
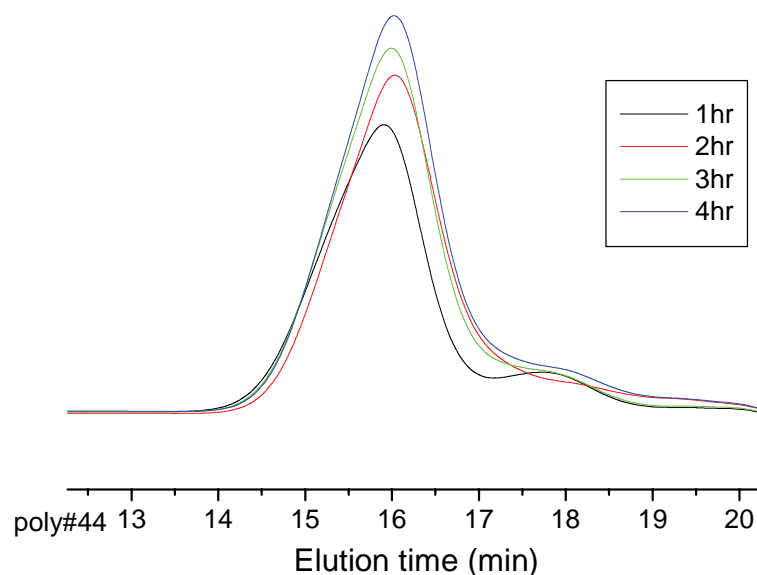
Figure 6.36 GPC traces of photopolymerization of MMA in toluene initiated by GAP-TDDC. (Polymerization conditions: [GAP-TDDC]/[MMA] = 2.23.).

The first-order time-conversion plot for this polymerization system is shown in **Figure 6.37**. Conversion was obtained by gravimetric measurements. The first-order time-conversion plot shows an increase in the conversion with the time. The increase in the conversion in the first period of polymerization was higher, and the reduction in the last stage could be attributed to an increase in the viscosity of polymerization solutions. In addition, the nature of the azide group could affect the effectiveness of dithiocarbamate in the polymerization. It is important to remember that a GAP chain functions as an activated group in the polymerization system.
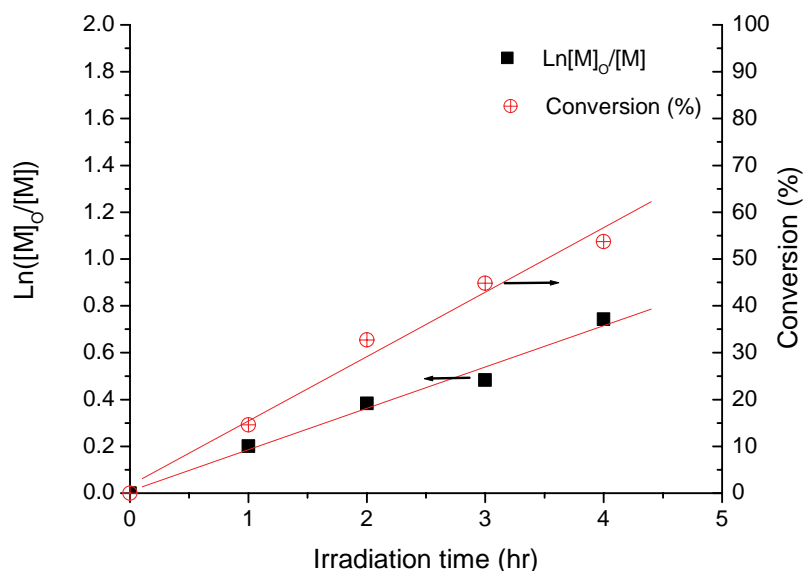
Figure 6.37 First-order time-conversion plots for the photopolymerization of MMA in toluene initiated by GAP-TDDC. (Polymerization conditions: [GAP-TDDC]/[MMA] = 2.23.).

The plot of $\overline{M_n}$ and $\overline{M_{wt}}/\overline{M_n}$ against conversion for the photopolymerization of MMA in the presence of GAP-TDDC is shown in Figure **6.38**. There is a high increase in the molecular weight within the first hour of the reaction time. But, the molecular weight did not change drastically as the reaction proceeded; also the polydispersity remained in the same range (1.3-1.6) based on polystyrene. There was a slight decrease for the polydispersity in the last two samples. The lower molecular weight of the block copolymer compared to the graft copolymer could be attributed to the low concentration of DDC groups in GAP-TDDC compared to the GAP-DDC macro-initiator. In any case, the results indicate that polymerization proceeded in a reasonably controlled fashion.
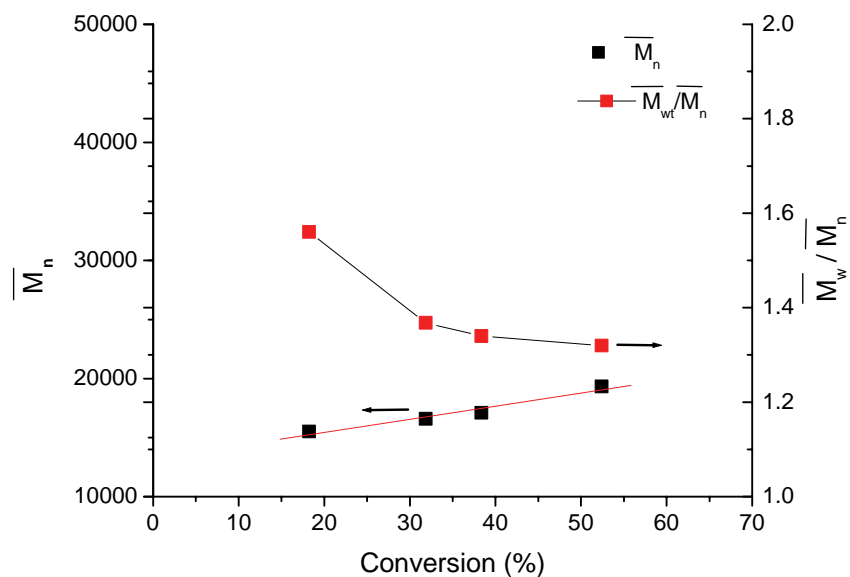
Figure 6.38 Plot of $\overline{M}_n$ or $\overline{M}_{wt}/\overline{M}_n$ against conversion for the photopolymerization of MMA in toluene initiated by GAP-TDDC. (Polymerization conditions: [GAP-TDDC]/[MMA] = 2.23).

Thermal analysis of GAP-*b*-PMMA is shown in **Figure 6.39**. The thermogram shows a broad glass transition temperature at about 92 $^{\circ}$C. This temperature is closer to the T_g of PMMA. The explanation for this is that most of the binder system is composed of PMMA segments; hence there is only a small effect of the elastomeric part in the glass transition behavior of copolymers. The glass transition of the copolymers was very broad, which could be attributed to the miscibility of two different pairs in each other.
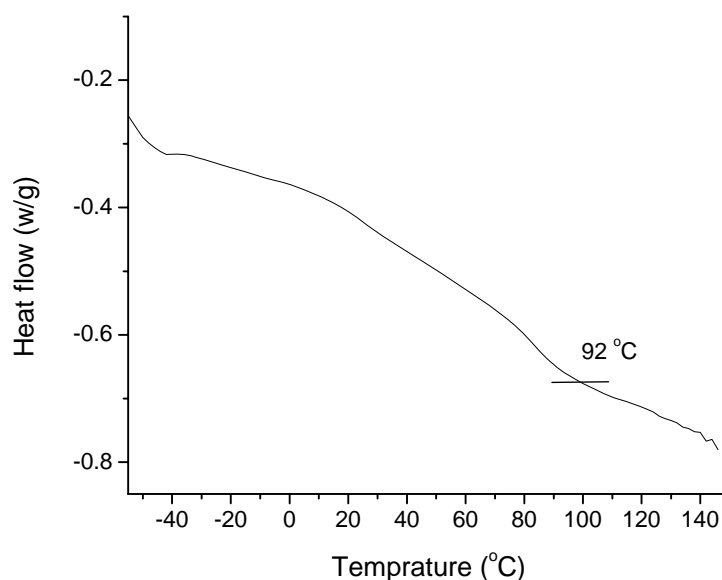
Figure 6.39 DSC thermogram of GAP-*b*-PMMA copolymer obtained by
photopolymerization of MMA in the presence of GAP-TDDC.

The DSC thermogram at high temperature scan recorded in **Figure 6.40**. The DSC
scan of GAP-*b*-PMMA copolymer shows an exothermic decomposition peak in the
temperature range 220-290 ^{o}C, with a maximum exothermic peak at about 260 ^{o}C.
The other interesting feature is the start of decomposition at a higher temperature than
the grafted copolymer. This could be attributed to a small amount of GAP segment in
the copolymer or little effect of the GAP segment on the decomposition behavior of
the binder due to the structural arrangement (block copolymer) of the two different
segments. The energy released from the decomposition of GAP-*b*-PMMA copolymer
was about 150 J/g, which is lower than the decomposition energy of the GAP-*g*-
PMMA copolymer, and gives further proof for the lower percentage of energetic
segment (GAP) in the block copolymer than grafted copolymer.
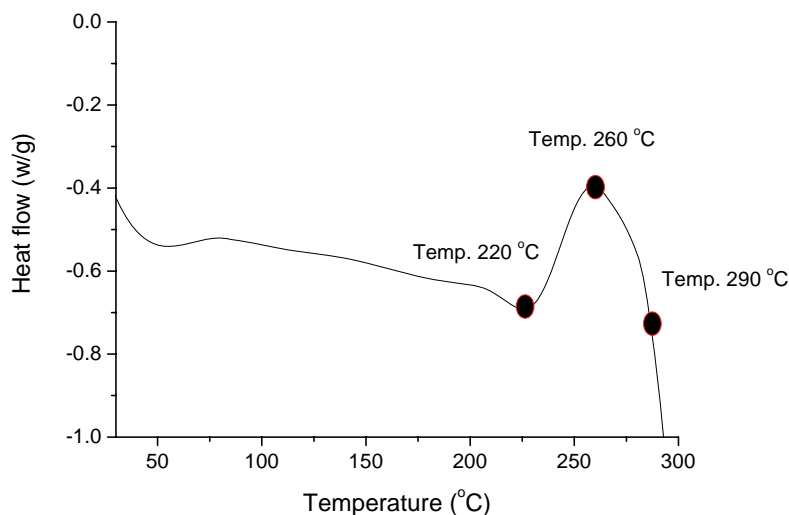
Figure 6.40 DSC thermogram of GAP-*b*-PMMA copolymer.

The thermal degradation of GAP-*b*-PMMA copolymer was also studied by TGA. **Figure 6.41** shows the result. The first degradation is about 166-336 ^{o}C, where about 23% of product was degraded. This part of the degradation is attributed to the GAP elastomers. Usually, the azide group will be decomposed in this temperature range. The second degradation step starts above 336 ^{o}C, where about 58% of weight loss occurs, which could be attributed to the PMMA main chains. In conclusion, different analytical techniques give proof about the formation of thermoplastic elastomer binder based on different microstructure, namely grafted and block GAP-PMMA copolymer, which was obtained, based on utilizing diethyl dithiocarbamate attached to GAP and by using photopolymerization.
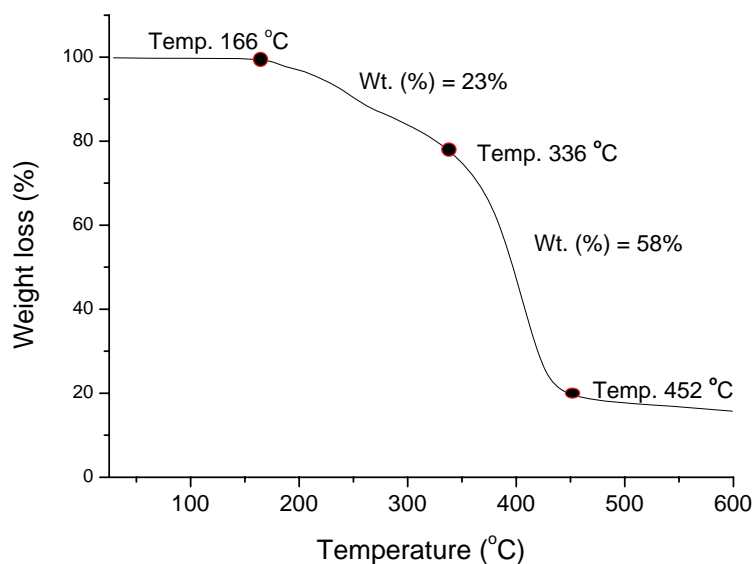
Figure 6.41 TGA analysis of GAP-*b*-PMMA copolymer.

6.3.5 Vacuum thermal stability test

The thermal stability test evaluates the reluctance of any explosive formulation to decompose at elevated temperatures. This method will give an indication about the presence of any unstable impurity in an explosives formulation that is stable at 100°C. Vacuum thermal stability test (compatibly test) are conducted to ensure that the explosive that is used will not react in a violent manner when it comes into contact with its surrounding media, for example the polymeric binder or the coating inside the shell. In this study, the thermal stability test of sensitized energetic binders has been conducted based on using RSA-MIL-STD-154 as described in Section 6.2.2.2. The energetic thermoplastic elastomers found to be most likely compatible with RDX as the gas evaluation was +2.3 cm^3 for GAP-*g*-PMMA. The gas evaluation of GAP-*b*-PMMA was about +2.8 cm^3 which is slightly higher than graft copolymer but still in the range of slight reactive and can be considered as compatibly according to

Picatinny arsenal, who developed the test [36]. However, another compatibly test needs to be carried out, such macro-calorimetery test, to ensure compatibility of new binder system with RDX.

6.4 Summery

In this study, an energetic thermoplastic elastomer was successfully prepared by using controlled free radical polymerization. In the first step, a macro-iniferter was prepared based on poly(epichlorohydrin) and *N,N*-diethyl dithiocarbamate by means of nucleophilic substitution of chlorine atoms in PECH with the DDC groups. This macro-iniferter was successfully transferred to *N,N*-diethyl dithiocarbamate-glycidyl azide polymer, by means of an azidation reaction of the remaining chloromethyl groups by using sodium azide in DMF solvent. The achievement of macro-initiators was proved by using different spectroscopy analysis techniques, such as UV, FI-IR, and NMR. Thermoplastic elastomers were obtained by the photopolymerization of methyl methacrylate and styrene monomers in the presence of poly(epichlorohydrin) macro-iniferter and an energetic thermoplastic elastomer was obtained by the photopolymerization of methyl methacrylate monomers in the presence of glycidyl azide macro-iniferter. The photopolymerization was run with photoreactor with UV radiation (λ>300 nm). The first-order time-conversion plot for the polymerization system under UV irradiation, and an increase in the molecular weight with a slight change in the polydispersity, confirmed that polymerization proceeded in a controlled manner. Spectroscopic analyses gave proof of the formation of copolymers. Thermal analysis showed a single glass transition temperature for copolymer with values between the values of the glass transitions temperatures of the two homopolymers. Thermal analysis of GAP-PMMA copolymer showed exothermic decomposition

starting at about 200 ^{o}C, providing proof for the synthesis of an energetic binder system. GAP-PMMA binder found to be compatible with RDX crystal based on an evaluation by vacuum thermal stability test. Success in the synthesis of energetic thermoplastic elastomers by using photopolymerization provides an opportunity to apply this method in the coating of internal solid rocket motors to prevent migration of the energetic plasticizers, which has been the goal of rocket materials research for over 20 years.

6.5 References

1. Yugci Y., Serhatli I. E., Kubisa P., Biedron T., Macromolecules 1993, 26, 2397.
2. Moad G., Rizzardo E., Thany S. H., Aust. J. Chem 2005, 58, 379.
3. Jenkins D. W., Hudson S. M., Chem Rev 2001, 101, 3245.
4. Sebenik A., Prog. Polym. Sci 1998, 23, 875.
5. Battaerd, H. A. J., Tergear, G. W., Graft Copolymers, John Wiley and Sons 1967, 238.
6. Chung, T. C., Janvikul W., Bernard R., Hu R., Li C. L., Liu S. L., Jiang G. J., Polymer 1995, 36, 3565.
7. Crivello J. V., Dietliker K., Photoinitiators for Free Radical Cationic & Anionic Photopolymerisation, 2nd Edition, Wiley 1998, 61.
8. Scranton A. B., Bowman C. N., Peiffer R. W., Photopolymerization Fundamentals and Applications, American Chemical Society 1996, 1-14.
9. Luo N., Hutchison J. B., Anseth K. S., Bowman C. N., J. Polym. Sci., Part A: Polym. Chem 2002, 40, 1885.
10. Ishizu K., Khan R. A., Furukawa T., Furo M., J. Appl. Polym. Sci 2004, 91, 3233.
11. Destarac M., Charmot D., Frank X., Zard S. Z., Macromol. Rapid Commun 2000, 21, 1035.
12. Georges M. K., Veregin R. P. N., Kazmaier P. M., Hamer G. K., Macromolecules 1993, 26, 2987.
13. Kajiwara A., Matyjaszewski K., Macromolecules 1998, 31, 3489.
14. Otsu T., Yoshida M., Macromol. Rapid Commun 1982, 3, 133.
15. Otsu T., Akikazu M., Advances in Polymer Science, Springer-Verlag Berlin Heidelberg 1998, Vol.13, 675.

16. Otsu T., Matsunaga T., Doi T., Matsumoto A., Eur. Polym. J 1995, 31(1), 67.

17. Kongkaew A., Wootthikanokkhan J., J. Appl. Polym. Sci 2000, 75, 938.

18. Otsu T., J. Polym. Sci., Part A: Polym. Chem 2000, 38, 2121.

19. Ishizu K., Mori A., Shibuya T., Designed Monomers and Polymers 2002, 5(1), 1.

20. Greszta D., Mardare D., Matyjaszewski K., Macromolecules 1994, 27, 638.

21. Denisov E. T., Denisova T. G., Pokidova T. S., Handbook of Free Radical Initiators, John Wiley & Sons Inc. 2003, 303-330.

22. Lakshmi S., Jayakrishnan A., Polym 1998, 39(1), 151.

23. Yang W., Guan J., Lui W., Ye S., Shen J., Eur. Polym. J 1997, 33, 5761.

24. Bhuyan P. K., Kakati D. K., J. Appl. Polym. Sci 2005, 98, 2320.

25. Shu-Hui Q., Kun-Yuan Q., Polym 2000, 42, 3033.

26. Shu-Hui Q., Kun-Yuan Q., Polym Bull 2000, 44, 123.

27. Kroeze E., Brinke T. G., Hadziioannou G., Macromolecules 1995, 28, 6650.

28. Otsu T., Yamashita K.,Tsuda K., Macromolecules 1986, 19, 287.

29. Arai K, Ogiwara Y., J. Appl. Polym. Sci 1988, 36, 1651.

30. Holden G., Understanding Thermoplastic Elastomers, Hanser 2000, 1-13.

31. Matyjaszewski K., Cationic Polymerizations Mechanisms, Synthesis, and Applications, Marcel Dekker, Inc. 1996, 46.

32. Guan J., Yang W., J. Appl. Polym. Sci 2000, 77, 2569.

33. Liu P., Su Z., J. Photochem. Photobiol. A. 2004, 167, 237.

34. Gaur B., Lochab B., Choudhary V., Varma I. K., J. Macromol. Sci., Polym. Rev 2003, C43(4), 505-545.

35. Subramanian K., Eur. Polym. J 1999, 35, 1403.

36. Ahad, U.S. Patent 1992, 5,130,381.

37. Mohan Y. M., Raju M. P., Raju K. M., J. Appl. Polym. Sci 2004, 93, 2157.

38. Hesse M., Meier H., Zeeh B., Spectroscopic Methods in Organic Chemistry, Georg Thieme Verlag 1997, 29-45.

39. Cakmak I., Baykara H., J. Appl. Polym. Sci 2006, 102, 2725.

40. Tasdelen M. A., Yagci Y., Demirel A. L., Biedron T., Kubisa P., Polym Bull 2006, 653.

41. O Schwarz's, Polymer Materials Handbook, Natal Witness Printing and Publishing Company (Pty) Ltd 1995, 86.

Chapter 7

Synthesis and characterization of poly(epichlorohydrin-methyl methacrylate) graft copolymers prepared using reversible addition-fragmentation chain-transfer polymerization

Synthesis and characterization of poly(epichlorohydrin-methyl methacrylate) graft copolymers prepared using reversible addition-fragmentation chain-transfer polymerization

Abstract

The synthesis of poly(epichlorohydrin-methyl methacrylate) graft copolymers based on using sodium dithiobenzoate as a reversible addition-fragmentation chain-transfer (RAFT) agent has been studied. Sodium dithiobenzoate was prepared in aqueous solution, before it was reacted with PECH via nucleophilic substitution reaction of a chloromethyl group on the PECH backbone. The formation of poly(epichlorohydrin) (PECH) with pendant dithiobenzoate groups as macro-initiators was proved by using different spectroscopic techniques. Thermal bulk polymerization of methyl methacrylate monomers in the presence of macro-initiator was studied and the controlled radical polymerization was confirmed by a linear increase of molecular weight of polymer with conversion. First-order time-conversions give an indication that polymerization proceeds via a controlled fashion. The polydispersity index was not changed considerably during polymerization. The copolymers were subjected to characterization with spectroscopic analysis which gives proof of the formation of two different segments in the final yield.

Keywords: Thermoplastic elastomer; dithiobenzoate; poly (epichlorohydrin-methyl methacrylate) graft copolymers, RAFT agent.

7.1 Introduction and Objectives

7.1.1 Living free radical polymerization

In the last decade, living polymerization has been shown to be a convenient method for obtaining polymers with low polydispersity, tailored molecular weights, and well-defined architectures [1, 2]. Living radical polymerization processes are of a great interest in macromolecular chemistry, both in academic and industrial sides. Since the first reports of living radical polymerization appeared, when Otsu and his colleagues reported photoiniferters in 1982 [1], these controlled/living techniques have put the free-radical polymerization in a new perspective. This is related to the possibility of combining free radical chemistry with a more sophisticated design of the polymer chain architecture. Block copolymers are an example of such a class of materials, for which careful tailoring of the block length and monomer composition yields materials with unique properties that are, not only of academic significance, but also of a commercial interest. Block copolymers can be used in many applications: novel surfactants, dispersants, coatings, adhesives, bio-materials, membranes, drug delivery media, and materials for microelectronics.

This research area has now become one of the most rapidly growing areas of polymer chemistry. These living techniques are based on either reversible termination of the propagating radicals to form dormant covalent species, as found with nitroxide-mediated polymerization (NMP) and atom transfer radical polymerization (ATRP), or the transfer of the radical to a different chain, as found in the reversible addition-fragmentation chain transfer (RAFT) process. Here, the focus will be on the latter method.

7.1.2 Reversible addition fragmentation chain transfer

Many reports addressing the third pseudo-living polymerization technique, which has termed reversible addition-fragmentation chain transfer polymerization [2, 3]. RAFT appears to offer advantages over other controlled polymerization methods since it is applicable to a wide range of monomers and can be performed in a wide variety of solvents (including water), under a broad range of experimental conditions. The basic structure of the transfer agent used in the RAFT process is shown in **Figure 7.1**., Z refers to the stabilizing group and R refers to the leaving group. The Z group should be able to activate the dithioester double bond for fast addition of the propagating polymeric radicals. The R group should be suitable for use with the monomer that needs to be polymerized and be a good leaving group, capable of reinitiating polymerization.

R is the leaving group

Z is the stabilizing group
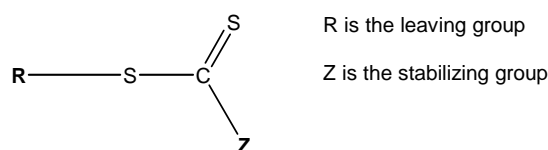
Figure 7.1 Basic structure of RAFT agent.

Radical polymerizations based upon a degenerative transfer system rely upon the rapid and reversible exchange of highly active transferable groups and growing polymeric radicals. While in conventional radical initiators compounds such AIBN or peroxides serve as a radical source to drive reversible exchange reactions between active and dormant states.

7.1.2.1 Types of RAFT

Different types of RAFT have been used, examples of which are dithiocarbamates (**1**), xanthates (**2**), trithiocarbonate (**3**), and other compounds (**Figure 7.2**).
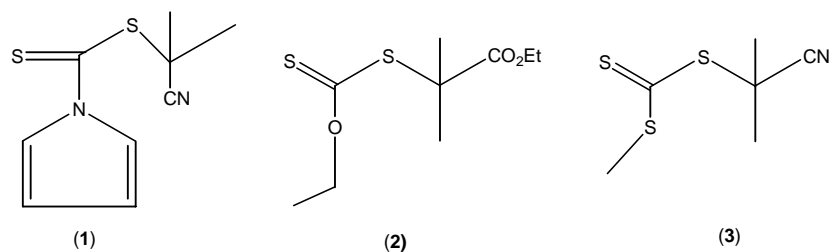
Figure 7.2 Examples of different types of RAFT agents.

Figure 7.3 shows examples for Z and R groups. Polarity, steric effects, bond strength and stereoelectronic effects are the major controllers of RAFT agent activity.
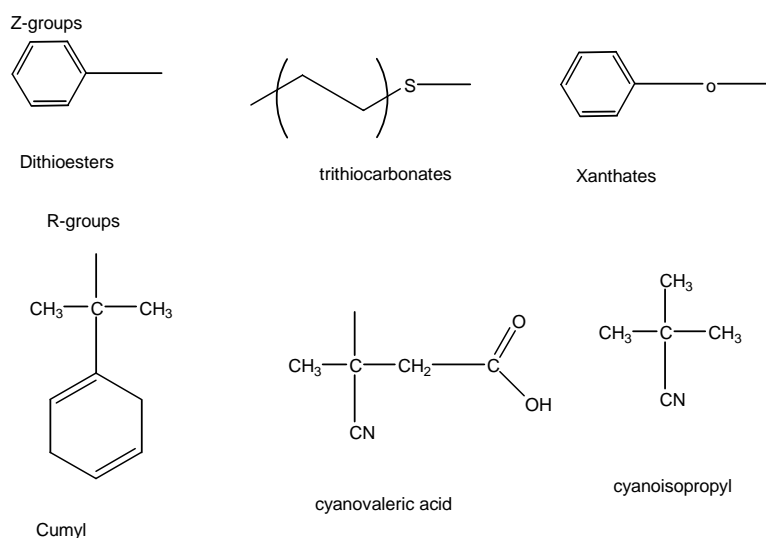
Figure 7.3 Examples of Z and R groups of RAFT agent.

7.1.2.2 RAFT mechanism

The key to a successful RAFT polymerization is the presence of a highly efficient dithioester chain transfer agent (CTA). The CTA reacts with either the primary radical (derived from the initiator; AIBN, for example) or a propagating polymer chain, forming a new CTA and eliminating R·, which in turn reinitiates

polymerization. "Living" characteristics are conferred via the RAFT reactions between active and dormant polymer chains and the S=C (Z) S– species (where Z is Ph for example). **Scheme 7.1** illustrates the reversible addition-fragmentation chain transfer polymerization [1, 3].

  a) Initiation and propagation:
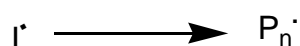
  b) Chain transfer
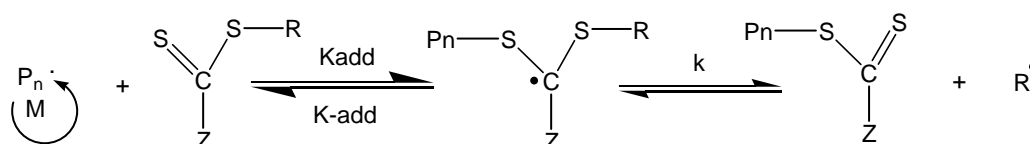
  c) Re-initiation and propagation:
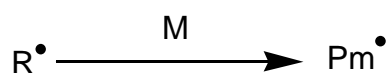
  d) Chain equilibrium:
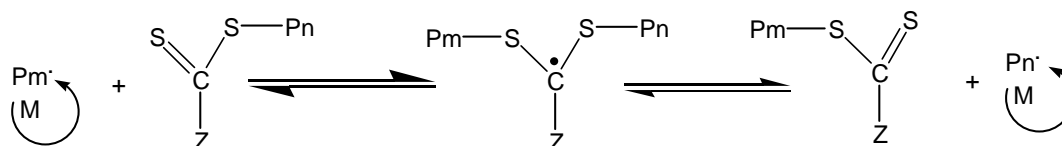
  e) Termination:
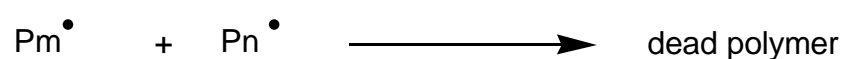
R=leaving group   Z=activating group

Scheme 7.1 Schematic representation of reversible addition-fragmentation chain transfer, in which a dithioester is used. a) Conventional initiation and propagation. b) Reaction of the initial transfer agent with a propagating radical, forming a dormant species and releasing radical R·. c) The expelled radical initiates polymerization and forms a propagating chain. d) Establishment of equilibrium between active propagating chains and dormant chains with a dithioester moiety. e) Termination reaction.
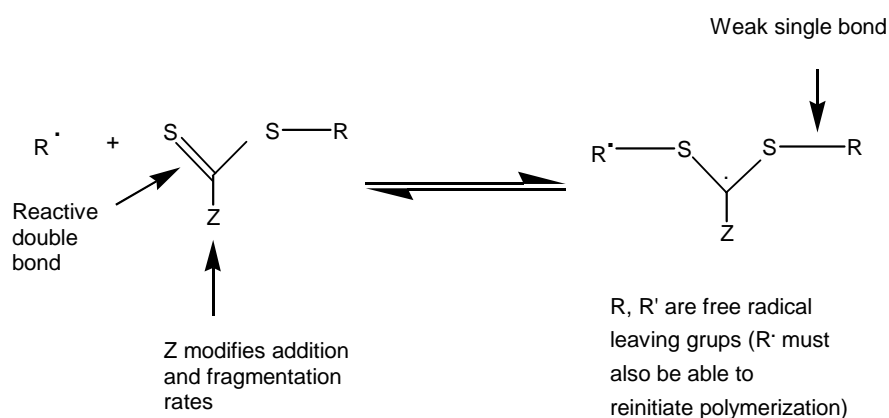
Figure 7.4 Structural features of thiocarbonylthio RAFT agent and the intermediate formed on radical addition (figure adopted from [2]).

There is a wide range of thiocarbonylthio compounds which can be used. These include trithiocarbonates, xanthates, dithiocarbamates, and other compounds [3, 4]. The effectiveness of the RAFT agent depends on the monomer being polymerized, and also depends strongly on the properties of the free-radical leaving group R and the group Z, which can be chosen to activate or deactivate the thiocarbonyl double bond and modify the stability of the intermediate radicals (see Figure 7.4). For an efficient RAFT polymerization the RAFT agent should have the following properties [3, 4]:

1. Have a reactive C=S double bond in order to achieve high rate of addition. It is reported that the rate of addition of radicals to the C=S double bond is strongly influenced by the Z group. The rate is higher when Z=aryl, alkyl (dithioester), or S-alkyl(trithiocarbonates), and lower when Z=O-alkyl(xanthates) or *N,N*-dialky (dithiocarbamates).

2. The intermediate radical rapidly fragments without side reactions. The chain transfer coefficients decrease in the series dithiobenzoates>trithiocarbonates ≈ dithoalkanoates > dithiocarbonates (xanthates) > dithiocarbamate. The low reactivity of the latter two types is attributed to the interaction between the

oxygen and nitrogen lone pairs and the C=S double bond. It is important to remember that the effectiveness of the RAFT agent is controlled by the interaction of Z with the C=S double bond to activate or deactivate that group towards the free-radical addition.

3. The expelled radicals (R⋅) should efficiently re-initiate polymerization. In order to achieve this, fragmentation must occur efficiently in the desired direction, and the substituent R must be a good homolytic leaving group, relative to the attacking radical P_n. For example, benzyl dithiobenzoate is reported to be a suitable chain-transfer agent in polymerizations with styrene, but not in the case of methacrylate. This is attributed to the inertness of the R in the case benzyl dithiobenzoate with respect to the PMMA propagating radical.

Moad *et al.* [2], reported that the reactivity of RAFT agents with different Z group decreases as follows: aryl > alkyl ≈ alkylthio ≈ pyrrole > aryloxy > amido > alkoxy > dialkylamino. On the other hand, it is reported that chain transfer coefficients decrease in the series dithiobenzoate > trithiocarbonates ≈ dithioalkanoates > dithiocarbonats (xanthates) > dithiocarbamates [5].

The nature of the R group on the RAFT agent affects the chain transfer constant. The choice of the R group depends on the monomer being polymerized. R should be a good leaving group, capable of reinitiating polymerization. If R is not efficient in reinitiating, retardation and inhibition may occur. This may lead to a slow conversion of the RAFT agent and a broad molar mass distribution. The leaving group ability decreases in the series R = tertiary >> secondary < primary [5].

7.1.2.3 Advantages and limitations of RAFT

RAFT appears to offer advantages above other controlled free radical polymerization methods. These advantages include the following [3, 4, 6]:

1. RAFT is applicable to a wide range of monomers and a wide range of functionalities in monomers.

2. RAFT can be performed in a wide variety of solvents (including water), under a broad range of experimental conditions.

3. RAFT polymerization has been viewed as the most robust and versatile method for controlling the molecular weight of polymers in heterogeneous media (emulsion, miniemulsion, suspension) and RAFT is tolerant of small amounts of impurities.

4. A variety of molecular architectures can be prepared. Stars, blocks, microgel and hyperbranched structures, supramolecular assemblies and other complex architectures are accessible and can have high purity [6].

5. It is possible to take RAFT polymerizations to high conversions and achieve commercially acceptable polymerization rates.

6. Polymers with well-controlled molecular weight and narrow polydispersity can be obtained. Also, RAFT yield polymers without metal ions.

RAFT does however have some limitations, which including the following [4]:

1. Polymerization (retardation, poor control) is frequently attributable to inappropriate choice of the RAFT agent for the monomer(s) and/or reaction conditions.

2. RAFT agents that perform well under a given set of conditions are not necessarily optimal for all circumstances.

3. The reaction scheme for RAFT copolymerization is relatively complex, when considered alongside that for NMP or ATRP.

4. Some types of RAFT such as trithiocarbonates, tend to produce polymers with a yellow color, where dithiocarbamates and xanthates produce white or low-colored compounds.

7.1.2.4 Copolymerization using RAFT

As mentioned previously, RAFT techniques can be used to make copolymers. There are generally two methods. The first method is based on using a polymer obtained from RAFT polymerization as the macro-initiator in the second polymerization. For example, RAFT of MMA with benzyl dithiobenzoate is used in the copolymerization of styrene with MMA, but very poor control is achieved [2]. The second method is based on attaching the RAFT agent to the first polymer and using this product as macro-initiator. An example of this is when an hydroxyl-terminated polymer (such as polyethylene glycol or poly(dimethyl siloxane)) is condensed with a carboxyl terminated RAFT agent, to be followed by radical polymerization to form the block copolymer [7].

Lae *et al*. [8], reported about using a controlled radical polymerization based on carboxyl- and hydroxyl- terminated polymers to prepare block copolymer. They utilized dithiocarbamates or xanthates with simple alkyl Z derivative. It is not practical to make block copolymers by this method due to slow reinitiation of the second block.

7.1.3 Objectives

The aim of this part of the study is to prepare poly(epichlorohydrin-*g*-methyl methacrylate) (PECH-*g*-PMMA) graft copolymer by using controlled free radical polymerization. This was to be carried out by reacting sodium dithiobenzoate solution with hydroxyl terminated poly(epichlorohydrin) (PECH-diol) to obtain a RAFT macro-initiator, which was then to be used as a CTA in the free radical polymerization of MMA.

7.2 Experimental

7.2.1 Materials

Sodium methoxide and benzyl chloride were obtained from Aldrich and used without further purification. AIBN was obtained from Fluka and recrystallized from methanol. PECH-diol was obtained via cationic ring-opening polymerization (Chapter 2, Section 2.2.3.1). Toluene and dichloromethane were purified by standard procedures. Methanol was used as received for precipitation of the polymer and it was dried over anhydrous molecular sieves before use in case of the synthesis of sodium dithiobenzoate. Diethyl ether and ethanol (absolute) were used as received. Magnesium sulfate and calcium chloride were obtained from Saarchem. Methyl methacrylate (MMA) was first washed with a 0.3 M KOH solution to remove inhibitor and then distilled under reduced pressure. MMA was stored over molecular sieves in a refrigerator and used within 1 week of purification. All purified solvents and reagents were stored over molecular sieves.

7.2.2 Analytical equipments and methods

7.2.2.1- UV, FTIR, NMR, GPC, and DSC analysis

The equipment and analytical methods used for the UV, FTIR, NMR, GPC, and DSC are described in Chapter 2, Section 2.2.2.

7.2.3 Experimental techniques

This section describes experimental techniques used to prepare dithiobanzoate-poly(epichlorohydrin) (PECH-DBZ) as macro-raft agent and polymerization of MMA monomers in the presence of macro-raft agent.

7.2.3.1 Synthesis of sodium dithiobenzoate

Sodium dithiobenzoate was prepared by the method of Mitsukami *et al*. [9]. The equipment comprised a dry three-necked bottomed-round flask equipped with a magnetic follower, addition funnel, thermometer, and rubber septum for liquid transfer. First, sodium methoxide (30% solution in methanol, 1 mol) was transferred to the flask. Then anhydrous methanol was added, followed by the rapid addition of elemental sulfur (1 mol), with stirring. Benzyl chloride (0.5 mol) was added dropwise via the addition funnel over a period of 1 hour, at room temperature, under a dry nitrogen atmosphere. Upon the addition of the benzyl chloride, a dark brown color appeared. The reaction mixture was heated in an oil bath at 70 $^{\circ}$C for 10 hours. The reaction mixture was cooled to 7 $^{\circ}$C using an ice bath. The precipitated salt was removed by filtration and the solvent removed under vacuum. The oily, brownish colored residue was taken up in water and the dispersion filtered a second time, through a glass filter. A second batch of the unidentified cooking salt was removed. A solution of sodium dithiobenzoate and dithiobenzoic acid in water remained. The following method was used to extract the dithiobenzoic acid.

Deionized water (500 mL) was added to the residue and mixture transferred to a 2 L separating funnel. Diethyl ether (600 mL) and 1N HCl (about 500 mL) were added, and the dithiobenzoic acid was extracted into the ether layer. To the residue, deionized water (300 mL) and 1N NaOH (500 mL) were added, and sodium dithiobenzoate was extracted to the aqueous layer. This washing process was repeated twice. Sodium dithiobenzoate solution was used directly in the grafting reaction of dithiobenzoate to PECH-diol.

7.2.3.2 Synthesis of dithiobenzoate-poly(epichlorohydrin) as RAFT-agent

PECH-DBZ was synthesized by refluxing poly(epichlorohydrin) (5 g) with sodium dithiobenzoate solution (50 mL) obtained from the previous step, for about 24 hours

in absolute ethanol **Scheme 7.2**. On completion of the reaction the mixture was cooled to room temperature and filtered. The solvent was removed under vacuum. Dichloromethane (100 mL) was added to the mixture of the product and water making two layers. PECH-DBZ was transferred to the organic layer. To the mixture of the product and water, dichloromethane to was added form two layers. In order to remove all of the unreacted sodium dithiobenzoate, the organic solution was transferred to a separation funnel and shocked well with distilled water. This was repeated three times. The product was dried over magnesium sulfate, the solvent removed by vacuum distillation, and the product dried under vacuum overnight at room temperature. Finally, the product was characterized by UV, FTIR and NMR.

^{1}H-NMR (CDCl$_3$): δ= 1.19 ppm [CH$_2$ of 1, 4-butanediol], δ= 3.1 ppm [hydroxyl group proton of PECH], δ= 3.37-3.8 ppm [CH$_2$Cl and CH$_2$ of PECH], δ= 4.05 ppm [CH of PECH], and δ= 7.5-8 ppm [C=C aromatic of dithiobenzoate].

^{13}C-NMR (CDCl$_3$): δ= 28 ppm [CH$_2$ of 1,4-butanediol], δ= 41-44 ppm [CH$_2$Cl of PECH], δ= 70 ppm [–O–CH$_2$– of PECH], δ= 79-80 ppm [CH of PECH], δ= 126-130 ppm [C=C aromatic of dithiobenzoate], and δ= 227 ppm [C=S of dithiobenzoate].

FTIR (NaCl): 3406 (s, –OH), 3050 (w, Aryl–H), 2906 (s, –CH$_2$), 2866 (s, –CH), 1590, 1670, 1715 (w, aromatic), 1433 (s) 1338 (w), 1525 (w), 1195 (w), 1109 (s), 966 (w), 833(w), 738(s), 960(w), 642(w) cm^{-1}. UV spectrum shows absorption of aromatic groups of dithiobenzoate at about 303 nm.
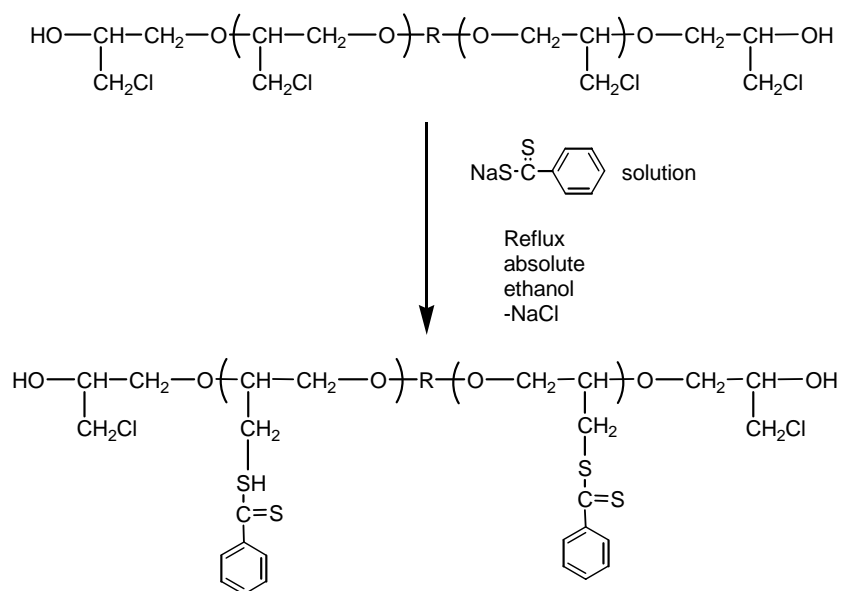
Scheme 7.2 Proposed reaction scheme for the synthesis of dithiobenzoate-
poly(epichlorohydrin) (R 1, 4-butanediol).

7.2.3.3 Polymerization of MMA in the presence of dithiobenzoate macro-RAFT agent

Polymerization reactions were conducted in a 250 mL three-necked round-bottomed flask, fitted with a condenser, stopper and a gas-inlet valve. Predetermined quantities of MMA, AIBN and PECH-DBZ (macro-initiators) were mixed together in the flask at room temperature. The flask and contents were purged with nitrogen for about 15 minutes prior to starting the reaction, to remove oxygen. The reaction flask was immersed in a temperature controlled oil bath at 80 $^{\circ}$C. All the reactions were conducted under nitrogen gas and samples were withdrawn at specific time intervals via a syringe, until the reaction reached its final conversion (when the sample could not be withdrawn due to the high viscosity of polymerization solution). The polymerization conversations were determined gravimetrically. A sample of the

cured reaction mixture (2 mL) was transferred to aluminum plates, for which excess monomer and solvent were removed by evaporation at ambient temperature. Finally, samples were dried overnight under a vacuum at room temperature. **Scheme 7.3** shows the proposed reaction scheme for the bulk thermal polymerization of MMA in the presence of PECH-DBZ to yield PECH-*g*-PMMA.

Scheme 7.3 Synthesis of poly(epichlorohydrin-*g*-methyl methacrylate) copolymer by bulk thermal polymerization of MMA in the presence of PECH-DBZ, and AIBN (R 1, 4-butanediol).

7.3 Results and discussion

The results obtained for the synthesis and the characterization of PECH-DBZ as macro-raft-agent and poly(epichlorohydrin-g-methyl methacrylate) copolymer obtained from the free radical polymerization of MMA in the presence of PECH-DBZ maro-raft-agent are presented and discussed.

7.3.1 Synthesis of dithiobenzoate-poly(epichlorohydrin)

The attachment of dithiobenzoate to PECH is achieved by a nucleophilic substitution of chlorine groups with sodium dithiobenzoate. The attachment of dithiobenzoate changes the color of PECH from colorless to pink. The successful synthesis of PECH-DBZ was confirmed by UV, FTIR, and NMR analyses. A UV spectrum of PECH-DBZ is shown in **Figure 7.4.** The absorption b and at about 303 nm is attributed to the aromatic ring of PECH-DBZ. The UV spectrum of PECH itself does not show a strong absorption peak at this region. This indicates that the dithiobenzoate is incorporated into the elastomers.

The FTIR spectrum of PECH with DBZ pendent groups is shown in **Figure 7.5**. The characteristic peaks due to the attachment of dithiobenzoate are assigned as follows: 3050 cm^{-1} attributed to the Aryl-H stretching vibration and several weak bonds for overtones and combination vibrations attributed to the aromatic ring of dithiobenzoate can be indicated in the region 2000-1600 cm^{-1} [10].
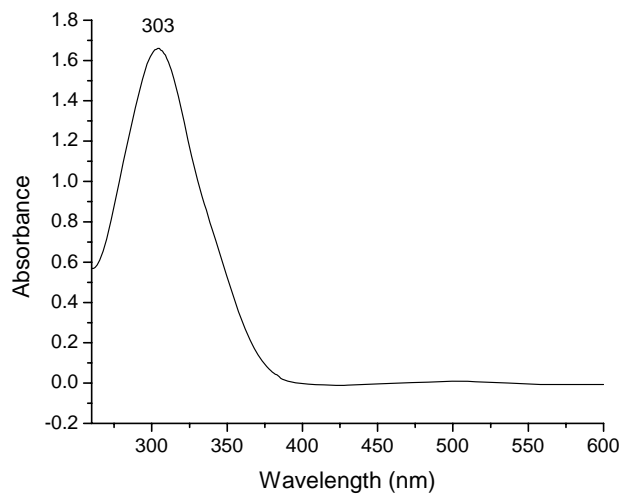
Figure 7.5 UV spectrum of dithiobenzoate-poly(epichlorohydrin). (solvent dichloromethane, concentration 1 mg/mL).
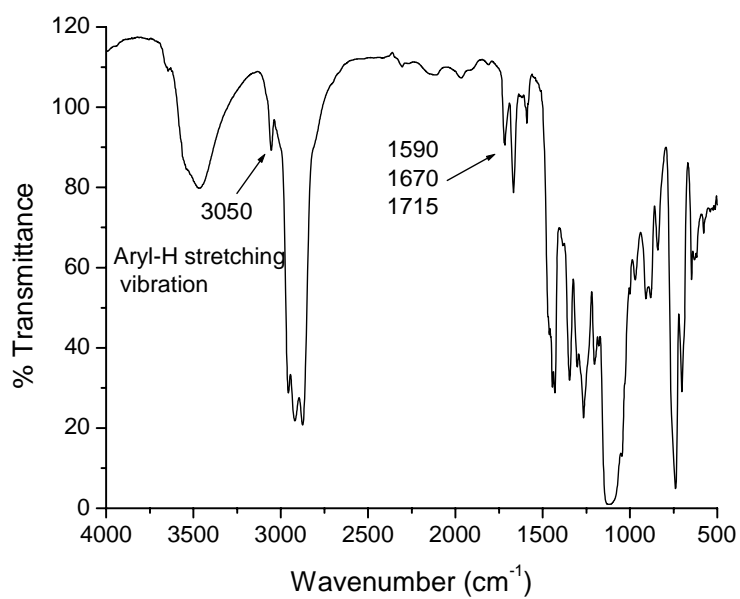
Figure 7.6 FTIR spectrum of dithiobenzoate-poly(epichlorohydrin).

The ^{1}H-NMR spectrum of PECH-DBZ is shown in **Figure 7.6**. The most important singnals are the methylene proton of diols at about 1.58 ppm (denoted 2), the chloromethyl proton, methylene, and ethylene of PECH at 3.2-4 ppm (denoted 3, 4 & 5), and the aromatic ring protons of dithiobenzoate at 7.5-8 ppm (denoted 6). The remaining assignments are indicated in the figure below.

The ^{13}C-NMR spectrum of PECH-DBZ is shown in **Figure 7.7**. Peak assignments are indicated in the figure. The most important peaks are those of the methylene carbon that link PECH to DBZ at about 33 ppm (denoted 1), the chloromethyl of PECH at about 46 ppm (denoted 2), the aromatic ring of DBZ at about 130 ppm (denoted 5), and the carbon disulfide at about 220 ppm (denoted 6).

Finally, the data gathered for analyses by UV, FTIR, and NMR confirmed the successful formation of PECH-DBZ as macro-RAFT agent. This macro-RAFT agent will be used in the next step, in the thermal bulk polymerization of MMA monomers, to yield poly(epichlorohydrin-g-methyl methacrylate) graft copolymer.
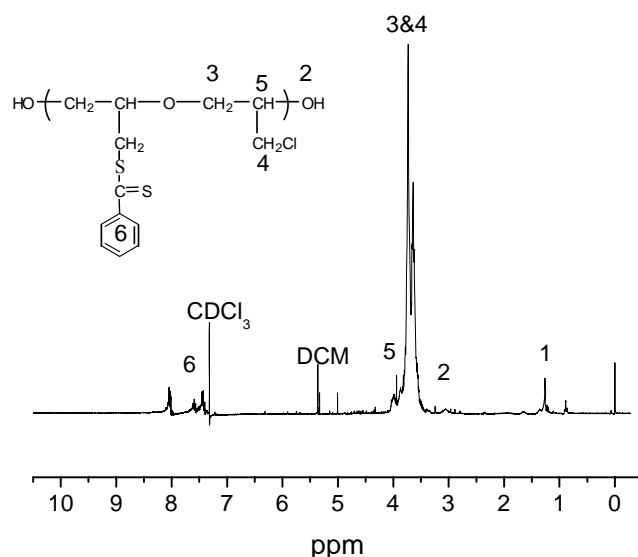
Figure 7.7 ^{1}H-NMR (CDCl$_3$) spectrum of dithiobenzoate-poly(epichlorohydrin).
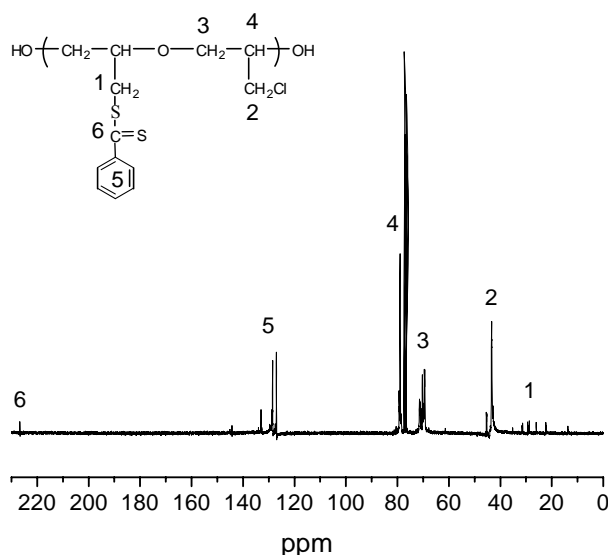
Figure 7.8 ^{13}C-NMR (CDCl$_3$) spectrum of dithiobenzoate-poly(epichlorohydrin).

7.3.2 Synthesis of poly(epichlorohydrin-methyl methacrylate) graft copolymer

Thermal polymerization of MMA was carried out in bulk and by mixing monomers with macro-RAFT agent and AIBN. In order to better understand the mechanism of initiation and propagation, a first-order time-conversion plot for this polymerization system was obtained. Conversion was estimated by gravimetric measurements. The first-order time-conversion plot is shown in **Figure 7.8**. The conversion after a reaction time of 2 hours was very low. Running the reaction for a further 10 hours only increased the conversion to about 22%. The viscosity of reaction mixture prevented the withdrawal of more samples for conversion analysis. A relationship between ln ([M]$_o$/[M]) and the reaction time indicated that the steady-state radical concentration was constant over the duration of the polymerization of MMA (in the presence of PECH-DBZ as mediated RAFT and AIBN as an initiator). There was an inhibition period lasting up to 4 hours. It is reported that the dithiobenzoate RAFT

agent causes this inhibition period, which is attributed to low fragmentation of the radical [6]. The inhibition period observed in the RAFT polymerization may be related to a sufficient stabilization of the intermediate macro RAFT radical or it could be attributed to the effect of chloromethyl groups of PECH (polarity effect). For longer reaction times, when the initial RAFT agent was converted into a polymeric species, the polymerization rate increased. It is thus expected that the inhibition period could be eliminated by a higher reaction temperature, which could accelerate the reaction between the reinitiating group and monomer, or it could increase the fragmentation rate of the pre-equilibrium RAFT radical.
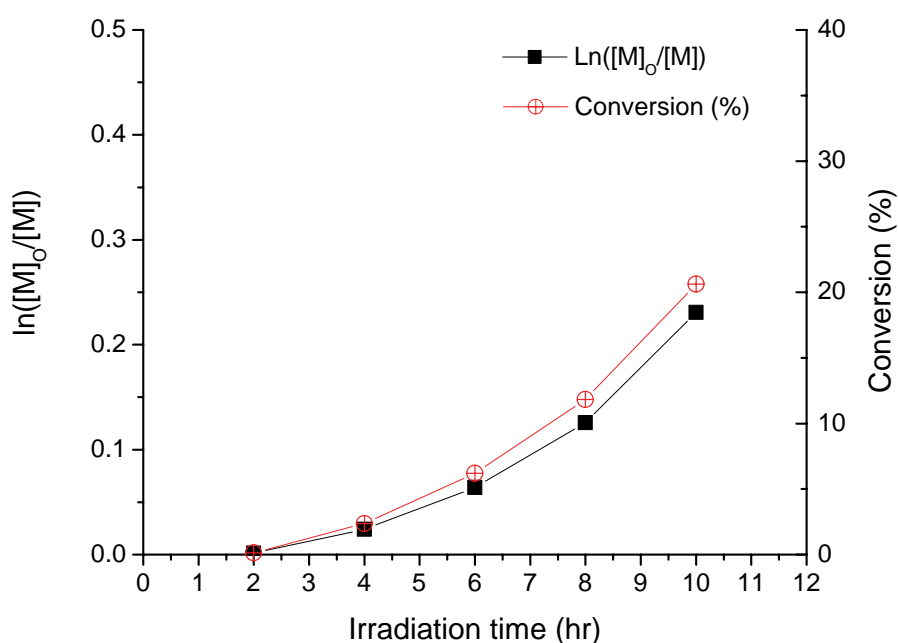
Figure 7.9 First-order time-conversion plots for the thermal bulk polymerization of MMA initiated by dithiobenzoate-poly(epichlorohydrin). (Polymerization conditions: [PECH-DBZ]/ [MMA] =0.0028, AIBN used as initiator.)

The effect of the reaction time on the molecular weight and polydispersity index of grafted copolymer is demonstrated in **Figure 7.9**. There is a slight increase in the molecular weight after a reaction time of 2 hours. After a reaction time of 4 hours, however there was a higher increase in the molecular weight compared to the first 2 hours. This could be attributed to the nature of the dithiobenzoate and the resulting inhibition period. The change in the molecular weight with reaction time was small and the polydispersity index remained in the range of 1.6-1.85. This indicates that polymerization proceeded in a reasonably controlled fashion.
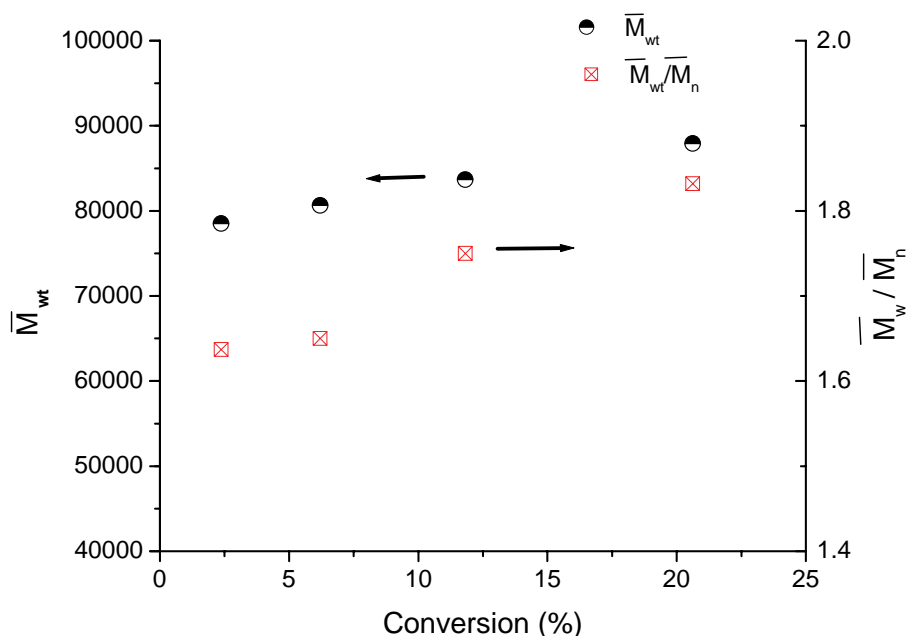
Figure 7.10 Plots of $\overline{M_{wt}}$ and $\overline{M_{wt}}/\overline{M_n}$ against conversion for the thermal bulk polymerization of MMA initiated by dithiobenzoate-poly(epichlorohydrin). (Polymerization conditions: [PECH-DBZ]/ [MMA] =0.0028, AIBN used as initiator.)

Polymerization kinetics of PECH-*g*-PMMA copolymer shows that polymerization proceeds in a controlled fashion and there was an inhibition period of 2 hours. FT-IR

showed the presence of two different segments in the final copolymer obtained from the thermal polymerization where, absorption of a carbonyl group found at about 1730 cm^{-1} and absorption of chloromethyl groups at about 745 cm^{-1} were detected.

7.4 Summery

Macro-raft agents were successfully prepared based on poly(epichlorohydrin) and dithiobenzoate by means of nucleophilic substitution of chlorine atoms in PECH with the DBZ groups, as confirmed by UV, FIIR, and NMR spectroscopy. These macro-raft agents were used in the bulk thermal polymerization of MMA to yield graft copolymer. The first-order time-conversion also showed a linear relationship between ln ([M]$_o$/[M]) and the reaction time and an increase in the molecular weight with only a slight change in the polydispersity index, which confirmed that polymerization, preceded in a controlled manner. FTIR spectroscopy proofed formation of graft copolymer. PECH-g-PMMA graft copolymer is thermoplastic elastomers and could be used as coatings, sealants and adhesives.

7.5 References

1. Otsu T., Yoshida M., Macromol. Rapid Commun 1982, 3, 133.
2. Moad G., Rizzardo E., Thany S. H., Aust. J. Chem 2005, 58, 379.
3. Moad G., Solomon D. H., The Chemistry of Radical Polymerization, First Edition, Elsevier 2006.
4. Destarac M., Charmot D., Frank X., Zard S. Z., Macromol. Rapid Commun 2000, 21, 1035.
5. Chiefari J., Mayadunne R. T. A., Moad C. L., Moad G., Rizzardo E., Postma A., Skidmore M. A., Thang S. H., Macromolecular 2003, 36, 2273.
6. Moad G., Chong Y. K., Postma A., Rizzardo E., Thang S. H., Polym 2005, 46, 8458.
7. Brouwer H. D., Schellekens M. A. J., Klumperman B., Mounteiro M. J., German A. L., J. Polym. Sci. Part A: Polym. Chem 2000, 38, 3596.
8. Lai J. T., Shea R., J. Polym. Sci. Part A: Polym. Chem 2006, 44, 4298-4316.
9. Mitsukami Y., Donovan M. S., Lowe A. B., McCormick C. L., Macromolecules 2001, 34, 2248.
10. Hesse M., Meier H., Zeeh B., Spectroscopic Methods in Organic Chemistry, Georg Thieme Verlag 1997, 29-45.
11. Mohan Y. M., Raju M. P., Raju K. M., J. Appl. Polym. Sci 2004, 93, 2157.

Chapter 8

Controlled radical polymerization of methyl methacrylate using *N,N′*-dithiocarbamate-mediated iniferter derivatives

Controlled radical polymerization of methyl methacrylate using *N,N'*-dithiocarbamate-mediated iniferter derivatives

Abstract

Four different photoiniferters namely benzyl diethyl dithiocarbamate (BDC), 2-(*N,N*-diethyldithiocarbamyl) propionic acid (PDC), 2-(*N,N*-diethyldithiocarbamyl) isobutyric acid (DTCA), and *N,N*-diethyl dithiocarbamate-epichlorohydrin (ECH-DDC) were synthesized and examined in the living/controlled radical polymerization of methyl methacrylate (MMA). The effect of the different iniferter structures on the molecular weight, polydispersity, and conversion of the polymer yield from photopolymerization has been investigated. Photoiniferters show controlled/living polymerization and the lowest molecular weight was obtained when BDC was used as photoiniferter, where ECH-DDC photoiniferter yielded polymer with the lowest polydispersity. The effect of the concentration (monomer-to-photoiniferter) and the reaction time on the polymerization has been studied and the conversion found to be controlled by a ratio of photoiniferters to monomers. The active PMMA precursor (macro-iniferter) obtained from this polymerization was also used in the photopolymerization of styrene monomer to yield poly(methyl methacrylate-*b*-styrene) copolymer. Photoiniferters and polymers were characterized by different spectroscopic methods and gel permeation chromatography. The conversion of polymerization was determined gravimetrically. Thermal analysis of copolymer was examined by using a differential scanning calorimetry (DSC).

Chapter 8

8.1 Introduction and objectives

8.1.1 Introduction

Living polymerization systems will be founded if there is a dynamic equilibrium between active and dormant species as a result of rapid reversible termination or reversible degenerative chain transfer reaction. The propagation and reversible termination should be much faster than any irreversible termination. Literature reported many radical polymerization methods, which exhibit controlled or living characteristics such as (I) dithiocarbamate iniferters [1-3], (II) nitroxide-mediated processes [4], (III) transition metal complex-dediated atom transfer radical polymerizations (ATRP) [5], (VI) reversible addition-fragmentation chain transfer (RAFT) processes [6]. Our interest in this section of the study is focused on using dithiocarbamate derivatives as photoiniferters in the free radical photopolymerization of methyl methacrylate (MMA).

Photopolymerization is one of the most rapidly expanding processes for materials production with more than 15% annual growth expected for the next several years. It is driven by the advantages afforded by the use of light, rather than heat, to drive the conversion of monomer to polymer [7]. Photopolymerization have many advantages such as: solvent-free formulations; very high reaction rates at room temperature; spatial control of the polymerization; low energy input; and chemical versatility since polymerization of a wide variety of monomers can be polymerized photochemically. Due to this unique set of advantages, photopolymerization have gained prominence in the recent years for the solvent-free curing of polymer films as well as emerging applications in dental materials, conformal coatings, electronic and optical materials, and rapid prototyping of three dimensional objects. Photoimaging, UV curing of coating and inks are another example of commercial processes of photoinitated polymerization [8].

Photopolymerization depends on using initiators that have the ability to convert the physical energy such as UV spectral (250-450 nm) into chemical energy in the form of reactive intermediates. These intermediates are radicals capable of initiating radical polymerization [2, 9-12]. For more information see page (173-175)

The two groups attached to the C=S double bond affect the polymerization throughout effectiveness and transfer coefficients **Figure 8.1**. Destarac *et al*. [3], reported that a

good iniferter (or RAFT agent) must have two characteristics. First, the rate of the addition to the (C=S) bond and fragmentation of the intermediate radical R (Figure 8.1) should be rapid relative to the rate of propagation. Second, the radical must reinitiate polymerization and it is preferable to have a rate equal to that of propagation in order to avoid any retardation. It is reported that dithiocarbamate has the lowest rate of addition and chain transfer coefficients compared to the other similar compounds containg thiocarbonyl double bonds. This is attributed to the interaction between the N and the C=S double bond [6]. On the other hand, dithiobenzoates possess a much higher rate of addition and chain transfer coefficient, which can be attributed to the presence of the benzyl ring of the dithiobenzoate.

Figure 8.1 Four different R groups of dithiocarbamate derivatives.

8.1.1 Objectives

The aim of this study is to synthesize different *N,N*-diethyldithiocarbamate iniferters and to investigate the effect of different iniferter structures on the molecular weight, polydispersity, and conversion of the polymer obtained by the photopolymerization. The effects of the concentration of monomer to the photoiniferter, and the reaction time on the polymerization are also studied.

8.2 Experimental

8.2.1 Materials

Sodium *N,N'*-diethyl dithiocarbamate, 2-bromopropionic acid, bromoisobutryic acid, epichlorohydrin, and benzyl chloride were obtain from Aldrich and used without further purification. Toluene was purified by standard procedures. Methanol, ethanol (absolute), dichloromethane, and diethyl ether were used as received. Methyl methacrylate and styrene (monomers) were first washed with a 0.3 M KOH solution to remove the inhibitors and then distilled under reduced pressure. The monomers were stored over molecular sieves in a refrigerator and were used within a week of purification. All purified solvents and reagents were kept over molecular sieves.

8.2.2 Analytical equipments and methods

8.2.2.1- UV, FTIR, NMR, GPC, and DSC analysis

Description of equipment and analysis methods applied for the UV, FTIR, NMR, GPC, and DSC analyses are given in Chapter 2 Section 2.2.2.

8.2.3 Experimental techniques

This section covers the synthesis of photoiniferters and the photopolymerization of MMA in the presence of these iniferters.

8.2.3.1 Synthesis of photoiniferters

The synthesis of the photoiniferters was based on nucleophilic displacement of bromine or chlorine atoms with sulfur atoms, which is associated with sodium *N,N'*-diethyl dithiocarbamate. Photoiniferters were subjected to different characterizations such as UV, FTIR, ^{1}H-NMR, and ^{13}C-NMR.

8.2.3.1. Synthesis of benzyl diethyl dithiocarbamate

Synthesis of benzyl diethyl dithiocarbamyl (BDC) was based on the reaction of benzyl chloride with sodium *N,N'*-diethyldithiocarbamate salts in an absolute ethanol [13, 14]. To a dried, three-necked round-bottomed flask equipped with a magnetic follower,

addition funnel, and condenser (with a calcium chloride guard tube), sodium *N,N'*-diethyl dithiocarbamate (10 g, 22.5 moles) dissolved in 60 mL of ethanol was added. Benzyl chloride (5.66 g, 22.5 moles) was dissolved in 60 mL of ethanol solvent and transferred dropwise through a dropping funnel over a period of 2 hours. After that, the reaction mixture temperature was raised to 50 °C and maintained at that temperature for about 10 hours. During this period, the formation of NaCl as a white salt was clearly observed, which indicates that the reaction was proceeding. After this time, the reaction mixture was cooled to room temperature. The reaction mixture was filtered, and the product was extracted from the filtered solution by using a mixture of dichloromethane and distilled water (1:1), three times, and the organic phase was collected and dried over magnesium sulfate for 18 hours. The dichloromethane was removed under vacuum (Buchi Rotavapor) and dried in the vacuum oven at room temperature. The product was characterized by UV, FTIR, ^{1}H-NMR, and ^{13}C-NMR spectroscopy. **Scheme 8.1** shows the proposed reaction scheme of or the synthesis of BDC.
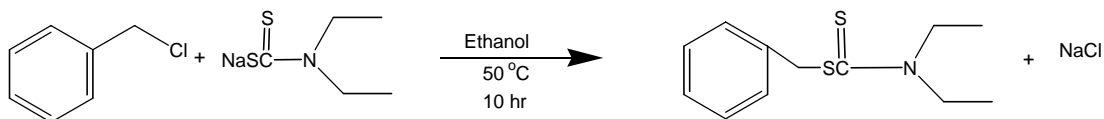
Scheme 8.1 Proposed reaction scheme for the synthesis of BDC photoiniferter.

^{1}H-NMR [CDCl$_3$]: δ= 1.23 ppm [–CH$_3$], δ= 3.7-4.05 ppm [–CH$_2$– of –(CH$_2$)$_4$], δ= 4.55 ppm [–CH$_2$–], δ= 7.2-7.4 ppm [aromatic ring].

FTIR (NaCl): 2970 (Stretching vibration of –CH, –CH$_2$, CH$_3$), 1590-1950 (overtones and combination vibration of aromatics), 1484 (s), 1410 (s), 1350 (w, CS–N), 1264 (s, –S–C=S–), 1204 (s, C=S), 1138 (S), 1068 (s, –SC(S)N), 982 (s), 920 (s), 830 (w), 770 (w, aromatic ring), 700 (s, aromatic ring) cm^{-1} [15, 16]. The UV spectrum (dichloromethane used as solvent) shows absorption peaks at 251 and 280 nm, which can be attributed to the –S–C(=S)– and –C(=S)–N groups, respectively. The product obtained was viscous yellow in color and typically the yield was about 30%.

8.2.3.1.2 Synthesis of 2-(*N,N*-diethyldithiocarbamyl) propionic acid

Synthesis of 2-(*N,N*-diethyldithiocarbamyl) propionic acid (PDC) was based on the reaction of 2-propionic acid with sodium *N,N'*-diethyldithiocarbamate salts in the mixture of an absolute ethanol/acetone (60/40) [13, 14]. To a dried three-necked round-bottomed flask equipped with a magnetic follower, addition funnel, and condenser with calcium chloride guard tube sodium *N,N'*-diethyl dithiocarbamate (10 g, 22.5 moles) dissolved in 60 mL of solvent mixture (ethanol/acetone, 60/40 mixture) was added. The mixture was stirred for about 30 minutes. 2-Propionic acid (6.8 g, 22.5 moles) dissolved in 60 mL of the solvent mixture was added dropwise over a period of 2 hours. After that, the reaction temperature was raised to 50 °C and left there for about 10 hours. During this period, the formation of NaBr as white salt was clearly observed. The reaction mixture was cooled to room temperature. Solids were filtered out and the solvent was removed under reduced pressure. The resultant products were dissolved in diethyl ether before being transferred to the separation funnel and extracted three times with water. Finally, the organic layer was dried over magnesium sulfate overnight and diethyl ether was removed by a Buchi Rotavapor and the product was dried under vacuum at ambient temperature. Photoiniferters were characterized by UV, FTIR, ^{1}H-NMR, and ^{13}C-NMR spectroscopy. **Scheme 8.2** below represents the proposed reaction scheme for the synthesis of PDC.
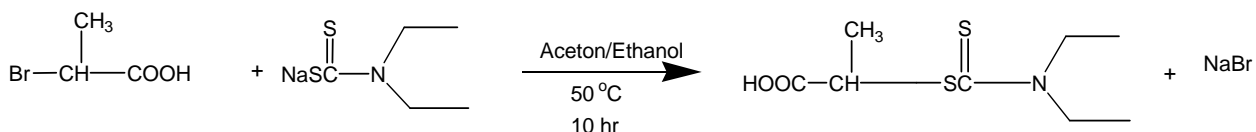

Scheme 8.2 Proposed reaction mechanism for the synthesis of 2-(*N,N*-diethyldithiocarbamyl) proponic acid photoiniferter.

^{1}H-NMR [DMSO]: δ= 1.1-1.5 ppm [–CH$_3$ of –(CH$_3$)$_2$–], δ= 1.47 ppm [CH–CH$_3$], δ=3.7-3.9 ppm [–CH$_2$– of –(CH$_2$)$_2$–], δ= 2.5 ppm [DMSO], δ= 4.55 ppm [–CH–].

^{13}C-NMR [DMSO]: δ= 11 ppm [–CH$_3$ of –(CH$_3$)$_2$–], δ= 17 ppm [CH–CH$_3$], δ= 40 ppm [DMSO], δ= 46 ppm [–CH$_2$– of –(CH$_2$)$_2$–], δ= 49 ppm [–CH–], δ= 172 ppm [COOH], δ= 192 ppm [C=S]. FTIR (KBr): 557, 595 ,642, 746, 765, 777, 829, 858, 914, 1201 (s, C=S), 1276 (s, -S-C=S-), 1301, 1351 (w, CS–N), 1376, 1409, 1430, 1442, 1454, 1488,

1637, 1700, 2584, 2692, 2931, 2973 (stretching vibration of -CH, -CH$_2$, CH$_3$), and 3000 (COO-H group) cm^{-1}. The UV (ethanol used as solvent) spectrum shows strong absorption peaks at about 251 and 280 nm, which is attributed to the –S–C(=S)– and –C(=S)–N groups, respectively. The obtained product was little white salts and recrystallization applied using petroleum ether to yield white salts and the typical yield was about 11%.

8.2.3.1.3 Synthesis of 2-(*N,N*-diethyldithiocarbamyl) isobutyric acid

2-(*N,N*-diethyldithiocarbamyl) isobutyric acid (DTCA) was synthesized by the reaction of 2-bromoisobutyric acid with sodium *N,N'*-diethyldithiocarbamate salts in a solvent mixture of ethanol/acetone (60/40) via a conventional nucleophilic substitution reaction [13, 14]. The following is a description of the followed experimental techniques: to a dried three-necked round-bottomed flask with a magnetic stir bar, addition funnel, and condenser with the calcium chloride guard tube were added. Sodium *N,N'*-diethyl dithiocarbaomate (10 g, 22.5 moles) dissolved previously in 60 mL of solvent mixture was transferred to the flask and stirred for about 30 minutes. 2-Bromoisobutyric acid (7.46 g, 22.52 moles) dissolved in 60 mL of the solvent mixture was added drop wise by using the addition funnel over a period of 2 hours. After that, the reaction mixture temperature was raised to 50 °C for about 10 hours and the formation of NaBr as white salt was clearly observed during this period. At the end of the reaction, the mixture cooled to room temperature then the unreacted sodium *N,N'*-diethyl dithiocarbamate and the formed salt were filtered, and the solvent was removed under reduced pressure to yield a viscous yellow product. The product was dissolved in diethyl ether before being transferred to a separation funnel and extracted three times with water. Finally, the organic layer was dried over magnesium sulfate and diethyl ether removed by a Buchi Rotavapor to yield a white solid which was dried under vacuum at room temperature. The photoiniferter was characterized by UV, FTIR, ^{1}H-NMR, and ^{13}C-NMR spectroscopy. **Scheme 8.3** below represents the proposed reaction scheme for the synthesis of the DTCA photoiniferter.

Scheme 8.3 Proposed reaction scheme for the synthesis of 2-(*N,N*-diethyldithiocarbamyl) isobutyric acid photoiniferter.

^{1}H-NMR [CDCl$_3$]: δ= 1.3 ppm [–CH$_3$ of –(CH$_3$)$_2$–], δ= 1.7 ppm [CH$_3$ of (C–CH$_3$)], δ= 3.7-3.9 ppm [–CH$_2$– of –(CH$_2$)$_2$–], δ= 7.3 ppm [CDCl$_3$].

^{13}C-NMR [CDCl$_3$]: δ= 10.6 ppm [–CH$_3$ of –(CH$_3$)$_2$–], δ= 24-26 ppm [C–CH$_3$], δ= 47 ppm [–CH$_2$– of –(CH$_2$)$_2$–], δ=77 ppm [CDCl$_3$], δ= 172 ppm [COOH], δ= 192 ppm [C=S].

FTIR (KBr): 561, 599, 655, 696, 742, 771, 825, 916, 935, 987, 1014, 1081, 1124, 1135, 1166, 1207(s, C=S), 1272(s, –S–C=S–), 1353 (w, CS–N), 1376, 1415, 1481, 1541, 1689, 2090, 2294, 2345, 2532, 2628, 2929, 2975 (Stretching vibration of –CH, –CH$_2$, CH$_3$), and 3000 (COOH group) cm^{-1}. The UV (ethanol used as a solvent) spectrum shows the absorption peaks at 251 and 280 nm which can be attributed to the –S–C(=S)– and –C(=S)–N groups, respectively. The product was obtained as a white solid and re-crystallization from petroleum gave a final yield of about 12%.

8.2.3.1.4 Preparation of epichlorohydrin-*N,N*-diethyl dithiocarbamate

The Epichlorohydrin attached to *N,N*-diethyl dithiocarbamate (ECH-DDC) was synthesized by refluxing epichlorohydrin with sodium diethyl dithiocarbamate for 18 hours in absolute ethanol (**Scheme 8.4**). At the end of the reaction, the formed sodium chloride was filtered out, and the solvent was removed under vacuum. The viscous light yellow product was dissolved in dichloromethane and residual NaCl and unreacted sodium dithiocarbamate were filtered out before transferring the solution to a separation funnel and washing three times with water in order to remove all formed and unreacted salts. The organic layer was dried over magnesium sulfate overnight, before the solvent was filtered and removed using vacuum distillation. Finally, the product was dried under

vacuum at room temperature for about 15 hours before being characterized using UV, FTIR, and ^{1}H-NMR spectroscopy.
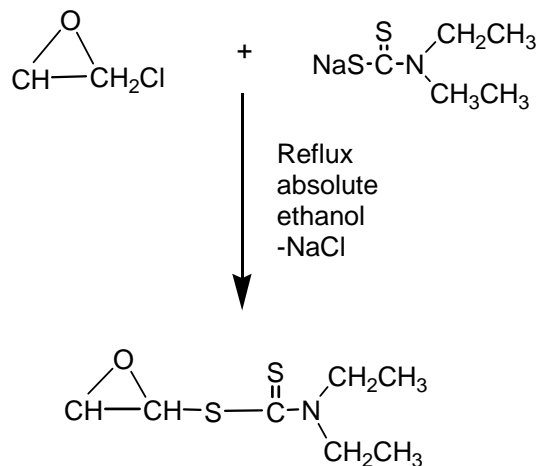
Scheme 8.4 Proposed reaction scheme for the synthesis of epichlorohydrin with sodium diethyl dithiocarbamate.

^{1}H-NMR (CDCl$_3$): δ= 1.18 ppm [CH$_3$ of DDC δ= 2.3-2.5 ppm [CH$_2$ of ECH], δ= 3 ppm [CH2 of ECH], and δ= 3.4 ppm [CH$_2$ of DDC].

FTIR (NaCl): 614 (s), 652 (s), 726 (w), 793 (w), 849 (s), 1103 (s), 1244 (s), 1395 (s), 1650 (s), 2977 (s), and 3450 (w) cm^{-1}. The yield of the yellowish product was about 70% and UV (dichloromethane used as solvent) shows strong absorptions at about 251 and 281 nm.

8.2.3.2 Photopolymerization

Photopolymerization reactions were carried out either in bulk or in toluene as a solvent. A mixture of appropriate amounts of MMA and photoiniferter was placed in a Pyrex tube and was purged with nitrogen for about 5 min prior to irradiation. A photoreactor equipped with 15 Philips 8 W/06 lamps emitting light nominally at λ > 300 nm and a cooling system was used for these reactions. The temperature of the photoreactor was maintained at 36 °C. Conversions of the polymerization reactions were determined gravimetrically. The obtained product was isolated by precipitating the polymerization solution in methanol before washing several times with large amounts of methanol in order to remove all non-consumed initiators. All samples were dried under a vacuum.

PMMA-*b*-PS block copolymer was synthesized by the irradiation of a mixture of PMMA obtained from photopolymerization as macro-iniferter and styrene monomer in toluene solution and under nitrogen atmosphere for 4 hours. At the end of the polymerization the product was precipitated in methanol and was Soxhlet-extracted with benzene and cyclohexane to remove the PMMA and PS homopolymer, respectively [17]. The block copolymer was then dried in a vacuum oven at 40 °C.

8.3 Results and discussion

This part is divided into two sections. The first section covers the synthesis of photoiniferters where, spectroscopic analyses results from synthesis of benzyl *N,N*-diethyl dithiocarbamate, 2-(*N,N*-diethyldithiocarbamyl) propionic acid, 2-(*N,N*-diethyldithiocarbamyl) isobutyric acid, and *N,N*-diethyl dithiocarbamate-epichlorohydrin is documented. The second section reports the polymerization of MMA in the presence of benzyl diethyldithiocabamate, the effect of photoiniferters structure on the MMA polymerization, the effect of [iniferter]/[monomer] ratio, and the synthesis of PMMA-*b*-PS block copolymer.

8.3.1 Synthesis of photoiniferters
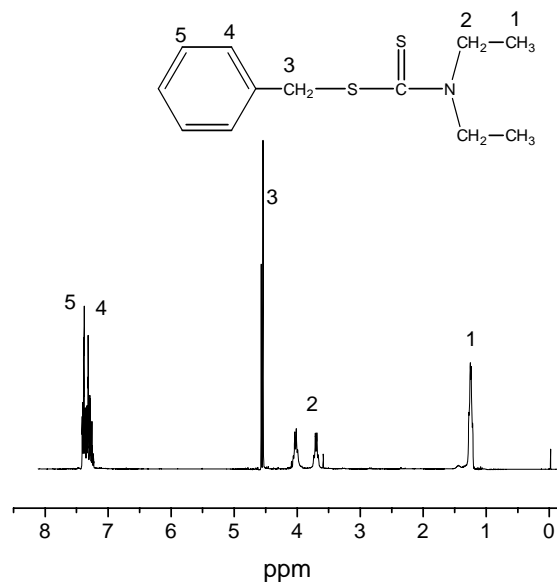
8.3.1.1 Synthesis of benzyl *N,N*-diethydithiocarbamate

Figure 8.2 shows the FTIR spectrum of benzyl *N,N*-diethydithiocarbamate (BDC). The presence of the benzyl group is proof by the C–H stretching peaks at about 3000cm^{-1}. The absorption at about 1600 and weak overtone bands at 2000-1667cm^{-1} are also evidence of the aromatic ring of BDC [18].
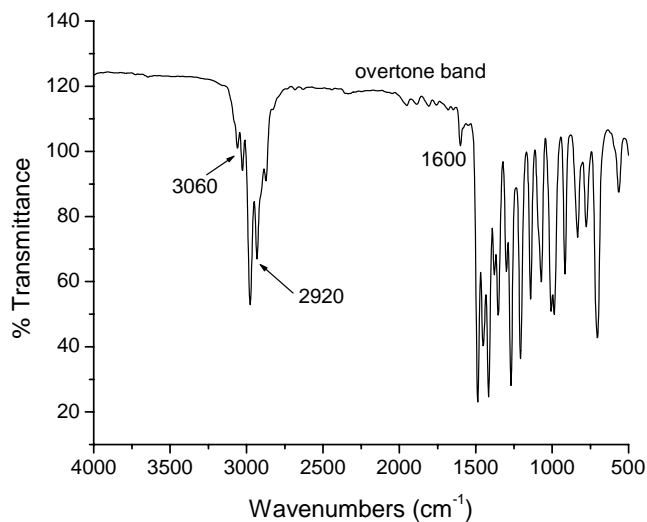
Figure 8.2 FTIR (NaCl) of benzyl *N,N*-diethyldithiocarbamate photoiniferter.

Figure 8.3 shows the ^{1}H-NMR spectrum of BDC. The peaks are identified in the figure. The most significant peaks of BDC are the methyl protons at about 1.2 ppm, denoted **1**, the methlylene protons at about 3.6-4.1 ppm, denoted **2**, the methylene of benzyl at about 4.65 ppm, denoted **3**, and the protons of aromatic ring at about 7.3-4.5 ppm, denoted **4** and **5**. FTIR and NMR data prove the formation of benzyl *N,N*-diethyl dithiocarbamate.

Figure 8.3 ^{1}H-NMR (CDCl$_3$) spectrum of benzyl *N,N*-diethyldithiocarbamate photoinferiter.

8.3.1.2 Synthesis of 2-(*N,N*-diethyldithiocarbamyl) propanic acid

2-(*N,N*-diethyldithiocarbamyl) propionic acid was synthesized by a conventional nucleophilic substitution reaction between sodium *N,N'*-diethyldithiocarbomate and 2-bromopropionic acid. **Figure 8.4** shows the ^{1}H-NMR spectrum of PDC. The most important features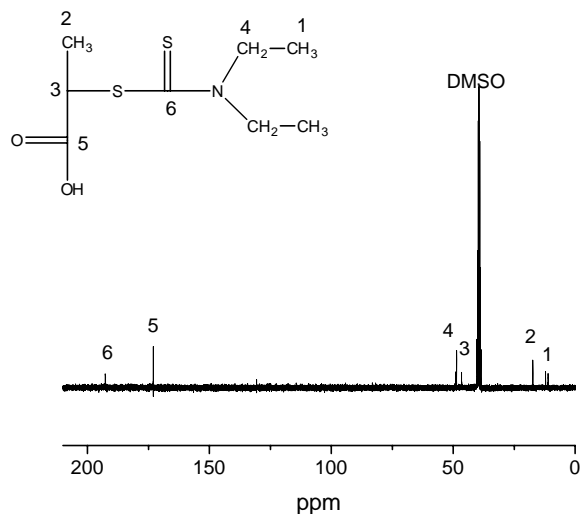 of this spectrum are the methyl protons at about 1.1-1.5 ppm, denoted **1**, the hydroxyl proton at about 3.2 ppm, denoted **2**, and the methylene protons peak at about 3.6-4.1 ppm, denoted **3**. The rest of the assignments are indicated in the figure.
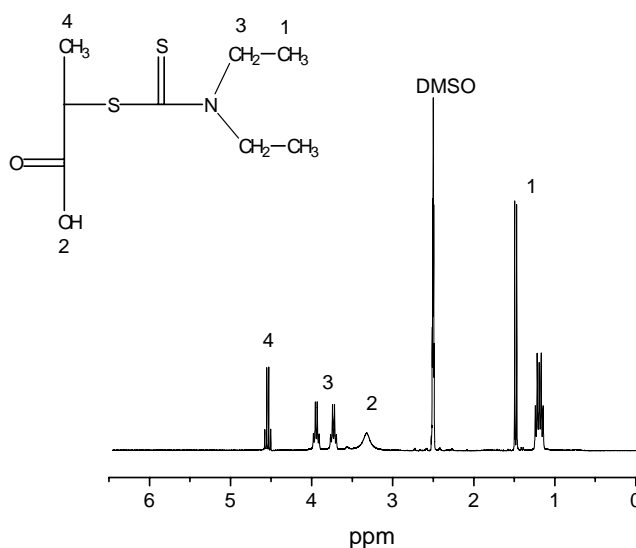
Figure 8.4 ^{1}H-NMR (DMSO) spectrum of 2-(*N,N*-diethyldithiocarbamyl) propanic acid.

Figure 8.5 shows the ^{13}C-NMR spectrum of PDC. The most important features of this spectrum are the methyl carbon peak of diethyl dithiocarbamate at about 10 ppm, denoted **1**, the carbonyl group peak at about 171 ppm, denoted **5**, and the carbon of the –C=S group at about 191 ppm, denoted **6**. The rest of the assignments are indicated in the figure.

Figure 8.5 ^{13}C-NMR (DMSO) spectrum of 2-(*N,N*-diethyldithiocarbamyl) propanic acid.

8.3.1.3 Synthesis of 2-(*N,N*-diethyldithiocarbamyl) isobutyric acid

The 2-(*N,N*-diethyldithiocarbamyl) isobutyric acid (DTCA) was synthesized by the reaction of 2-bromoisobutyric acid with sodium *N,N*-diethyldithiocarbamate salts. The ^{1}H-NMR spectrum of DTCA can be seen in **Figure 8.6**. The most important peaks are those of the methyl protons at about 1.1-1.5 ppm, denoted **1**, and the methlylene protons at about 3.6-4.1 ppm, denoted **3**. The rest of the assignments are indicted in the figure below.

Figure 8.6 ^{1}H-NMR (CDCl$_3$) spectrum of 2-(*N,N*-diethyldithiocarbamyl) isobutyric acid.

Figure 8.7 shows the ^{13}C-NMR spectrum of DTCA. The most important features of this spectrum are the peaks associated with the methyl carbon of diethyl dithiocarbamate at about 10 ppm, denoted **1**, the carbonyl carbon at about 180 ppm, denoted **5**, and the carbon of the C=S group at about 191 ppm, denoted *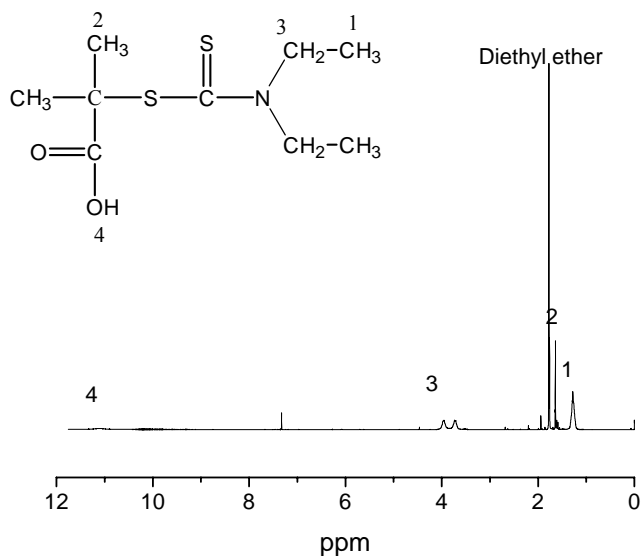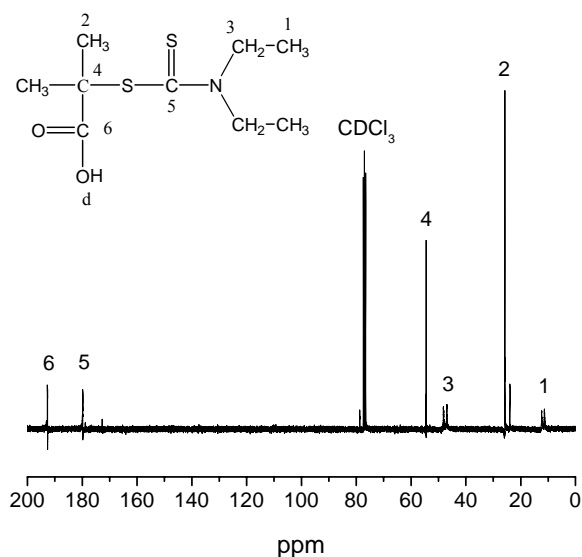*6**. The rest of the assignments are indicted in the figure below. NMR analysis confirmed the formation of DPC and DTCA photoiniferters, which were to be used in the polymerization of MMA.

Figure 8.7 ^{13}C-NMR (CDCl$_3$) spectrum of 2-(*N,N*-diethyldithiocarbamyl) isobutyric acid.

8.3.1.3 Synthesis of *N,N*-diethyl dithiocarbamate-epichlorohydrin

The successful synthesis of ECH-DCC was confirmed by FTIR, UV, and NMR analyses. The FTIR spectra of epichlorohydrin, and epichlorohydrin with the DDC pendent groups, are shown in **Figure 8.8**. The characteristic peaks due to the –S–C(=S)– and –C(=S)–N groups appear at 604, 661, 1415 cm^{-1} and 1207, 1644 and 3400 cm^{-1}, respectively [10,16-21]. Some of these peaks overlap with the ECH monomer peaks at 1644 cm^{-1}. There is a weak absorption at 3450 cm^{-1}, which could be attributed to some ring-opening of ECH monomers during the nucleophilic substitution reaction.

The UV spectrum of ECH-DDC (**Figure 8.9**) also confirms the attachment of DDC groups to the ECH monomers. There are two strong absorption peaks at about 281, and

251 nm, which can be attributed to the –S–C(=S)– and –C(=S)–N groups, respectively [16,20].
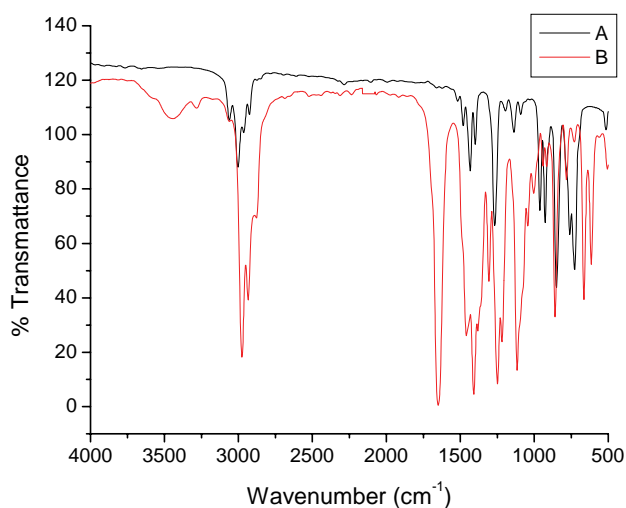
Figure 8.8 FTIR (NaCl) spectrum of (A) Epichlorohydrin monomers, and (B) *N,N*-diethyl dithiocarbamate-epichlorohydrin.
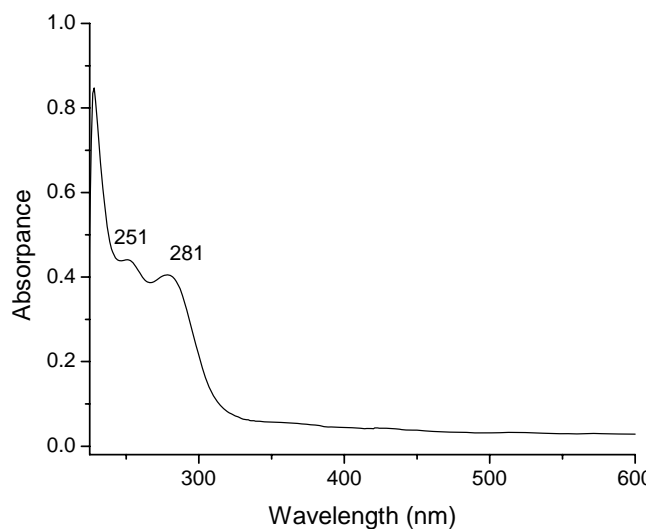
Figure 8.9 UV spectrum of *N,N*-diethyl dithiocarbamate-epichlorohydrin. (Analysis conditions: dichloromethane used as solvent, concentration 1 mg/mL.)

^{1}H-NMR analysis confirmed formation of the desired product. **Figure 8.10** shows the ^{1}H-NMR spectrum of ECH (in the top left) and ECH-DDC. The most important features are peaks at 1.182, 3.41, and 4 ppm, which are attributed to protons of the methylgroup (CH$_3$) of DDC, the methylene carbon (CH$_2$) of DDC, and traces of PECH monomer

formed during the nucleophilic substitution reaction, respectively. The rest of the assignments are indicated in the figure below.
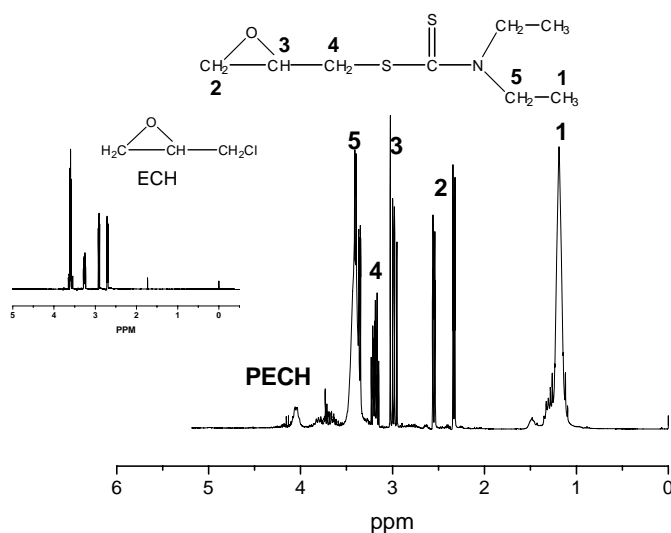
Figure 8.10 ^{1}H-NMR (CDCl$_3$) spectrum of epichlorohydrin monomer and *N,N*-diethyl dithiocarbamate-epichlorohydrin.

8.3.2 Photopolymerization of PMMA in the presence of photoiniferters

The photopolymerization of MMA in the presence of BDC photoiniferters is expected to proceed as proposed in **Scheme 8.5**.
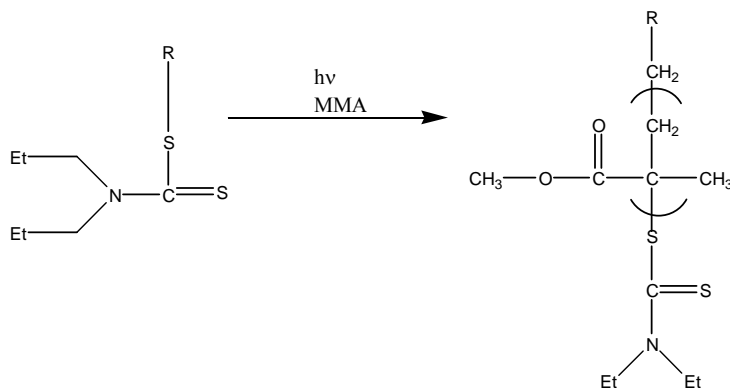
Scheme 8.5 Proposed reaction scheme for the polymerization of PMMA via photopolymerization in the presence of R-DDC, where R = benzyl.

The first-order time-conversion plot is shown in **Figure 8.11**. The conversion after 30 min of radiation was about 7% and after 120 min the conversion had reached about 40%. The low conversion rate recorded as polymerization proceeded was attributed to the increase in the viscosity of the polymerization solution. In addition, polydispersity did not change considerably during this polymerization. This result showed that the polymerization proceeded via controlled fashion.

Figure 8.11 First-order time-conversion plots for photopolymerization of MMA initiated by benzyl diethyldithiocarbamate as a function of different UV irradiation times. (Polymerization conditions: [MMA]/[BDC] = 80, toluene used as solvent.)

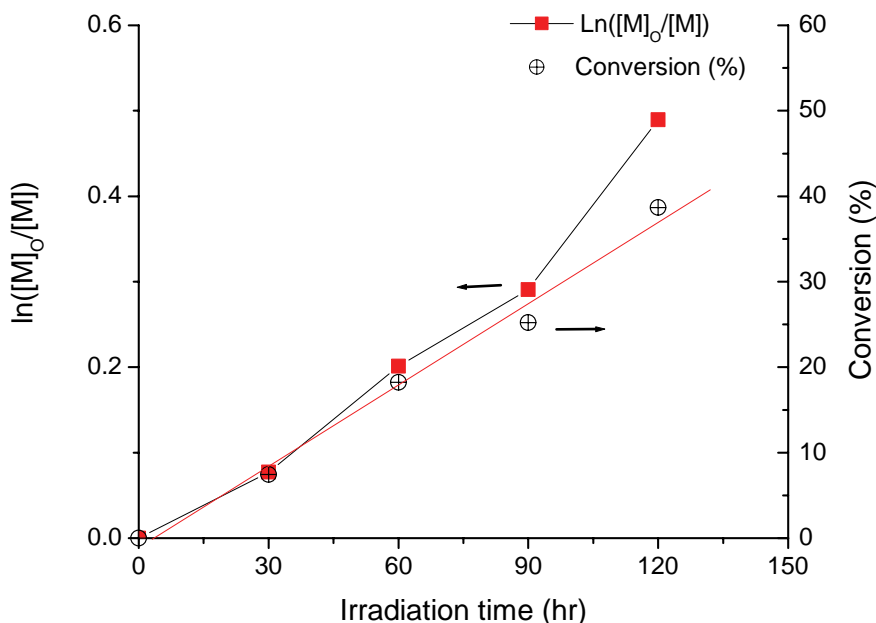Typical GPC traces of photopolymerization of MMA using BDC ([MMA]/[BDC] = 80) and varying the UV irradiation times are shown in **Figure 8.12**. All GPC curves show a unimodal distribution. Further, the elution peaks shifted to the high-molecular weight as reaction times increased. The increase in molecular weight was lower as polymerization proceeded. This could be attributed to the viscosity of the reaction mixture. This was also noticed during polymerization experiment and from the first-order time-conversion. On the other hand, polymerization without iniferter or macro-iniferter yielded small amounts of polymer with high molecular weight and polydispersity, while adding small

quantity of iniferter caused a remarkable change in the reaction (see chapter 6, Section 6.3.2).
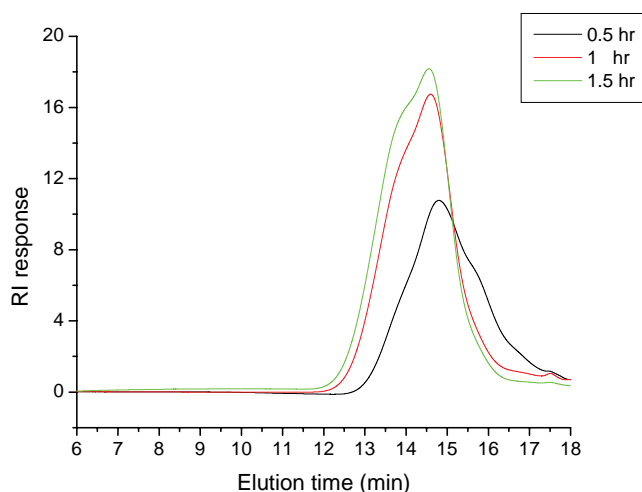
Figure 8.12 GPC traces of photopolymerization of methyl methacrylate initiated by benzyl *N,N*-diethyldithiocarbamate, as a function of different UV irradiation time. (Polymerization conditions: [MMA]/[BDC] = 80, and toluene used as solvent.)

Photopolymerization of MMA in toluene was carried out in the presence of ECH-DDC and samples were taken at various UV irradiation times. The GPC profiles of PMMA obtained from polymerization, as reaction time proceeded are shown in **Figure 8.13**. The presence of a peak at about 18.4 min could be attributed to the unreacted macro-iniferters. This could be attributed to some ring-opening polymerization of ECH monomers during the attachment of dithiocarbamate.

The GPC traces of PMMA recorded by using UV at 254 nm and RI detector are shown in **Figure 8.14**. These chromatograms are of the final polymerization product, where polymer was precipitated and washed several times with methanol in order to extract all un-reacted ECH-DDC. The overlaps of the two peaks (UV and RI) indicate that the polymer chains contain dithiocarbamate, where PMMA chains do not have an absorption at this region. The UV peak did not completely superimpose on the RI. This could be attributed to some PMMA chains initiated without photoiniferter. There is no clear explanation for the formation of PMMA without photoiniferters, whereas using MMA

monomers to UV irradiation yielded trace amount of polymer with high molecular weight and high polydispersity, which was not founded in our case.
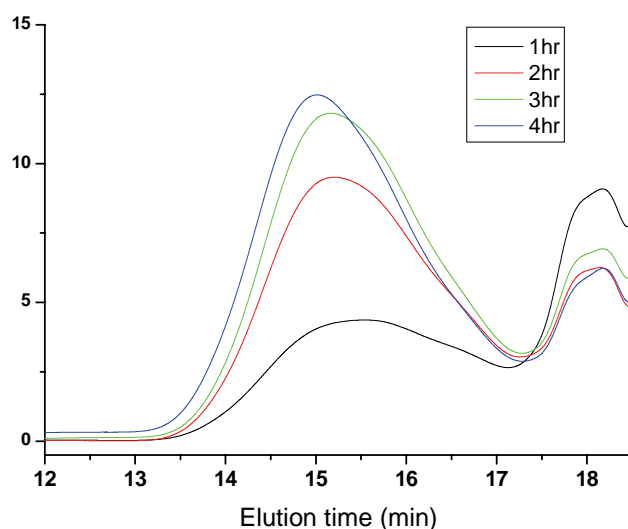

Figure 8.13 GPC traces of photopolymerization of methyl methacrylate initiated by the *N,N*-diethyl dithiocarbamate-epichlorohydrin, samples were taken as the irradiation time increased. (Polymerization conditions: [ECH-DDC]/ [MMA] = 0.0167 and toluene used as solvent.)
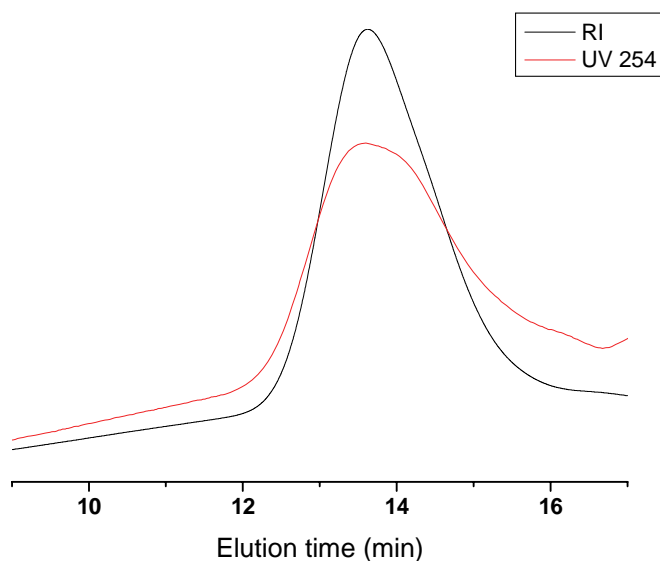
Figure 8.14 GPC traces of photopolymerization of MMA initiated by *N,N*-diethyl dithiocarbamate-epichlorohydrin. (Polymerization conditions: [ECH-DDC]/ [MMA] = 0.0167 and toluene used as solvent.)

8.3.2.1 Effect of different photoiniferters on PMMA polymerization

The effect of using different *N,N*-diethyl dithiocarbamate iniferters on the polymerization of PMMA was investigated. Results of the conversion, the molecular weight and the polydispersity were recorded in **Table 8.1**. The use of PDC and DTCA shows almost the same trend in the molecular weight and the polydispersity, whereas PDC gives the highest conversion. On the other hand, BDC yielded polymer with lower molecular weight and polydispersity. This could be attributed to the benzyl ring of BDC as it can work as inert radicals more efficiently than propanoic and isobutyric groups. Chong *et al*. [22], reported that benzyl dithiobenzoate appears almost inert because benzyl is a poor leaving group. On the other hand, the high polydispersity of PMMA in the case of PDC or DTCA could be attributed to the effect of the carboxylic functional group or low fragmentation of the R group during the polymerization [3]. The relatively high polydispersity (>1.4) and low conversion could be attributed to the nature of dithiocarbamate, due to the interaction between the N and the C=S double bond, as mentioned previously [6]. On the other hand, the use of ECH-DDC resulted in a lower polydispersity compared to the rest of the photoiniferters used. This could be attributed to the effect of ring on the polymerization.

Table 8.1 Photopolymerization of PMMA with different diethyl dithiocarbamate iniferters. (Polymerization conditions: bulk, and time 30 min.)

Iniferters	Conversion (%)	$\overline{M}_n$	PDI
BDC [MMA]/ [Iniferters] =80	9.7	9255	1.8
PDC [MMA]/ [Iniferters] =80	12	25159	2.0
DTCA [MMA]/ [Iniferters] =80	6.2	21870	2.0
ECH-DDC ([MMA]/[Iniferter]=50	15.6	17203	1.3

8.3.2.2 Effect of [iniferter]/ [MMA] molar ratio on PMMA polymerization

The effect of the [BDC]/ [MMA] mol ratio on the molecular weight, polydispersity index and conversion were investigated and **Table 8.2** records the results. The conversion increased as the molar ratio increased, until a certain point, whereafter the conversion declined again. This means that the conversion was controlled by the ratio of photoiniferters to monomers and that there was a maximum point. On the other hand, the number average molecular weight and polydispersity showed a slight difference as the mole ratio changed. It is possible that, the use of a higher difference in the molar ratio between iniferters and monomers could give more information about the trend of the polymerization. A similar trend has been reported by Kongkaew and Wootthikanokkhan [13]. Added to that, the alteration in the concentration of PDC and DTCA photoiniferters with the MMA monomers shows the same trend as BDC.

Table 8.2 The relationship between [BDC]/[MMA] ratio and molecular weight, polydispersity index, and the conversion of PMMA. (Polymerization conditions: bulk, time 30 min.)

[BDC]/[MMA]	$\overline{M_{wt}}$	PDI	Conversion (%)
0.005	10540	1.68	6.7
0.01	10110	2.29	7.5
0.0125	9255	1.88	9.7
0.015	7610	1.96	5.5

8.3.2.3 Synthesis of poly(methyl methacrylate-styrene) block copolymer

The UV spectrum of the PMMA obtained from the photopolymerization in the presence of benzyl *N,N*-diethyldithiocarbamate is shown in **Figure 8.15**. There are two different peaks at 251 and 280 nm, which can be explained by the formation of the photoiniferters

at the end of the polymer chains. It is worth mentioning that, PMMA obtained from conventional thermal polymerization does not show any UV absorption above 230 nm.
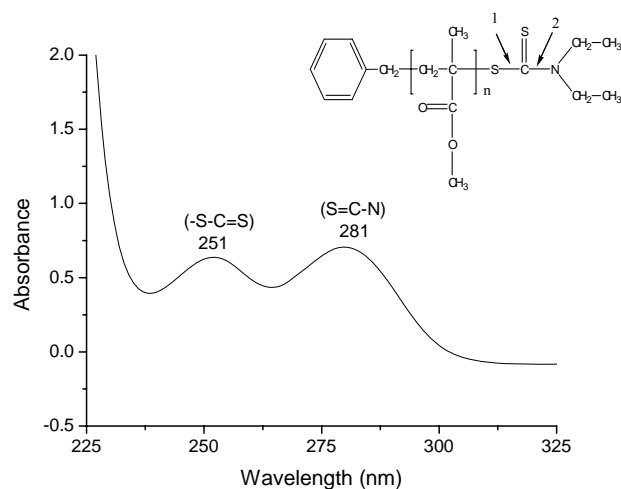
**Figure 8.15** UV spectrum of PMMA yielded by using benzyl *N,N*-diethyldithiocarbamate photoiniferters. (Analysis conditions: dichloromethane used as solvent and concentration 1 mg/5 mL.)

^{1}H-NMR spectrum of PMMA produced from photopolymerization in the presence of BDC is shown in **Figure 8.16**. The most important feature of this spectrum is the chemical shift of the methyl protons of the DDC group as can be seen from the intensity at about 1.67 ppm. This result indicates the formation of the *N,N*-diethyldithiocarbamate group on the ends of PMMA chains, and the possibility of utilizing this product as a macro-initiator.

The ^{1}H-NMR spectrum of the PMMA obtained from the photopolymerization in the presence of ECH-DDC and after precipitation in methanol is shown in **Figure 8.17**. Characteristics peaks of PMMA at 3.6 ppm (-OCH_3), and DDC at 1.03 ppm (CH_3), can be seen in the spectrum. The rest of the assignments are indicated in the figure.
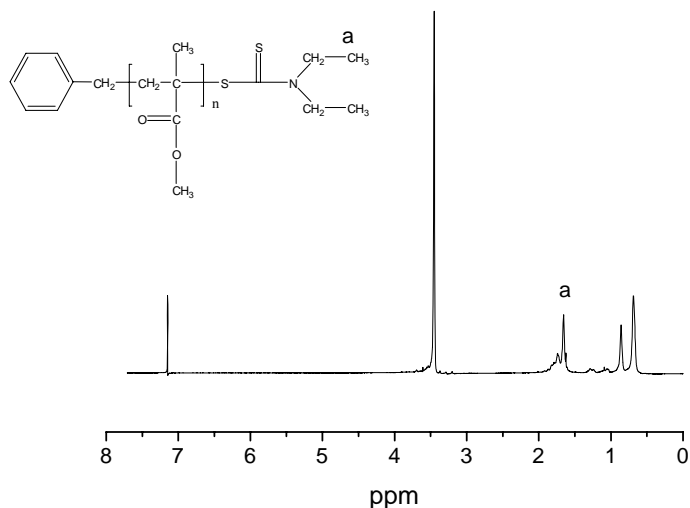
Figure 8.16 ^{1}H-NMR (CDCl$_3$) spectrum of PMMA ($\overline{M}_{wt}$ =30 000 g/mol) obtained from photopolymerization in the presence of benzyl *N,N*-diethydithiocarbamate inferter.
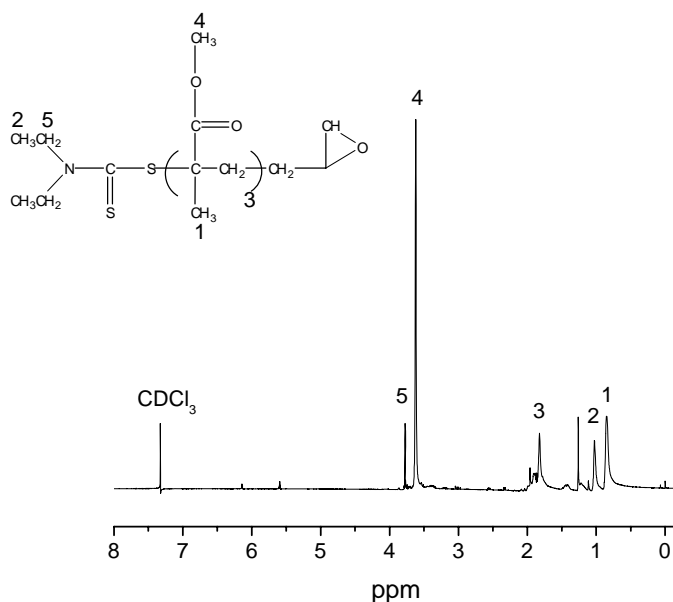
Figure 8.17 ^{1}H-NMR (CDCl$_3$) spectrum of PMMA obtained from photopolymerization in the presence of *N,N'*-diethyl dithiocarbamate-epichlorohydrin macro-photoinitiators.

It is expected that the polymer terminated by *N,N'*-diethyl dithiocarbamyl could be used for further block copolymerization with other vinyl or acrylate monomers [2]. Also, the cyclic ring in other side of the PMMA chain could be opened by using cationic ring-opening polymerization and by so doing attach the PMMA chain to an epichlorohydrin

chain. This reaction could be difficult after the precipitation of PMMA in methanol due to the small concentration of these cyclic rings in the whole product. Nonetheless, ring-opening reaction of the cyclic ring could be done in the same solution, which usually used in CROP of ECH monomers (see Chapter 2, Section 2.3.2) [23, 24].

The FTIR spectrum of PMMA yield from photopolymerization in the presence of ECH-DDC macro-photoinitiators is shown in **Figure 8.18**. The FTIR spectrum shows the characteristics peaks of PMMA at 1730 (C=O) and 1150 (C-O-C), where absorption at 1660 cm^{-1} could be attributed to the DDC.
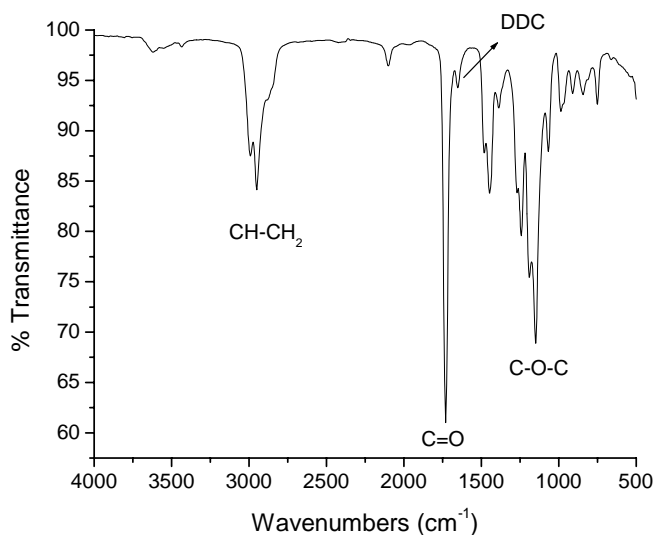

Figure 8.18 FTIR spectrum of PMMA obtained from photopolymerization in presence of ECH-DDC macro-photoinitiators.

PMMA produced from photopolymerization in the presence of BDC was used as a macrointiator for styrene. The formation of PMMA-block-PS was examined by FTIR and NMR spectroscopy. The FTIR spectrum of the PMMA-*b*-PS copolymer is shown in **Figure 8.19** and it shows the characteristic peaks of PMMA at 1734 (C=O) and 1150 cm^{-1}(C-O-C) where, PS peaks appears at 1600 and 1960 cm^{-1} due to the aromatic ring [16].
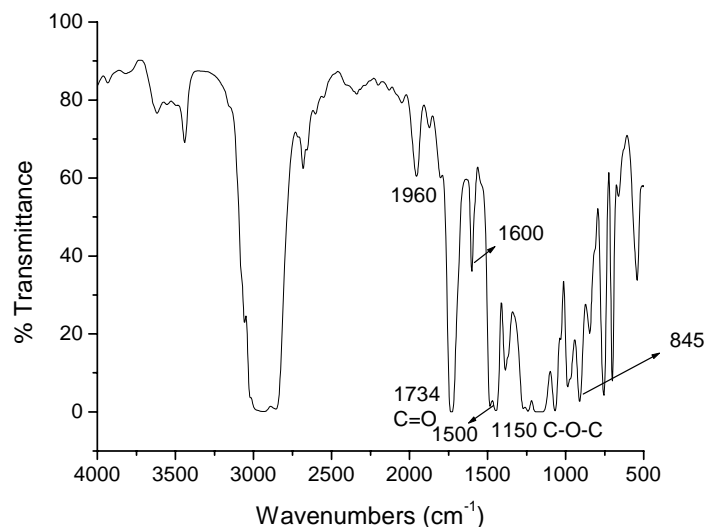
Figure 8.19 FTIR spectrum of poly(methyl methacrylate-styrene) block copolymer.

^{1}H-NMR (CDCl$_3$) spectrum of PMMA-*b*-PS block copolymer was recorded and is shown in **Figure 8.20**. The chemical shifts for both PMMA and PS appear in the spectrum. The most important feature of this spectrum is the peak at about 6.4-6.9 ppm, which is due to the aromatic ring protons of polystyrene and the peaks at about 1.8 and 3.5 ppm which could be attributed to the methyl group protons of PMMA.
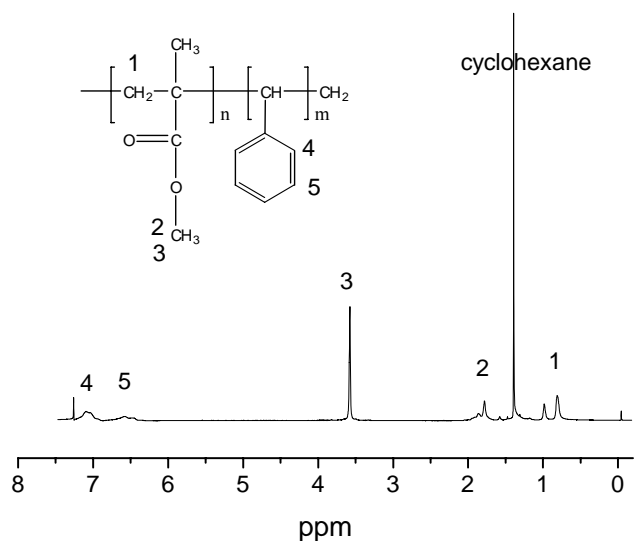
Figure 8.20 ^{1}H-NMR (CDCl$_3$) spectrum of poly(methyl methacrylate-styrene) block copolymer.

The GPC analysis of the PMMA-PS block copolymer gives further confirmation about the formation of block copolymer throughout the increase in the molecular weight and the shift of the elution time as can be seen in **Figure 8.21**. The elution peak at about 14.6 min is attributed to the PMMA macro-initiator with $\overline{M}_{wt}$ =29 689 g/mol and the elution time at about 13.6 min is attributed to the PMMA-*b*-PS block copolymer with $\overline{M}_{wt}$ =47 957 g/mol. The composition of the PS block was determined to be about 38 mol %, based on the GPC results (M_{wt}). Also, the polydispersity of block copolymer was lower than macro-initiator.
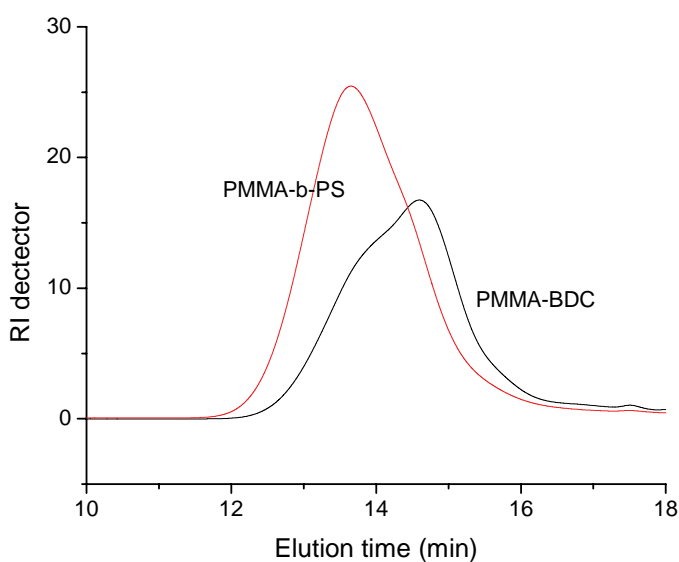
Figure 8.21 GPC traces of PMMA-BDC (macro-iniferter) and PMMA-*b*-PS. (Polymerization conditions: toluene used as solvent, [PMMA-BDC]/[St]= 150, irradiation time 4 hr.).

PMMA-PS product obtained by photopolymerization was subjected to a thermal analysis using DSC. **Figure 8.22** shows the thermograms of this analysis; there is a single glass transition temperature at about 110 $^{\circ}$C, which is between the T_g values of the two homopolymers [17].
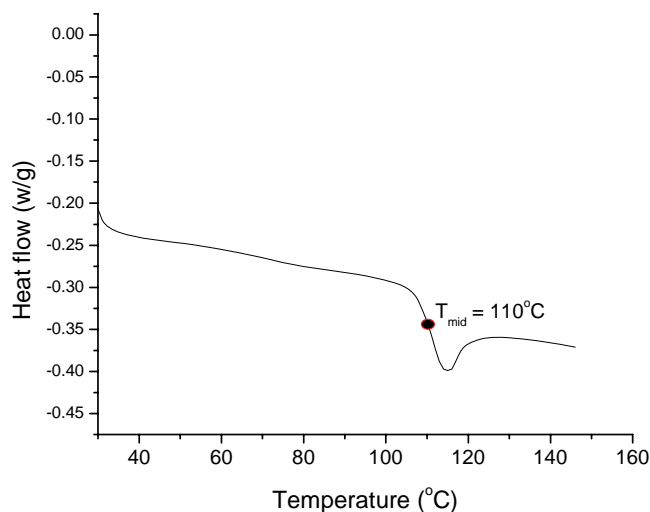
Figure 8.22 DSC thermogram of PMMA-*b*-PS block copolymer.

8.4 Summery

Four different diethyldithiocarbmate iniferters were prepared and characterized. The desired products were all of good purity as proofed by spectroscopic analysis techniques. First-order time-conversion and the increase in the molecular weight with irradiation time proofed that photopolymerization MMA in the presence of the iniferter proceeded via a controlled/living fashion. Effect of the molecular structure of the iniferter on the molecular weight, polydispersity, and conversion was evaluated. Of the types of photoiniferters used, benzyl diethyl dithiocarbamate provided the lowest polydispersity and molecular weight, which could be attributed to the inertness of the benzyl ring. Variations of the molar ratio between the monomer and the iniferter affect the conversion more than the polydispersity of the obtained polymer. ECH-DDC yielded the polymer with the lowest polydispersity. PMMA was obtained from the photopolymerization posses DDC groups and used as macro-initiator precursor to the architecture of PMMA-PS block copolymer. The T_g of block copolymer was between the glass transition of two homopolymers.

Chapter 8

8.5 References

1. Ishizu K., Khan R. A., Furukawa T., Furo M., J. Appl. Polym. Sci 2004, 91, 3233.

2. Sebenik A., Prog. Polym. Sci 1998, 23, 875.

3. Destarac M., Charmot D., Frank X., Zard S. Z., Macromol. Rapid Commun 2000, 21, 1035.

4. Georges M. K., Veregin R. P. N., Kazmaier P. M., Hamer G. K., Macromolecules 1993, 26, 2987.

5. Kajiwara A., Matyjaszewski K., Macromolecules 1998, 31, 3489.

6. Moad G., Rizzardo E., Thany S. H., Aust. J. Chem 2005, 58, 379.

7. Scranton A. B., Bowman C. N., Peiffer R. W., Photopolymerization Fundamentals and Applications, American Chemical Society 1996, 1-14.

8. Crivello J. V., Dietliker K., Photoinitiators for Free Radical Cationic & Anionic Photopolymerisation, Second Edition, Wiley 1998, 61.

9. Otsu T., J. Polym. Sci. Part A: Polym. Chem 2000, 38, 2121.

10. Otsu T., Yamashita K.,Tsuda K., Macromolecules 1986, 19, 287.

11. Otsu T., Yoshida M., Macromol. Rapid Commun 1982, 3, 133.

12. Otsu T., Matsunaga T., Doi T., Matsumoto A., Eur. Polym. J 1995, 31(1), 67.

13. Kongkaew A., Wootthikanokkhan J., J. Appl. Polym. Sci 2000, 75, 938.

14. Ishiz K., Katsuhara H., Kawauchi S., Furo M., J. Appl. Polym. Sci 2005, 95, 413.

15. Cakmak I., New Polym. Mat 1998, 5(2), 159.

16. Bhuyan P. K., Kakati D. K., J. Appl. Polym. Sci 2005, 98, 2320.

17. Brandrup J., Immergut E. H., Grulke E. A., Abe A. B., Daniel R., Polymer Handbook, 4th Edition,1999.

18. Pavia D. L., Lampman G. M., Kriz G. S., Introduction to spectroscopy. Third Edition, Thomson Learning 2001, 13-101.

19. Lakshmi S., Jayakrishnan A., Polym 1998, 39(1), 151.

20. Guan J., Yang W., J. Appl. Polym. Sci 2000, 77, 2569.

21. Yugci Y., Serhatli I. E., Kubisa P., Biedron T., Macromolecules 1993, 26, 2397.

22. Chong Y. K., Krstina J., Le T. P., Moad G., Potma A., Rizzardo E., Thang S. H Macromolecules 2003, 36, 2256.

23. Ivin K. J., Sagusa T., Ring Opening Polymerization, Elsevier 1984, 185.

24. Moad G., Solomon D. H., The Chemistry of Radical Polymerization, 1st Edition, Elsevier 2006.

Chapter 9

Conclusions and Recommendations

9.1 Conclusions

The aim of this study was the synthesis of the energetic thermoplastic elastomer with a controlled free radical polymerization. This aim was achieved successfully via controlled free radical polymerization. This was achieved throughout the following steps:

- The synthesis of the elastomeric segment was achieved via cationic ring-opening polymerization.
- Attaching different groups, such as dithiocarbamate, to produce macro-initiators which have the ability to initiate the free radical polymerization of vinyl and acrylate monomers.
- Using the macro-initiators in free radical polymerization of an acrylate monomer to obtain an energetic thermoplastic elastomer.

The following is a summary for each chapter in this manuscript. The elastomeric component was made via the cationic ring-opening polymerization of ECH. The resultant hydroxy-terminated PECH was used as is or transformed into hydroxy-terminated glycidyl azide polymer (GAP). The latter was successfully used to form urethane-like polymers by react the prepolymer with suitable diisocyanates.

Macro-azo initiators were synthesized from both the PECH and GAP prepolymers, utilizing the terminal hydroxyl groups and reacting them with 4,4'-azobis (4-cyanopentanoyl chloride). These macro-azo-initiators were utilized in the thermal polymerization of methyl methacrylate monomer to yield PECH-PMMA and GAP-PMMA block copolymers as energetic thermoplastic elastomers. These polymers exhibited a single glass transition temperature which was attributed to the miscibility of two different segments. This was again proven with miscibility studies of PMMA with PECH and GAP, although high molecular weight (rubbery) PECH showed signs of phase separation when mixed with PMMA.

Two different macro-iniferters namely *N,N*-diethyl dithiocarbamate-poly(epichlorohydrin) and *N,N*-diethyl dithiocarbamate-glycidyl azide polymer were also successfully prepared and used in the photopolymerization of MMA ($\lambda > 300$nm). Macro-raft agents were successfully prepared based on the reaction of poly(epichlorohydrin) and glycidyl azide polymer with dithiocarbamate via a nucleophilic substitution reaction. The macro-raft-agent was used in the photopolymerization of MMA to yield graft copolymers. The linear relationships of the first-order time-conversion give an indication that polymerization proceeded in a controlled manner. Poly(epichlorohydrin-methyl methacrylate) graft copolymer produced from bulk thermal polymerization of MMA in presence of dithobenzoate-poly(epichlorohydrin) macro-raft agents.

The last chapter reported the successful synthesis of four different diethyldithiocarbmate iniferters, namely, benzyl diethyl dithiocarbamate (BDC), 2-(*N,N*-diethyldithiocarbamyl) proponic acid (PDC), 2-(*N,N*-diethyldithiocarbamyl) isobutyric acid (DTCA), and epichlorohydrin-diethyl dithiocarbamate.

9.2 Recommendations

The synthesis of energetic thermoplastic elastomers in general and the utilization of the controlled free radical polymerization still need a significant investigation before it becomes commercially viable. The following are some of most important suggestions for future investigations:

1. Investigate the polymerization of other vinyl monomers with *N,N*-diethyl dithiocarbamate-glycidyl azide polymer and other GAP-macro-initiators.

2. Study the decomposition behavior of *N,N*-diethyl dithiocarbamate iniferter during the radical polymerization.

3. Study the utilization of the other active groups such as xanthates and trithiocarbonate with GAP in free radical polymerization.

4. Study the possibility to produce a binder based on other energetic segment like Poly(3-nitratomethyl-3-methyl-oxetane), 3,3-bis(azidomethyl)oxetane, and 3-azidomethyl-3-methyl oxetane throughout controlled free radical polymerization.

5. Investigate using new binders such as GAP-*g*-PMMA or GAP-*g*-PS as coating agents for internal solid rocket motors to prevent the migration of the energetic plasticizers, which has been the goal of rocket materials research for over 20 years.

6. Make a different mixture of the new energetic binder with other ammunition ingredients and study the solids loading capability, processblity, and storage stability.

7. Investigate the possibility to run the control free radical polymerization with the rest of the formulation ingredients (running polymerization during the mixing of formulation ingredients).

8. Study the interaction of new binders systems with different plasticizers (nitro and azide) utilized in the production of insensitive munitions formulations.

9. Study the utilization of photopolymerization to the synthesized energetic binder as coating for some internal part of rockets and missiles.